

---

# **Investigations of the Carbonyl-Olefin Metathesis and $\beta$ -Glycosylation inside the Supramolecular Resorcinarene Capsule**

**Inauguraldissertation**

zur Erlangung der Würde eines Doktors der Philosophie

vorgelegt der

Philosophisch-Naturwissenschaftlichen Fakultät

der Universität Basel

von

**Fabian Huck**

2022

Originaldokument gespeichert auf dem Dokumentenserver der Universität Basel

[edoc.unibas.ch](http://edoc.unibas.ch)

Genehmigt von der Philosophisch-Naturwissenschaftlichen Fakultät

auf Antrag von

Prof. Dr. Konrad Tiefenbacher, Prof. Dr. Housecroft und Prof. Dr. Nguyen.

Basel, den 22. 02. 2022

Prof. Dr. Marcel Mayor

(Dekan)

Die vorliegende Arbeit wurde von Oktober 2017 bis November 2021 an der Universität Basel unter Leitung von Prof. Dr. Konrad Tiefenbacher angefertigt. Teile dieser Arbeit wurden veröffentlicht:

**Expanding the Protecting group Scope for the Carbonyl-olefin Metathesis Approach to 2,5-Dihydropyrroles** Huck, F.; Catti, L.; Reber, g. L.; Tiefenbacher, K., *J. Org. Chem.* **2022**, *87* (1), 419-428.

## Acknowledgements

I want to thank my supervisor Prof. Dr. Konrad Tiefenbacher for giving me the opportunity to work in his group and pursue my research. I am thankful for his support, his input and the scientific discussion which helped me to develop my projects.

I am thankful to my second supervisor Prof. Dr. Housecroft and to Prof. Dr. Nguyen to read this thesis and helping me to improve it.

I want to thank the Tiefenbacher group and the great atmosphere in the lab and on our group trips. Special thanks to Dr. Lorenzo Catti for introducing me to this group and for his input even though he has already taken his position in Japan. Thanks to Suren Nemat who read this thesis and gave me input to improve it. I want to mention all the people from the middle lab giving me a great time during these four years of exploring new music. An honorable mention has to go to the participants of the thirsty Thursday, I really enjoyed the nice evenings with you and a cold beer.

The entire staff of the chemistry department is greatly acknowledged for their support, with a special mention of the workshop crew, who are always ready to help and find solutions despite my bad swiss-german understanding. I am also grateful to Isa Worni for always being of great help concerning any administrative issues.

I want to thank my family, especially my parents who made this all possible by supporting me my whole life. I want to specially mention my mother Sabine who did everything to support me after the passing of my father and helped me to finish my degrees. To my sister Johanna and my brother Moritz, who are always there for me if I need advice.

My deepest gratitude goes to my partner Olivia Witan, she is always there on my side believing in me even when I lost belief in myself. Her love and support over the years made this thesis possible.

## Deutsche Zusammenfassung

Für die Entwicklung einer umweltfreundlichen Chemie, werden neue «grüne» Katalysatoren benötigt, welche für neuartige und effiziente Reaktionen eingesetzt werden können. Das Resorcinaren Hexamer **II** kann als solcher gezählt werden und seine Fähigkeit komplexe Reaktionskaskaden zu katalysieren wurde an der tail-to-head Terpenzyklisierung demonstriert.

Im ersten Teil dieser Arbeit, wurde die Anwendung von **II** mit HCl als Co-Katalysator in der Katalyse der Carbonyl-Olefin Metathese getestet. Die Carbonyl-Olefin Metathese ist eine vergleichsweise neue Reaktion zur Bildung einer Kohlenstoff-Kohlenstoff Bindung.

Im ersten Teil wurde die Synthese von 2-5-Dihydropyrrolen untersucht. Die Startmaterialien wurden aus chiralen, tosylgeschützten Aminosäuren synthetisiert. Obgleich gute Ausbeuten für die von Glycin und Alanin abgeleiteten Substrate erhalten wurden, führten grössere  $\alpha$ -Substituenten zum einen zu einer verringerten Ausbeute, zum anderen zur vermehrter Dealkylierung. Als alternative Schutzgruppe wurden Mesyl und 4-Trifluoromethylbenzenesulfonyl getestet. Die Schützung mit Mesyl lieferte gute Ausbeuten, wobei die beste Ausbeute erstaunlicherweise wurde für das grösste getesteten Substrate, dem Phenylalanin-Derivat, beobachtet wurde. Mit 4-Trifluoromethylbenzenesulfonyl hingegen wurden nur niedrige Ausbeuten erhalten und welche auf die Zersetzung des Startmaterials zurückzuführen sind.

Eine mechanistische Untersuchung von drei repräsentativen Substraten mit Hilfe einer Eyring Analyse und der Bestimmung des sekundären kinetischen Isotopeneffektes zeigte, dass verschiedene geschwindigkeitsbestimmende Schritte für die unterschiedlichen Substrate möglich sind. Die Experimente wurden mit dem in der Literatur bekannten Eisen(III)chlorid Katalysator wiederholt, mit ähnlichen Beobachtungen. Das Abfangen von intermediären Carbokationen mit Hilfe von mechanistischen Prüfsubstanzen war erfolgreich. Jedoch konnte in nachfolgenden Studien gezeigt werden, dass die verwendete *ortho*-Phenolgruppe selbst den Reaktionspfad beeinflusst und deswegen keine allgemeine Aussage über den Mechanismus anhand dieser Ergebnisse getroffen werden kann.

Um den Umfang an Substraten der mit **II**/HCl katalysierten Carbonyl-Olefin Metathese zu erweitern, wurden Alkylketone und die intermolekulare ringöffnende Carbonyl-Olefin Metathese untersucht. Unglücklicherweise wurden keine vielversprechenden Resultate in beiden Fällen erzielt.

Im zweiten Teil dieser Arbeit wurde der Mechanismus der  $\beta$ -Glykosylierung im Hexamer **II** mittels der Bestimmung der Reaktionsordnung, Bestimmung des sekundären kinetischen Isotopeneffektes, sowie einer Protonen-Inventar Studie, analysiert. Die experimentel bestimmte Reaktionsordnung und der sekundäre kinetische Isotopeneffekt weisen auf einen losen  $S_N2$  Übergangszustand hin. Nachfolgende Rechnungen zeigten eine zweifache Aktivierung des Glycosyldonatoren und des Nucleophils durch ein kommunizierendes Wasserstoffbrückennetzwerk. Diese Ergebnisse der Protoneninventar Studie deuten auf eine Beteiligung von mehr als zwei Wasserstoffbindungen am Übergangszustand hin.

## English Abstract:

In order to access environmentally friendly chemistry, new «green» catalysts have to be developed and applied in novel and efficient reactions. The resorcinarene hexamer **II** can be regarded as such and has already demonstrated its capability to access complex reaction cascades like tail-to-head terpene cyclization.

In the first part of this work, the capability of **II** to catalyze the emerging carbonyl-olefin metathesis in presence of HCl was investigated. Carbonyl-olefin metathesis is a comparably new reaction for carbon-carbon bond formations.

First, the synthesis of 2-5-dihydropyrroles was investigated. The starting material was synthesized from chiral amino acids with a tosyl protecting group. Although good yields were obtained for the glycine and alanine derived substrates, larger  $\alpha$ -substituents lead to little product formation on the one hand and more dealkylation on the other. Mesyl and 4-trifluoromethylbenzenesulfonyl protecting groups were tested as an alternative. Protection with mesyl showed good yields but astonishingly the best result was obtained with the phenylalanine substrate, the biggest amino acid derivative tested in this substrate scope. 4-trifluoromethylbenzenesulfonyl derivative on the other hand resulted in low yields and mainly decomposition of starting material.

Mechanistic investigations of three representative substrates by an Eyring analysis and determination of secondary isotopic effects showed that diverging rate-limiting steps are possible for different substrates. The experiments were repeated with the literature known catalyst iron(III)chloride with a similar observation. Attempts to intercept the intermediate carbocations with mechanistic probes were successful. Nevertheless, subsequent studies showed that the *ortho*-phenol group in the mechanistic probe alters the reaction pathway and therefore cannot be used to make statements about the general mechanism.

In order to expand the substrate and reaction scope, alkyl ketones and the intermolecular ring-opening cross carbonyl-olefin metathesis were tested. Unfortunately, no promising results were obtained in both cases.

In the second part of this thesis, the mechanism of  $\beta$ -glycosylation inside hexamer **II** was investigated by determination of the reaction order, determination of the secondary kinetic isotope effect, and by a proton inventory study. The experimentally determined reaction order and the secondary kinetic isotope effect were indicative of a loose  $S_N2$  transition state.

Subsequent calculations suggested a dual activation of the glycosyl donor and the nucleophile via a communicating hydrogen bond network. Results from the proton inventory study indeed suggest the participation of more than two hydrogen bonds in the transition state.



## Table of Content

1. Introduction .....	1
2. Carbonyl-Olefin Metathesis .....	3
2.1 Introduction.....	3
2.1.1 Carbonyl – Olefin Exchange.....	3
2.1.2 Carbonyl-Olefin Metathesis .....	11
2.1.3 Objectives within this Thesis .....	42
2.2 Results and Discussion .....	44
2.2.1 Synthesis of 3-aryl-2,5-dihdropyrroles <sup>105</sup> .....	44
2.2.2 Mechanistic Investigation .....	50
2.2.3 Alkyl-Ketones .....	61
2.2.4 Intermolecular Ring-Opening Cross Carbonyl-Olefin Metathesis .....	66
2.3 Summary and Outlook.....	71
3. Glycosylation.....	73
3.1 Introduction.....	73
3.2 Results and Discussion .....	81
3.2.1 Reaction Order .....	81
3.2.2 Secondary Kinetic Isotopic Effect .....	83
3.2.3 Proton Inventory.....	85
3.3 Summary and Outlook.....	89
4. Index of Abbreviations .....	90
5. Bibliographic Data of Complete Publications.....	92
6. Reprints and Reprint Permissions.....	93
7. Experimental Part .....	104
7.1 General Information .....	104
7.2 Carbonyl-Olefin Metathesis.....	106

7.2.1	Mechanistic investigation .....	106
7.2.2	Kinetic Analysis .....	132
7.2.3	Alkyl-Ketones .....	183
7.2.4	Intermolecular Ring-opening cross carbonyl-olefin Metathesis.....	195
7.3	Glycosylation .....	206
7.3.1	Reaction Order .....	206
7.3.2	Secondary Kinetic Isotopic Effect .....	220
7.3.3	Proton inventory study .....	225
8.	References .....	237

# 1. Introduction

Catalysis shapes life as we know it and provides the solutions to the problems of its time. Even before the seminal scientific description of catalytic processes dating back to the 16<sup>th</sup> century, catalysis had been utilized by humans for millennia. The fermentation of sugars to alcohol through yeast can be counted as one of the first catalytic processes used deliberately by mankind.<sup>1</sup> In the 19<sup>th</sup> century, empirical studies revealed that chemical reactions can be performed with additives that are not consumed during the course of the process. In an early example by *Valerius Cordus* in 1552, the formation of ethers from alcohols in the presence of sulphuric acid was observed.<sup>2</sup> *Döbereiner* developed a hydrogen-powered lamp based on the observation that hydrogen can be ignited on a platinum surface in 1823.<sup>3</sup> At the beginning of the 20<sup>th</sup> century, the *Haber-Bosch* process provided ammonia on an industrial scale and enabled the production of synthetic fertilizers, which increased the production of food and still secures the supply to this day.<sup>4</sup> Processes like the cracking of petroleum or the production of polymers are essential for today's way of life.<sup>5</sup> From the end of the 20<sup>th</sup> century up till now, catalysis has developed towards environmentally friendly chemical processes which are used to tackle the most current problems, such as climate change. In 1998 *Paul Anastas* and *John C. Warner* formulated the twelve principles of green chemistry in order to provide a guideline for designing reactions with as little as possible formation of waste and hazardous byproducts.<sup>6</sup> Catalysis fulfills most of these points as it combines atom economy, waste prevention and energy efficiency and therefore helps to substitute stoichiometric processes. Stoichiometric processes are a double threat to the environment firstly with the production of additional reagents and secondly with the production of waste. The latter has to be stored in landfills or incinerated, both causing further environmental damage.<sup>7,8</sup>

One example of green chemistry is the catalytic olefin-olefin metathesis which plays an important role in the synthesis of natural products.<sup>9-11</sup> The reaction provides access to highly substituted olefins while using easily accessible alkenes as starting materials. Previously reported carbon-double bond formations rely on stoichiometric amounts of reagents like *Wittig*-olefination or carbenes. Furthermore, the necessity to use organic solvents is one of the biggest contributors to the waste products of chemical processes. The production, disposal or recycling of these solvents are energy intensive and are a potential threat to the environment due to the toxic nature of many organic solvents. Water is therefore the preferred choice of solvent since it is abundant and non-toxic. Efforts to realize olefin-olefin metathesis in water have shown promising results with ring-closing metathesis and cross-metathesis realized in conjunction

with both homogeneous and heterogeneous catalysts.<sup>12, 13</sup> In waste treatment, the olefin-olefin metathesis plays an important role in the degradation of rubber-waste towards reusable building blocks.<sup>14, 15</sup> Therefore the olefin-olefin metathesis enables recycling of waste and prevents the release of harmful degradation products via incineration. A similar approach is the synthesis of raw materials from renewable feedstock like seed oil or lipids via olefin-olefin metathesis.<sup>16-18</sup>

In conclusion, the olefin-olefin metathesis plays an important role in industry and the development of greener chemistry.<sup>19</sup> Carbon-carbon bond formation strategies are essential if new important pharmaceutical products are to be developed. Therefore the development of new sustainable strategies is of great interest to synthetic chemists.

## 2. Carbonyl-Olefin Metathesis

### 2.1 Introduction

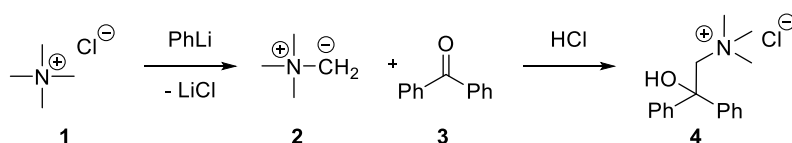
#### 2.1.1 Carbonyl – Olefin Exchange

In this section, stoichiometric carbonyl olefination strategies are discussed, in order to give an overview of the developments which have led to the emergence of catalytic carbonyl-olefin metathesis.

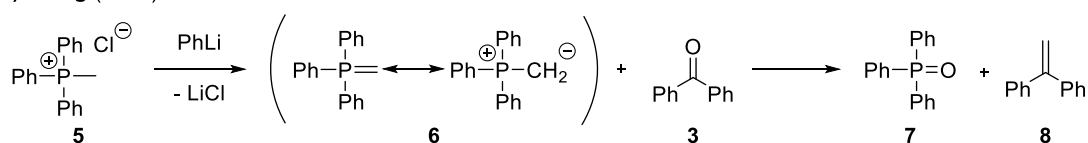
##### 2.1.1.1 Wittig Olefination

One of the first general and reliable methods used to access olefins was the *Wittig* reaction which was published in early 1950 (Scheme 1a).<sup>20,21</sup> The initial efforts of *Wittig* to investigate pentavalent nitrogen, led to the discovery of nitrogen-ylid (**2**), which readily reacted with benzophenone (**3**) (Scheme 1b).<sup>22</sup> The expansion of this concept towards the next higher element, phosphorus, provided an almost quantitative reaction with benzophenone (**3**). High yields and good stereoselectivity are key characteristics of the *Wittig* reaction, which make it attractive for applications in synthesis.

##### a) Wittig (1947)



##### b) Wittig (1953)

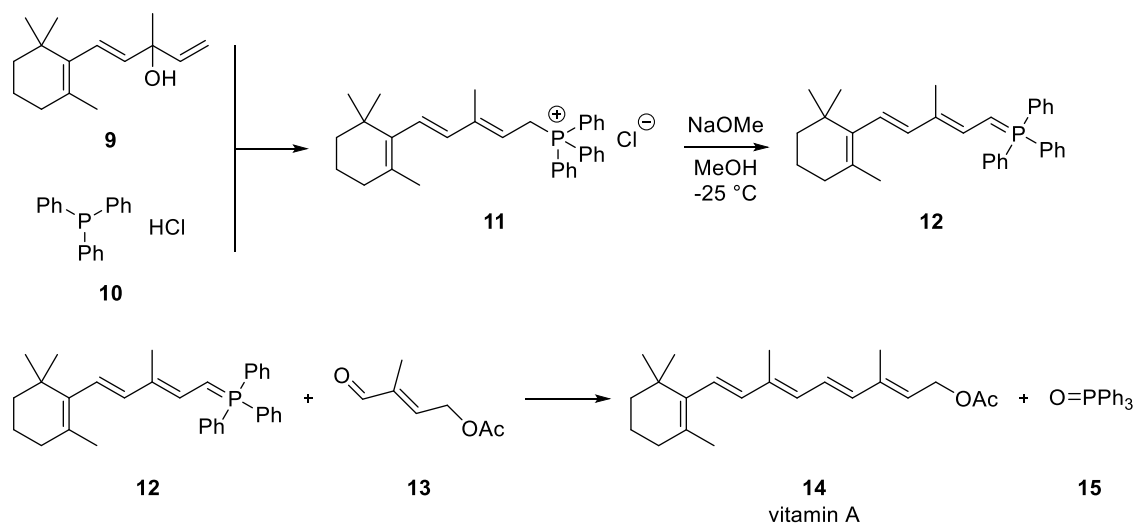


Scheme 1 a) Discovery of nitrogen-ylid **2** b) Reaction of phosphor-ylid **6** with benzophenone (**3**).

As an early example, the *Wittig* reaction played a key role in the synthesis of vitamin A by BASF, (Scheme 2).<sup>23</sup> However, the *Wittig* reaction also suffers from significant drawbacks. The ylid has to be prepared before the reaction thereby requiring the alkylation of a phosphane with the subsequent deprotonation using stoichiometric amounts of base.<sup>24</sup> The ylid also has to be used in stoichiometric quantities, which leads to the quantitative formation of phosphoxides. This is not only ineffective regarding the atom economy of the reaction, but the thereby generated phosphoxid is often very hard to separate from the product and therefore requires

intensive purification.<sup>25</sup> In addition, the stability of the formed P-O double bond prohibits efficient recycling of the phosphoxide, often resulting in its incineration.<sup>23</sup>

**BASF Synthesis of Vitamin A (1971)**



Scheme 2 Synthesis of vitamin A by BASF.

The originally presumed mechanism for the *Wittig* reaction involved a nucleophilic attack of the ylid at the carbonyl under the formation of an intermediate betaine, which subsequently cyclizes to an oxaphosphetane.<sup>21</sup> This oxaphosphetane undergoes cycloreversion to release the alkene and the respective phosphine oxide. However, the mechanism is a topic of recent debate, since calculations and experimental data suggest, that the betaine-intermediate seems not to display the standard mechanistic pathway. The isolation of betaine-LiBr complexes as a product of the reaction of a phosphor ylid with an aldehyde in the presence of HBr was interpreted as evidence for the betaine-intermediate.<sup>21</sup> Nevertheless, it was shown that oxaphosphetanes under acidic conditions form the betaine complex, thereby putting the previous findings into perspective. Experimental data suggest, that in most cases, the oxaphosphetane is formed irreversibly as the initial step. Synthesis of stable oxaphosphetanes derived from a *Wittig* reaction or separately synthesized betaines showed different ratios of the formed pseudo rotamers, indicating that betaines are no prior intermediates in the *Wittig* reaction.<sup>26</sup> In the mechanism proposed by *Vedejs*, a direct [2+2] cycloaddition of the carbonyl to the ylid has been suggested, which is supported by computational studies.<sup>27-30</sup> The *E/Z* selectivity of the reaction is determined by the state of hybridization and substituent arrangement of the phosphorus center in the transition state and is therefore under kinetic control. The approaching angle and alignment of the carbonyl are influenced by the steric environment of the ylid and the carbonyl itself. During the formation of the oxaphosphetane the phosphorus undergoes a

change from a tetrahedral-substituted center to a trigonal-bipyramidal- substituted one. The structure of the transition state depends on the stabilization of the ylid: alkyl substituents lead to unstabilized, highly reactive ylids, while aryl or alkenyl substituents are considered to be semi-stabilized.

Electron-withdrawing groups like esters or carbonyls give the most stable ylids. Unstabilized ylids react in an early transition state, with a tetrahedral arrangement of the phosphorus substituents resulting in a higher *Z*-selectivity (**22**) (Figure 1b). Semi-stabilized ylids have a later transition state compared to unstabilized ylids. As a consequence, the phosphorus substituents are already in a more trigonal bipyramidal, rather than tetrahedral configuration and show a less defined *E/Z* selectivity (Figure 1c). Stabilized ylids have a late transition state and therefore the forming bonds are more developed and shorter compared to semi- or unstabilized ylids. The phosphorus substituents have a more trigonal bipyramidal configuration than a tetrahedral one, which favors the *trans*-transition state (**27**), and therefore they show a high *E*-selectivity (Figure 1d).

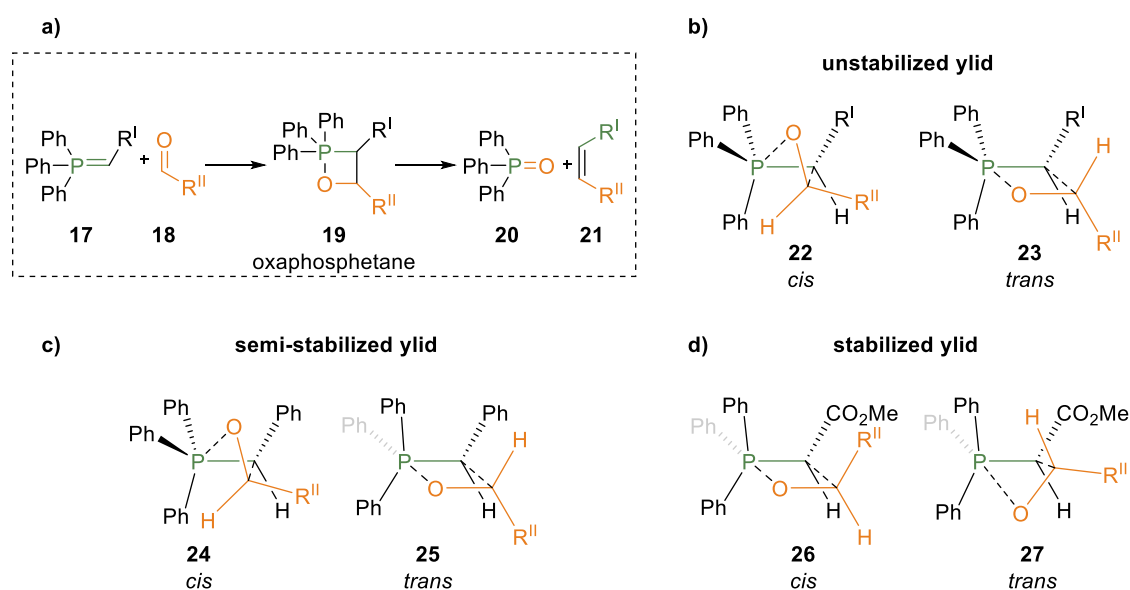


Figure 1 a) Reaction overview of the *Wittig* reaction. b) Transition states for the unstabilized ylid and the carbonyl. c) Transition states for the semi-stabilized ylid and the carbonyl. d) Transition states for the stabilized ylid and the carbonyl.

### 2.1.1.2 Schrock Carbenes

*Schrock* carbenes (**28**) are a subclass of carbenes widely used for carbonyl alkylation. The advantages of this reaction are its mildly basic conditions alongside the high reactivity of the carbene. Moreover, the alkylation of carboxylic acid derivatives like esters or lactones is possible unlike in the *Wittig* reaction. *Schrock* carbenes consist of a carbene coordinated to an oxidized early-transition metal complex with Ta or Ti for example. The metal complex requires electron rich ligands like cyclopentadiene (Cp) for stabilization. The carbene is in its triplet state, which allows the formation of both a  $\sigma$ - and a  $\pi$ -bond with the metal center. Due to the higher electronegativity of the carbon compared to the metal, the complex is polarized towards the carbene carbon, which corresponds to the nucleophilic site.<sup>31</sup>

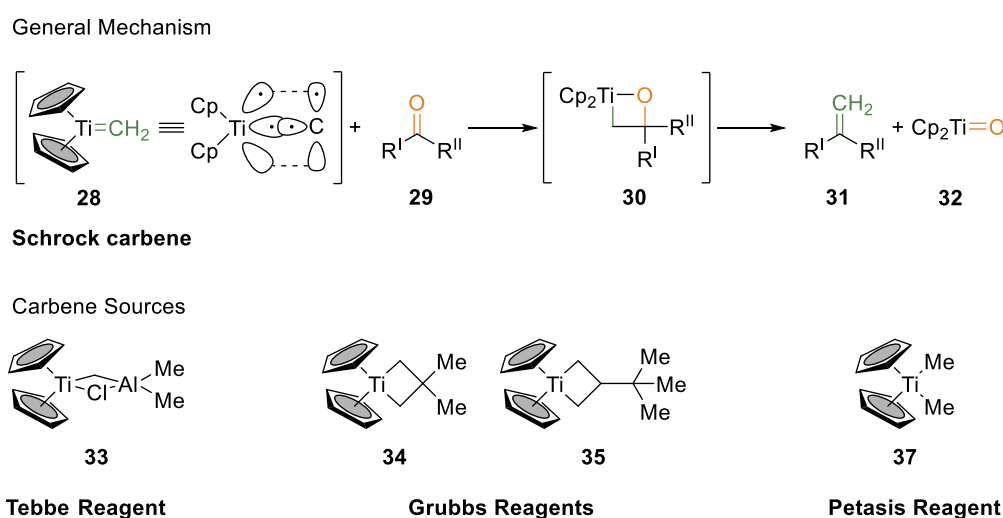


Figure 2 General mechanism for the reaction of *Schrock* carbenes with carbonyls.

The nucleophilic carbene can easily attack carbonyls (**29**) and form an oxatitanacyclobutane (**30**), which undergoes cycloreversion to release the alkyldiene (**31**). The reaction is driven by the formation of the stable titanium oxygen double bond in the by-product (**32**), which precludes the catalytic usage of *Schrock* carbenes (Figure 2). Several reagents have been developed as stable carbene precursors (Figure 2). In general, the addition of a weak Lewis-base such as pyridine and THF, or the use of an elevated temperature are enough to generate the carbene *in situ*.<sup>32</sup>

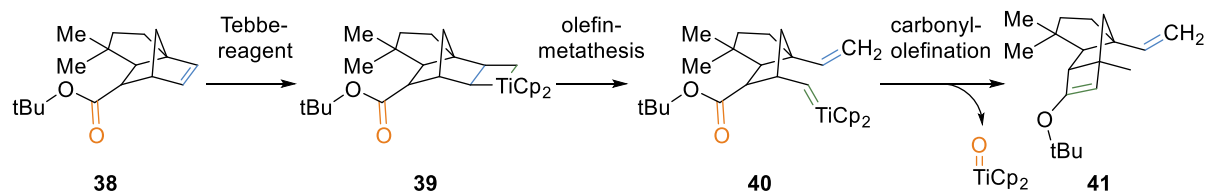
Olefin-olefin metathesis is also accessible via organotitanium complexes<sup>33</sup> and can be used in combination with the carbonyl-olefination to achieve a pseudo carbonyl-olefin metathesis. In the strict definition of a metathesis reaction, a new carbonyl compound has to be formed, which is not the case with titanium reagents due to the formation of stable titanium oxides. In a work of *Grubbs* in 1986 (Scheme 3a) the *Tebbe* reagent was used to first open up the strained



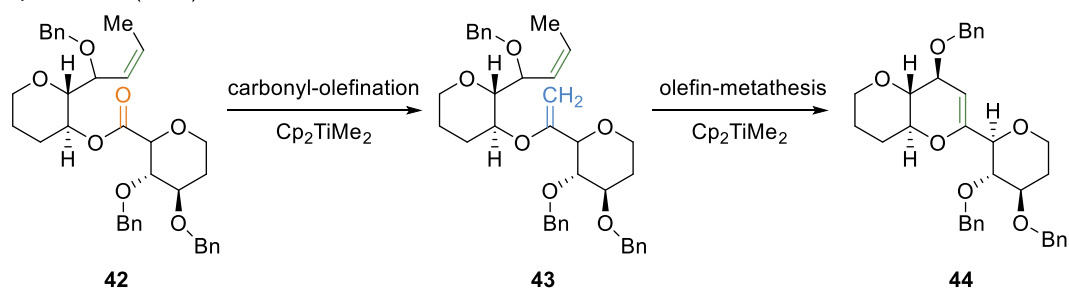
norbornene ring in a ring-opening olefin-olefin metathesis. The metal alkylidene (**40**) reacted with the carbonyl of the *tert*-butyl ester towards the cyclobutene (**41**) and titan oxide.<sup>34</sup>

A similar approach was chosen in the synthesis of the JKL rings of maitotoxin by *Nicolaou* (Scheme 3b), but instead of the initial olefin metathesis, the carbonyl olefination of **42** is the first step.<sup>35</sup> The formed dialkene (**43**) undergoes subsequent olefin metathesis in the presence of super stoichiometric amounts of *Tebbe* reagent.

**a) Grubbs (1986)**



**b) Nicolaou (1996)**



Scheme 3 a) Synthesis of **41** by Grubbs. b) Synthesis of the JKL rings (**44**) of maitotoxin.

Metal alkylidenes were key to one of the few methods available at the time to enable a carbonyl-olefin exchange reaction in natural product synthesis besides the *Paterno Büchi* reaction. Nevertheless, the necessary super stoichiometric amount of metal alkylidynes makes this approach uneconomical compared to the comparable olefin-olefin metathesis.

### 2.1.1.3 Paterno Büchi reaction

*Scharf* and *Korte* observed the formation of benzaldehyde and norbornene in their attempt to perform a photodimerization of norbornene (**46**) (Figure 3a).<sup>36</sup> Instead of the expected alkene [2+2] cycloaddition, the benzophenone, intended as a photosensitizer, reacted with norbornene (**46**) to form oxetane **47**. The addition of acid led to cycloreversion of the oxetane (**47**) and therefore provided one of the first examples of a carbonyl-olefin metathesis (**48**) (Figure 3b).<sup>36</sup>

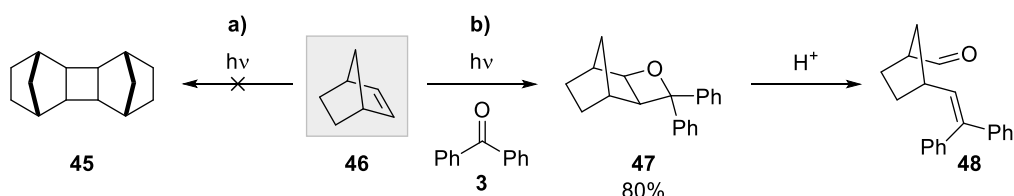


Figure 3 a) Intended photo-dimerization of norbornene (**46**). b) [2+2] cycloaddition of benzophenone and norbornene with subsequent acidic oxetane opening.

The *Paterno Büchi* reaction is a photochemical [2+2] cycloaddition of a carbonyl and an olefin. Under photon irradiation, the carbonyl (**49**) is transferred to its singlet state (**50**) via  $n-\pi^*$  absorption.<sup>37</sup> Depending on the substitution pattern the carbonyl either reacts in its singlet state (**50**) for alkyl substituents or by intersystem crossing via the triplet state (**51**) for aryl substituents (Figure 4).

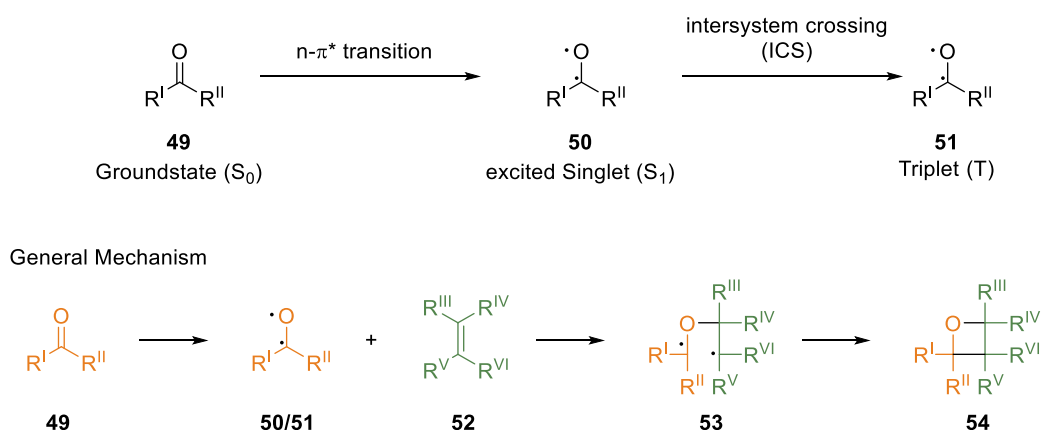


Figure 4 Excitation of the carbonyl ground state to the biradical.

Due to the amphoteric character of the excited carbonyl, electron donating, as well as electron withdrawing groups at the alkene, are beneficial for the reaction.<sup>38</sup> If several double bonds are available, the attack of the carbonyl occurs at the more nucleophilic double bond. For electron withdrawing groups like acetate, the electrophilic double bond is preferred over the unsubstituted one. After the initial attack on the alkene (**52**), the lifetime of the formed biradical

(53) is crucial for the stereoselectivity of the reaction. The biradical (53) is in its triplet state and over time de-excites via intersystem crossing (ISC) to a singlet state, in order to recombine. If this process is slow in the case of a very stable triplet state, such as observed for aryl-substituted carbonyls, the former alkene bond has time for rotation, which leads to a loss of stereo information. If the alkene bears a sterically demanding group, the stereo information of the formed oxetane (54) can be predicted. In order to avoid interaction between the two spin-equal electrons in the triplet state, the orbitals of the radicals occupy the conformation with the least orbital interaction, which is orthogonal. Depending on the substituents, steric interactions will favor the conformation with the least strain (Figure 5).<sup>39,40</sup>

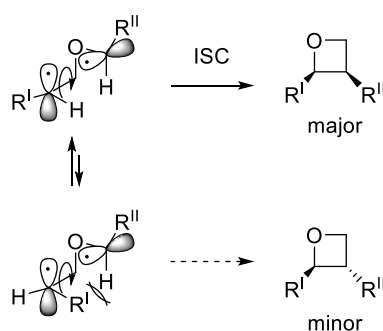
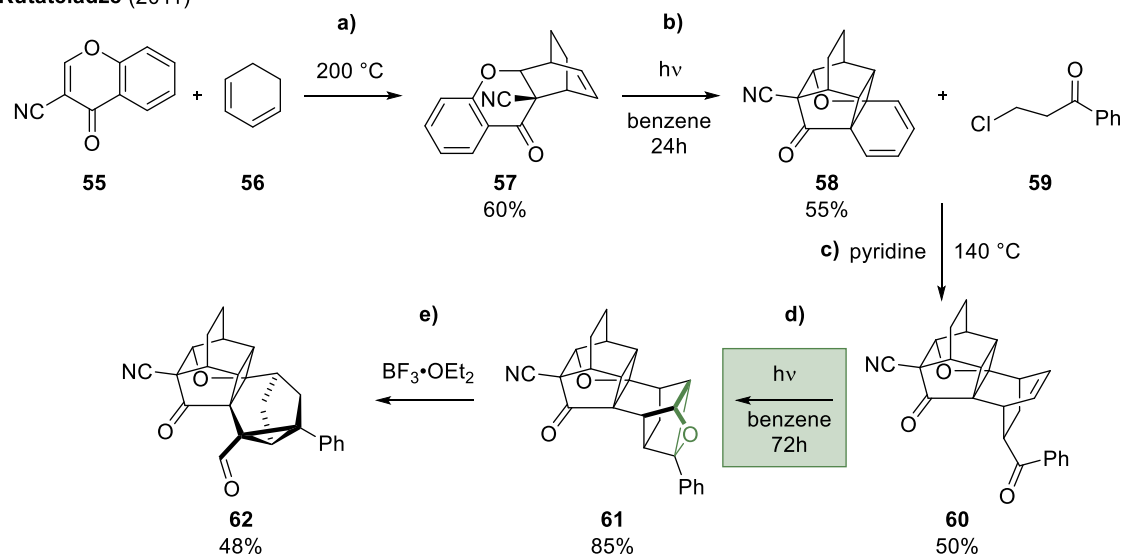


Figure 5 Conformation of the intermediate biradical in its triplet state.

Oxetanes are an important motif in natural products, like in the case of merrilactone A, or as a precursor to more complex structures.<sup>41</sup> The combination of a *Paterno-Büchi* reaction followed by oxetane opening was used to access an “interrupted” carbonyl-olefin metathesis. Early studies by *Jones* were focused on the thermal cycloreversion of the oxetane at high temperatures. This pyrolytic approach only enabled access to simple and stable molecules, therefore other approaches with milder conditions such as acidic oxetane fragmentation are more appealing.<sup>42, 43</sup> In 2009 *Kutateladze* and *Valiulin* developed a two-step acid-catalyzed metathesis, based on the formation of a strained oxetane via a *Paterno Büchi* reaction with successive acid catalyzed oxetane openings.<sup>44</sup> This concept was further developed by *Kutateladze* towards the synthesis of more complex organic structures (Scheme 4).<sup>45, 46</sup>

Kutateladze (2011)



Scheme 4 Creating chemical complexity with simple starting materials: a) *Diels-Alder* reaction, b) Intramolecular [2+2] arene-alkene photocyclization, c) *In situ* generation of vinyl phenyl ketone with subsequent *Diels-Alder* reaction, d) *Paterno Büchi* reaction and e) Acidic oxetane opening.

The work on photochemical oxetane formation with successive fragmentation was the starting point for the subsequent studies on catalytic carbonyl-olefin metathesis protocols. In order to access more complex molecules, milder strategies were developed combining the advantages of the photochemical approach, without the need for stoichiometric additives, and the use of the mild conditions of carbene chemistry. The combination of both worlds led to the development of the catalytic carbonyl-olefin metathesis.

### 2.1.2 Carbonyl-Olefin Metathesis

Carbonyl-olefin metathesis describes the exchange of a carbonyl double bond and an olefinic double bond.<sup>47</sup> By definition, a metathesis requires that both motives have to be preserved in both substrate and product. This distinguishes carbonyl-olefin metathesis from carbonyl olefination such as the previously described *Wittig* reaction. Three main reactions of the carbonyl-olefin metathesis are frequently discussed in literature (Figure 6):

#### 1. Ring-closing metathesis 2. Cross-metathesis 3. Ring-opening metathesis

In the ring-closing metathesis, the carbonyl and the olefin are both parts of the substrate (**63**) and form an unsaturated cyclic product (**64**). Commonly accessible ring sizes are five and six-membered rings, but also seven-membered rings have been realized by *Lin* and co-workers.<sup>47</sup> The cross-metathesis aims for more complex olefins as compared to the starting material;<sup>48</sup> therefore, simple alkenes (**67**) are used in these reactions. So far, cross-metathesis was realized with aryl aldehydes and trisubstituted alkenes. In this process, the carbonyl substituent is transferred to the newly formed olefin (**68**) whereby *E*-isomer formation is favored.<sup>49-51</sup> Ring-opening metathesis requires strained unsaturated rings (**71**) which can react with the carbonyl to give the respective unsaturated carbonyl. For the ring-opening metathesis, the required reactivity of the substrates can lead to undesired side reactions and therefore has to be adjusted carefully. Examples of Lewis acid catalyzed ring-openings have been demonstrated by *Nguyen* and *Schindler* with methylcyclopentene.<sup>50, 52, 53</sup> *Lambert* and co-workers were able to show the conversion of cyclopropenes and norbornenes with their hydrazine catalyst.<sup>54, 55</sup> The field of the carbonyl-olefin metathesis is rapidly expanding with the use of new catalysts, which make more and more transformations accessible.<sup>47, 56, 57</sup>

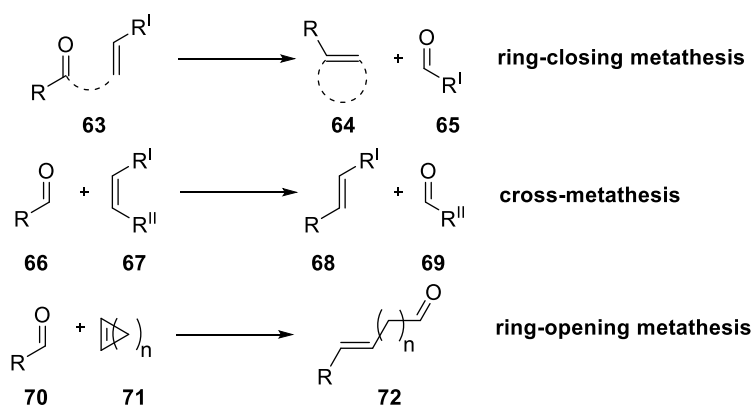


Figure 6 Classes of the carbonyl-olefin metathesis discussed in literature.<sup>47</sup>

### 2.1.2.1 Lewis acid mediated and catalyzed reactions

One of the earliest reported examples of a Lewis acid initiated [2+2] cycloaddition can be found in the synthesis of carotol-like sesquiterpenes (**74**) by *Demole, Enggist* and *Borer* (Figure 7a).<sup>58</sup> The first acid catalyzed carbonyl-olefin metathesis was presented in the work of *Bickelhaupt* in 1994 (Figure 7b).<sup>59</sup> In the presence of ZnCl<sub>2</sub> clay catalyst EPZ-10, benzaldehyde (**75**) and amylene (**76**) formed *trans*-1-propenylbenzene (**80**). For the mechanism, *Bickelhaupt* proposed a *Prins* type activation of the carbonyl (**77**), with a subsequent attack of the olefin on the carbonyl and the formation of an intermediate oxetane (**79**). Under the acidic conditions, the oxetane underwent a *Grob* fragmentation and acetone (**81**) and the metathesis product (**80**) were released.

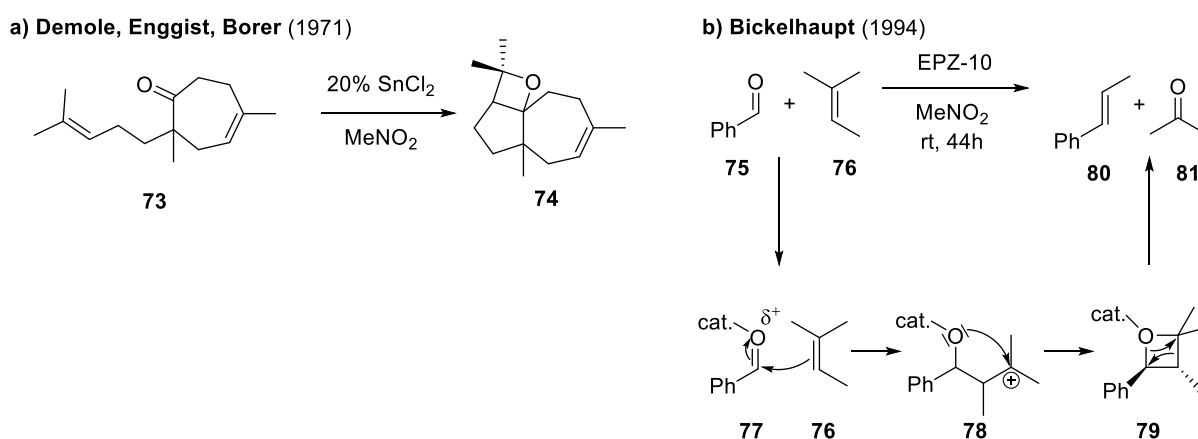
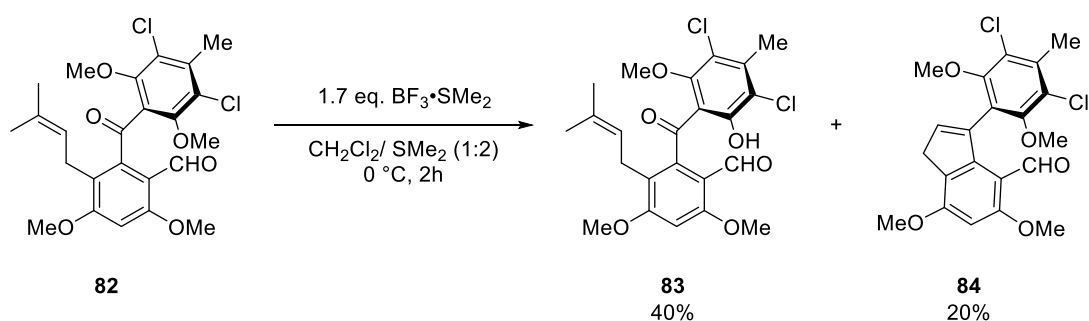


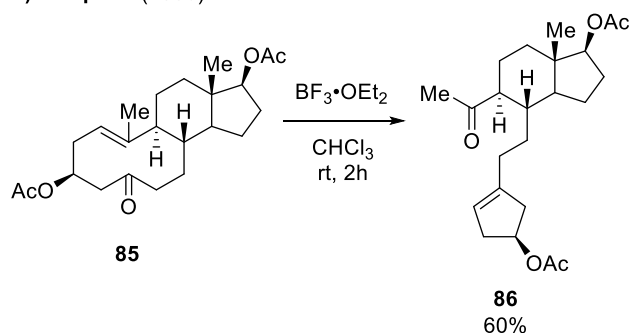
Figure 7 a) Cyclisation of **73** under Lewis acidic conditions to oxetane **74** by *Demole, Enggist* and *Borer*. b) Carbonyl-olefin cross-metathesis of benzaldehyde (**75**) and amylene (**76**) catalyzed by ZnCl<sub>2</sub> clay catalyst EPZ-10 by *Bickelhaupt*.

*Schmalz* and co-workers observed that during the methoxy deprotection of **82** with BF<sub>3</sub>·SMe<sub>2</sub>, the carbonyl-olefin metathesis product (**84**) was formed with considerable yield (Scheme 5a).<sup>60</sup> Based on these observations, BF<sub>3</sub>·OEt<sub>2</sub> was tested for its catalytic potential for carbonyl-olefin metathesis.<sup>61</sup> Syntheses of indene and 2-dihydronaphtalene were demonstrated from ortho alkenylated acetophenones, with up to 87 % yield for stoichiometric amounts of BF<sub>3</sub>·OEt<sub>2</sub>. The principle of a [2+2] cycloaddition/reversion initiated by BF<sub>3</sub>·OEt<sub>2</sub> was also observed by *Khripach et al.* for the rearrangement of steroid **85** to **86** in the presence of BF<sub>3</sub>·OEt<sub>2</sub> (Scheme 5b).<sup>62</sup>

a) Schmalz (2010)

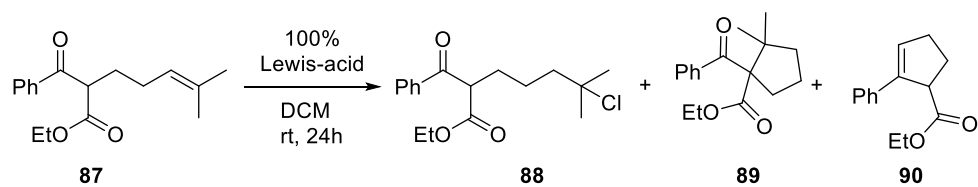


b) Khripach (2006)



Scheme 5 a) Methoxy deprotection of **82** with 1.7 eq  $\text{BF}_3 \cdot \text{SMe}_2$  with metathesis product **84** as a side product. b) Transannular carbonyl-olefin metathesis of **85** in the presence of  $\text{BF}_3 \cdot \text{OEt}_2$ .

After the pioneering work of *Franzen* and *Lambert*, a milestone of catalytic promoted carbonyl-olefin metathesis was realized by the *Schindler* group in 2016, with  $\text{FeCl}_3$  as a catalyst.<sup>49, 54, 63</sup>  $\text{FeCl}_3$  showed superior reactivity when tested on  $\beta$ -ketoester **87**, compared to similar Lewis acids used in stoichiometric amounts (Figure 8). From the other tested Lewis acids, only  $\text{SnCl}_4$  showed product (**90**) formation. Optimization of the reaction conditions showed 5 %  $\text{FeCl}_3$  in 1,2-dichloroethane at room temperature to be the most effective combination.

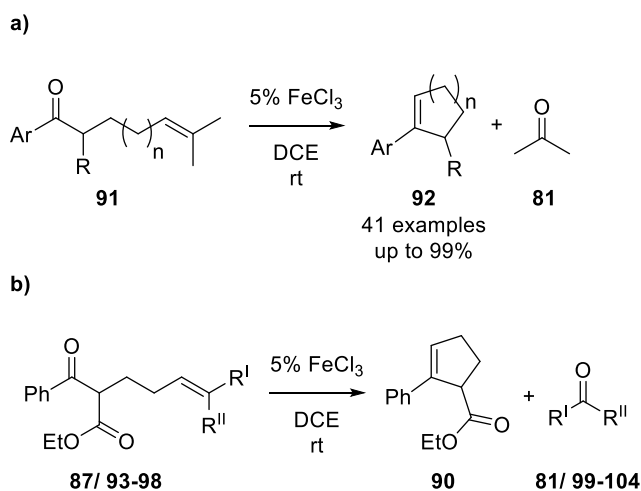


Lewis-acid	<b>88</b>	<b>89</b>	<b>90</b>
AlCl <sub>3</sub>	66%		
TiCl <sub>4</sub>		74%	
SnCl <sub>4</sub>		47%	24%
FeCl <sub>3</sub>			50%

Figure 8 Lewis acid screening for carbonyl-olefin metathesis of **87**.

The catalyst demonstrated a vast versatility with 41 examples, which had up to 99 % yield (Figure 9a). Cyclopentenes, as well as cyclohexenes, were synthesized with a high tolerance of functional groups. Screening for different olefin moieties revealed acetone (**81**) as the preferred leaving group (Figure 9b).





	R <sup>I</sup>	R <sup>II</sup>	90
<b>87/81</b>	Me	Me	99%
<b>93/99</b>	Ph	Me	49%
<b>94/100</b>	Ph	H	60%
<b>95/101</b>	H	Ph	49%

	R <sup>I</sup>	R <sup>II</sup>	90
<b>96/102</b>		H	60%
<b>97/103</b>		H	62%
<b>98/104</b>		H	70%

Figure 9 a) Optimized conditions for the intramolecular ring-closing carbonyl-olefin metathesis catalyzed by FeCl<sub>3</sub> b) Leaving group screening.

Initially, two possible mechanistic pathways were proposed: stepwise or asynchronous concerted (Figure 10a). Moreover, two mechanistic probes were designed to intercept a cationic intermediate (**106/ 109**). In the first set-up, equimolar amounts of alcohols were added, to form the respective ether (**111/ 112**) (Figure 10b). In the second set-up, the β-ketoester was reduced to a primary alcohol (**113**), which is then able to form an alternative oxetane via an intermediate benzylic cation (Figure 10c). Nevertheless, no cationic species were trapped and only the metathesis products (**90/ 114**) were received. Based on these findings, a detailed mechanistic study was carried out.<sup>64</sup> The first measurements revealed a first-order dependence of the reaction on the FeCl<sub>3</sub> concentration. EPR-spectroscopy showed that FeCl<sub>3</sub> interacts with the carbonyl group of the substrate throughout the reaction, without changing its oxidation state. In addition, an Eyring analysis was performed on **87**, **116** and **117** (Figure 10d).

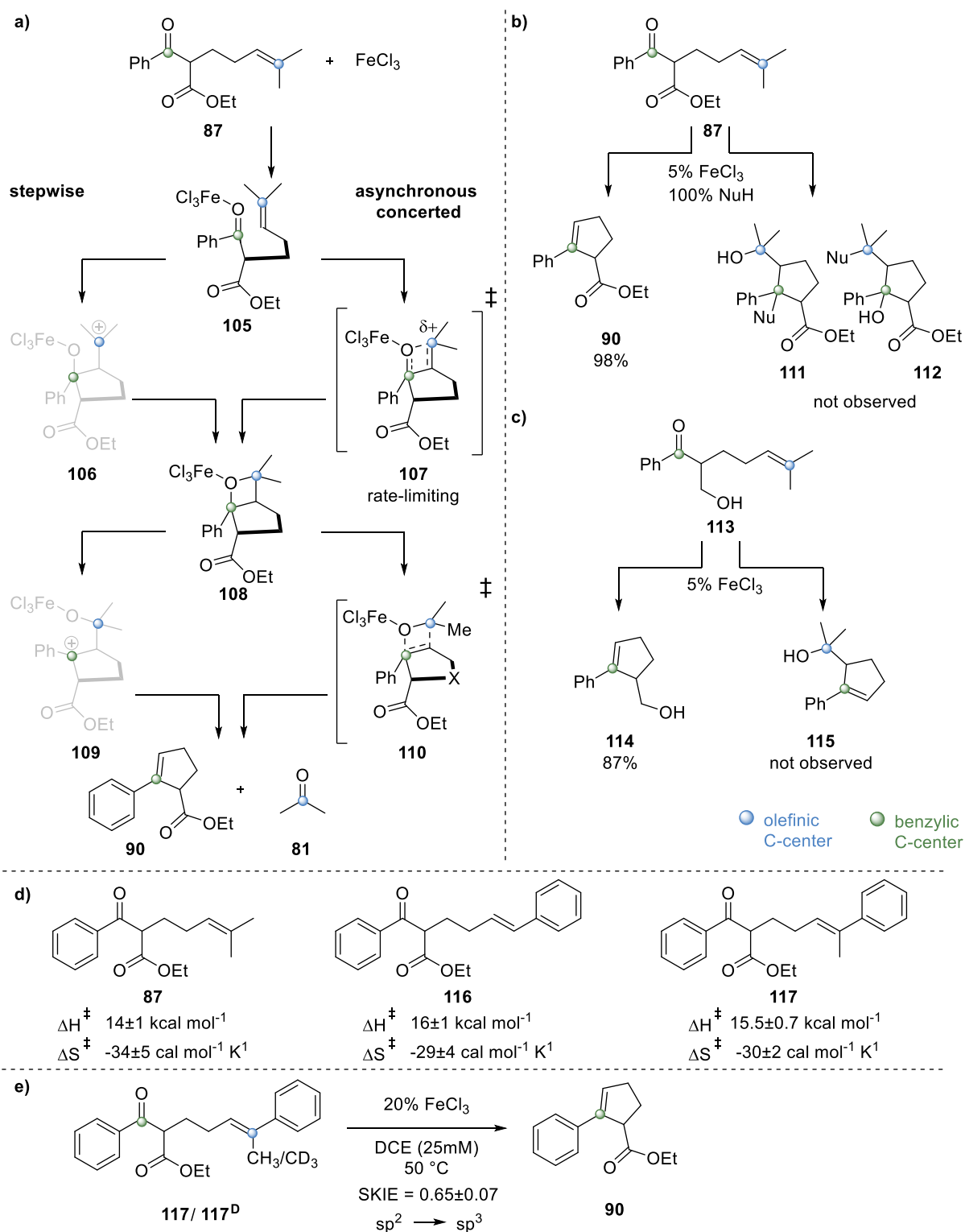


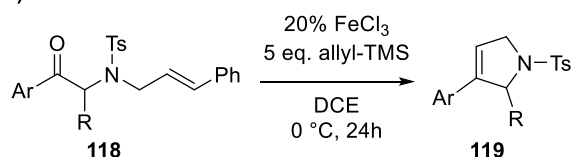
Figure 10 a) Mechanistic pathways for the intramolecular ring-closing carbonyl-olefin metathesis of **87**. b) Probe for cation **106** or **109** by addition of nucleophiles c) Intramolecular mechanistic probe for **109**. d) Eyring analysis of **87**, **116** and **117** e) Inverse SKIE for the reaction of **117/117<sup>D</sup>**.

The study by Ludwig *et al.* showed that all transition states in the rate-limiting step show a positive activation enthalpy and negative entropy of activation, which is indicative of an ordered transition state and therefore it is in accordance with the existence of an oxetane as intermediate. A kinetic isotope study with the substrates **117** and **117<sup>D</sup>** showed an inverse effect, which was interpreted as being due to the transition of an  $sp^2$  center to an  $sp^3$  center during the rate-limiting step (Figure 10e). Calculations by Ludwig *et al.* showed that the rate-limiting step consists of the asynchronous concerted oxetane formation over a partially charged transition state.<sup>64</sup> Through the asynchronous course of the [2+2] cycloaddition, the orbital symmetry is preserved during the transition state and therefore does not violate the *Woodward-Hoffmann* rules. Interestingly, calculations for the cycloreversion showed that it is dependent on the olefin moiety whether the mechanism is stepwise or asynchronous concerted.

In a similar reaction setup with a sulfonamide substrate **120** in the presence of allyltrimethylsilane and  $FeCl_3$  (20%), Li and co-workers isolated the side product **125**, stemming from the formation of a benzyl cation at the olefin moiety (**124**). This demonstrates stepwise oxetane formation as being an alternative pathway to the asynchronous concerted one observed for the  $FeCl_3$  catalyzed carbonyl-olefin metathesis (Figure 11).<sup>65</sup> The use of allyltrimethylsilane was necessary to scavenge the aldehyde side product as otherwise no catalytic turnover was observed.

Li (2016)

a)



b)

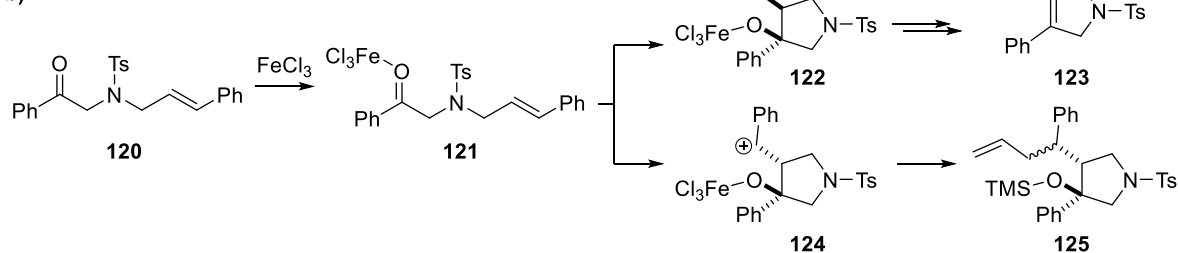


Figure 11 a) Conditions for the intramolecular ring-closing carbonyl-olefin metathesis towards 3-aryl-2,5 dihydropyrroles (**119**) by Li. b) Isolation of side product **125** from **109**.

*Schindler* and co-workers investigated a different approach, in which they suggest that the low catalytic turnover stems from the competitive binding of the catalyst by the sulfone (Figure 12b).<sup>66</sup> To reduce the binding affinity of the protection group, electron-withdrawing

substituents were installed. 4-trifluoromethylbenzenesulfonyl was identified as the most effective protecting group, thereby delivering the desired products in high yield. Interestingly alanine-derived substrates did not require electron-poor protection but readily reacted with *N*-tosyl protection. The authors theorized the presence of a *Thorpe-Ingold* like effect leading to a favorable formation of the substrate as a reason for this observation. The FeCl<sub>3</sub> catalyzed carbonyl-olefin metathesis proved to be stereo preserving and therefore suitable for the access of chiral products (Figure 12a). The substrates were derived from chiral amino acids via a three-step synthesis. Deprotection with SmI<sub>2</sub> and the installation of alternative protection groups like Boc or tosyl provided the desired product in up to 98 % yield. By optimizing the reaction conditions towards higher temperatures, tetrahydropyridines were accessible via FeCl<sub>3</sub> catalyzed carbonyl-olefin metathesis, which showed similarly good yields as obtained for 2,5-dihydropyrroles.<sup>67</sup>

Schindler (2018)

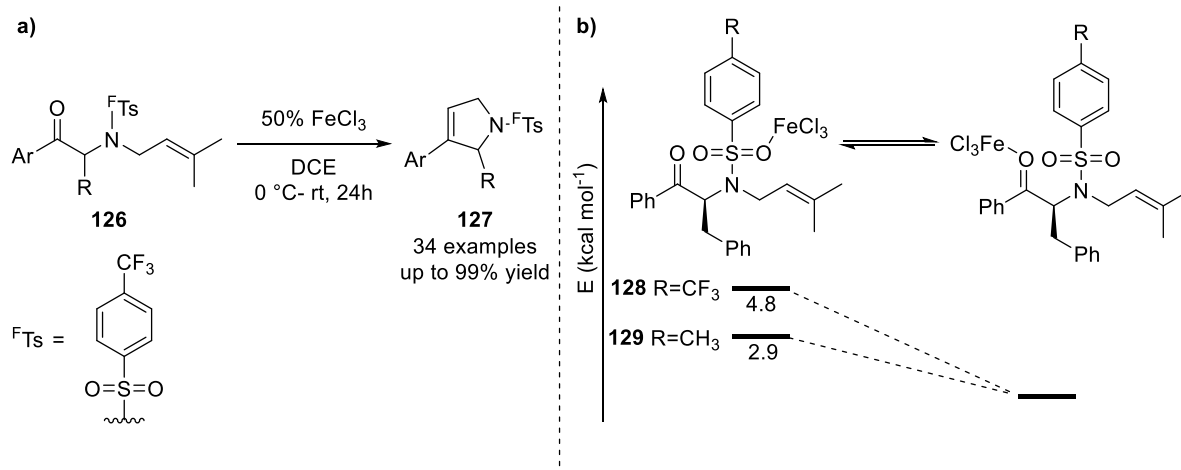


Figure 12 a) FeCl<sub>3</sub> catalyzed intramolecular ring-closing carbonyl-olefin metathesis by Schindler towards 3-aryl-2,5-dihydropyrroles. b) Equilibrium between the two coordinating sites of **128** and **129**.

FeCl<sub>3</sub> is a versatile catalyst that can be used for a broad variety of substrates to access cyclopentenes, cyclohexenes, 2,5-dihydropyrroles or tetrahydropyridines.<sup>63, 66-68</sup> All these substrates require an aryl ketone to provide substantial yield. Aliphatic ketones exhibit lower reactivity due to the diminished binding affinity of the aliphatic ketone towards FeCl<sub>3</sub> compared to aryl ketones.<sup>69</sup> This not only leads to a higher activation barrier for the reaction but also enhances the competitive binding with the formed by-product. Albright *et al.* investigated a variety of Lewis acids for aliphatic ketones.<sup>69</sup> Surprisingly, strong Lewis acids such as AlCl<sub>3</sub> did not provide the desired compound while weak Lewis acids like GaCl<sub>3</sub> or SnCl<sub>4</sub> were able

to catalyze the reaction, but only small amounts of product were isolated. FeCl<sub>3</sub> was shown to provide the best yield with a catalyst loading of 10 %. In order to further optimize the reaction, different solvents were tested where only 1,2-dichloroethane was found to be suitable. The optimized conditions were applied to a variety of substrates (**130**) and showed a good yield of up to 94 % for 41 examples (**131**) (Figure 13a). Nevertheless, the high dependency on the applied solvent and the catalyst load on the reaction prompted the authors to take a deeper look into these effects. The reaction order on the catalyst concentration of the classical aryl ketone substrates is of first order. The results from aliphatic ketones on the other hand showed a second-order dependency on FeCl<sub>3</sub> (**134**). Lewis acid monomers can form single bridged dimers, which display higher activity and fall under *Olahs* definition of superelectrophiles (Figure 13b).<sup>70</sup>

In order to investigate the formation of FeCl<sub>3</sub> dimers, an IR study was performed by *Albright et al.* on the shift of the carbonyl absorption frequency with one and two equivalents of FeCl<sub>3</sub> per substrate.<sup>69</sup> As expected, the carbonyl absorption band shifted upon the addition of one equivalent of FeCl<sub>3</sub>. With the addition of the second equivalent, another absorption band arose at a lower frequency, which indicates the formation of the FeCl<sub>3</sub> dimer.

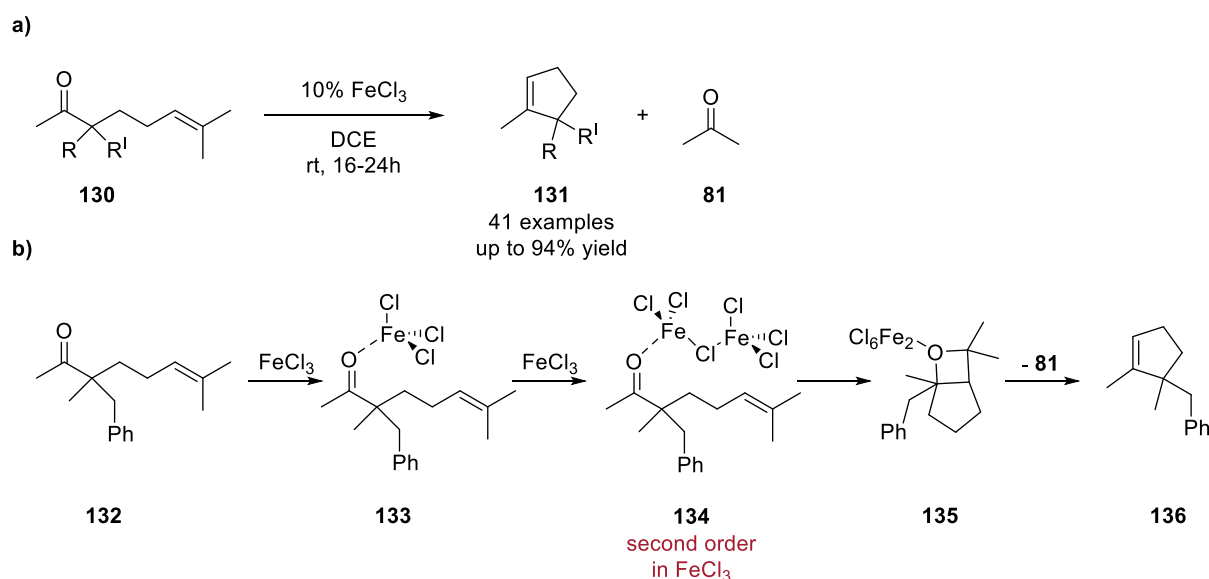


Figure 13 a) FeCl<sub>3</sub> catalyzed intramolecular ring-closing carbonyl-olefin metathesis by *Schindler* towards alkyl-ketones. b) Carbonyl activation via superelectrophilic FeCl<sub>3</sub>-dimer (**134**).

To further confirm their theory of a superelectrophile FeCl<sub>3</sub>-dimer, a heterodimer from FeCl<sub>3</sub> and FeBr<sub>3</sub> was applied to substrate **132**, since a stronger Lewis acid was expected to give a



### 2.1.2.2 Hydrazine catalyzed reactions

One of the earliest approaches used to realize catalytic carbonyl-olefin metathesis was the hydrazine catalyzed reaction developed by *Lambert*.<sup>54</sup> To circumvent the symmetry forbidden [2+2] cycloaddition of acid-catalyzed carbonyl-olefin metathesis, *Lambert* designed the catalyst to form an *in situ* azomethine imine which can react in a [3+2] cycloaddition with the olefin.

The catalyst design was based on symmetric alkyl hydrazines (**141**), which can react with aldehydes (**142**) toward azomethine imines (**143**).<sup>54</sup> The so formed 1,3 dipole (**143**) and the alkene (**144**) undergo a [3+2] cycloaddition (**145**) with subsequent cycloreversion (**146**, **147**) (Figure 15a). Cyclopropenes (**149**) were chosen as alkene sources due to their inherent ring strain. Catalyst screening showed, that the bicyclic hydrazine HCl (**150**) salt was most effective for this reaction. The optimization of the reaction conditions showed that 10 % catalyst loading was the most effective, along with elevated temperatures of 70 - 90 °C, in 1,2-dichloroethane. The catalytic system was demonstrated for 14 examples with up to 95 % yield and the *E*-isomer as the only product (Figure 15b). This approach proved to be limited to strained cyclopropenes and attempts with norbornene or stilbenes were not successful.

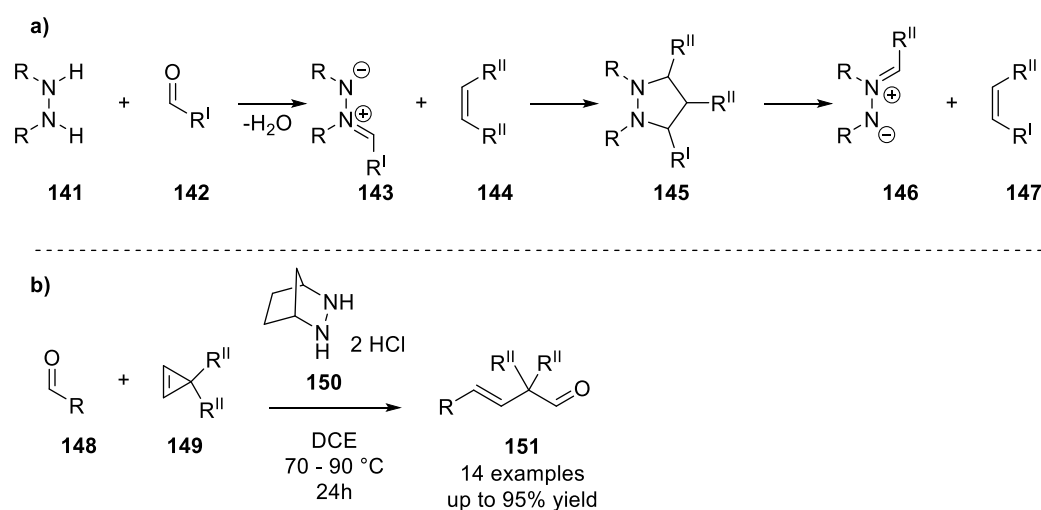


Figure 15 a) General reaction scheme for a [3+2] dipole cycloaddition b) Carbonyl-olefin cross-metathesis catalyzed by hydrazine catalyst **150**.

A detailed computational study was carried out regarding the overall mechanism and the influence of different types of olefins.<sup>71</sup> The general mechanism (Figure 16) was demonstrated by the ring-opening metathesis of cyclopropene (**153**) with benzaldehyde (**75**) and catalyst (**150**). The reaction was found to be initiated by the exergonic condensation of benzaldehyde (**75**) with the catalyst (**150**). Two isomers of the intermediate azomethine imine can be formed

**151** (*E*) and **152** (*Z*), while the *Z*-isomer (**152**) is thermodynamically more favored. Nevertheless, the reaction proceeds via the *E*-isomer (**156**), since in the subsequent cycloaddition of cyclopropene (**153**), the formed *E*-intermediate (**154**) is energetically favored over the *Z*-isomer (**155**). Proton transfer leads to the intermediate (**157**), which is ready to undergo [3+2] cycloreversion (**158**). The catalyst (**150**) and the product (**160**) were generated by the hydrolysis of **159**.



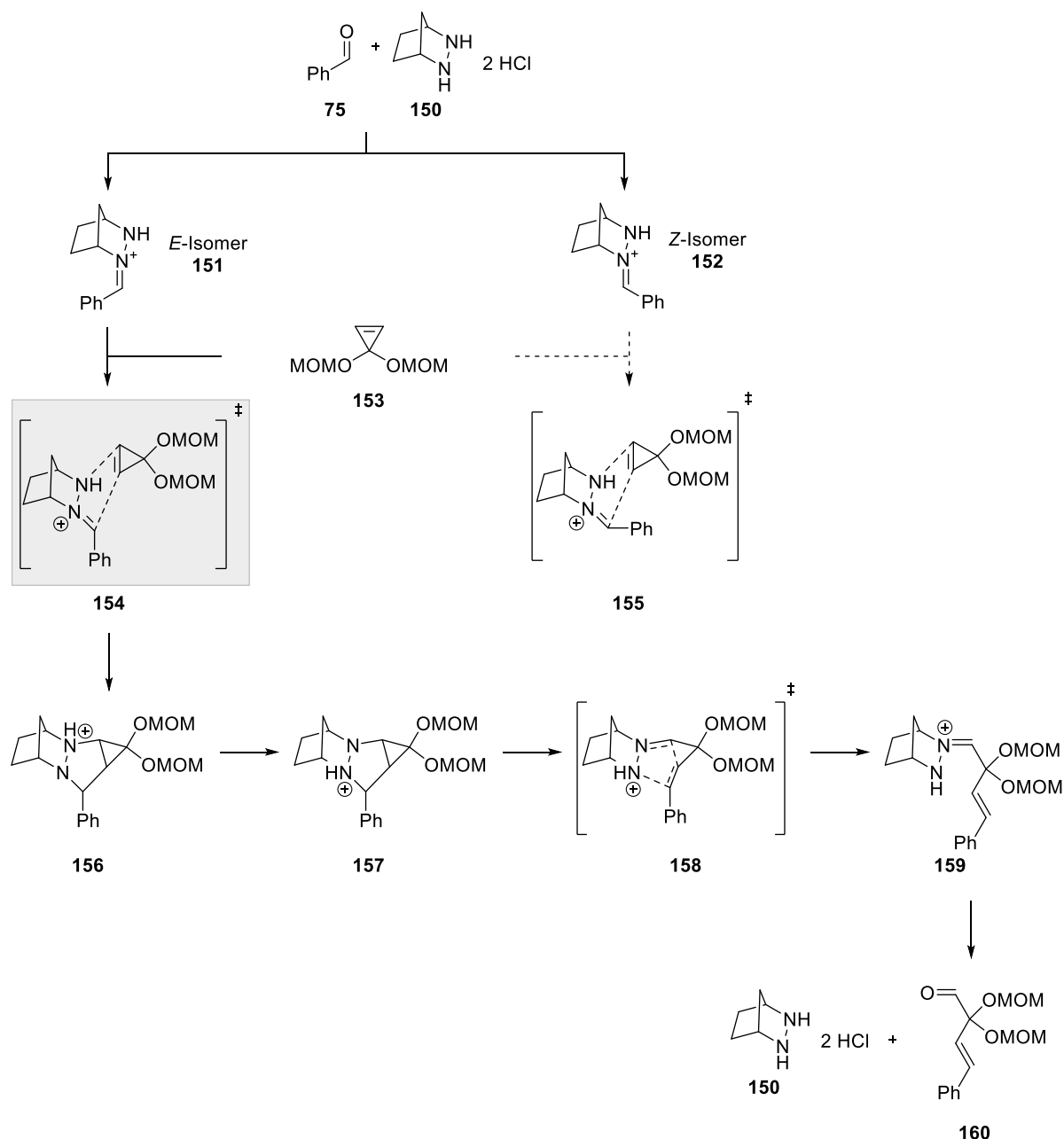


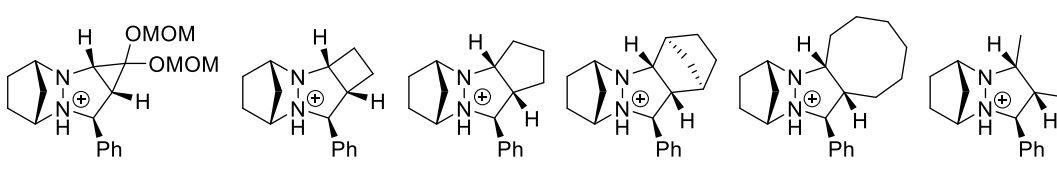
Figure 16 Intermediates and transition states of the [3+2] catalyzed carbonyl-olefin metathesis determined by DFT calculations.

The cycloaddition and reversion of the cyclopropene substrate were studied by *Hong et al.* in more detail, in order to understand whether the reactions rely exclusively on the high ring strain of cyclopropenes, or if other factors influence the reactivity of the substrate.<sup>71</sup> It can be suggested from the associated calculations, that for the cycloaddition, the release of strain from the double bond is not the most influential factor. It was instead found that the distortion energy of the bond angles of the double bond protons in the cycloaddition product was determining the

reaction barrier. This was so significant, that systems with low distortion energy like cyclopropene or pre-distorted systems like *trans*-cyclooctene, readily undergo cycloaddition.

Intermediate (**157**) had to undergo cycloreversion to release **159**. The driving force for this reaction is derived from the release of the ring strain of the intermediate cycloalkane.<sup>71</sup> Unstrained rings do not provide enough energy for the reaction to proceed, which leads to accumulation at the stage **161-165**.

Table 1 Ring strain for different ring sizes of the intermediate adducts.



The image shows six chemical structures of norbornene-based intermediates, labeled 157 through 165. Each structure features a bicyclic norbornene core with a protonated nitrogen atom (N-H<sup>+</sup>), a phenyl group (Ph), and a hydrogen atom (H) on the bridgehead carbons. The structures vary in the size of the ring fused to the norbornene system: 157 has a three-membered ring with two OMOM groups; 161 has a four-membered ring; 162 has a five-membered ring; 163 has a six-membered ring; 164 has a seven-membered ring; and 165 has an eight-membered ring.

	<b>157</b>	<b>161</b>	<b>162</b>	<b>163</b>	<b>164</b>	<b>165</b>
$\Delta E_{\text{strain}}$ [kcal mol <sup>-1</sup> ]	-28.1	-26.9	-7.2	-10.4	-10.0	0.0

The studies with hydrazine catalyst **150**, showed it to be compatible with a broad variety of benzaldehyde derivatives. The reaction scope in terms of the olefin was limited to cyclopropenes.<sup>54</sup> Based on the properties of the hydrazine catalyst a targeted design of the system was achieved in order to successfully enable the ring-opening metathesis of norbornene.<sup>55</sup>

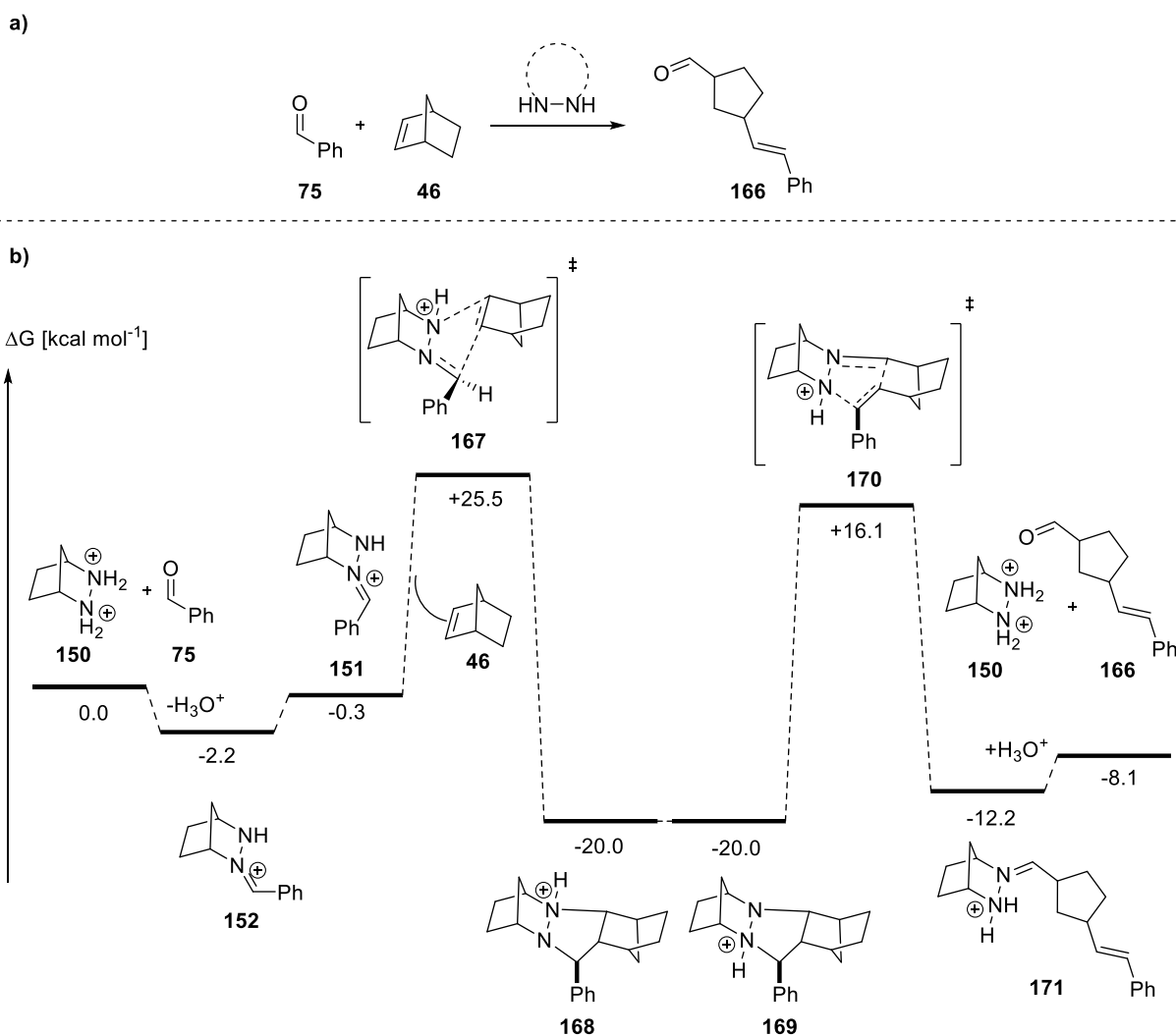


Figure 17 a) Ring-opening carbonyl-olefin metathesis of norbornene b) DFT-calculated reaction mechanism of the ring-opening carbonyl-olefin metathesis of norbornene and benzaldehyde catalyzed by **150**.

Based on the calculated mechanism (Figure 17) of catalyst **150** with norbornene (**46**) and benzaldehyde (**75**), the activation energies for different cyclic hydrazine catalysts were calculated (Figure 18).<sup>55</sup> The cycloreversion of **169** was identified as the biggest factor for catalyst optimization due to the high barrier of this step. The computational catalyst screening showed the lowest barrier to occur for the cycloreversion using catalyst **174**. An Eyring analysis of the intermediate **179** confirmed the calculated data (Figure 18).

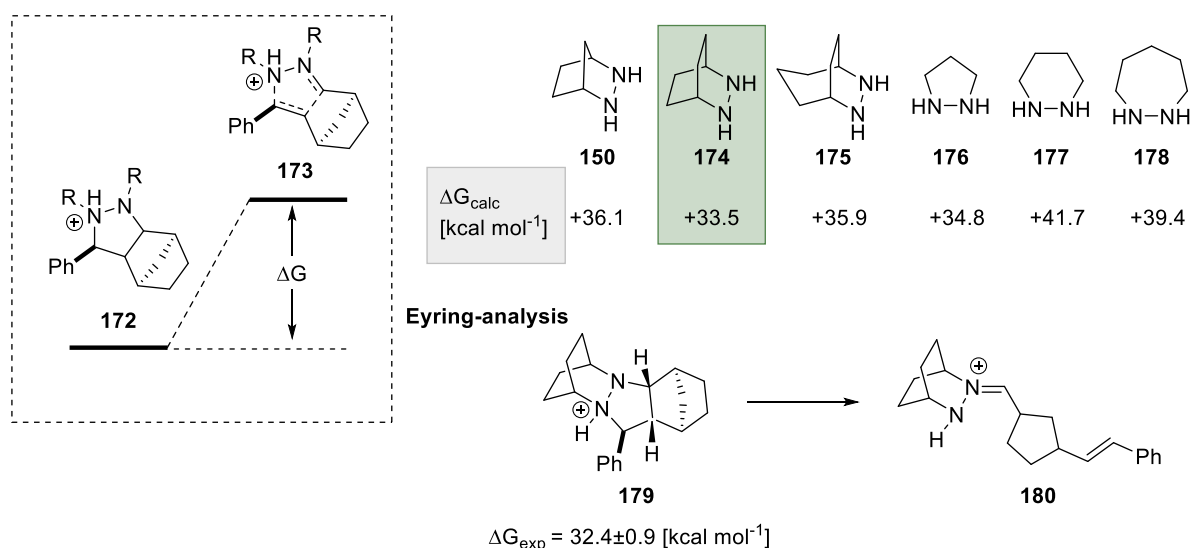


Figure 18 Activation energies for the cycloreversion of different hydrazine catalyst.

From the calculations by *Jermaks et al.*, it has been suggested, that the cycloreversion is favored by catalysts with higher nitrogen-bond angles. Through the transition of intermediate (**181**) with full  $sp^3$ -hybridization, towards the imine (**182**) with  $sp^2$ -hybridization, the bond angles change from  $109^\circ$  to  $120^\circ$  degrees (Figure 19). Systems with higher bond-angles, like intermediate (**179**) facilitate this transition and therefore lower the overall barrier of this step.

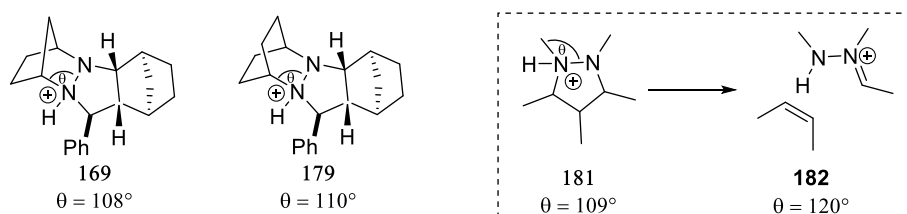


Figure 19 Bond angles for catalyst/ norbornene adduct **169** and **179**.

The achieved isolation of **184** indicates, that the reaction reaches a steady state on this step. Further catalysis with  $\text{Sc}(\text{OTf})_3$  showed, that **184** can be transformed to acetal **185** in the presence of ethylene glycol (Figure 20a).<sup>55</sup> Hydrolysis of **186** proved to be an unexpected bottleneck of the reaction. Cycloaddition of a second equivalent of norbornene to the ring-opened intermediate (**186**) was observed, leading to diminished yield and inactivation of the catalyst. In order to destabilize intermediate **186** by the introduction of additional strain, norbornene (**46**) was replaced with methylnorbornene (**188**). Destabilization proved to be effective and the product (**189**) was obtained with 70 % yield (Figure 20c).

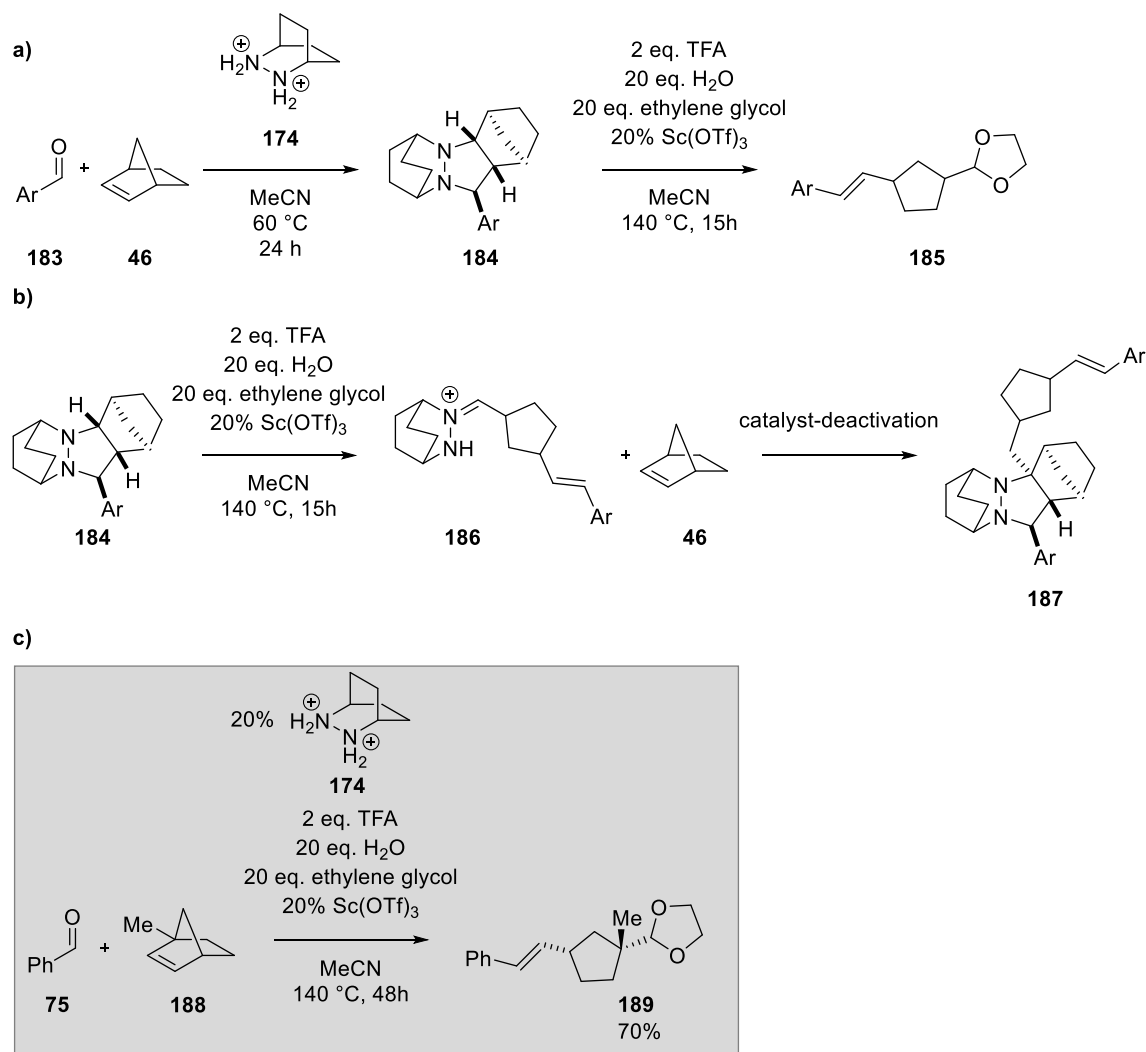


Figure 20 a) Formation of the stable intermediate **184** with subsequent cycloreversion in presence of  $\text{Sc}(\text{OTf})_3$ . b) Catalyst deactivation by the addition of norbornene (**46**) to intermediate **186**. c) One-pot conditions of carbonyl-olefin cross-metathesis of benzaldehyde (**75**) and methyl norbornene (**186**).

In 2019 the principle of [3+2] cycloaddition/ reversion was successfully applied to ring-closing carbonyl-olefin metathesis for the synthesis of 2H-chromenes.<sup>72</sup> The tested reaction used salicylaldehyde allylic ethers as feedstock and was demonstrated in 21 examples with up to 90 % yield. In addition, ketones were proved to be inferior to aldehyde substrates, with only traces of the desired product obtained due to the additional strain. Diethylallyl showed the best performance as the leaving group. A similar approach was successful for the synthesis of 1,2-dihydroquinolines. The authors mentioned, that due to the donating effect of the nitrogen, the cycloreversion step was facilitated, which enabled the use of commercially available prenyl groups instead of diethylallyl.<sup>73</sup>

### 2.1.2.3 Carbocation catalyzed reactions

Based on the work of *Bickelhaupt*, *Franzen* and co-workers envisioned tritylium tetrafluoroborate (TrBF<sub>4</sub>) to be a suitable Lewis acid to catalyze intermolecular carbonyl-olefin cross-metathesis (Figure 21).<sup>49, 59</sup> This marked the first attempts towards an organocatalyzed carbonyl-olefin metathesis via a [2+2] cycloaddition.

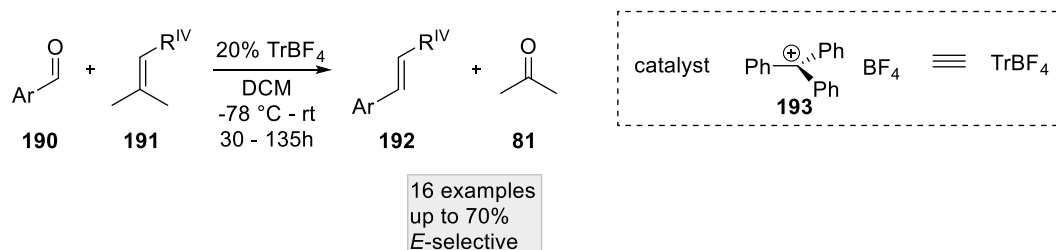


Figure 21 Tritylium catalyzed carbonyl-olefin cross-metathesis.

Starting from the conditions of *Bickelhaupt*, amylene (**76**) and benzaldehyde (**75**) were converted in the presence of 7 % TrBF<sub>4</sub>. These initial reaction conditions provided the desired product only with a 20 % yield despite a high conversion of 77 %. Optimization of the reaction conditions by varying the substrate ratio and the catalyst loading, showed a catalyst load of 20 % at -78 °C over the course of 4 days with benzaldehyde (**75**) in excess, to be the most effective. Low temperatures reduced polymer formation as a major side reaction. Interestingly, tracking of the reaction components showed that amylene (**76**) was consumed within the first 3h, even though at this time the product formation only reached 40 %. Over a period of 30 h, the product yield grew to 68 %. <sup>1</sup>H-NMR analysis showed the formation of unidentified intermediates within the first hours which were consumed in parallel to the formation of the product.

Solvent optimization showed, that coordinating solvents like acetonitrile or ethers tend to block the Lewis-acidic site of TrBF<sub>4</sub> and shut down the reaction. Benzaldehydes with weak electron donating substituents showed the best yield (55-85 %), whereas strong donating substituents led to product decomposition. Other tertiary olefins showed reduced reactivity and needed adjustments regarding the reaction condition, while tetrasubstituted olefins proved to be unreactive. Aliphatic aldehydes were observed to decompose under the given reaction conditions and only amylene was recovered. The reaction was demonstrated on 16 examples with up to 70 % yield where the *E*-isomer was the exclusive product.

Based on the proposed mechanism by *Bickelhaupt* two assumptions were made regarding the TrBF<sub>4</sub> catalyzed carbonyl-olefin metathesis. In general, the reaction is initiated with the

activation of the carbonyl (**194**) followed by a successive attack of the olefin (**191**) which is comparable to a *Prins* reaction. Two possible mechanisms (A and B) can proceed from **194**.

For mechanism A (Figure 22), the tertiary carbocation (**195**) reacts with the former carbonyl oxygen and an oxetane (**196**) is formed. Under stepwise cycloreversion first, a benzylic cation (**197**) is formed and under the elimination of **198**, a new double bond is obtained (**192**). In mechanism B (Figure 22), the tertiary carbocation (**195**) is attacked by a second equivalent of benzaldehyde (**75**) and intermediate **199** is formed. The benzylic-position of the charged moiety is attacked by the triphenylether and a six-membered intermediate (**200**) is formed. Cycloreversion of **200** releases acetone (**81**), the desired product (**192**) and the activated carbonyl species (**194**).

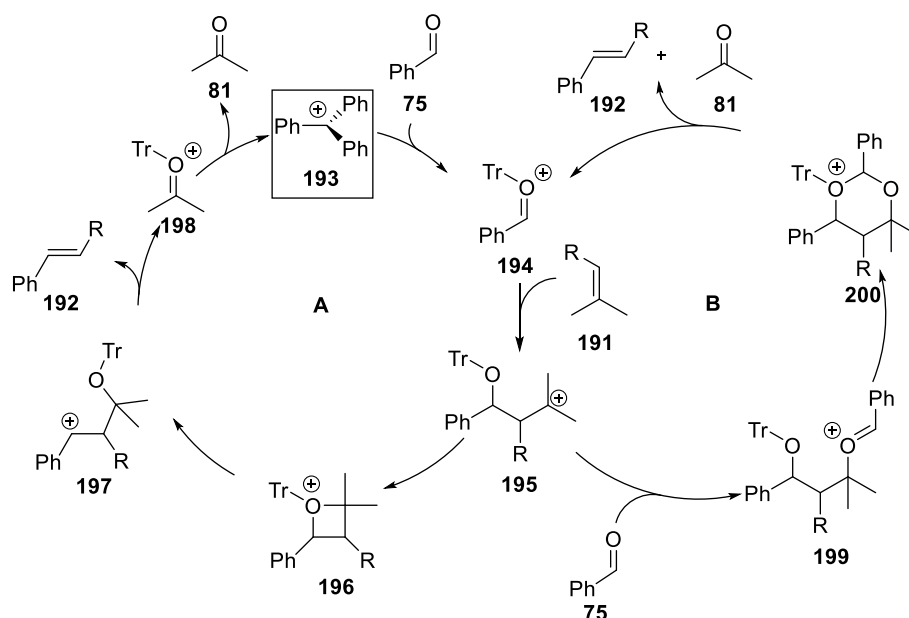


Figure 22 Mechanistic proposals for tritylium catalyzed carbonyl-olefin cross-metathesis.

Ring-closing metathesis was achieved with enals (**201**) in DCM at room temperature using catalyst **206** (Figure 23).<sup>74</sup> Investigation of the leaving group showed *ortho* tolylaldehyde (**203**) to be superior compared to unsubstituted benzaldehyde (**75**). Investigation of R<sup>I</sup> (Figure 23) showed that methyl substitution at the 3-position accelerated the reaction, most likely through a *Thorpe-Ingold* effect. Methoxy substitution at the 5-position showed the same effect. Electron donating substituents at the 4-position had a negative effect on the yield by enhanced product decomposition. Substitution at the R<sup>II</sup> (Figure 23) position was beneficial for the reaction and allowed a reduction of the catalyst load down to 2 %.

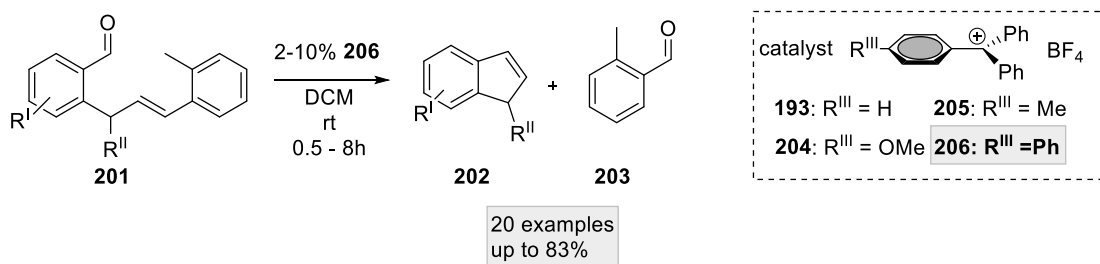


Figure 23 Intermolecular ring-closing metathesis catalyzed **206**.

The tropylium ion is another easily accessible and stable carbocation that can act as a Lewis acid. The electrophilicity of the tropylium ion is of similar magnitude to the methoxy substituted trityl cation according to the *Mayr* nucleophilicity/ electrophilicity chart.<sup>75-80</sup> The success of the *Franzen* group with trityl derived catalysts for carbonyl-olefin metathesis reactions, inspired *Nguyen* and co-workers to investigate tropylium ions as catalyst.<sup>50</sup>

The *Nguyen* group started their investigation of the catalytic capability of tropylium tetrafluoroborate (**207**) for the intramolecular carbonyl-olefin metathesis of ketone **208**. Optimization of the reaction revealed neat conditions at 90 °C for 24h with 15 % catalyst loading to be the best conditions for **210**. Under these conditions, good yields were achieved for the intramolecular cyclization (Figure 24). Double bond rearrangement was observed for substrates with a methyl-substituent in the  $\alpha$ -position of the ketone, whereas carboxy-, or aryl substituents resulted in the regular carbonyl-olefin metathesis product. Biphenyl substrates led to the carbonyl-ene product as the major species (**214/ 215**).



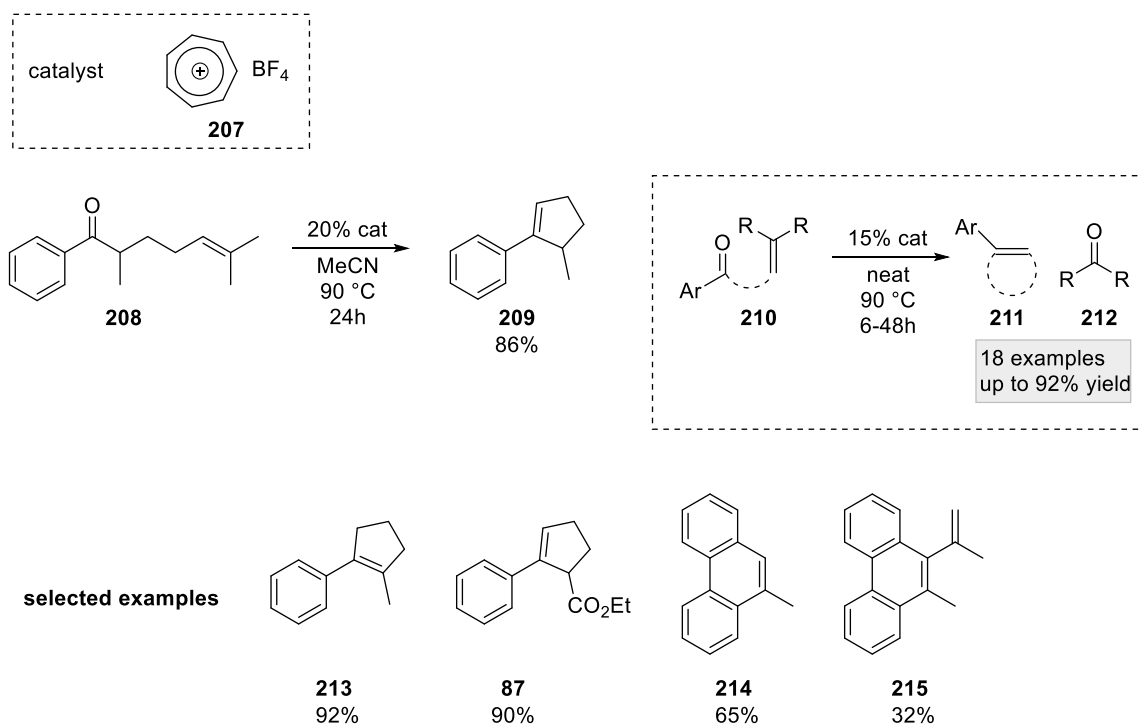


Figure 24 Intramolecular carbonyl-olefin metathesis catalyzed by tropylium ion.

Intermolecular cross-metathesis was tested on aldehyde (**216**) and amylene (**76**) in acetonitrile at 90 °C and provided the desired product in 14 % yield. Based on these initial results, reaction conditions were optimized with DCM at 80 °C in the microwave, which led to a yield of 52 % after 0.5h (Figure 25). These conditions were applied to a variety of olefins but proved to be unproductive for ketone substrates or heteroatomic aldehydes. A general problem of these types of reactions is the tendency of the olefinic compound (**219**) to polymerize under such conditions, thereby lowering the achievable yield.

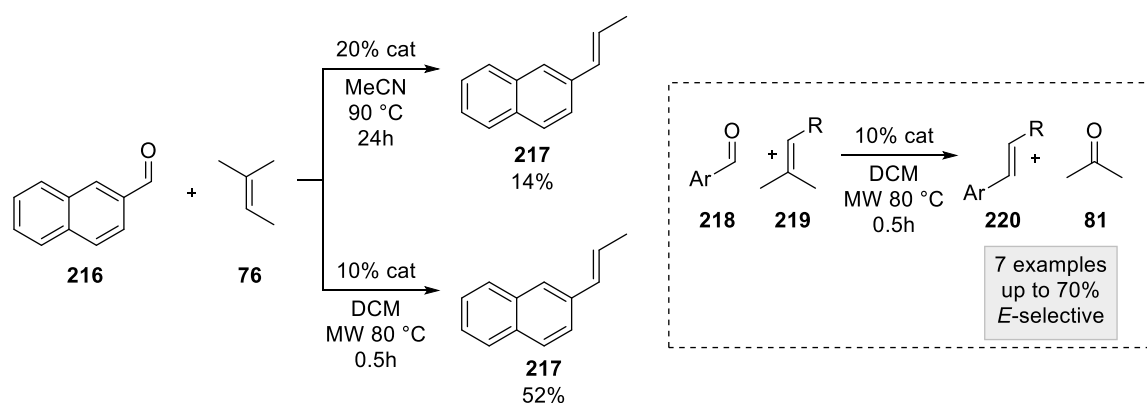


Figure 25 Tropylium catalyzed cross-metathesis.

One of the first examples of ring-opening metathesis based on [2+2] cycloaddition/ reversion was achieved with the tropylium catalyst (Figure 26a). Benzaldehyde and *para*-

methylbenzaldehyde showed good reactivity towards cyclobutene and cyclopentene. Larger rings did not show reactivity, most probably due to the reduced ring strain of such systems. A methyl substituent at the olefinic double bond proved to be important to initiate the reaction, as only methyl-cyclopentene (**236**) showed reactivity compared to aryl (**227**) or unsubstituted cyclopentene (**228**), which did not react. The use of cyclobutene (**235**) and especially cyclopropene (**234**) led to problems regarding the volatility of the starting material. Addressing this problem by performing the reaction under pressurized conditions did not improve the reaction and only led to oligomerization. Sterically more demanding substituents on the substrate (**226**) were found to be incompatible with the reaction (Figure 26b).

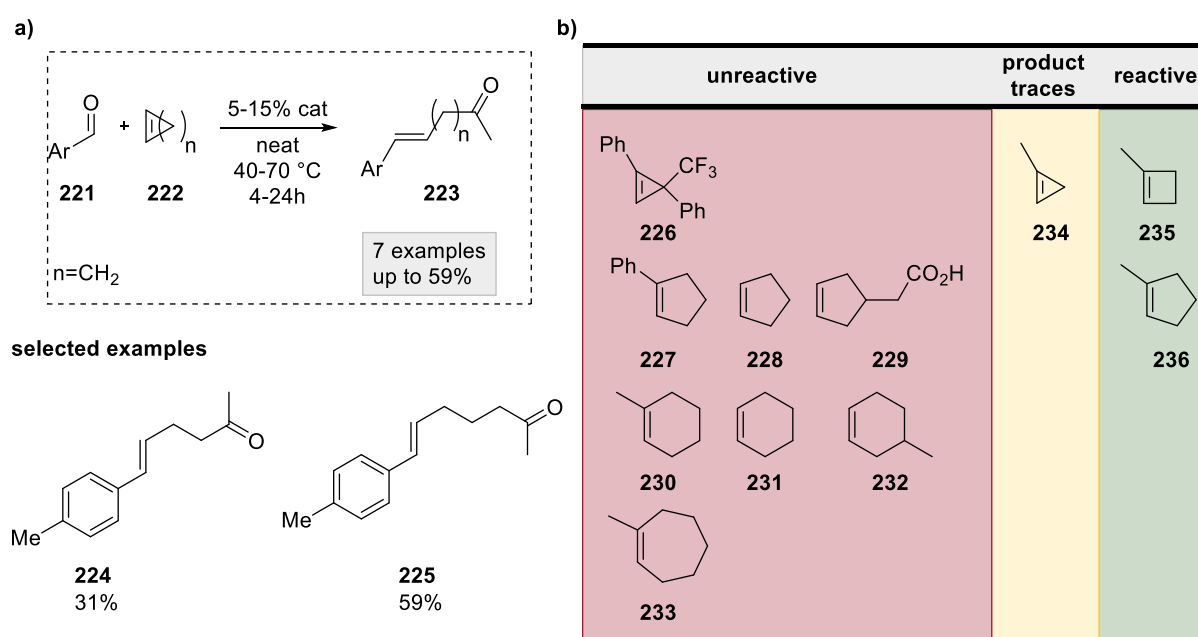


Figure 26 a) Optimized conditions for ring-opening carbonyl-olefin metathesis with tropylium catalyst. b) Screening for cyclic alkenes: (red) unreactive substrates, (yellow) only product traces were isolated, and (green) suitable alkenes for ring-opening.

DFT calculations for the carbonyl-olefin cross-metathesis of amylenes and benzaldehyde provided insight into the character of the mechanism since both, an asynchronous concerted and a stepwise mechanism were plausible. The calculation showed a significant reduction of the activation energy necessary for the oxetane formation and opening in the presence of the tropylium catalyst (**207**) and therefore the reaction was found to proceed via cationic intermediates. This is similar to mechanism A (Figure 22) proposed by *Franzen* for the trityl catalyzed intermolecular cross-metathesis, which proceeds via a *Prins* like activation with subsequent oxetane formation.

#### 2.1.2.4 Iodonium catalyzed reactions

Based on studies of the activation of oxygen-containing compounds, *Nguyen* and co-workers envisioned  $I_2$  to be a suitable activator for the carbonyl group in carbonyl-olefin metathesis.<sup>52, 81</sup> Iodine a simple, cheap and easy to handle substance in comparison to other carbonyl-olefin metathesis catalysts. Initial reactions at 50 °C showed good results where carbonyl-olefin metathesis products **90** and **237** were produced with a 62 % yield (Figure 27). Optimization of the reaction showed that solvent-free conditions at room temperature were the most effective and provided a yield of 93 % (**90** +**237**) for the cyclization of **87**. A broad scope of substrates for intramolecular carbonyl-olefin metathesis was tested using the optimized conditions, in addition to some examples of intermolecular cross-metathesis and ring-opening metathesis, which highlighted the versatility of this catalytic system. For intramolecular ring-closing metathesis, 27 substrates were tested and achieved up to a 96 % yield (Figure 28a). Comparable to the studies with  $FeCl_3$ , double bond isomerization was observed, most likely due to the formation of HI in the presence of moisture. Two tests were additionally performed on a gram scale, which demonstrated the scalability of this reaction.

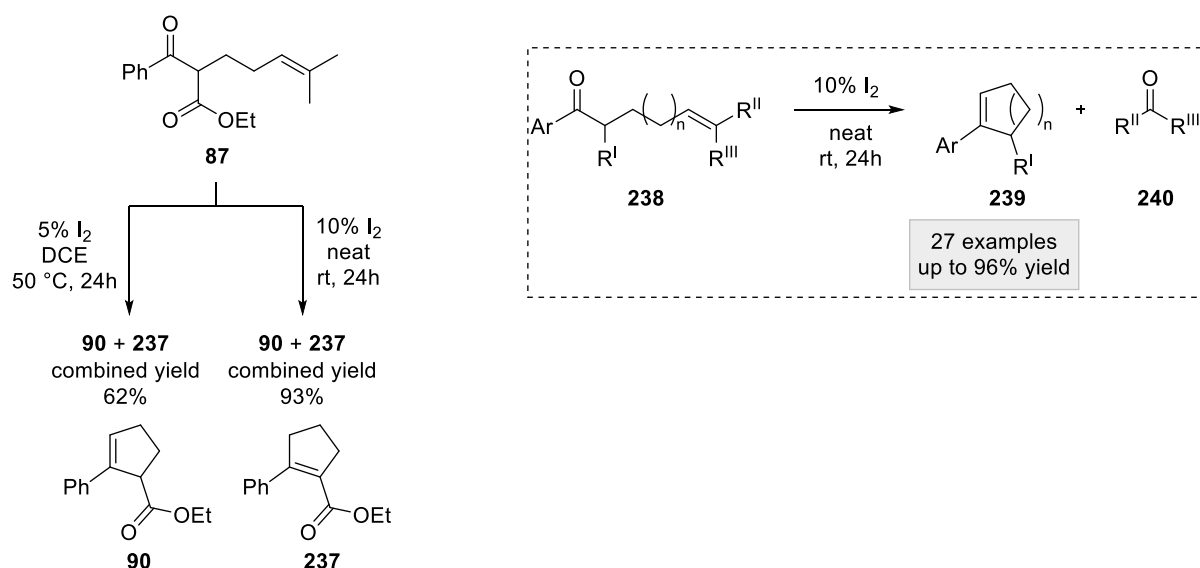


Figure 27 Conditions for the  $I_2$  catalyzed ring-closing carbonyl-olefin-metathesis.

Interestingly, when substrate **241**, with  $n=1$ , was applied to the reaction, a *6-endo trig* cyclization was observed. However, the synthesis of cyclohexenes from **241**  $n=3$  was not achieved (Figure 28). From DFT calculations it has been suggested, that a complete stepwise mechanism for the oxetane formation and opening occurs.

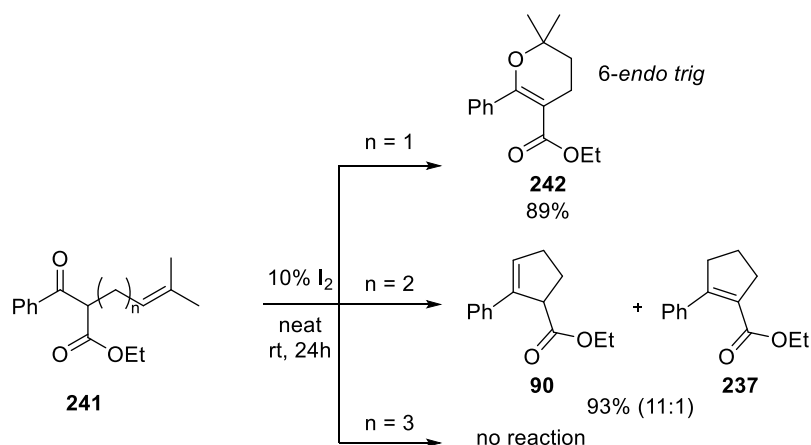


Figure 28 Carbonyl-olefin metathesis with different chain lengths.

Four catalytic active species were proposed for the  $I_2$  catalyzed carbonyl-olefin metathesis:

1. Formation of Brønsted acid
2. Formation of radicals
3. Halogen bonding
4. Iodonium-ions

When the reaction was performed with HI or KI, no conversion was observed, which was a clear indication, that neither  $H^+$  nor  $I^-$  were catalytic active species. In order to test the formation of radicals in the reaction, the experiment with  $I_2$  was conducted once under the exclusion of light and in a second experiment with butylated hydroxytoluene (BHT) as a radical scavenger. When the reactions were carried out under air, both experiments ran to 100 % conversion, which indicates that no radicals participate in the reaction. Interestingly, under an  $N_2$ -atmosphere, both experiments showed a significantly reduced yield. Since oxygen seemed to play an important role in the reaction, it was repeated with an oxidative environment by adding either *m*-CPBA or  $H_2O_2$ . However, both approaches failed and did not lead to the conversion of the starting material. When halogen-bond donors like pentafluorophenyl iodide or triphenylphosphine diiodide were tested, no reaction was observed which excludes halogen-bonding as a promotor. To test if the reaction could be catalyzed by iodonium-ions, *N*-iodosuccinimide (NIS) and iodine monochloride (ICl) were tested as iodonium sources. In both cases, full conversion was achieved after 72 h. To test if this reactivity stemmed from the iodonium-ion, the experiment was conducted with the addition of DMSO, which is known as a good iodonium-binding solvent, or with KI. In this case, the reactivity was stopped, demonstrating that iodonium ions are the catalytic active species. In a follow-up study, the

authors were able to demonstrate that NIS and ICl are suitable catalysts for carbonyl-olefin metathesis.<sup>82</sup>

### 2.1.2.5 Supramolecular Catalysis

The resorcinarene hexamer **I** was first reported by *Atwood* and *MacGillivray* in a crystal structure of **238**.<sup>83</sup> The reported structure had eight water molecules incorporated and formed a hydrogen-bonding network consisting of 60 hydrogen bonds, with a cavity of 1400 Å<sup>3</sup> (Figure 29). In works by *Rebek* and *Cohen*, the solution hexamer-formation of **239** was shown in apolar solvents.<sup>84, 85</sup> Important for the formation of the hexamer **II** are long aliphatic chains which enhance the lipophilicity and therefore solubility of the system. The incorporation of water into the hydrogen bonding network of the hexamer in the solution was demonstrated in DOSY-NMR studies.<sup>86, 87</sup> The dependence of the diffusion coefficient of the assembly on the water concentration was measured, which revealed that also in solution eight equivalents of water are part of the assembly.<sup>86, 87</sup> Guest uptake studies showed that hexamer **II** is capable of encapsulating tetraalkylammonium or tetralkylphosphonium salts via a cation- $\pi$  interaction.<sup>88</sup> The uptake and the release of the guest proceed most likely occur via one resorcinarene subunit detaching from the hexamer, thereby leaving a portal for molecules to enter and exit the cavity.<sup>88</sup>

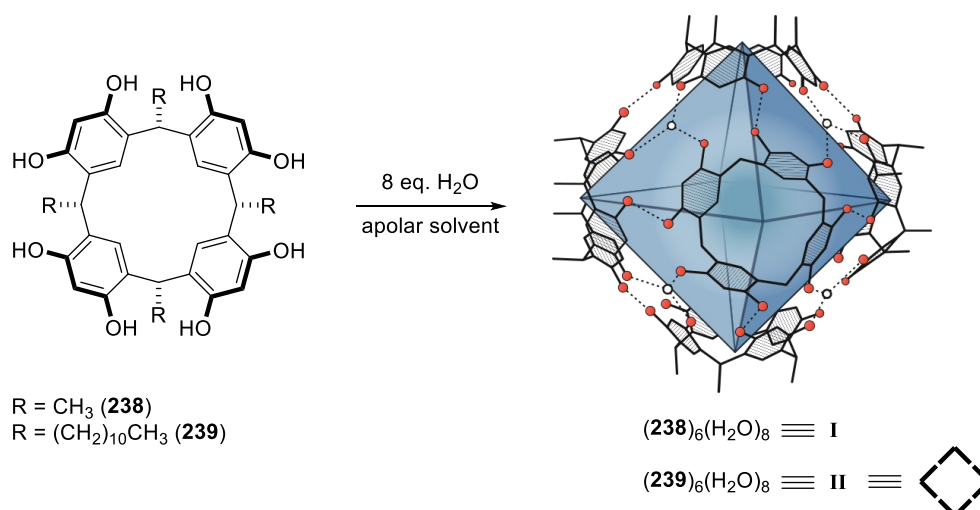


Figure 29 Formation of the resorcinarene hexamer **I** and **II** in apolar solvents.

The cation-stabilizing properties and the dynamic guest exchange of the cavity make the resorcinarene hexamer attractive for catalytic applications. This was first demonstrated by *Scarso* and *Reek*, who showed the capability to change the reaction outcome of gold-catalyzed hydration of alkyne **240**.<sup>89</sup> Under standard conditions the *Markovnikov* product (**241**) is formed as the main product. In the presence of the hexamer **II**, the anti-*Markovnikov* product (**243**) was formed as well as the intramolecular cyclization product (**242**). The authors suspected the catalyst is encapsulated by **II** along with alkyne **240**, which leads to an unusual folding of **240**,

thereby promoting the intramolecular rearrangement respectively the anti-*Markovnikov* product (Figure 30).

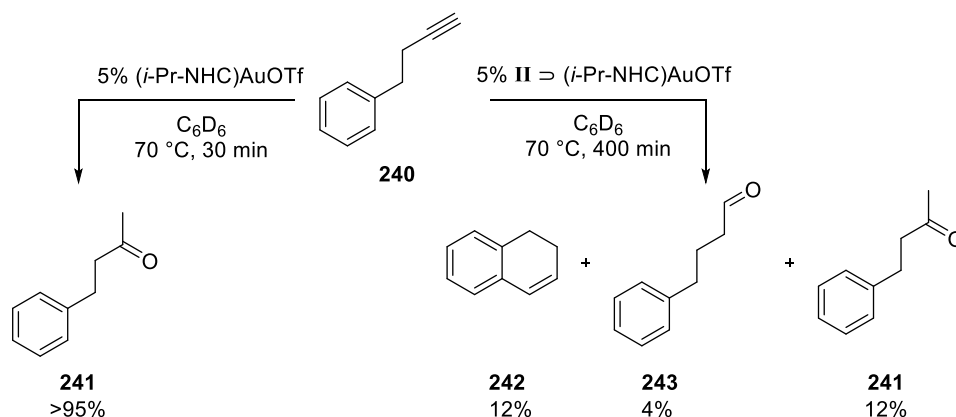


Figure 30 Product distribution of the gold-catalyzed alkyne hydration with and without **II**.

*Tiefenbacher* and co-workers showed via an NMR study, that hexamer **II** provides a weak acidic environment with a  $pK_A$  of 5-6.<sup>90</sup> In following studies they reported the capability of the hexamer (**II**) in combination with HCl as a cocatalyst, to function as a supramolecular catalyst for a broad range of reactions.<sup>91, 92</sup> In their work from 2015 *Tiefenbacher* and *Zhang* were able to perform tail-to-head (THT) cyclizations of monoterpenes under mild conditions in the presence of catalytic amounts of hexamer **II** and in the presence of HCl as co-catalyst.<sup>93</sup> In bulk solution the activation of monoterpene alcohols requires strong Brønstedt or Lewis acids, which leads to undesirable side product formation. In nature, terpene cyclases activate phosphorylated alcohols via metal centers.<sup>94</sup> Moreover, the intermediary carbo-cations are stabilized in the active pocket of the enzyme by cation- $\pi$ -interactions or cation-dipole interactions, through amino acid sidechains such as phenylalanine, tyrosine, or tryptophan. Hexamer **II** provides unique properties which can be used to mimic terpene cyclases. The cation- $\pi$  interactions from the capsule walls facilitate the formation and stabilization of carbo-cations. Treatment of nerol (**246**) in the presence of 10 % **II** with 3 % HCl leads to the formation of eucalyptol (**255**) with a 39 % yield. By tracking the reaction course via gas chromatography, the formation of reaction intermediates could be studied. For geraniol (**244**), the formation of linalool (**253**) was observed in the first 10 hours, which is in agreement with the formation of an allylic cation quenched by water. Besides linalool (**253**),  $\alpha$ -terpinene (**257**) and  $\alpha$ -terpinol (**254**) were formed in the initial phase of the reaction. Over the course of the reaction, these initial products decreased in concentration in favor of eucalyptol (**255**). The formation of linalool (**253**) as an intermediate was in agreement with the common theory for the isomerization of the former *cis*-double (**252**) bond to the *trans*-configuration (**253**), which is necessary for the subsequent cyclization. The

reaction profile of nerol (**246**) differed from that of geraniol (**244**), with  $\alpha$ -terpineol (**254**) being the major initial product, which was then converted to eucalyptol (**255**). The reaction with nerol (**246**) provided a cleaner reaction with fewer side products as compared to geraniol (**244**). In order to prevent the interception of the cationic intermediates, acetate was introduced as a less nucleophilic leaving group compared to water. Geranyl acetate (**245**) displayed completely different reaction profiles than its corresponding alcohol. For **245** no formation of linalyl acetate was observed in the reaction profile, instead,  $\alpha$ -terpinene (**257**) was selectively formed. This observation highlighted, that the *transoid* cationic intermediate (**247**) was transformed into the *cisoid* intermediate (**248**) with the subsequent formation of a terpinene cation (**249**). The terpene cation underwent a 1,2 hydride shift to form  $\alpha$ -terpinene (**257**), which demonstrated that a non-stop terpene cyclization inside the resorcinarene capsule occurred (Figure 31).

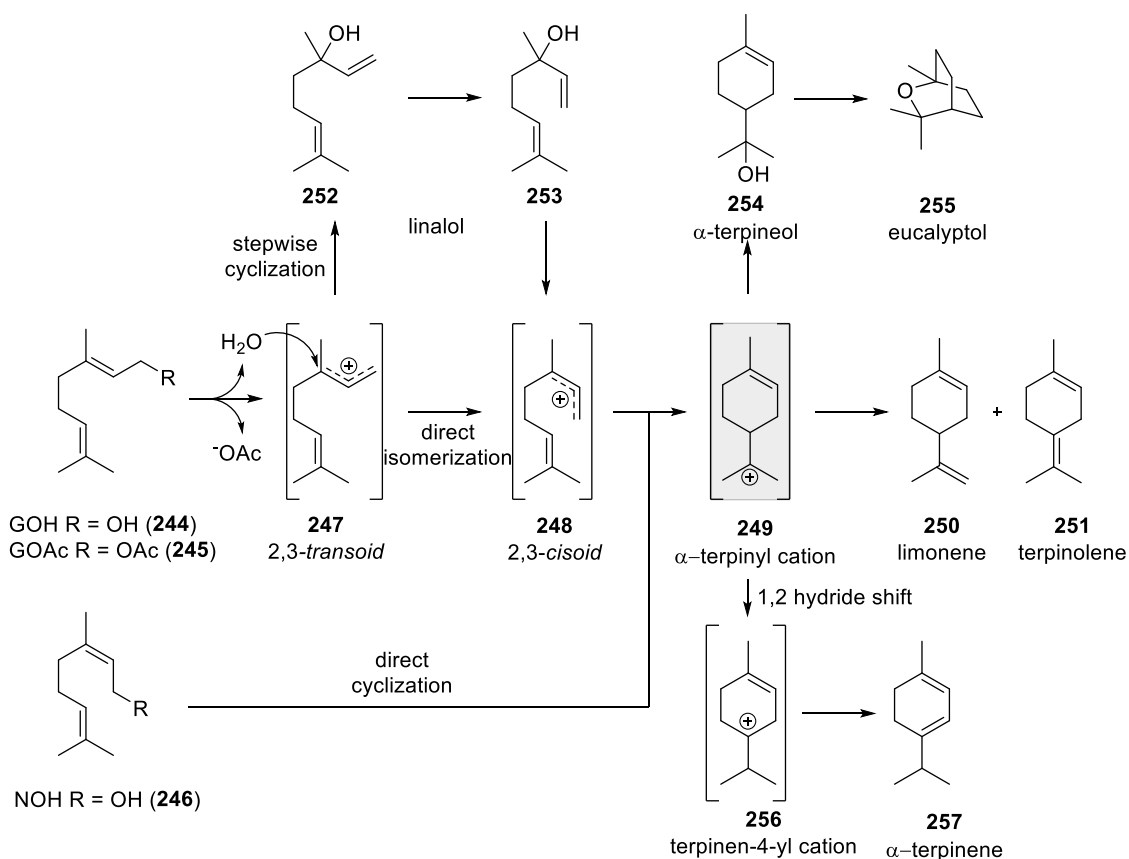


Figure 31 Mechanism for the tail-to-head terpene cyclization catalyzed by HCl/ **II**.

An Eyring analysis of the geranyl acetate (**245**) cyclization showed, that the rate-limiting step features a positive entropy of activation. Therefore, a more disordered transition state is formed, which is only the possible case for two steps in the reaction cascade: release of solvent through substrate encapsulation (Figure 32a) or cleavage of the acetate-leaving group (Figure 32b). In order to test, which of both steps is rate-limiting, two deuteriums were introduced at the 1-



position of **245**. In the case of a rate-limiting encapsulation, the isotopic labeling should not induce any change in the reaction rate. For the release of the leaving group, the former  $sp^3$  center transforms into an  $sp^2$  center, which is expected to show a positive secondary kinetic isotope effect (SKIE). The measured SKIE of 1.22 is in agreement with the release of the leaving group, being the rate-limiting step.<sup>93</sup> The principle of terpene cyclization was expanded to various terpene cyclizations and these could be used to demonstrate the capabilities of **II** as a man-made enzyme.<sup>95, 96</sup>

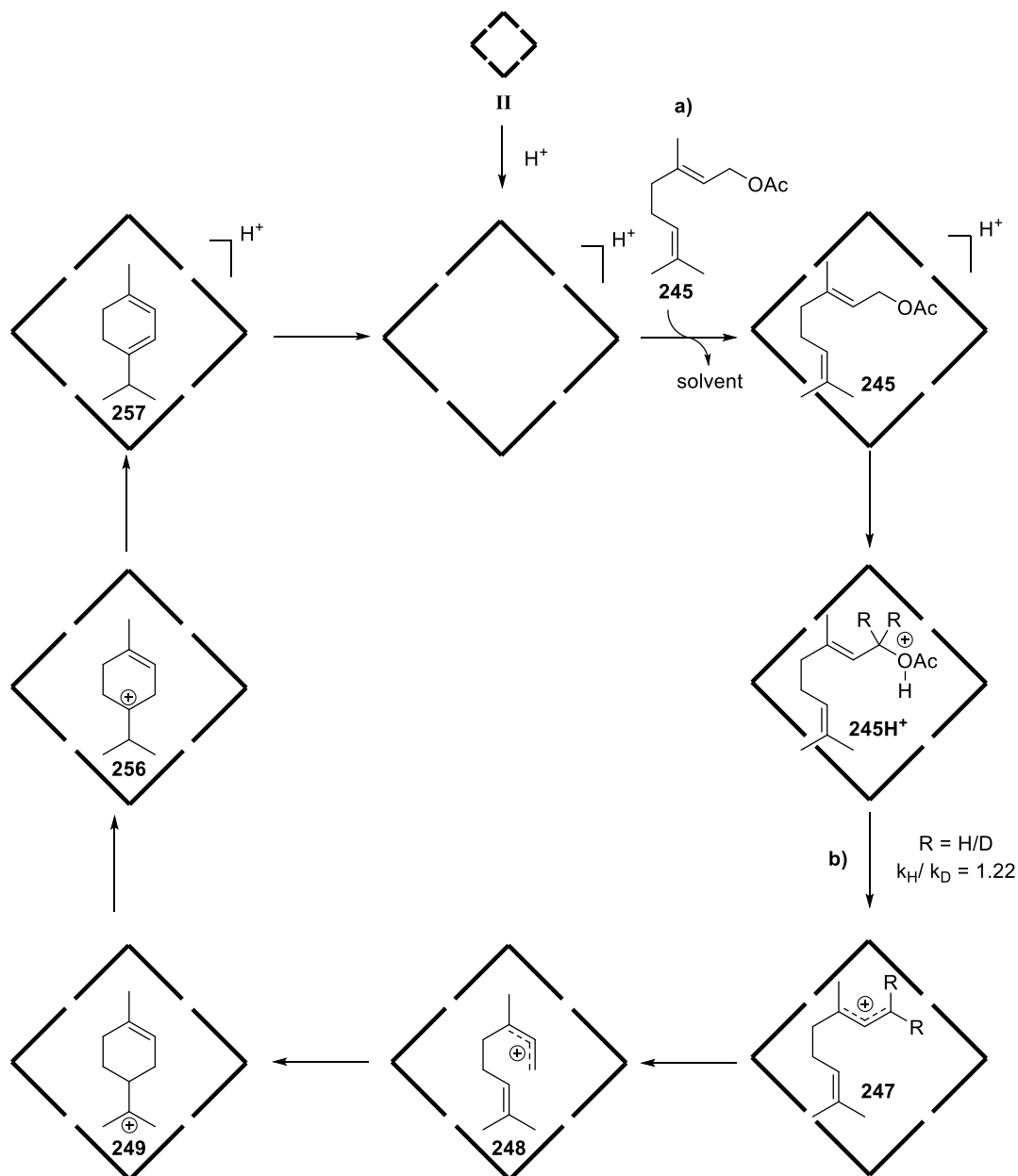


Figure 32 Mechanism of the catalytic cycle of the terpene cyclization of **245** in **II**.

In addition, the insights obtained about the mechanism of the terpene cyclization, and the exact route of how the acidic activation of substrates by **II** proceeds was revealed in 2020 by

*Merget et al.*<sup>97</sup> In this study, different resorcinarene derivatives were tested. The respective assemblies were found to incorporate between eight to zero equivalents of water in their related hexamer. Assemblies without water did not show any catalytic activity for the terpene cyclization of **245**. This demonstrated the crucial role water plays for the catalytic activity of the resorcinarene capsules. Quantum mechanical/molecular mechanic calculations revealed that water in the hydrogen bond network is protonated by HCl in the first step of the catalytic cycle (Figure 33b). The so formed hydronium ion is subsequently replaced by the chloride anion and released into the inner capsule cavity. The chloride is stabilized through hydrogen bonds by the phenols of the adjacent resorcinarene units. The hydronium ion is transferred onto the substrate, which is then activated by protonation (Figure 33c).

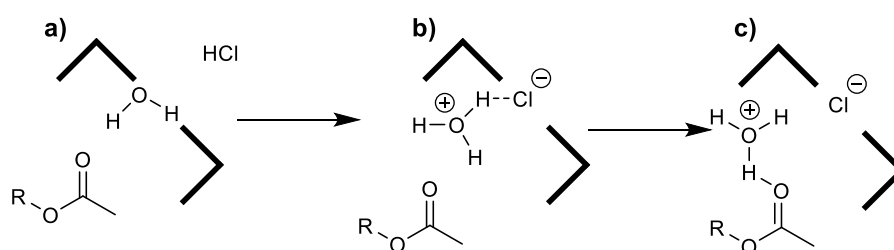


Figure 33 Proton shuttle mechanism.

Since **II** displays cation stabilizing properties and provides an acidic environment, it was tested with regards to its catalytic performance for carbonyl-olefin metathesis by *Catti et al.* in 2018.<sup>98</sup> For comparison with the benchmark catalyst FeCl<sub>3</sub>,  $\beta$ -ketoester (**87**) was subjected to **II** in combination with HCl. The optimized conditions showed, that 10 % **II** and 5 % HCl at 50 °C in CHCl<sub>3</sub> provided the best yield with 91 % for **90**. The optimized conditions were demonstrated on 14 examples with up to 98 % yield (Figure 34a).

To test whether the reaction took place inside **II** several control experiments were performed (Figure 34b). In the absence of **II** or HCl, no conversion was observed, indicating that both components are necessary for the reaction. In the presence of the strong binding guest tetrabutylammonium bromide, only a small amount of the product was formed after 4d, which indicates that the reaction likely takes place inside the cavity. Disassembling the hexamer by adding 9000 % of MeOH also prohibited product formation, which indicates, that the capsule monomer was not the catalytic active species.

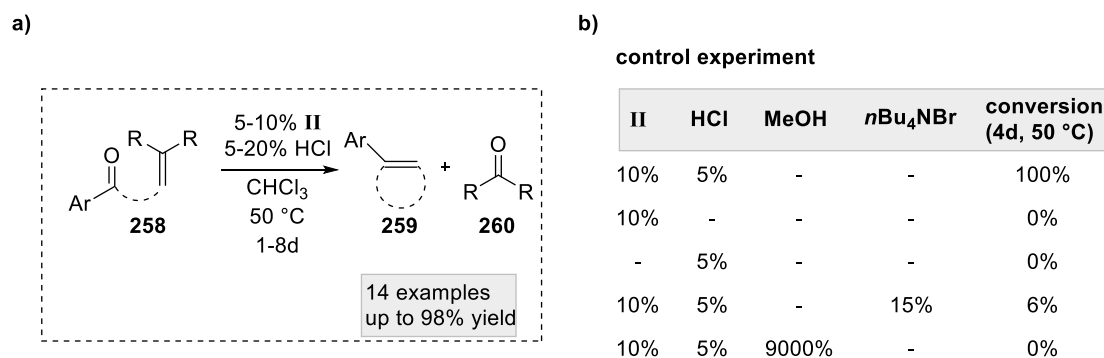


Figure 34 a) Optimized conditions for the intramolecular ring-closing metathesis with **II** b) control experiments.

Due to the cation-stabilizing properties of **II**, *Catti et al.* proposed that a stepwise mechanism was more likely than an asynchronous concerted mechanism. Consequently, a mechanistic probe (**261**) was designed to intercept a potential tertiary carbocation at the olefin moiety (Figure 35). The intercepting product (**263**) was isolated with a 66 % yield, indicating the formation of a cationic intermediate.

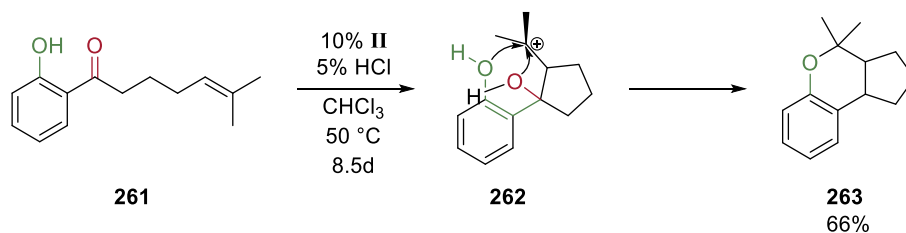


Figure 35 Mechanistic probe for the **II** catalyzed carbonyl-olefin metathesis.

In studies of *Neri* and co-workers on **II** the reaction scope was expanded towards [2+3]-dipolar cycloaddition between nitrones and unsaturated aldehydes, the conjugate addition of pyrroles to nitroalkenes and *Friedel-Crafts* alkylations by the activation of benzylchlorides.<sup>99-103</sup>

### 2.1.3 Objectives within this Thesis

The combination of the hexameric resorcinarene capsule (**II**) and HCl has been shown to be a potent catalyst for the intramolecular carbonyl-olefin metathesis. However, several open questions still remained at the time, and this work was aimed at addressing these. Specifically, the objectives of this thesis were:

- 1) Expanding the substrate scope to 2,5-dihydropyrroles
- 2) Mechanistic investigation of the carbonyl-olefin metathesis
- 3) Expanding the substrate scope to alkyl ketone substrates
- 4) Expanding the substrate scope to intermolecular ring-opening cross carbonyl-olefin metathesis
- 5) Due to the mechanistic know-how gained in this work, a glycosylation reaction discovered in the working group was investigated by kinetic analysis (see chapter 3).

1) Other researchers have demonstrated the successful synthesis of 2,5-dihydropyrroles via the carbonyl-olefin metathesis. Starting with amino acids, chiral 2,5-dihydropyrroles are valuable precursors for natural product synthesis. Therefore, the synthesis of these products with **II**/ HCl is highly desirable.

2) The mechanism for this kind of reaction was reported in literature to be either asynchronous concerted or stepwise. One aim within this thesis was the investigation of the mechanistic pathway of the carbonyl-olefin metathesis inside the resorcinarene hexamer (**II**). In addition, there was a desire to consolidate the different mechanistic proposals by expanding the investigated substrate scope of the well-established iron(III) catalyst.

3-4) In order to establish a generally applicable method also alkyl ketones and intermolecular ring-opening cross-metathesis were of significant interest, especially since these reactions are not as accessible as the well-established metathesis of aryl ketone substrates.

5) The **II**-catalysed  $\beta$ -selective glycosylation investigated by *T.-R.* Li is a remarkable new method that has been proven to apply to a wide range of glycosyl donors and nucleophiles.<sup>104</sup> The objective of this part of the work was to elucidate the mechanism of the  $\beta$ -selective glycosylation by utilizing a determination of the reaction order, secondary kinetic isotope effects and proton inventory techniques. The methods applied in point 2) to determine the cationic or non-cationic character of the rate-limiting step in the carbonyl-olefin metathesis, were also applied in order to answer the question of the rate-limiting step in the glycosylation

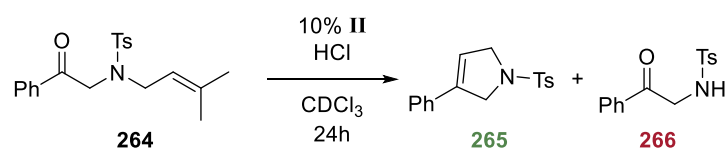
reaction. The knowledge gained through the mechanistic study of the carbonyl-olefin metathesis helped with the development of new methods to study glycosylation.

## 2.2 Results and Discussion

### 2.2.1 Synthesis of 3-aryl-2,5-dihydropyrroles<sup>105</sup>

On the basis of previous publications on the **II**/ HCl catalyzed carbonyl-olefin metathesis, investigations were started in order to expand the substrate scope to access 3-aryl-2,5-dihydropyrroles. The conditions used for the carbonyl-olefin metathesis of aryl ketones (**258**, Figure 34) were applied to substrate **264** (Table 2, entry 1), which showed a moderate yield of 30 % of the desired product (**256**) after 24h. Deallylation of the product (**266**) was observed as a major side reaction. Lower temperatures suppressed the formation of the side reaction, but the reaction only ran to 48 % conversion (Table 2, entry 8). Increasing the acid concentration improved the formation of the carbonyl-olefin metathesis product, with an optimal amount being 20 % HCl (Table 2, entry 6). Higher acid concentration led to a decrease in product formation (Table 2, entry 5). In order to establish reproducible reaction conditions, 30 °C was chosen as the reaction temperature (Table 2, entry 4).

Table 2 Optimization of the reaction conditions for **264**



entry	1	2	3	4	5	6	7	8	9	10
T [°C]	50 °C	50 °C	30 °C	30 °C	rt	rt	rt	rt	rt	4 °C
HCl [mol%]	5%	2.5%	30%	20%	30%	20%	10%	5%	2.5%	30%
Conversion <sup>a</sup>	100%	95%	100%	100%	100%	100%	89%	48%	26%	33%
Yield <sup>b</sup> <b>265</b>	30%	37%	69%	80%	75%	85%	68%	30%	9%	27%
Yield <sup>b</sup> <b>266</b>	45%	53%	15%	20%	17%	15%	26%	4%	0%	0%

<sup>a</sup>conversion was determined by <sup>1</sup>H NMR, with tetraethylsilane as internal standard after 24h;

<sup>b</sup>yields were determined by <sup>1</sup>H NMR, with tetraethylsilane as internal standard after 24h

An investigation of the alkene substituents was carried out with dimethyl (**264**), phenyl (**268**) and unsubstituted olefin moiety (**267**) (Figure 36). Substrate **267** did not show any reactivity, even at elevated temperature (50 °C) and high HCl loadings. The reaction of **268** resulted only

in deallylation. Thus, all further studies were performed with the dimethyl substituted olefin moiety.

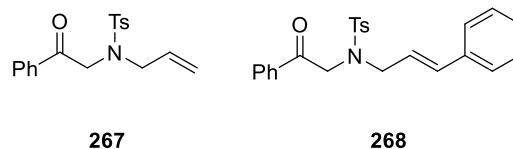


Figure 36 Substrates with alternative olefin moieties.

In the next step, the effect of different protection groups on the substrate scope was tested. Toluenesulfonyl (Ts) protected substrates **269** and **270** showed good yield (Table 3). Interestingly, increasing the size of **270** by one CH<sub>2</sub>-group (**271**) led to a dramatic drop in the yield of product **271A**. Increasing the size of the substituent by the introduction of a phenyl group (**272**) led to an even further reduced yield of the carbonyl-olefin metathesis product **272A**.

Introduction of the electron poor protecting group 4-trifluoromethyl benzene sulfonyl (trifluorotosyl, <sup>F</sup>Ts) generally lead to lower yields compared to Ts-protection and required a higher temperature of 50 °C, high HCl concentration of 40 % and long reaction times to run to completion.

Interestingly, the more electron rich mesyl (Ms) protection group showed good conversion at 50 °C with 20 % HCl. Moreover, the best yield was obtained for the most sterically demanding substrate (**280**), which contrasts with the other protecting groups, where smaller substrates provided better yields.

The alanine-derived substrates (**270**, **274** and **278**) showed surprisingly good yields, especially for Ts and <sup>F</sup>Ts, where increasing the size of the substituent led to decreased formation of the carbonyl-olefin metathesis product. It is the case, that this observation most likely stems from a *Thorpe-Ingold* effect, which was also discussed by the *Schindler* group for substrate **270**. Experiments with the racemic and enantio enriched substrate **270** showed, that the stereo information is preserved during the reaction.

Table 3 Evaluation of the protecting group influence

10% **II**  
HCl  
CHCl<sub>3</sub>

**A** + **B**

20% HCl, 30 °C, 24h			
 <b>269</b> A: 74±2% <sup>a</sup> B: 25±3% <sup>a</sup> Iso. yield: 62% (A) <sup>b</sup>	 <b>270</b> A: 84±0.8% <sup>a</sup> B: 11±0.5% <sup>a</sup> Iso. yield: 79% (A) <sup>b</sup>	 <b>271</b> A: 31±0.8% <sup>a</sup> B: 30±5% <sup>a</sup> Iso. yield: 34% (A) <sup>b</sup>	 <b>272</b> A: 24±0.4% <sup>a</sup> B: 66±0.6% <sup>a</sup> Iso. yield: 17% (A) <sup>b</sup>
40% HCl, 50 °C, 14d			
 <b>273</b> A: 9±1% <sup>a</sup> B: 22±0.6% <sup>a</sup> Iso. yield: 6% (A) <sup>b</sup>	 <b>274</b> A: 58±3% <sup>a</sup> B: 35±2% <sup>a</sup> Iso. yield: 52% (A) <sup>b</sup>	 <b>275</b> A: 18±0.5% <sup>a</sup> B: 52±0.9% <sup>a</sup> Iso. yield: 18% (A) <sup>b</sup>	 <b>276</b> A: 32±2% <sup>a</sup> B: 16±1% <sup>a</sup> Iso. yield: 35% (A) <sup>b</sup>
20% HCl, 50 °C, 48h			
 <b>277</b> A: 27±2% <sup>a</sup> B: 43±5% <sup>a</sup> Iso. yield: 25% (A) <sup>b</sup>	 <b>278</b> A: 54±0.2% <sup>a</sup> B: 30±0.1% <sup>a</sup> Iso. yield: 57% (A) <sup>b</sup>	 <b>279</b> A: 45±0.4% <sup>a</sup> B: 38±0.3% <sup>a</sup> Iso. yield: 41% (A) <sup>b</sup>	 <b>280</b> A: 83±2% <sup>a</sup> B: 12±2% <sup>a</sup> Iso. yield: 62% (A) <sup>b</sup>

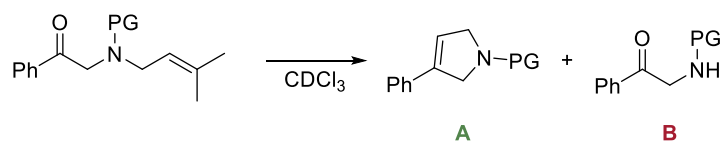
<sup>a</sup>reactions run in triplicate and analyzed by <sup>1</sup>H NMR with tetraethylsilane as internal standard (std. deviation reported).  
<sup>b</sup>isolated yield

In order to confirm that the reaction takes place inside the cavity of **II** control experiments were carried out (Table 4). In the presence of the strong-binding guest tetrabutylammonium bromide, no formation of the carbonyl-olefin metathesis product was observed (Table 4, entry 1). For **269** a small amount of the deallylation product was formed. Tetrabutylammonium bromide occupies the cavity of **II** and therefore blocks it for other substrates to enter. The addition of



superstoichiometric amounts of methanol disrupts the hydrogen bonding network of **II** so that the monomer (**239**) is present in the solution (Table 4, entry 2). No formation of the carbonyl-olefin metathesis product nor the deallylation product was observed, which excludes a catalytic activity of the monomer (**239**). Without **II** or HCl, no carbonyl-olefin metathesis product was observed, thereby demonstrating that both components have to be present to catalyze the reaction. For **269** and **277** the deallylation product was observed in both cases, which indicates that the deallylation reaction is independent of **II**/ HCl but is accelerated by the catalytic system.

Table 4 Control experiments



		0	1	2	3	4	
<b>II</b>		10%	10%	10%	0%	10%	
	HCl	20%	20%	20%	20%	0%	
	<i>n</i> Bu <sub>4</sub> NBr	-	150%	-	-	-	
	MeOH	-	-	6000%	-	-	
		30°C, 1d		30°C, 7d			
<b>269</b>	A <sup>a</sup>	74%	n.d.	n.d.	n.d.	n.d.	
	B <sup>a</sup>	25%	14%	n.d.	15%	13%	
		50°C, 14d		50°C, 14d			
<b>273</b>	A <sup>a</sup>	9%	n.d.	n.d.	n.d.	n.d.	
	B <sup>a</sup>	22%	n.d.	n.d.	n.d.	n.d.	
		50°C, 2d		50°C, 7d			
<b>277</b>	A <sup>a</sup>	27%	n.d.	n.d.	n.d.	n.d.	
	B <sup>a</sup>	43%	n.d.	n.d.	3%	2%	

<sup>a</sup>analyzed by <sup>1</sup>H NMR with tetraethylsilane as internal standard; n.d. = not detectable via <sup>1</sup>H NMR

The results from the protection group screening indicate, that the limited size of the cavity of **II**, leads to a limitation in the conformational freedom of the substrates. Sterically demanding substrates are therefore hindered from undergoing conformational changes necessary for the carbonyl-olefin metathesis. This limitation was addressed by introducing the smaller Ms-protection group. The deallylation does not require substantial conformational changes and can

therefore outcompete the carbonyl-olefin metathesis in the case of sterically demanding substrates.

In summary, the synthesis of 3-aryl-2,5-dihydropyrroles via carbonyl-olefin metathesis was realized with the catalytic system of **II** and HCl. The used Ms-protection can be deprotected selectively in the presence of Ts-protection as shown in the literature.<sup>106</sup> Due to the electron-rich character of the Ms-group, Lewis-acidic catalysts like FeCl<sub>3</sub> are incompatible because of coordination. Therefore, the combination of **II**/ HCl and Ms-protection displays an interesting orthogonal approach to the synthesis of more complex molecules.

## 2.2.2 Mechanistic Investigation

The mechanism of the Lewis acid catalyzed carbonyl-olefin metathesis, displayed in literature presents either an asynchronous concerted or cationic-stepwise pathway. The *Schindler* group has demonstrated that the iron(III)chloride catalyst favors an asynchronous concerted pathway via **TS<sub>AC1</sub>** and **TS<sub>AC2</sub>** for substrates **87**, **116**, **117** (Figure 10d). Isotopic labeling of the olefin position of **117** (Figure 10e) leads to an inverse isotopic effect (SKIE = 0.65±0.07), which is interpreted as the transition from an sp<sup>2</sup> to an sp<sup>3</sup> center in **TS<sub>AC1</sub>**.

An overview of the two possible pathways is depicted in Figure 37. For each transition state (**TS**) it includes the expected SKIE at the olefin moiety and  $\Delta S^\ddagger$ , for the case that the reaction step is rate-limiting.

The carbonyl-olefin metathesis to form **INT1**, is initiated by the activation of the carbonyl group through the catalyst (Figure 37). Catalyst binding should not induce an SKIE at the olefin moiety, however for the case of this step being rate-limiting for **II/HCl** a positive entropic change is expected. The encapsulation of substrates triggers the release of solvent molecules from the cavity which is an entropically favorable process. Similar effects were demonstrated for other substrates by the *Tiefenbacher* group.<sup>95</sup> The binding of iron(III) chloride, however, is expected to result in a negative  $\Delta S^\ddagger$ .

The subsequent oxetane formation proceeds in an asynchronous concerted (**AC**) or stepwise (**S**) fashion (Figure 37). In the stepwise mechanism, a tertiary carbocation is formed at the former olefin moiety (**TS<sub>S1</sub>**), which is stabilized via hyperconjugation from the neighboring methyl groups. The weaker stabilization of the cation by the CD<sub>3</sub>-groups compared to CH<sub>3</sub>-groups would be expected to result in a normal SKIE (1.1-1.5) in case this step is rate-limiting.<sup>107-109</sup> The formed cation (**INT2**) is subsequently converted to oxetane (**INT3**). In the corresponding TS (**TS<sub>S2</sub>**), the hybridization change from sp<sup>2</sup> to sp<sup>3</sup> would result in an inverse SKIE (0.4-0.9).<sup>110, 111</sup>

If the energy of the intermediate cationic species (**INT2**) is too close to the energy of the transition state (**TS<sub>S2</sub>**), an asynchronous concerted pathway is observed.<sup>112</sup> In such a case, the reaction proceeds over a partially charged transition state (**TS<sub>AC1</sub>**). The hybridization change (sp<sup>2</sup> to sp<sup>3</sup>) would be expected to result in an inverse SKIE. In the stepwise, as well as in the asynchronous concerted pathway, the formed transition states have fewer degrees of freedom than the ground state, resulting in a negative  $\Delta S^\ddagger$ .

The oxetane opening can also proceed in a stepwise manner, as well as asynchronously concerted. In the stepwise mechanism, a carbon-oxygen bond is broken to form a benzylic

cation (**INT4**, Fig. 5). As the isotopic CD<sub>3</sub> labels are distant ( $\gamma$ -position), no significant SKIE is to be expected ( $k_H/k_D = 1$ ). In the final step, acetone is eliminated from intermediate **INT4**. The hybridization change ( $sp^3$  to  $sp^2$ ) should result in a normal SKIE. Since a bond is broken during the transition state (**TSs4**) and the molecule is fragmented, the entropic change ( $\Delta S^\ddagger$ ) should be positive. In the case of an asynchronous concerted opening, a normal SKIE can be expected due to the hybridization change ( $sp^3$  to  $sp^2$ ) during **TS<sub>AC2</sub>**. The transition state is closely related to the transition state **TS<sub>AC1</sub>** so a negative  $\Delta S^\ddagger$  can be expected.

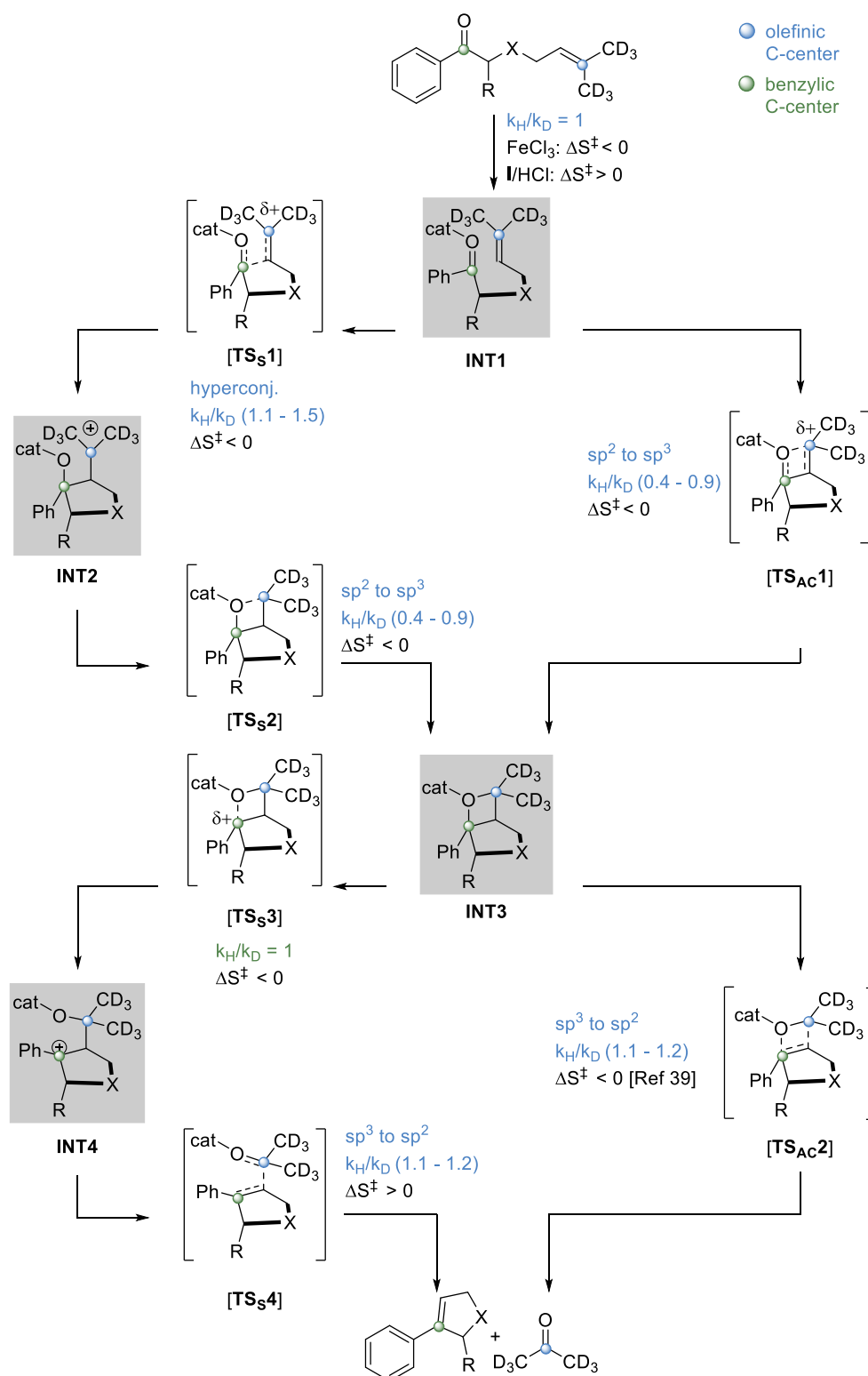


Figure 37 Overview of the available mechanistic pathways for the stepwise (TS<sub>s</sub>) and asynchronous concerted (TS<sub>AC</sub>) carbonyl-olefin metathesis. The expected values for  $\Delta S^\ddagger$  and  $\beta$ -SKIE are given below the respective transition state.

In order to investigate the underlying mechanism of the carbonyl-olefin metathesis inside **II**, substrates **87**, **281** and **270** (Figure 38) were analyzed by an Eyring analysis as well as with

regard to their SKIE. Results from *Catti et.al.* suggest the existence of a cationic intermediate during the carbonyl-olefin metathesis inside **II** (Figure 35).<sup>98</sup>

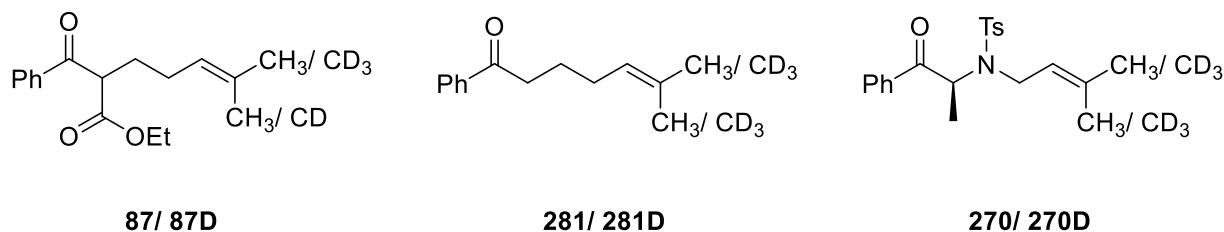
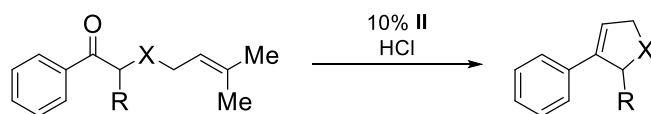


Figure 38 Substrates analyzed by an Eyring analysis and determination of secondary isotope effect.

All reactions were analyzed by <sup>1</sup>H NMR. For substrates **87** and **281**, the reactions were run at 50 °C, 40 °C and 30 °C in CDCl<sub>3</sub> with 10 % **II** and 5 % HCl. Substrate **270** required a higher HCl loading (20 %) and was run at 30 °C, 20 °C and 11 °C under otherwise identical reaction conditions. Reaction rates were determined by observing the consumption of the starting material. Each reaction was carried out in triplicate. All substrates showed negative  $\Delta S^\ddagger$  and positive  $\Delta H^\ddagger$  activation parameters (Table 5). Due to the negative entropy of activation ( $\Delta S^\ddagger$ ), the release of acetone as the rate-limiting step (**TSs4**, Figure 37) could be excluded for all three substrates. In contrast to the catalyst FeCl<sub>3</sub>, also the formation of the substrate catalyst complex could be excluded already at this stage, as the encapsulation of the substrate inside **II** would be expected to release solvent molecules, leading to entropically favorable processes as demonstrated for sesquiterpene cyclization inside **II**.

Table 5 Activation parameters and SKIE ( $k_H/k_D$ ) with **II**/HCl



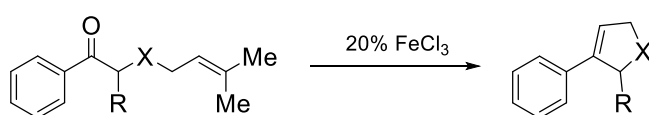
entry	substrate	isolated Yield	$\Delta H^\ddagger$	$\Delta S^\ddagger$	$k_H/k_D$
1	<b>87</b> (R = COOEt; X = CH <sub>2</sub> )	91% <sup>Ref. 98</sup>	11.0±0.8 kcal mol <sup>-1</sup>	-47±3 cal mol <sup>-1</sup> K <sup>-1</sup>	1.00±0.01
2	<b>281</b> (R = H; X = CH <sub>2</sub> )	73%	17.4±0.3 kcal mol <sup>-1</sup>	-27±1 cal mol <sup>-1</sup> K <sup>-1</sup>	1.26±0.04
3	<b>270</b> (R = CH <sub>3</sub> ; X = NTs)	79%	17.9±0.4 kcal mol <sup>-1</sup>	-17±1 cal mol <sup>-1</sup> K <sup>-1</sup>	1.12±0.05

No  $\beta$ -SKIE ( $1.00 \pm 0.01$ ) was measured for **87** (Table 5, entry 1). Therefore, no change occurs at the olefin moiety in the rate-limiting transition state (**TS<sub>S3</sub>**) from the oxetane intermediate (**INT3**) towards the benzylic cation (**INT4**). As discussed before, a negative  $\Delta S^\ddagger$  most likely stems from a partially cyclized transition state. The formation of a benzylic carbocation (**Int4**, Figure 37) in a stepwise oxetane opening comprises a cyclized structure as well as a center of reaction which is distant enough from the labeled position.

The SKIE for **281** and **270** were determined with  $1.26 \pm 0.04$  and  $1.12 \pm 0.05$ , respectively, (Table 5, entries 2 and 3), which indicates either that there is a carbocation in hyperconjugation (**TS<sub>S1</sub>**) or a change from an  $sp^2$  to an  $sp^3$  center (Figure 37). The change from  $sp^2$  to  $sp^3$  could only occur during the asynchronous concerted oxetane opening (**TS<sub>AC2</sub>**) or stepwise cleavage of acetone (**TS<sub>S4</sub>**). In the stepwise case, a significant bond cleavage takes place in the transition state (**TS<sub>S4</sub>**), which would be expected to lead to a positive  $\Delta S^\ddagger$ . The asynchronous concerted transition state (**TS<sub>AC2</sub>**) is expected to show a negative entropic change since its structure is closer to the oxetane. Therefore, the stepwise oxetane formation (**TS<sub>S1</sub>**), as well as the asynchronous oxetane opening (**TS<sub>AC2</sub>**), are possible mechanisms for **281** and **270**.

Astonishingly, the substrates did not show similar SKIE and therefore they seemingly have different rate-limiting steps for the carbonyl-olefin metathesis. To see if this was an effect induced by **II/HCl** or substrate-specific, the same substrates were tested with the well-established iron(III) catalyst (Table 6).

Table 6 Activation parameters and SKIE ( $k_H/k_D$ ) with iron(III)chloride



entry	substrate	$\Delta H^\ddagger$	$\Delta S^\ddagger$	$k_H/k_D$
1	<b>87</b> (R = COOEt; X = CH <sub>2</sub> )	$14 \pm 1$ kcal mol <sup>-1</sup> [Ref. 64]	$-34 \pm 5$ cal mol <sup>-1</sup> K <sup>-1</sup> [Ref. 64]	$0.64 \pm 0.04$
2	<b>281</b> (R = H; X = CH <sub>2</sub> )	$12 \pm 1$ kcal mol <sup>-1</sup>	$-39 \pm 4$ cal mol <sup>-1</sup> K <sup>-1</sup>	$0.98 \pm 0.05$
3	<b>270</b> (R = CH <sub>3</sub> ; X = NTs)	$13.3 \pm 0.3$ kcal mol <sup>-1</sup>	$-34 \pm 1$ cal mol <sup>-1</sup> K <sup>-1</sup>	$0.85 \pm 0.03$



The activation parameters were determined by an Eyring analysis for substrates **281** and **270**, as the activation parameters for **87** had been determined by the *Schindler* group already (Figure 10d).<sup>64</sup> The reactions were monitored by *in situ* IR measurements, as NMR was hampered due to the paramagnetism of the iron(III) catalyst. Substrate **281** was studied at 50 °C, 40 °C and 30 °C in DCE with 20 % FeCl<sub>3</sub> by monitoring the carbonyl band of the starting material. For substrate **270**, due to a substantial overlap of the carbonyl band, a switch in the solvent, as well as in the observed band was required. The study for this was performed at 30 °C, 20 °C and 11 °C in toluene with 20 % FeCl<sub>3</sub>. The reaction rates were determined by observing the consumption of the starting material. Each reaction was carried out in triplicate. The Eyring analysis showed a positive  $\Delta H^\ddagger$  and negative  $\Delta S^\ddagger$  for both substrates, which is comparable to the data for **87** obtained by the *Schindler* group (Table 6). Due to the negative  $\Delta S^\ddagger$ , the release of acetone could be excluded as the rate-limiting step (**TSs4**, Figure 37) for all three substrates.

The *Schindler* group showed there to be an asynchronous concerted mechanism for substrate **87**, where the oxetane formation (**TS<sub>AC1</sub>**) was identified as the rate-limiting step (Figure 10a). From the calculation of the transition state for the asynchronous concerted reaction and the cationic intermediate, it has been suggested that the latter is not stable enough to be populated. The activation parameters and  $\beta$ -SKIE determined by the *Schindler* group support the presence of an ordered transition state, where the sp<sup>2</sup> center changes to an sp<sup>3</sup> center. The  $\beta$ -SKIE from the *Schindler* group was determined from the phenyl-methyl substituted olefin substrate **117**.<sup>64</sup> The experiment was repeated in this work, with the methyl-methyl substituted substrate **87** and a negative  $\beta$ -SKIE ( $\beta$ -SKIE 0.64±0.04) was observed, which is in accordance with the results from the *Schindler* group.

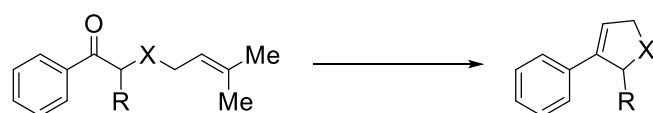
For substrate **280**, no  $\beta$ -SKIE (0.98±0.05) was observed, which excludes changes of hybridization or the formation of a carbocation at the olefin moiety. For this case, either the oxetane opening or the catalyst binding qualifies as a rate-limiting step. The binding of FeCl<sub>3</sub> would be expected to result in a more ordered system and therefore a positive  $\Delta S^\ddagger$ . Therefore, the formation of an intermediate benzylic cation via **TSs3** is more likely to be rate-limiting.

Substrate **270** showed an inverse SKIE (0.85±0.03, Table 6) similar to substrate **87**. Since no computational study has been performed on these substrates, either the asynchronous concerted transition state (**TS<sub>AC1</sub>**,) or the cyclization of the carbocation of **TSs2** (Figure 37) can be accounted as an inverse effect. In both cases, the sp<sup>2</sup> center is changed to an sp<sup>3</sup> center. Experiments by the *Li* group of similar substrates in the presence of allyl-TMS have shown an

interception product of a carbocation (Figure 11b) similar to **INT2**. Therefore, **TS<sub>S2</sub>** is more likely but **TS<sub>AC1</sub>** cannot be excluded.

For both catalytic systems, no general trend was observed. Substrates **281** and **270** both showed an SKIE in the presence of **II/HCl**. For **FeCl<sub>3</sub>**, substrates **87** and **270** displayed a similar SKIE and therefore most likely a related rate-limiting transition state. In order to address these conflicting results computational simulations were carried out by *Prof. Dr. B. Goldfuss* -a collaboration partner- for both catalysts with the three substrates. Although these calculations were unsuccessful with regard to explaining the differences of the SKIE, the first results suggested that there were complex interactions between the catalyst and the substituents in alpha and beta positions and complex influences of the substrate conformers on the mechanism. It was also found that the transition states are close in energy, so the mechanism is influenced by small changes in the reacting system. In Table 7 the most likely rate-limiting steps are summarized for both catalysts.

Table 7 Rate-limiting steps obtained from the Eyring analysis and SKIE



	catalyst	substrate		
		<b>87</b> (R = COOEt; X = CH <sub>2</sub> )	<b>281</b> (R = H; X = CH <sub>2</sub> )	<b>270</b> (R = CH <sub>3</sub> ; X = NTs)
rate limiting	<b>II/HCl</b>	TS <sub>S3</sub>	TS <sub>S1/</sub> TS <sub>AC2</sub>	TS <sub>S1/</sub> TS <sub>AC2</sub>
	<b>FeCl<sub>3</sub></b>	TS <sub>AC1</sub>	TS <sub>S3</sub>	TS <sub>S2/</sub> TS <sub>AC1</sub>

In order to identify possible cationic intermediates, mechanistic probes were designed based on the previous substrates (**87**, **281**, **270**). The design allowed the intramolecular interception of a cation formed at the olefin moiety. The *Schindler* group tried two interception experiments based on a *Prins* reaction with an inter and intramolecular nucleophile (Figure 10b). Intermolecular nucleophiles must compete with the intramolecular carbonyl-olefin metathesis and therefore might not be fast enough to catch an intermediate cation. The intramolecular experiments were realized by introducing primary alcohol in the alpha position of the ketone, which is capable of forming an alternative oxetane. This oxetane or the respective elimination

product might be too reactive to be isolated. However, the design used in this work led to the formation of a stable oxane that can be isolated.

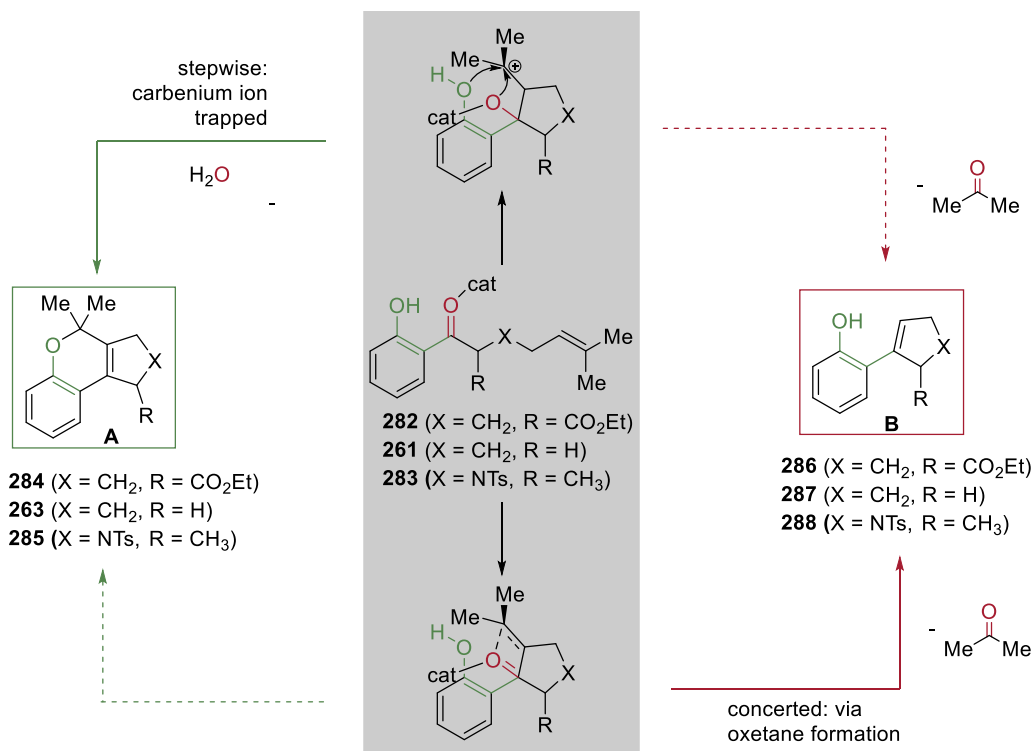


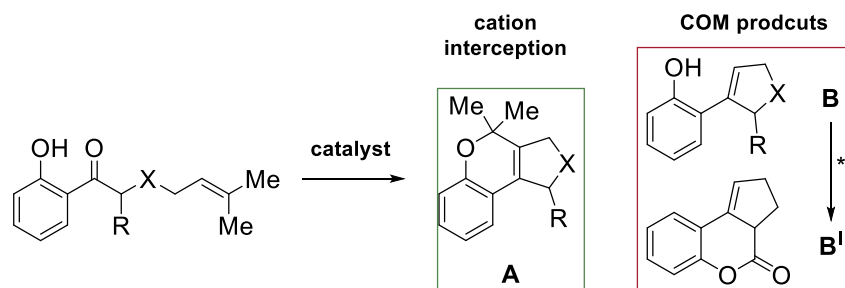
Figure 39 Overview concerning the reactivity of the mechanistic probes. (Top) The formation of a carbenium ion should result in the formation of oxane A (green). (Bottom) A concerted transition state should result in the formation of oxetane B (red).

Reactions with the mechanistic probes **282** and **261** were carried out at 50°C in CHCl<sub>3</sub> with 10 % **II** and 5 % HCl. Reaction conditions for **283** were adjusted to match the conditions of the mechanistic investigations of **270** (30°C, 10 % **II**, and 20 % HCl). For the mechanistic probes **282** and **261**, the cation-trapped products A (**284** and **263**, respectively) were exclusively isolated (Table 8). **283** formed both products, with the carbonyl-olefin metathesis product B (**288**) dominating (47 % isolated yield).

For the iron(III) catalyst, reactions with **282** and **261** were carried out at 30°C in DCE with 20 % FeCl<sub>3</sub>. The reaction conditions for **283** were adjusted to match the conditions of the mechanistic investigations of **270** (30°C in toluene with 20 % FeCl<sub>3</sub>). In the case of substrate **282**, no conversion for the standard conditions was achieved. Additional FeCl<sub>3</sub> (120 % in total) led to the formation of a mixture of cation interception product A (**284**) and COM-product B (**286**), which lactonized under these conditions to produce B<sup>I</sup> (Table 8).

Conversion of **282** and **261** in the presence of **II/HCl** resulted in the formation of the oxane **A** with a good yield, whereas **283** resulted in a mixture of **A** and **B** (Table 8). In the case of the **iron(III)** catalyst, conversion of **282** and **283** give a mixture of **A** and **B**. For substrate **261** only oxane **A** was observed (Table 8).

Table 8 Isolated products from the conversion of the mechanistic probes



catalyst	substrate			
	<b>282</b> (R = CO <sub>2</sub> Et; X = CH <sub>2</sub> )	<b>261</b> (R = H; X = CH <sub>2</sub> )	<b>283</b> (R = CH <sub>3</sub> ; X = NTs)	
<b>II/HCl</b>	<b>A</b>	80%	66%	21%
	<b>B</b>	0%	0%	47%
<b>FeCl<sub>3</sub></b>	<b>A</b>	25%	90%	27%
	<b>B / B'</b>	37% <sup>1,2</sup>	0%	29%

<sup>1</sup>additional FeCl<sub>3</sub> was added (1eq.)

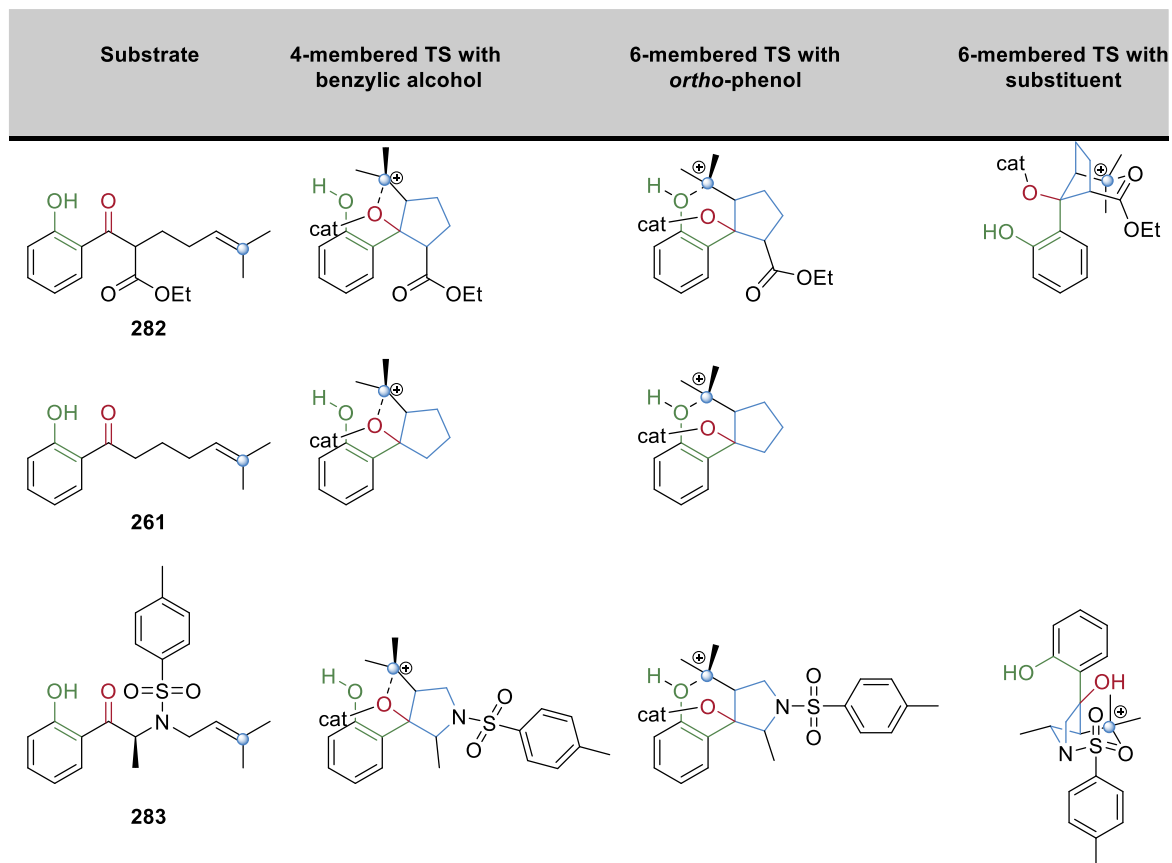
<sup>2</sup>B' isolated

Interestingly, also for the case of the mechanistic probes, no obvious trend was observable. Although substrate **261** and **283** showed the same behavior for **II/HCl** and FeCl<sub>3</sub>, substrate **282** seems to be a special case.

The phenol can form a six-membered transition state with a carbocation at the olefin moiety, which should lead to a stabilization of the charged intermediate (Figure 39). Therefore, it is astonishing, that substrate **283** with both catalysts and **282** with FeCl<sub>3</sub> showed a mixture of the oxane **A** and the carbonyl-olefin metathesis product **B**. In the case of substrate **261**, only the oxane was observable. Substrate **282** and **283** both possess potential coordinative sites, an ester in the case of **282** and a sulfonamide in the case of **283**, which might form a six-membered transition state with the carbocation (Table 9). Since these coordinative sites are unreactive, the oxetane formation is expected to be in a more favorable position and compete with the oxane

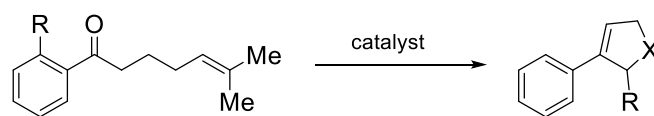
formation. Nevertheless, this effect does not explain the observed sole formation of oxane **A** in the case of substrate **282** in the presence of **II**/HCl. This could be an effect of the capsule environment, which offers the ester other coordinative possibilities. However, at this stage of the investigation, no final conclusion could be drawn from the results.

Table 9 Potential coordination of the tertiary carbocation by the mechanistic probes



In order to see if the results from the mechanistic probes (**282**, **261**, **283**) could be used to provide insight into the mechanism of the substrates (**81**, **281**, **270**), derivative **284** (Table 10) was investigated with regard to its SKIE and compared with the results from **281**. This substrate was expected to show the influence of an *ortho*-substituent on the rate-limiting step. The SKIE from **281** ( $1.26 \pm 0.04$ ) and **284** ( $1.03 \pm 0.09$ ) differ for the **II**/HCl catalyzed reaction. Therefore, these substrates display different rate-limiting steps, which shows that the *ortho*-substituent has too much influence on the mechanism to draw any conclusions from the mechanistic probes on the “normal” substrates.

Table 10 Comparison of the SKIE of 281 and 284 for **II**/HCl and FeCl<sub>3</sub>



substrate	SKIE	
	II/ HCl	FeCl <sub>3</sub>
<b>281</b> (R = H)	1.26±0.04	0.98±0.05
<b>284</b> (R = OMe)	1.03±0.09	0.99±0.07

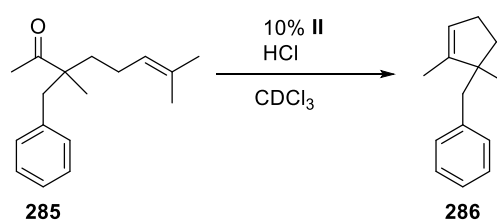
Even though the results from the mechanistic probes **282**, **261**, **283** did not provide any insights into the related substrates **81**, **281**, **270**, they did provide evidence for the formation of a tertiary cation at the olefin moiety. Future experiments should, therefore, feature intermolecular mechanistic probes which do not alter the substrate itself. The *Li*-group showed the interception of a tertiary cation in the presence of allyl-TMS, which is a promising approach for a mechanistic study of the carbonyl-olefin metathesis inside **II**. Furthermore, a Hammett plot with different substituted aryl substrates would be interesting for the quantification of the effect of electron donating and withdrawing groups on the mechanism. Moreover, it might indicate the formation of a positive charge on the carbonyl moiety.<sup>113, 114</sup>

### 2.2.3 Alkyl-Ketones

The previously in chapter 2.2.1 and 2.2.2 discussed substrates for the ring-closing intramolecular carbonyl-olefin metathesis, all have an aryl-ketone as electrophilic site. *Schindler* and co-workers discussed the problem of alkyl-ketones in their publication from 2019.<sup>69</sup> They showed that the substrate and the cleaved carbonyl side product are too similar in energy and require both higher activation energies than their aryl counterparts. Therefore, it was interesting how alkyl-ketone substrates behave in the cation-stabilizing environment of **II**.

The investigations of alkyl-ketone substrates started with the reaction of **285** in the presence of **II/HCl**. The temperature, as well as the acid concentration, were varied, where partial conversion at room temperature was observed, even with high acid concentrations (Table 11, entries 1 and 2). A complete conversion was obtained at 50 °C (Table 11, entries 3 and 4). New signals in the GC, with a shorter retention time compared to the substrate, occurred for entries 1-4 (Figure 40). A shorter retention time is promising since acetone is cleaved and the product becomes lighter and less polar. The research of this work was performed before the work of *Schindler* and co-workers, so no reference NMR spectra were available. Moreover, the product could not be identified as the obtained crude NMR spectra only provided information about newly formed species. The same information can be drawn from GC measurements. NMR spectroscopy was only performed on isolated substances.

Table 11 Reaction conditions for substrate **285**



substrate	entry	HCl	time	T	Conversion
<b>285</b>	1	10%	7d	25 °C	42%
	2	20%	7d	25 °C	65%
	3	5%	2d	50 °C	100%
	4	10%	2d	50 °C	100%

Although new signals (9.03 – 9.88 min, Figure 40) were observable in the GC, only unidentifiable mixtures were obtained after column chromatography. No separation was achievable via TLC or column chromatography.

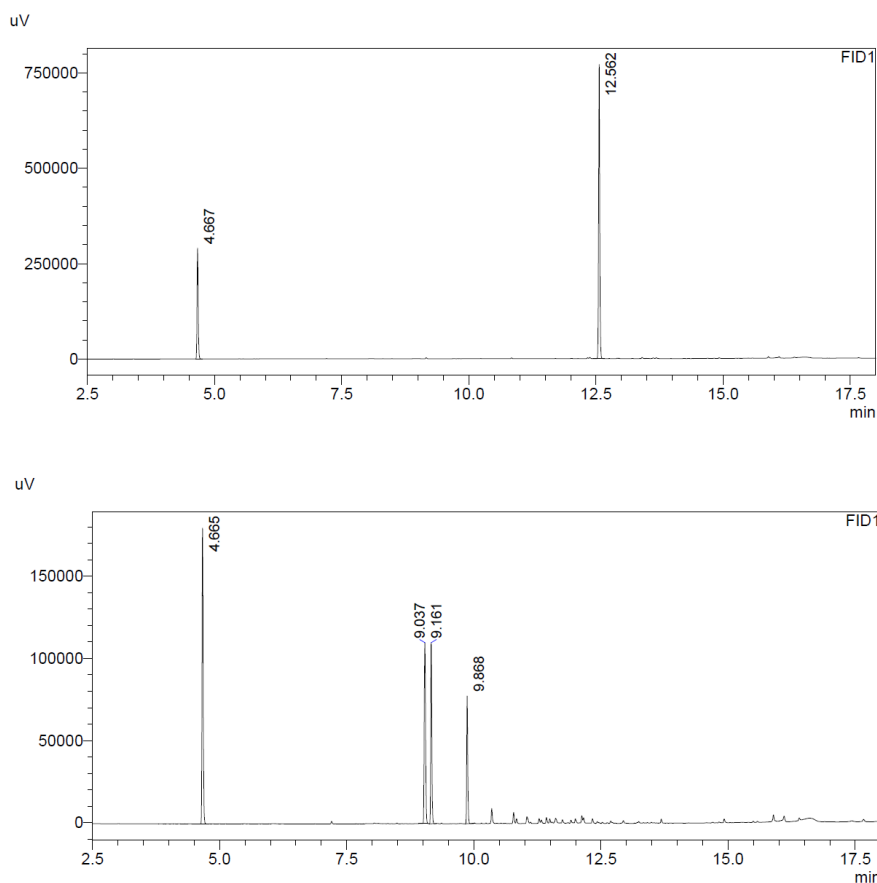
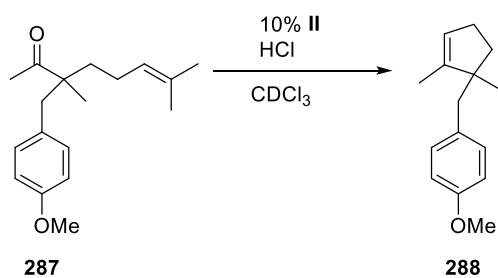


Figure 40 (Top) GC measurement of **285** with internal standard (Bottom) GC measurement for the conversion of substrate **285** at 50 °C with 10 % HCl.

In order to get a better separation, a slightly more polar derivative **287** was synthesized. The substrate showed similar reaction behavior to **285** (Table 12).

Table 12 Reaction conditions for substrate **287**



substrate	entry	HCl	time	T	Conversion
<b>287</b>	1	20%	6d	30 °C	70%
	2	40%	7d	25 °C	100%



The polar derivative **287** has a longer retention time than its apolar counterpart **285**. Moreover, new signals after conversion were observable (11.12 – 12.00 min), which have a shorter retention time than the substrate (14.24 min) (Figure 41).

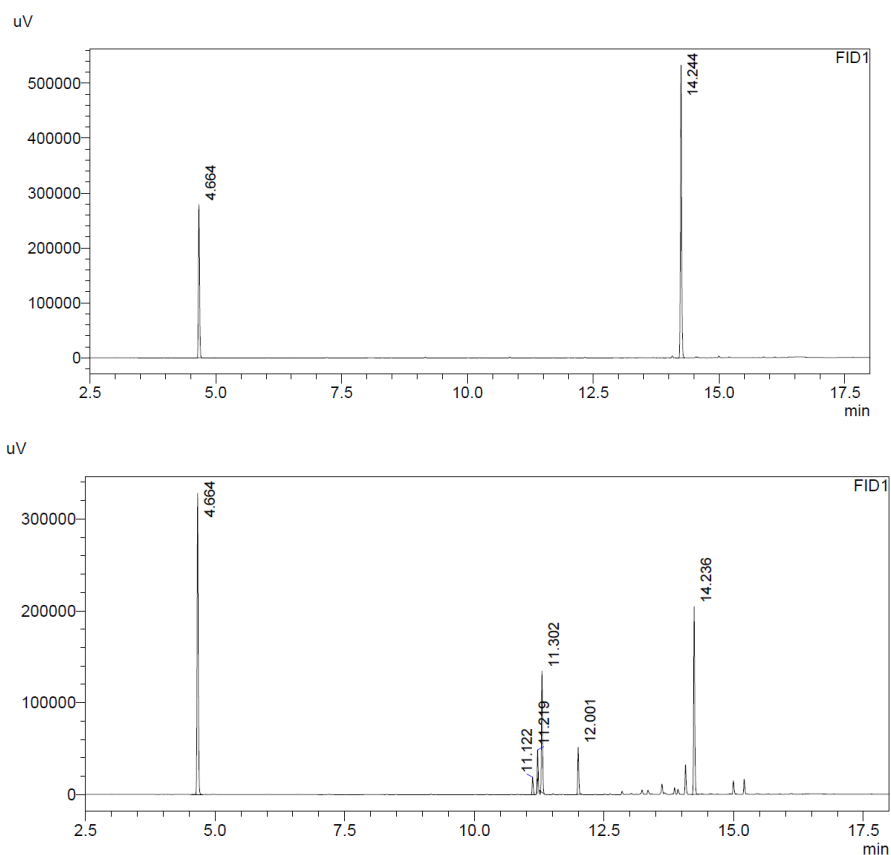


Figure 41 (Top) GC measurement of **287** with internal standard (Bottom) GC measurement for the conversion of substrate **287** at 30 °C with 20 % HCl.

These promising results meant that it was desirable to perform a reaction on a larger scale in order to isolate the formed products. Two new spots were observable on TLC, which separated into four spots on an AgNO<sub>3</sub>-silica TLC. Two main fractions were isolated by column chromatography but subsequent analysis of these fractions by GC did not match any of the main signals from the crude mixture.

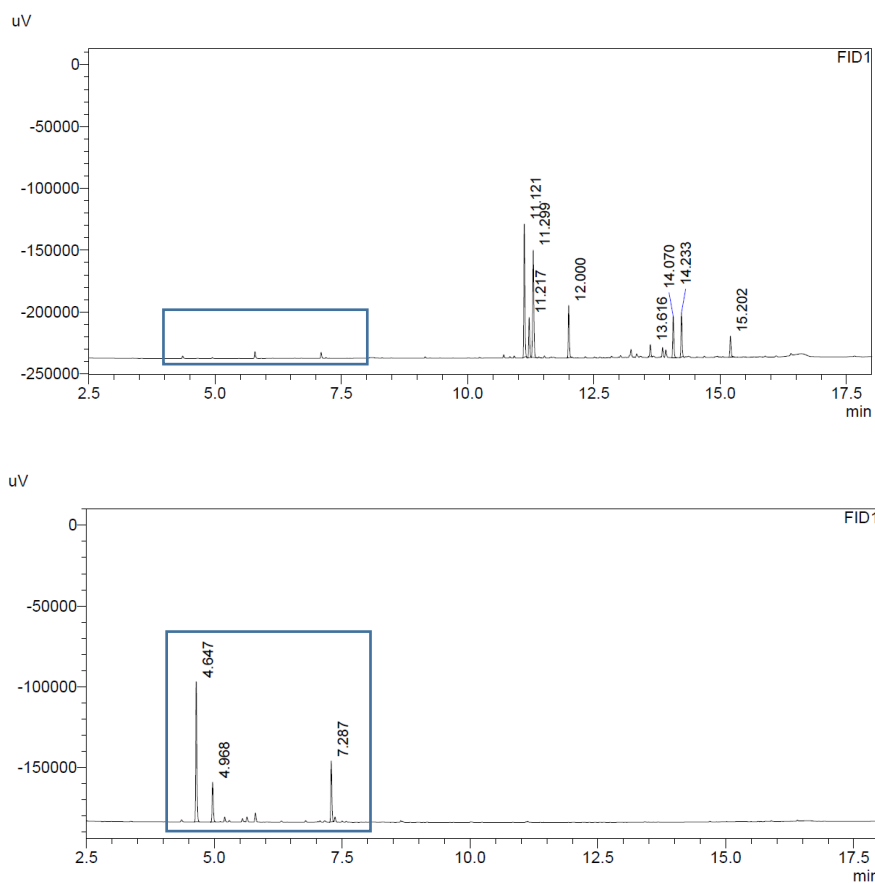


Figure 42 (Top) Crude GC measurement after the conversion of **287** (Bottom) GC measurement of the isolated fraction.

Nevertheless, analysis by NMR (Figure 43) of the isolated fraction and comparison with spectra from the literature showed, that small quantities of the metathesis product were formed.<sup>69</sup> A comparison with the GC of the crude material showed, that only traces of the desired product was formed (blue box Figure 42).

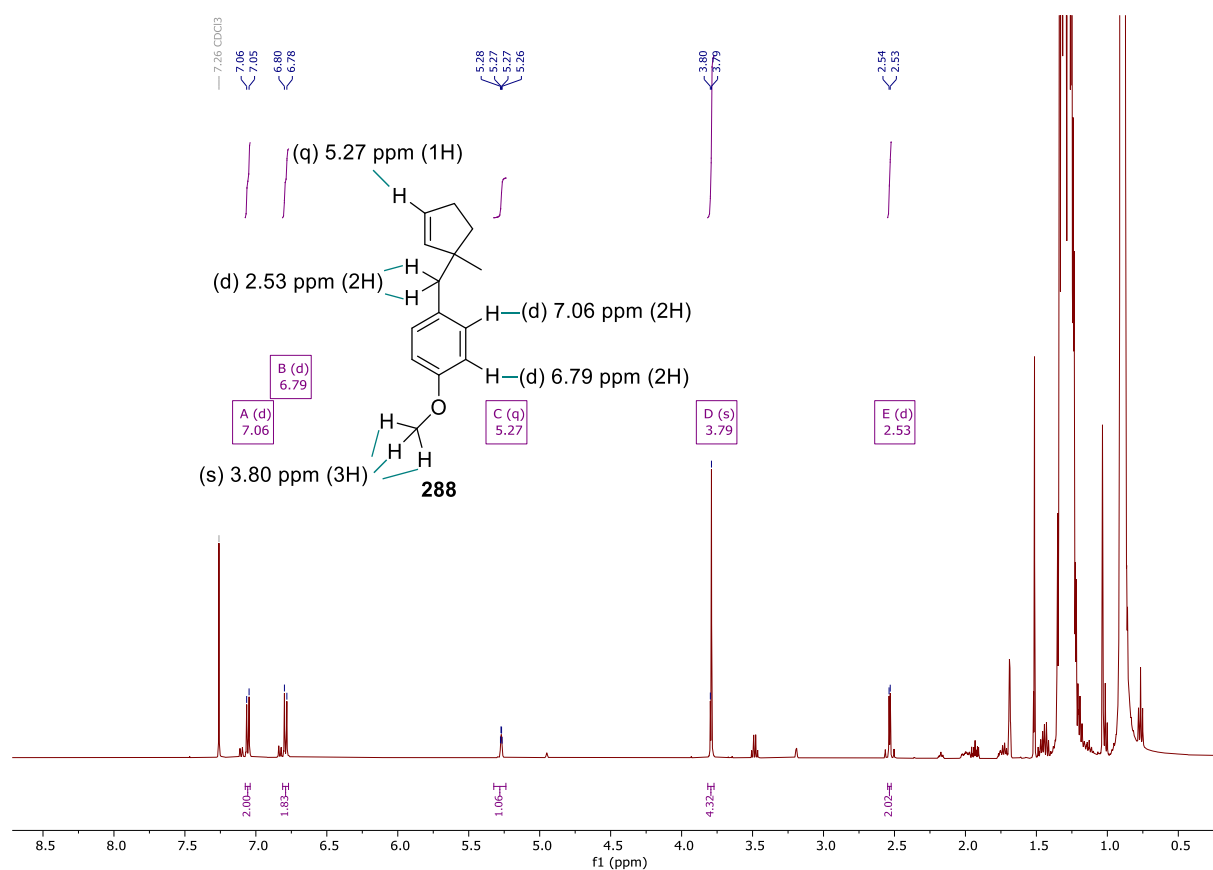


Figure 43  $^1\text{H}$  NMR-spectra of the isolated fraction with marked peaks according to literature known spectra of **288**.<sup>69</sup>

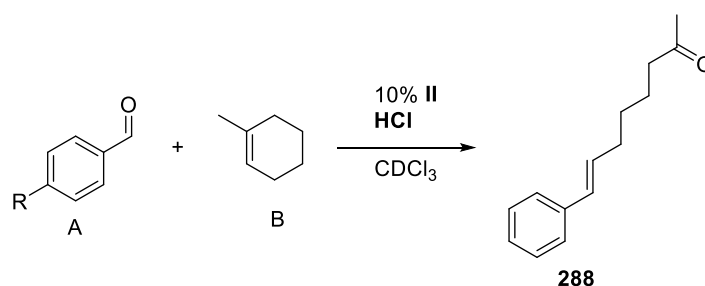
Although the metathesis product is formed in this case, the main part of the starting material seems to decompose. Since the results did not lead to initial results which looked promising, alkyl ketones were considered as being not suitable substrates for **II/HCl**.

## 2.2.4 Intermolecular Ring-Opening Cross Carbonyl-Olefin Metathesis

Ring-opening cross carbonyl-olefin metathesis differs from the previously discussed reactions in chapter 2.2.1, 2.2.2 and 2.2.3 since it contains two reaction partners. Benzaldehyde derivatives were tested with various alkenes of different reactivities.

The screening process was started with 1-methylcyclohexene and benzaldehyde in a 1:1 ratio (Table 13, entry 1). After three days only moderate conversion of benzaldehyde was observed. Longer reaction times of 3 additional days led to complete decomposition of the starting materials with no defined signals left in the NMR spectrum. In order to facilitate the reaction, 4-nitrobenzaldehyde was chosen as a better electrophile compared to benzaldehyde. Another problem of this reaction is the weak affinity of the capsule cavity toward non-polar components, therefore the concentration of 1-methylcyclohexene was enhanced in order to force it into the capsule cavity. Although decomposition of 4-nitrobenzaldehyde was not that prominent in comparison to benzaldehyde, no defined product was observable neither in GC, NMR or TLC.

Table 13 Screening for reaction conditions for 1-methylcyclohexene with benzaldehyde and 4-nitrobenzaldehyde

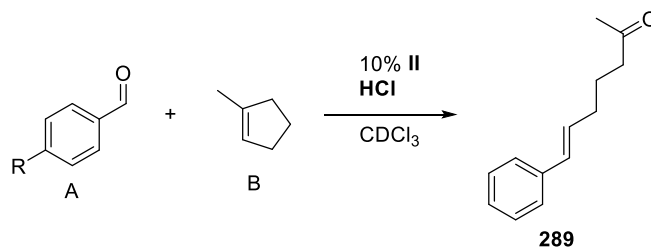


entry	R	ratio A:B	HCl	time	T	Consumption A
1	H	1:1	10%	3 d	60 °C	20%*
2	NO <sub>2</sub>	1:4	30%	5 d	30 °C	11%
3	NO <sub>2</sub>	1:4	30%	5 d	60 °C	23%
4	NO <sub>2</sub>	1:4	40%	5 d	30 °C	3%
5	NO <sub>2</sub>	1:4	40%	5 d	60 °C	27%

\*6 d decomposition

Since strained alkenes are more reactive, 1-methylcyclopentene and norbornene were tested with benzaldehyde and 4-nitrobenzaldehyde. In the case 1-methylcyclopentene a clean and sharp signal was observable after five days in the GC measurements for entries 1-3 with benzaldehyde and 4-7 with 4-nitrobenzaldehyde (Table 14).

Table 14 Screening for reaction conditions for 1-methylcyclopentene with benzaldehyde and 4-nitrobenzaldehyde



entry	R	ratio A:B	HCl	time	T	Consumption A
1	H	2:1	30%	5 d	30 °C	35%
2	H	2:1	30%	5 d	50 °C	51%
3	H	1:4	30%	3 d	50 °C	17%
4	NO <sub>2</sub>	1:4	30%	5 d	30 °C	80%
5	NO <sub>2</sub>	1:4	30%	5 d	60 °C	86%
6	NO <sub>2</sub>	1:4	40%	5 d	30 °C	65%
7	NO <sub>2</sub>	1:4	40%	5 d	60 °C	84%
8	NO <sub>2</sub>	1:100	30%	5 d	60 °C	100%
9	NO <sub>2</sub>	2:1	30%	5 d	30 °C	40%
10	NO <sub>2</sub>	2:1	30%	5 d	30 °C	40%
236	NO <sub>2</sub>	2:1	30%	5 d	50 °C	52%

Nevertheless, attempts to isolate the related product led to undefinable product mixtures in the NMR. For entries, 9-11 in Table 14, an excess of 4-nitrobenzaldehyde led to the same GC signal as for entries 4-7. After conversion the signals in the GC for benzaldehyde (11.128 min, Figure 44) and 4-nitrobenzaldehyde (14.105 min, Figure 45) displayed a different retention time, therefore these signals most likely are not caused by oligomerization of 4-methylcyclopentene. Interestingly, with 4-nitrobenzaldehyde in excess, no complete decomposition was observed, therefore it would seem that 1-methylcyclopentene reacts with the aldehyde first, which ultimately leads to decomposition.

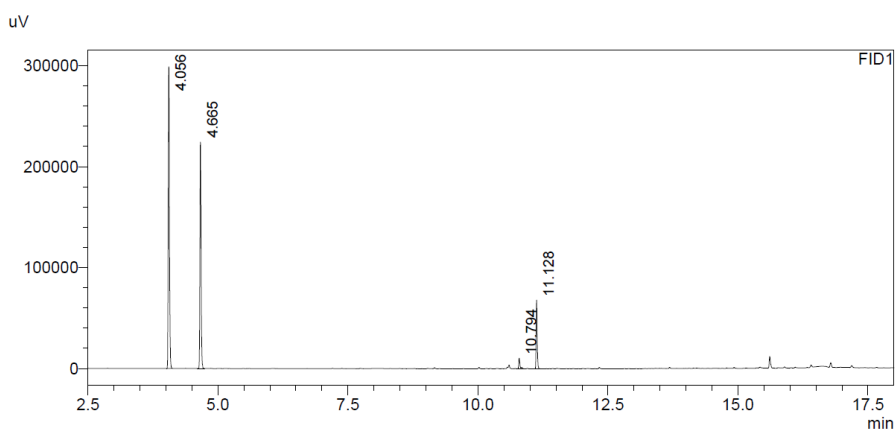
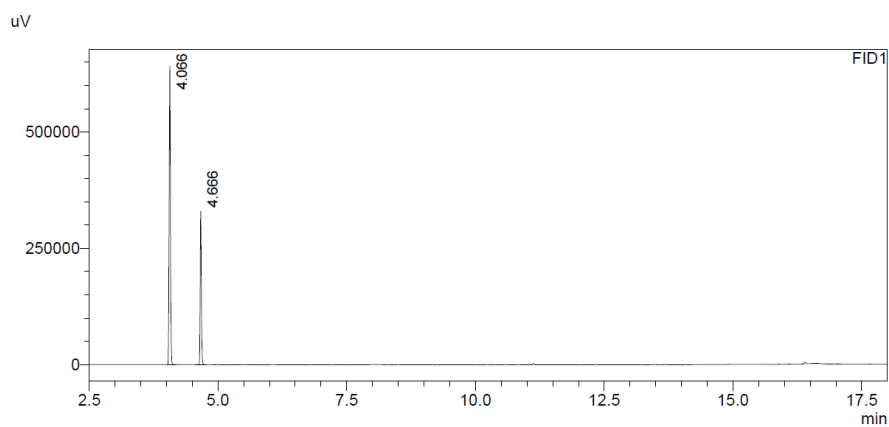


Figure 44 (Top) GC measurement: startpoint 0 d, 30 % HCl 30 °C for aldehyde (A) and 1-methylcyclohexene (B) 2:1 (entry 1 Table 14) (Bottom) GC measurement: conversion after 5 d.

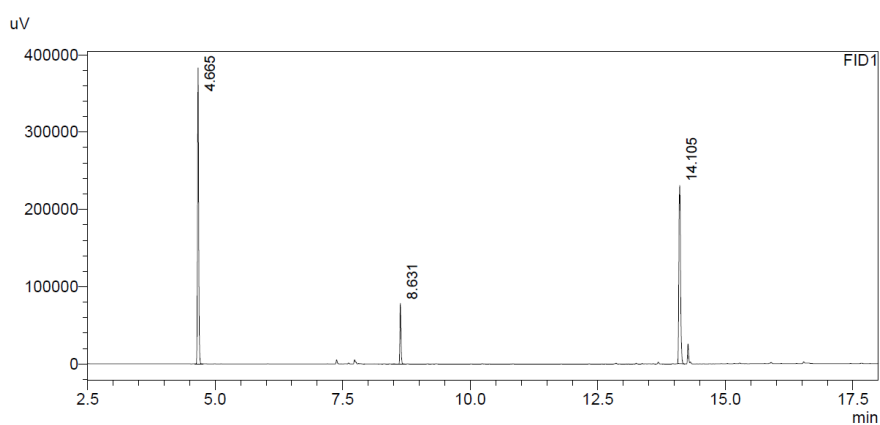
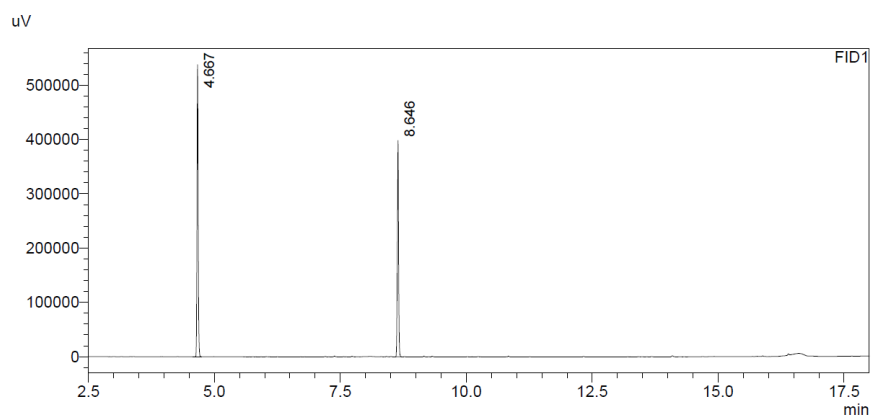
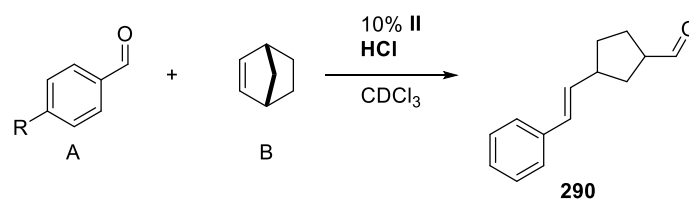


Figure 45 (Top) GC measurement: startpoint 0 d, 30 % HCl 30 °C for aldehyde (A) and 1-methylcyclohexene (B) 1:4 (entry 4 Table 14) (Bottom) GC measurement: conversion after 5 d.

Even though norbornene has a more strained double bond than cyclohexane, no conversion of the 4-nitrobenzaldehyde was observed (Table 15).

Table 15 Screening for reaction conditions for norbornene with 4-nitrobenzaldehyde



entry	R	ratio A:B	HCl	time	T	Consumption A
1	NO <sub>2</sub>	1:4	20%	9d	60 °C	0%
2	NO <sub>2</sub>	1:4	30%	7d	30 °C	0%
3	NO <sub>2</sub>	1:4	40%	7d	30 °C	0%
4	NO <sub>2</sub>	1:4	30%	7d	60 °C	1%
5	NO <sub>2</sub>	1:4	40%	7d	60 °C	3%

In summary, no metathesis product could be isolated, although in the presence of cyclohexene and cyclopentene new signals were observable in the GC measurement. Most likely these signals are caused by the decomposition of the respective aldehyde and not by metathesis. Even experiments with a high excess of the alkene did not lead to a defined product. Since the cavity of **II** is a bad host for non-polar guests, it is plausible that the alkene is unable to come into contact with the encapsulated aldehyde.



### 2.3 Summary and Outlook

Carbonyl-olefin metathesis is an emerging field with the potential to achieve the same universal applicability as the related olefin-olefin metathesis. Numerous catalytic systems have proven to be useful for the enablement of different types of carbonyl-olefin metathesis.<sup>47, 56</sup> The hexameric resorcinarene capsule has been shown to catalyze a broad scope of reactions, like terpene cyclization or carbonyl-olefin metathesis.

In the first part of this thesis, the scope of the ring-closing carbonyl-olefin metathesis to chiral 3-aryl-2,5-dihydropyrroles was expanded. Size limitations of the capsule cavity led to the investigation of *N*-sulfonyl protecting groups on four different amino acid derivatives. Mesyl proved to be an alternative to the larger tosyl-protecting group. The <sup>F</sup>Ts-protection group used for iron(III) catalysis did not provide satisfactory results. The cyclization catalyzed by **II**/HCl was found to be stereo preserving and also applicable for gram-scale synthesis.

In a second study, the mechanism of the intramolecular ring-closing carbonyl-olefin metathesis was investigated. Two possible mechanistic pathways for the [2+2] cycloaddition/ reversion have been reported or proposed in the literature, either an asynchronous concerted pathway or a stepwise pathway. Three representative substrates were tested with the catalyst **II** and FeCl<sub>3</sub>, in order to clarify if the mechanistic pathway is universal for one catalytic system. The activation parameters of the substrates were determined by an Eyring analysis and showed a negative  $\Delta S^\ddagger$  for every substrate with both catalysts and therefore an ordered transition state. Nevertheless, the determination of SKIE revealed different rate-limiting steps for the substrates even within a catalytic system. Attempts to intercept intermediate carbocations at the olefin moiety were successful. Subsequent analysis of an inactive mechanistic probe showed, that the ortho substituent by itself alters the mechanism and therefore no general conclusions could be drawn. So far, the rationale behind the different steps could not be finally determined. Therefore, additional mechanistic probes need to be tested, which do not alter the reactivity of the substrate too much. Based on the observation by the Li group, allyl-TMS is a promising candidate for such experiments. With the expected new insights from these tests, more specific calculations can be started in order to complete the picture of the carbonyl-olefin metathesis mechanism.

Expansion of the substrate scope towards alkyl ketones did not provide the metathesis product in useful quantities. Even though the conversion of the starting material was complete, analysis by GC showed that mostly decomposition of the starting material occurred.

Intermolecular ring-opening cross-metathesis catalyzed by **II**/ **HCl** led to the conversion of the respective aldehyde, nevertheless, no product was isolated. Most likely the non-polar properties of the alkenes prohibit encapsulation by **II** and therefore the formation of any metathesis product.

### 3. Glycosylation

#### 3.1 Introduction

Glycosides and glycans are one of the most important building blocks in an organism. However, control of the stereochemistry of glycosylation reactions remains challenging.

One of the first reported synthesis protocols for glycosylation was the synthesis of **293** by *Michael* in 1879 (Figure 46).<sup>115</sup> The reaction conditions led to the cleavage of the acetyl protection groups. In 1893 *Fischer* published a method for the glycosylation of the unprotected sugar with alcohols under acidic conditions (Figure 46).<sup>116</sup> Although many methods are available for the glycosylation reaction, most of them lack control over the stereoselectivity.<sup>117</sup>

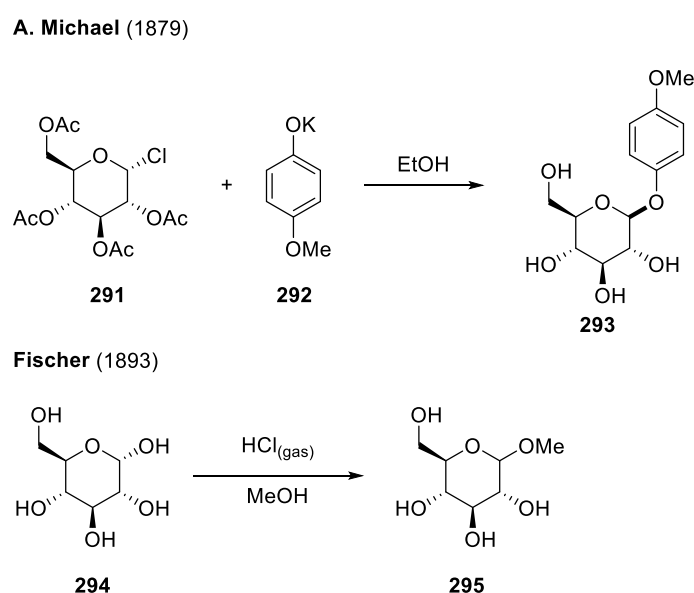


Figure 46 Glycosylations by *Michael* and *Fischer*.

*Koenig* and *Knorr* developed a glycosylation method based on heavy metals and glycosyl halides.<sup>118</sup> The mild conditions of this reaction allowed the preservation of the protection groups. The mechanism relies on the participation of the acetyl group next to the anomeric center, which reacts with the intermediate oxonium ion to form a dioxolanium ion. The nucleophile subsequently reacts via an  $S_N2$  mechanism under stereo-inversion (Figure 47).

Koenig and Knorr (1901)

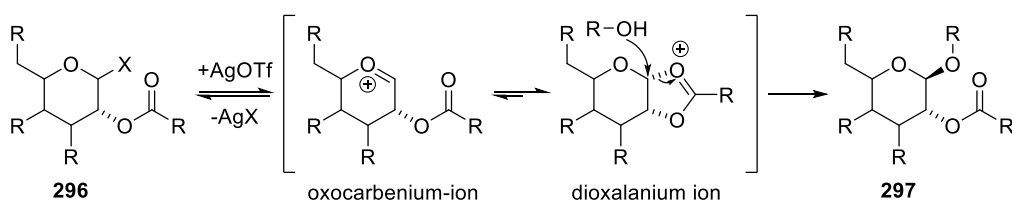


Figure 47 Mechanism of the *Koenig-Knorr* glycosylation.

To obtain complex oligoglycosides, more general methods have had to be developed. So far, protecting groups and coupling methods have had to be adjusted for every substrate and desired conformation. Instead of modeling every substrate, a catalyst that selectively performs glycosylation is desirable. A promising candidate was found with thiourea derivatives which are known to catalyze acetalizations.<sup>119</sup>

In 2007 the *Schreiner* group was able to install a THP protecting group on various alcohols under acid-free conditions with the thiourea catalyst **300**.<sup>120</sup> This method was applied to a broad range of alcohols, including tertiary or other sterically hindered ones. Within the group of tested substrates was glycosyl **301** which gave the 6-position (Figure 48).

Schreiner (2007)

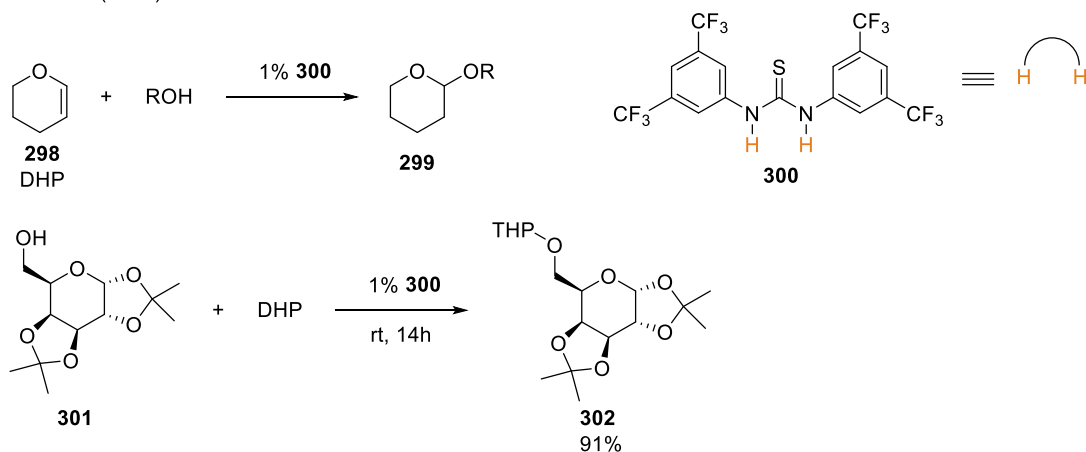


Figure 48 Acid-free acetalization of DHP with thiourea catalyst **300**.

The addition of the alcohol to DHP is a formal [2+2] cycloaddition. Since a concerted addition is forbidden, the mechanism proceeds asynchronously. The mechanism starts with the complexation of the alcohol by the thiourea catalyst (**304**), which enhances the acidity and polarizability of the alcohol (Figure 49). This activated alcohol interacts with the DHP from complex **305**. During the addition of the alcohol, catalyst **300** stays attached. The collapse of the product-catalyst complex **307** releases the final product **308** and enables the catalyst to enter a new catalytic cycle.

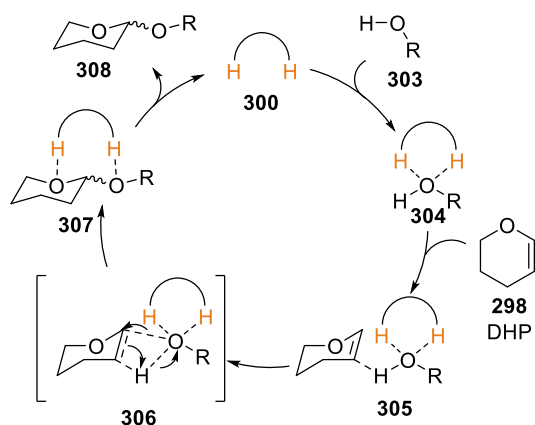


Figure 49 Activation of alcohols by **300** and addition to **298**.

Based on the results of the *Schreiner* group, *Galan* and *McGarrigle* developed an  $\alpha$ -selective synthesis of 2-deoxygalactosides from glycals (Figure 50).<sup>121</sup> The mild reaction conditions were compatible with a broad range of protection groups, even labile ones like MOM. The reaction showed a high  $\alpha$ -selectivity independent of the environment of the nucleophile.

Galan/ McGarrigle (2012)

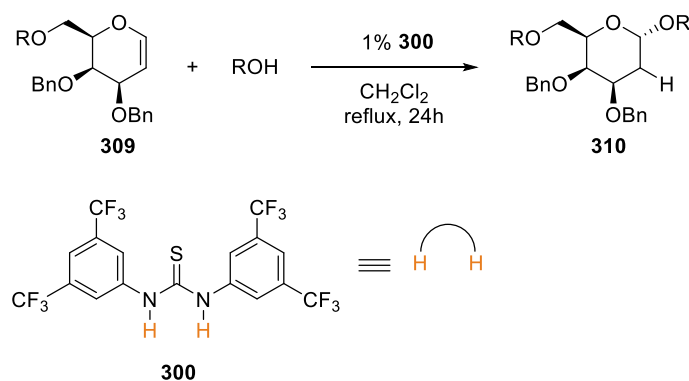


Figure 50 Mild addition of alcohols to glycals catalyzed by **300**.

The thioacetals remained untouched during the reaction, which enabled the synthesis of a trisaccharide in a one-pot reaction (Figure 51). In the first step, the thioglycoside **312** was added via the free 6-position to the glycal (**311**). In the next step, NIS and TMSOTf were added to activate the thioacetal thereby causing it to react with the third building block **313**.

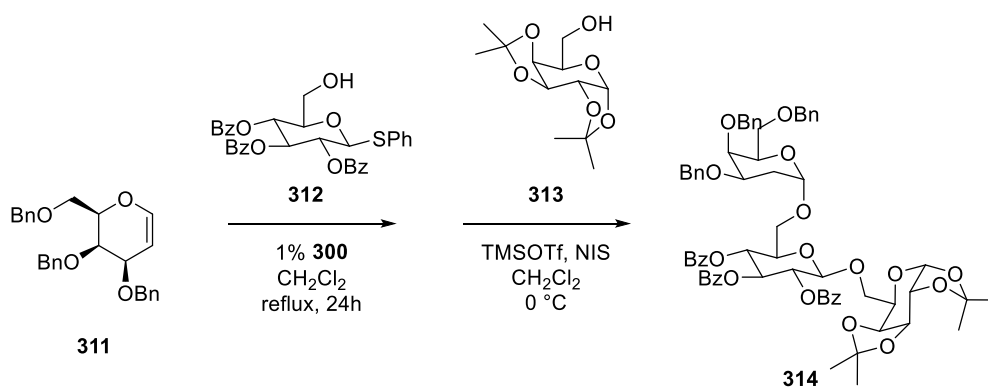


Figure 51 One-pot synthesis of trisaccharide **314**.

Experiments with the D-labelled glycal **311D** showed a *syn*-addition of the alcohol to the enol-ether (Figure 52). The underlying mechanism was hypothesized to be related to a thiourea alcohol complex similar to the mechanism proposed by Schreiner. This favors the less hindered side of the glycal.

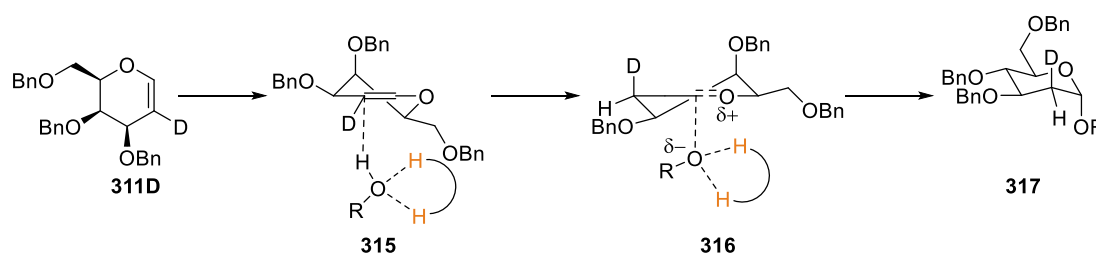


Figure 52 Mechanism of the *syn*-addition of alcohols to glycal.

In 2016, the *Ye* group successfully demonstrated the capability of the urea catalyst **300** to promote *Koenigs-Knorr* glycosylation of glycosyl halides.<sup>122</sup> The addition of the urea catalyst alone led to good yields but only poor stereoselectivity (Figure 53).

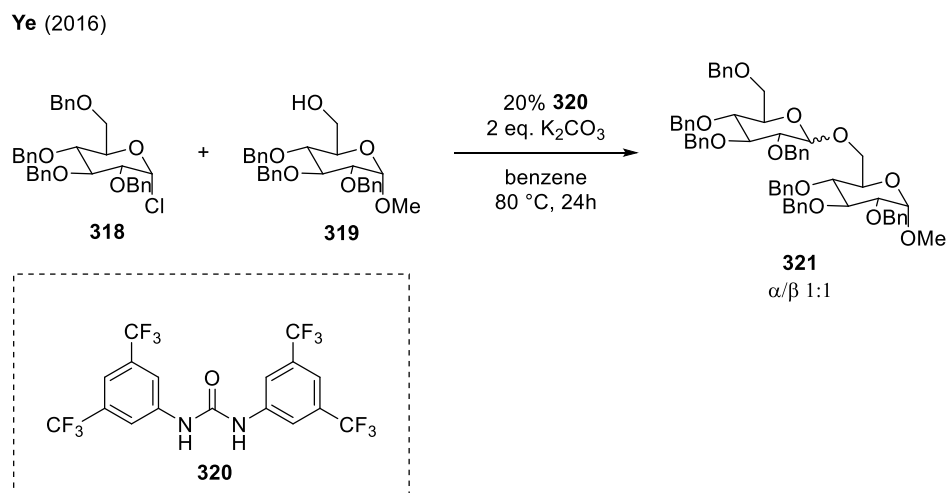


Figure 53 First glycosylations of **318** and **319** with solely **320** lead to an anomeric mixture.

Obtaining high  $\alpha$ -selectivity with perbenzylated glycosides is challenging, therefore the *Ye* group tried to influence the selectivity by chiral catalysts. Only catalysts with diphenylphosphino substituents led to a better  $\alpha$ -selectivity. Addition of phosphines as co-reagent indeed led to a higher selectivity, thus tri-(2,4,6-trimethoxyphenyl)-phosphine gave the best results (Figure 54). The *Ye* group hypothesized that there was a non-covalent interaction of the phosphine with the  $\beta$ -face of the anomeric center, favoring the attack from the  $\alpha$ -site.

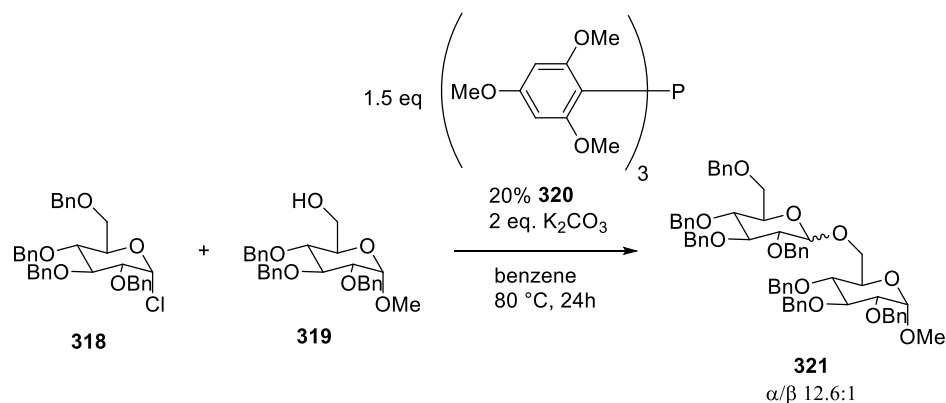


Figure 54 Stereoselectivity induction by the addition of tri-(2,4,6-trimethoxyphenyl)-phosphine.

The *Jacobsen* group designed a generally applicable catalyst to access  $\beta$ -glycosides from  $\alpha$ -glycosides (Figure 55).<sup>123</sup> The catalyst (**324**) was designed to activate the glycosyl halide (**322**) as well as the nucleophile via its thiourea moiety. Indoline-substituents were shown to provide a superior nucleophile binding site. Replacement of the indoline with less Lewis basic substituents led to a significant reduction of selectivity.

Jacobsen (2017)

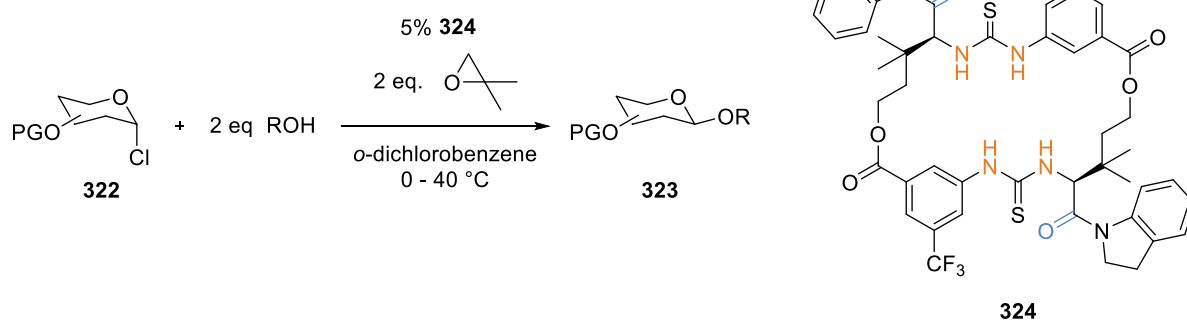
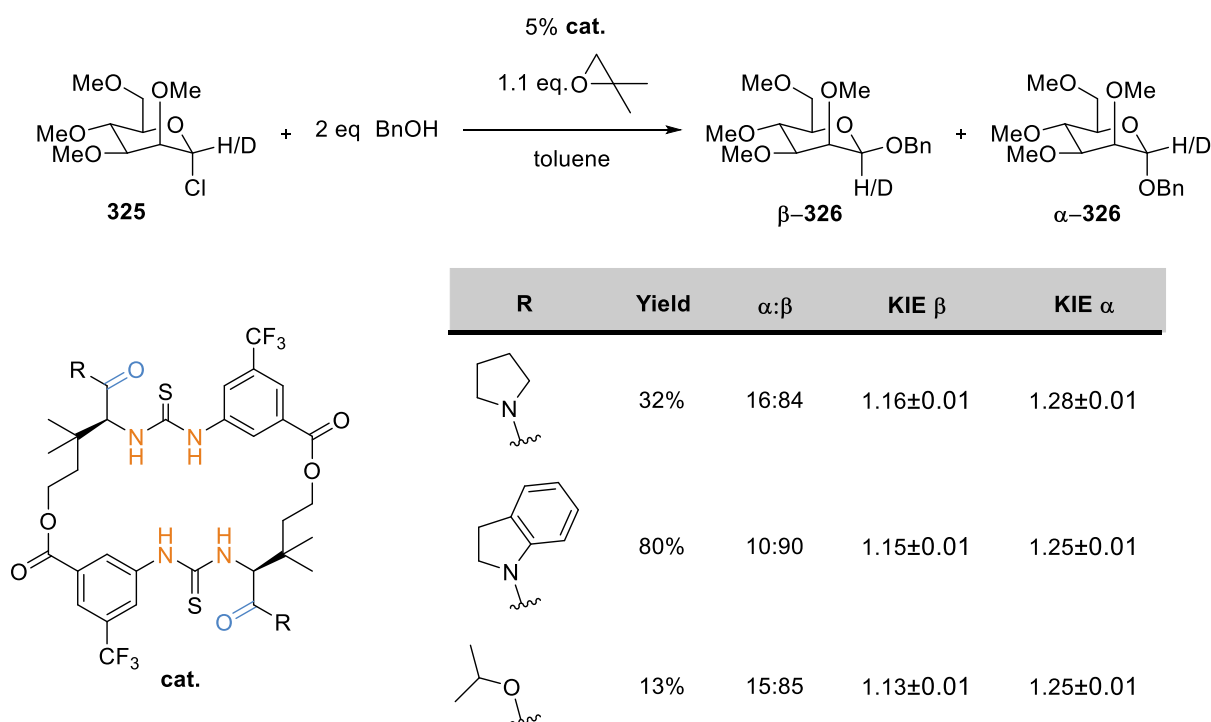


Figure 55  $\beta$ -selective glycosylation catalyzed by **324**.

Experiments by the *Jacobsen* group with **325** showed an increase of the observed isotopic effect with increased Lewis basicity of the substituents. Isotopic effects at the borderline to what is interpreted as carbocation were considered to be due to an increasing C-O bond distance in the transition state. Nevertheless, the obtained values were in the range of what is thought applicable for an S<sub>N</sub>2 transition state (Table 16, entries for KIE  $\beta$ ). Measurements of the minor  $\alpha$ -product resulted in higher values for the isotopic effect, which was interpreted as an S<sub>N</sub>1 reaction (Table 16, entries KIE  $\alpha$ ).

Table 16 Isotopic effects for different Lewis basic binding sites (R)



Density functional theory calculations by the *Jacobsen* group have shown there to be a loose and asynchronous transition state structure for the formation of the  $\beta$ -product, whereas the



halide of the glycosyl donor is activated by the thiourea moiety of **324** and the nucleophile is activated by the indoline moiety (Figure 56). The catalyst stabilizes the  $S_N2$  transition state and therefore enables the stereo-inversion of the deployed  $\alpha$ -substrates.

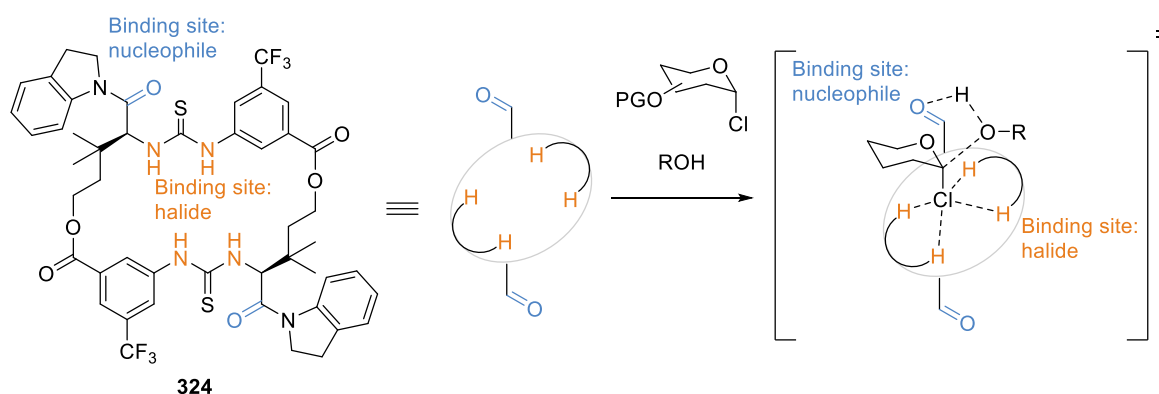


Figure 56 Dual activation of the glycosyl donor by the thiourea and the nucleophile by the indoline moiety.

The principle of a dual activation of the glycoside and nucleophile can also be found in the inverting cellulase enzyme.<sup>124</sup> In this case, the binding sites become active via a communicating hydrogen bond network.

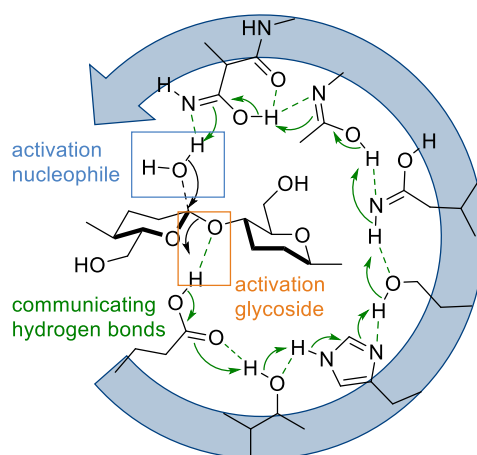


Figure 57 Dual activation of water and oligoglycoside by the communicating hydrogen bonding network of inverting cellulase.

A similar mode of activation has been found in 2020 for glycosylation reactions inside the hexamer **II**.<sup>104</sup> Reaction of mannose with methanol in the presence of **II** resulted in high yields of the desired  $\beta$ -product.

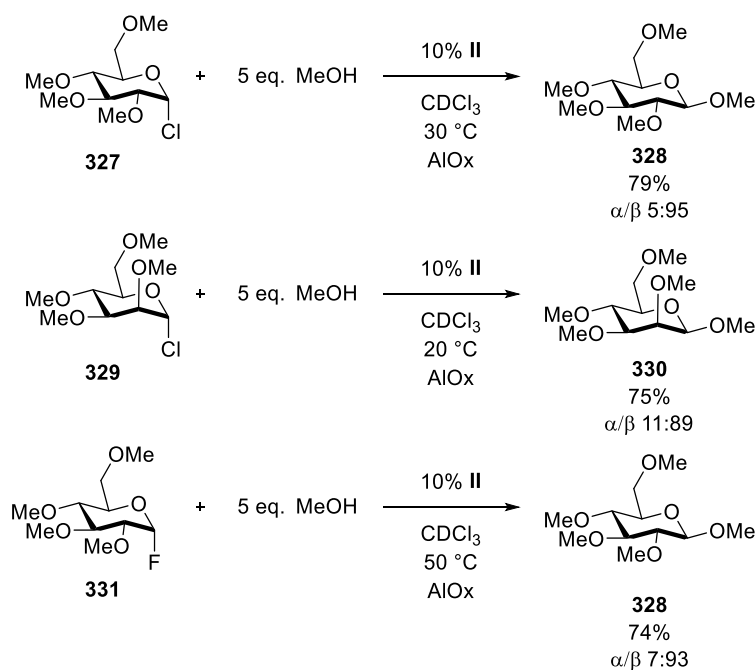


Figure 58 Initial glycosylation experiments with different glycosyl-donors.

Control experiments with strong-binding ammonium guests and size-exclusion experiments showed, that the reaction takes place inside the cavity of **II**. Reactions with the disassembled capsule and with the structural subunit, 4-hexylbenzene-1,3-diol showed the necessity of the assembly for catalysis. Pyrogallolarene, which is known to form similar assemblies like **II** but without water, was found to be unproductive for the reaction.

Glycosyl fluorides turned out to be the superior glycoside donor. Even challenging nucleophiles like secondary alcohol, such as cyclohexanol or sensitive alcohols such as 2-bromethanol were compatible with the reaction conditions. Moreover, disaccharides could be synthesized and even the steroid androsterone was successfully converted, thereby demonstrating the potential of **II** as a catalyst. The limited size of the cavity of **II** limits the scope of useable protecting groups for the glycoside donor. Allyl and acetate protection proved to be compatible with **II**. These can both be cleaved under mild enough conditions in order to prohibit anomerisation.

Although a broad substrate scope was revealed, the underlying mechanism causing the high  $\beta$ -selectivity of the reaction remained unknown. With the knowledge gained through the experiments for the mechanism of the carbonyl-olefin metathesis in chapter 2.2.2, a mechanistic investigation of the nature of the  $\beta$ -selectivity of the glycosylation inside **II** was started.

## 3.2 Results and Discussion

### 3.2.1 Reaction Order

In general, two scenarios may be used to explain the selectivity of the reaction, either an  $S_N2$  reaction or the formation of an oxocarbenium ion with a contact ion pair shielding the  $\alpha$ -face of the glycosyl donor (Figure 59).<sup>125</sup>

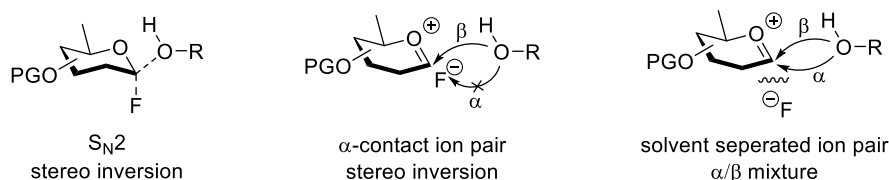


Figure 59 Stereo-inversion can be expected for an  $S_N2$  transition state or an  $\alpha$ -contact ion pair, solvent separation of the ion pair leads to a mixture of  $\alpha$  and  $\beta$ -anomer.

To gain insight into the reaction, the rate dependence of the glycosyl donor **331** as well as methanol as the nucleophile was determined. If the formation of an oxocarbenium ion is the rate-limiting step, the reaction is independent of the methanol concentration and displays a classic  $S_N1$  behavior (Figure 60).

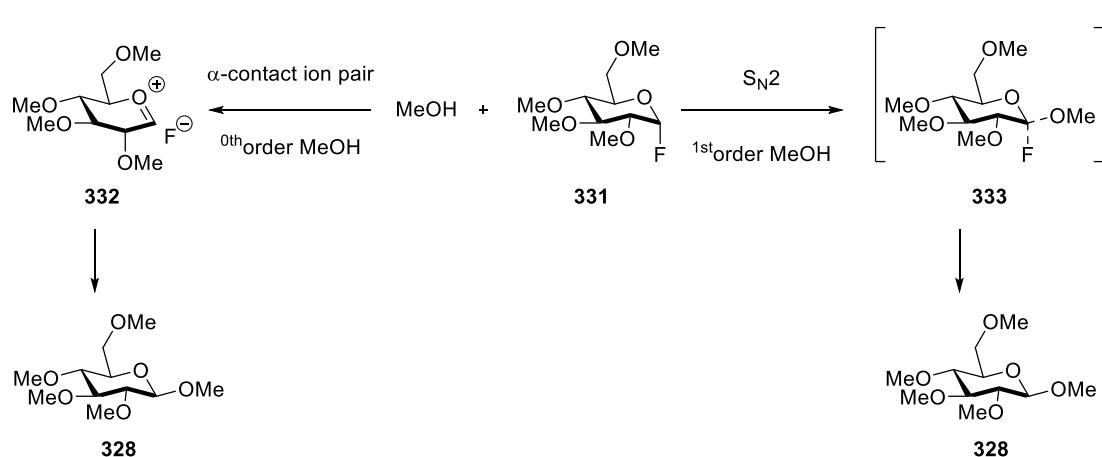


Figure 60 The reaction rate depends on the overall mechanism; the formation of an oxonium ion is independent of the methanol (0<sup>th</sup> order) concentration in contrast to an  $S_N2$  reaction (1<sup>st</sup> order).

The first measurement was performed with one, two and seven equivalents of methanol and one equivalent of **331**. The product (**328**) formation was tracked by analyzing aliquots of the reaction mixture by NMR with tetraethyl silane (TES) as the internal standard, thereby giving the rate of the reaction. The double logarithmic plot of the reaction rate versus the methanol concentration gave a slightly negative slope of -0.23 (Figure 61). The negative trend could stem

from a destabilization of the capsule at high methanol concentrations. Therefore, the slope can be interpreted as a 0<sup>th</sup> order dependence on methanol, so an S<sub>N</sub>1 reaction is plausible. However, saturation effects could not be excluded from these experiments at this point. In the case of an S<sub>N</sub>1 reaction, the rate dependence on methanol should display a 0<sup>th</sup> order even at lower methanol concentrations, therefore another set of experiments was carried out with 0.50 and 0.25 equivalents of methanol. In the range from 0.25 – 1.00 equivalents, the reaction showed a first-order (slope: 1.031, Figure 61) dependence on methanol and therefore showed saturation for the whole curve with the maximum reaction speed reached at one equivalent methanol. Therefore, the reaction showed an S<sub>N</sub>2 behavior rather than an S<sub>N</sub>1.

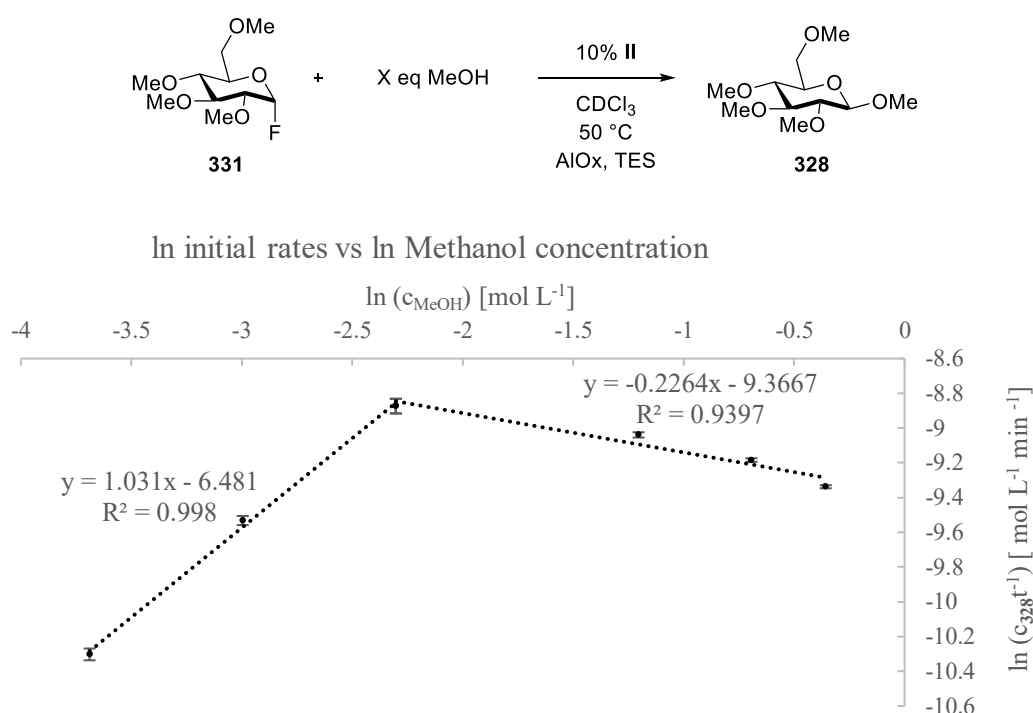
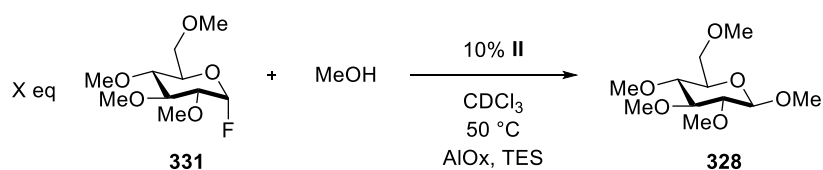


Figure 61 The dependence of the rate dependence of the glycosylation of **331** with MeOH on MeOH.

For the glycoside donor a first-order dependence was also observed, which showed that the transition state contains a 1:1 ratio of glycosyl donor and nucleophile (Figure 62).



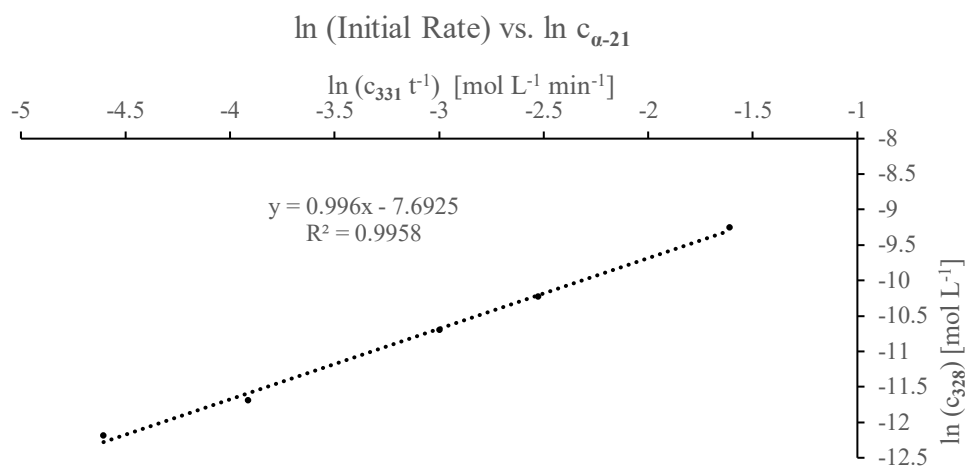


Figure 62 The dependence of the rate dependence of the glycosylation of **331** with MeOH on **331**.

### 3.2.2 Secondary Kinetic Isotopic Effect

Secondary kinetic isotope effects play an important role in the determination of transition state characteristics. In particular, in glycosylation chemistry, there are often no sharp distinctions between  $S_N1$  and  $S_N2$  transition states for nucleophilic substitutions at the anomeric center.<sup>125</sup> The possible transition state can vary from a classical  $S_N2$  reaction to more or less separated ion pairs or a discrete oxocarbenium intermediate (Figure 59). In order to obtain information about the transition state characteristics, kinetic experiments with labeled compound **331D** were carried out. The experiments were performed according to the *Singleton* method, where the isotopic ratio of the educts and the product were determined before and after conversion (F) (Figure 63). The ratio was determined after the initial conversion between 20 – 30 %.<sup>126</sup>

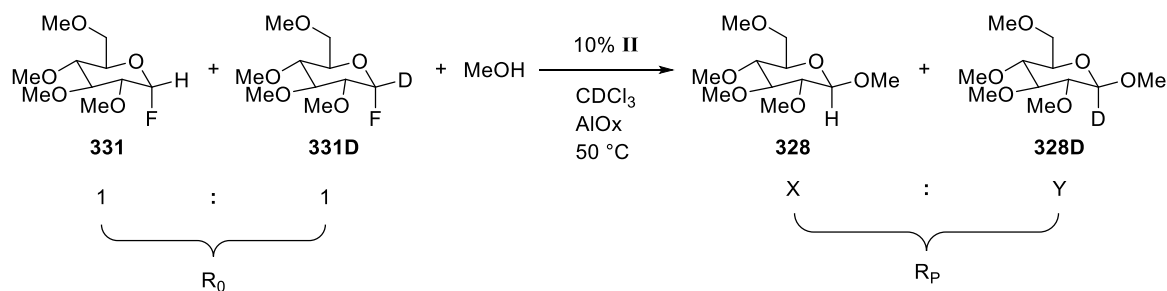


Figure 63 SKIE determination according to the *Singleton* method. The isotopic ratio of the educts (**331/331D**) ( $R_0$ ) is 1:1 at the beginning. After 20-30 % conversion the isotopic ratio of the products (**328/ 328D**) ( $R_P$ ) is determined.

The reaction was then quenched, and the products were isolated by column chromatography which allows easier access to the desired NMR signals due to obtaining a cleaner spectrum compared to the one obtained for a reaction aliquot. The conversion of the reaction was determined via such a reaction aliquot with an internal standard in order to obtain more precise data which are not altered by-product losses through columns or similar. The KIE can be determined with Equation 1

Equation 1

$$KIE = \frac{\ln(1 - F)}{\ln\left(1 - \left(F * \frac{R_P}{R_0}\right)\right)}$$

$F$  = conversion

$R_0$  = isotopic ratio educts starting point

$R_P$  = isotopic ratio products at the time of  $F$

The KIE for the reaction of glycosyl **331/331D** with methanol was determined to be  $1.19 \pm 0.02$ . This value is at the borderline of what is reported to be an  $\text{S}_{\text{N}}2$  transition state or an oxocarbenium ion.<sup>127, 128</sup> This together with the reaction order of two, means that a loose  $\text{S}_{\text{N}}2$  transition state is the most plausible one for the explanation of the high selectivity of the reaction. Although the results gave an explanation for the selectivity, they do not provide a satisfactory answer to the question of how the hexamer **II** is able to activate the nucleophile and glycosyl donor.

### 3.2.3 Proton Inventory

The acidity of the hexamer ( $pK_A$ : 5.5-6) is not sufficient to promote the reaction, as it was demonstrated by *T.-R. Li* with a control experiment using acetic acid ( $pK_A$ : ~5).<sup>90, 104</sup>

The hexamer is interconnected via a network of 60 hydrogen bonds. It can be envisioned that this network could perform a dual activation of the nucleophile and glycosyl donor via a communicating proton transfer, similar to the inverting cellulase enzyme (Figure 57). In an QM/MM enhanced sampling molecular dynamics (metadynamics) simulation by *GM. Piccini* -a collaboration partner- energy profiles were shown in which such a communicating hydrogen-bonding network can be identified (Figure 64).

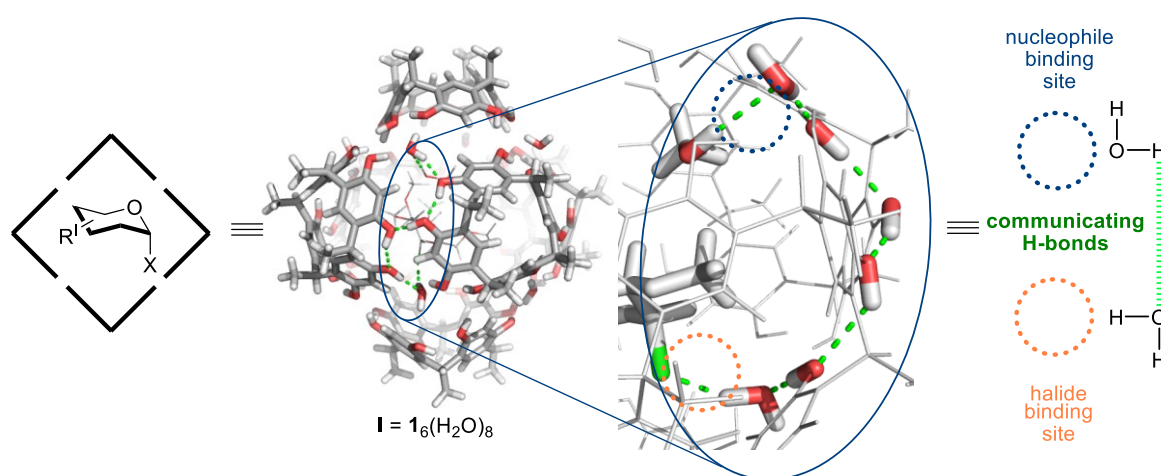


Figure 64 Dual activation of the glycoside donor and nucleophile by the communicating hydrogen-bond network of **II**.

Experimentally, the participation of multiple hydrogens in the transition state can be probed by a proton inventory experiment. Such experiments were first developed to analyze enzyme mechanisms.<sup>129</sup> The experiment is based on a collection of multiple single experiments in which the exchangeable protons are substituted by deuterium. In enzyme chemistry, this is often realized by applying different mixtures of H<sub>2</sub>O and D<sub>2</sub>O as solvents. The maximum isotope effect is reached, when the system is completely saturated with deuterons, in the example with water as a solvent, this would be at 100 % D<sub>2</sub>O as solvent. The D/H ratio is therefore the proportion of deuterium to the exchangeable hydrogens in the reaction.

Different D/H ratios cause isotopic effects of different magnitude. The obtained isotopic effects can be plotted against the D/H ratio, where the shape of the obtained plot depends on the number of hydrogen bonds in the transition state. The overall isotopic effect is the product of the isotopic effects induced by every single hydrogen bond. A single hydrogen bond in the transition state,

therefore, would result in a linear relationship between the isotopic effect and the D/H ratio, two hydrogen bonds in a quadratic relationship and multiple bonds in an exponential effect.<sup>130</sup>

The challenge of performing a proton inventory study with hexamer **II** lies in the use of chloroform as a solvent. Therefore, the D/H ratio cannot be adjusted by the use of different solvent ratios, but rather has to be adjusted by the compounds in the system which possess exchangeable hydrons. Hydrons are provided by the water and the phenols of **II**, the hydroxy group of methanol and the water present in the solvent (Table 17). In order to obtain the maximum KIE, every subcomponent has to be completely deuterated in theory, all other ratios can therefore be obtained by partially or completely exchanging one or two subcomponents. For methanol, this is easily achievable by using the commercially available methanol-d<sub>1</sub>. Methanol-d<sub>4</sub> was neglected as a deuterium source since the interaction of the methyl group and the hydrogen bonding was not clear and should not be altered. To control the water content of the used chloroform, two possibilities have been considered: use of dry solvent or saturation of dry chloroform with H<sub>2</sub>O respectively D<sub>2</sub>O. The use of dry solvent is not feasible since it leads to solubility issues of **II**. Therefore, a saturation of dry CDCl<sub>3</sub> with H<sub>2</sub>O or D<sub>2</sub>O was chosen as being more practical. The water content was determined via NMR of the H<sub>2</sub>O saturated chloroform sample. Karl-Fischer titration of both H<sub>2</sub>O and D<sub>2</sub>O saturated chloroform revealed, that the uptake capacity of chloroform for D<sub>2</sub>O is roughly 20 % lower than for H<sub>2</sub>O. Therefore, the initial non-deuterated sample was adjusted with dry solvent to match the D<sub>2</sub>O content of the other probes. All other experiments were carried out solely with D<sub>2</sub>O saturated CDCl<sub>3</sub> in order to avoid error-prone adjustments. The D/H exchange of the resorcinarene monomer **238** was achieved by the use of several cycles of drying **238** under high vacuum and dissolving it in a mixture of dry THF with 20 % D<sub>2</sub>O. With this method, 52 % of protons could be exchanged with deuterium.

Table 17 Proportion of the overall hydron concentration of the reaction by subcomponents

Proton Source	Hydrons [mmol]	Proportion
CDCl <sub>3</sub>	6.45E-02	11.3%
<b>II</b>	2.54E-01	44.7%
MeOH	2.50E-01	44.0%
Sum	5.67E-01	100%



Unfortunately, **238** is slightly hygroscopic and therefore the D/H ratio is not stable over time. Consequently, the experiments necessary for the proton inventory needed to be carried out at the same time. To avoid strong deviations from the deuterium-enriched **238**, only the last two experiments were carried out with it. Plotting the KIE of the experiments against their D/H ratio resulted in the graph of

Figure 65. The data points do not follow a linear dependency and instead either display a quadratic or exponential shape. To see if a quadratic function fits the datapoints, a linear function was fitted to the square root of the KIE values (

Figure 66). Only a poor fit was obtained for this plot and therefore it was the case that more than two hydrogens participate in the transition state. This supports the model of a communicating hydrogen-bond network as the dual activation for the glycosylation of **331** and methanol.

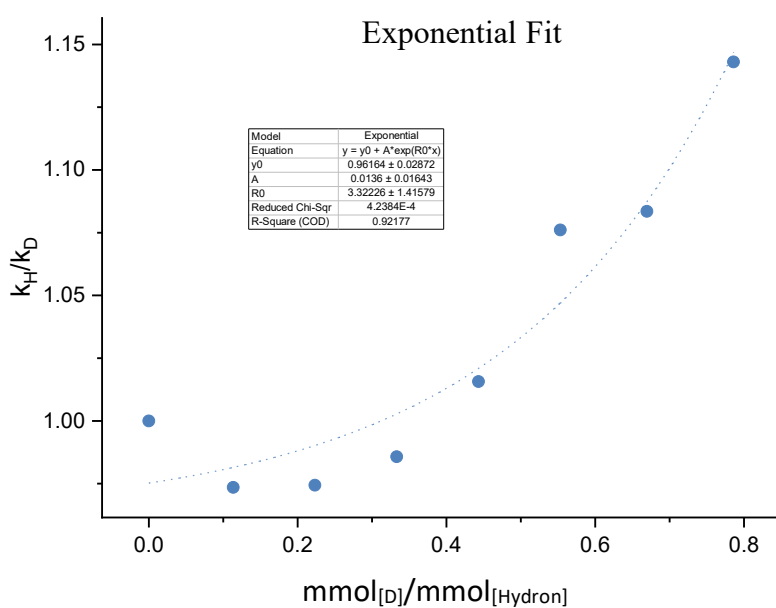


Figure 65 Kinetic isotope effect ( $k_H/k_D$ ) vs. the D/H ratio with an exponential fit.

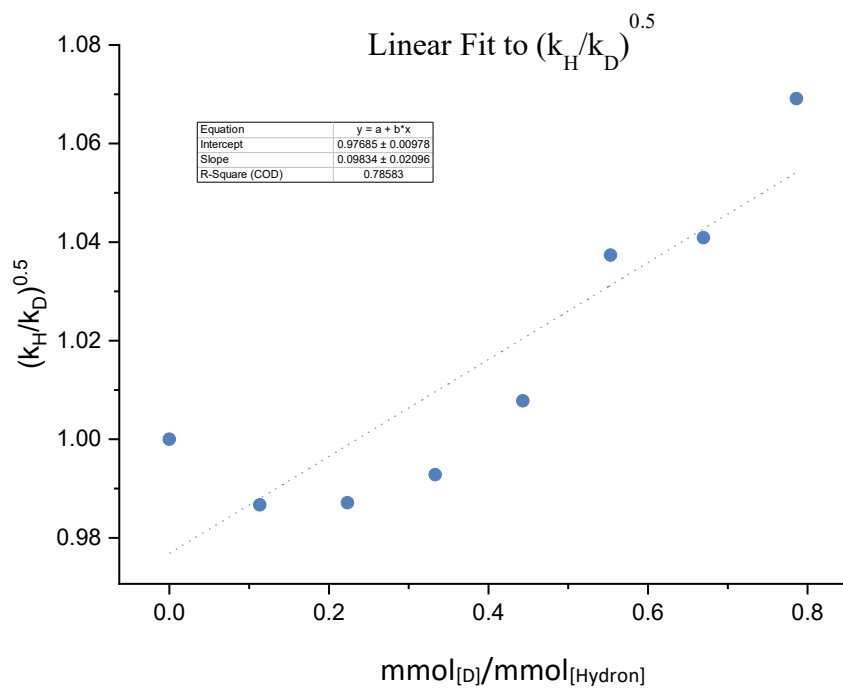


Figure 66 Square root of the kinetic isotope effect ( $k_H/k_D$ ) vs. the D/H ratio with a linear fit.

### 3.3 Summary and Outlook

An initial kinetic analysis with **331** showed that the capsule catalyzed glycosylation occurs via a second-order reaction. The SKIE of 1.19 indicates a loose S<sub>N</sub>2 mechanism. However, a comparison to literature values is not conclusive about this, as similar values were interpreted either as consistent with an intermediate with oxo-carbonium ion character or a loose S<sub>N</sub>2 mechanism. Since the results did not provide a distinct explanation for the high β-selectivity, model calculations by *GM. Piccini* -a collaboration partner- indicated a double activation of a communicating hydrogen bond network as a possible explanation. To provide further evidence for this hypothesis, a proton inventory study was carried out, to evaluate if multiple hydrogen bonds participate in the transition state. Indeed, the obtained data indicated that multiple hydrogen bonds are being formed and broken in the transition state. Nevertheless, further studies have to be performed to gain a complete picture of the reaction. The proton inventory study should be expanded to other nucleophiles and glycosyl donors. Moreover, natural abundance <sup>13</sup>C measurements could help in identifying potential charge formation at the anomeric center. Understanding the mechanism is essential to expanding the substrate scope and identifying other reactions that may benefit from such a dual activation mode.

## 4. Index of Abbreviations

°C	degree Celsius
Å	Ångström
Ac	acetyl
Ar	aryl
Boc	tert-butyloxycarbonyl
Cat.	catalyst
cHex	cyclo hexane
δ	chemical shift
d	day
DCE	1,2-dichloroethane
DCM	dichloromethane
DFT	density functional theory
DMF	N,N-dimethylformamide
DMSO	dimethylsulfoxide
DOSY	diffusion ordered spectroscopy
ESI	electrospray ionization
Et	ethyl
<i>et al.</i>	et alii (and others)
EPR	electron paramagnetic resonance
eq.	equivalent
<sup>F</sup> Ts	4-trifluoromethylbenzenesulfonyl
g	gram
GC	gas chromatography
GOAc	geranyl acetate
GOH	geraniol
h	hour
HPLC	high performance liquid chromatography
Hz	hertz
ISC	intersystem crossing
Iso.	isolated
K	kelvin
L	liter
LOAc	linalyl acetate
LOH	linalool

μL	microliter
μmol	micromol
μg	microgram
M	molar
Me	methyl
mg	milligram
MHz	Megahertz
min	minute
mL	milliliter
mm	millimetre
mmol	millimol
mol	mol
MOM	methoxymethyl
MS	mass spectroscopy
Ms	mesyl
MW	microwave
n. a.	not analyzed
<i>n</i> -BuLi	<i>n</i> -butyllithium
NMR	nuclear magnetic resonance
NOESY	nuclear Overhauser effect spectroscopy
NOAc	neryl acetate
NOH	nerol
Nu	nucleophile
OAc	acetate
PG	protecting group
Ph	phenyl
ppm	parts per million
R	organic residue
rt	room temperature
SKIE	secondary kinetic isotope effect
TBAB	tetrabutylammonium bromide
TFA	trifluoroacetic acid
THF	tetrahydrofuran
TMS	trimethyl silane
Tr	tritylium

## 5. Bibliographic Data of Complete Publications

### Expanding the protecting group scope for the Carbonyl-olefin Metathesis approach to 2,5-dihydropyrroles

Fabian Huck,<sup>1</sup> Lorenzo Catti,<sup>2</sup> Gian Lino Reber,<sup>1</sup> Konrad Tiefenbacher<sup>1,3\*</sup>

1] Department of Chemistry, University of Basel, Mattenstrasse 24a, CH-4058 Basel, Switzerland

2] Laboratory for Chemistry and Life Science Institute of Innovative Research Tokyo Institute of Technology, 4259-R1-28, Nagatsuta, Midori-ku, Yokohama 226-8503, Japan

3] Department of Biosystems Science and Engineering, ETH Zurich, Mattenstrasse 26, CH-4058 Basel,

Switzerland

\*Corresponding Author: [konrad.tiefenbacher@unibas.ch](mailto:konrad.tiefenbacher@unibas.ch); [tkonrad@ethz.ch](mailto:tkonrad@ethz.ch)

Originally published in *J. Org. Chem.* 2022, 87, 1, 419–428

DOI: <https://doi.org/10.1021/acs.joc.1c02447>

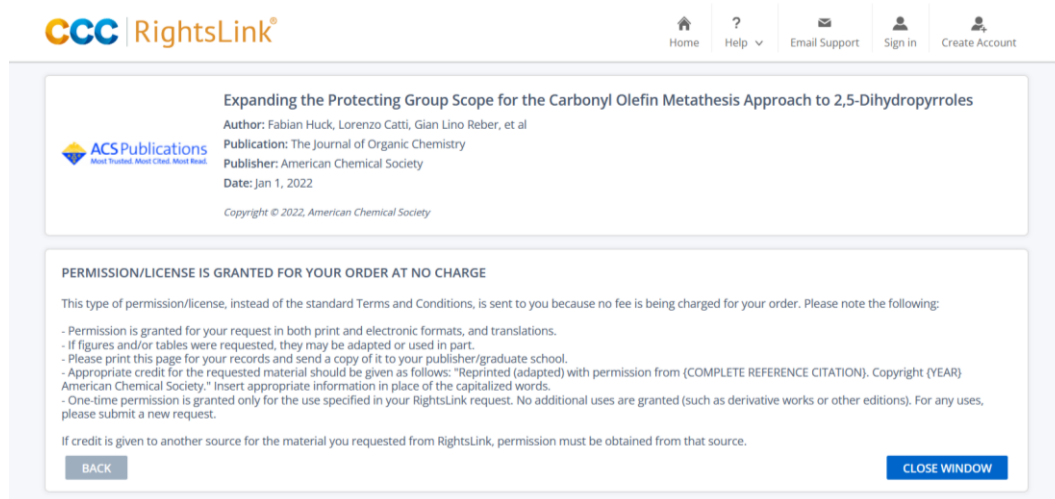
URL <https://pubs.acs.org/doi/10.1021/acs.joc.1c02447>

## 6. Reprints and Reprint Permissions

The manuscript published in *Journal of Organic Chemistry* is reproduced with the permission of *American Chemical Society*.

Expanding the protecting group scope for the Carbonyl-olefin Metathesis approach to 2,5-dihydropyrroles

Huck, F.; Catti, L.; Reber, g. L.; Tiefenbacher, K., Expanding the Protecting group Scope for the Carbonyl-olefin Metathesis Approach to 2,5-Dihydropyrroles. *J. Org. Chem.* **2022**, *87* (1), 419-428.



The screenshot shows the CCC RightsLink interface. At the top left is the logo "CCC RightsLink®". On the top right are navigation links: Home, Help, Email Support, Sign in, and Create Account. The main content area displays the following information:

**Expanding the Protecting Group Scope for the Carbonyl Olefin Metathesis Approach to 2,5-Dihydropyrroles**  
Author: Fabian Huck, Lorenzo Catti, Gian Lino Reber, et al  
Publication: The Journal of Organic Chemistry  
Publisher: American Chemical Society  
Date: Jan 1, 2022  
Copyright © 2022, American Chemical Society

**PERMISSION/LICENSE IS GRANTED FOR YOUR ORDER AT NO CHARGE**

This type of permission/license, instead of the standard Terms and Conditions, is sent to you because no fee is being charged for your order. Please note the following:

- Permission is granted for your request in both print and electronic formats, and translations.
- If figures and/or tables were requested, they may be adapted or used in part.
- Please print this page for your records and send a copy of it to your publisher/graduate school.
- Appropriate credit for the requested material should be given as follows: "Reprinted (adapted) with permission from (COMPLETE REFERENCE CITATION). Copyright (YEAR) American Chemical Society." Insert appropriate information in place of the capitalized words.
- One-time permission is granted only for the use specified in your RightsLink request. No additional uses are granted (such as derivative works or other editions). For any uses, please submit a new request.

If credit is given to another source for the material you requested from RightsLink, permission must be obtained from that source.

Buttons: BACK, CLOSE WINDOW

## Expanding the Protecting Group Scope for the Carbonyl Olefin Metathesis Approach to 2,5-Dihydropyrroles

Fabian Huck, Lorenzo Catti, Gian Lino Reber, and Konrad Tiefenbacher\*

Cite This: *J. Org. Chem.* 2022, 87, 419–428

Read Online

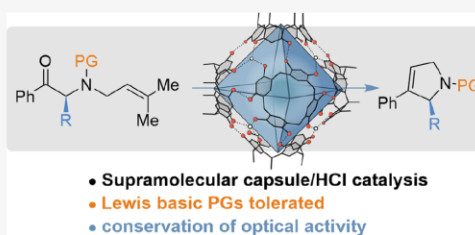
ACCESS |

Metrics & More

Article Recommendations

Supporting Information

**ABSTRACT:** Chiral pyrrolidine derivatives are important building blocks for natural product synthesis. Carbonyl olefin metathesis has recently emerged as a powerful tool for the construction of such building blocks from chiral amino acid derivatives. Here, we demonstrate that the supramolecular resorcinarene catalyst enables access to chiral 2,5-dihydropyrroles under Brønsted acid catalysis. Moreover, this catalytic system even tolerated Lewis-basic-protecting groups like mesylates that are not compatible with alternative catalysts. As expected for conversion inside a closed cavity, the product yield and selectivity depended on the size of the substrates.



### INTRODUCTION

Pyrroles and pyrrolidines are found in many natural products and play an important role as a precursor in drug synthesis.<sup>1–4</sup> However, their synthesis, especially of optically active derivatives, remains challenging.<sup>5,6</sup> Recently, carbonyl olefin metathesis (COM) has emerged as a useful tool to prepare chiral 2,5-dihydropyrroles, also termed 3-pyrrolines (Figure 1).<sup>7,8</sup> The COM reaction is related to the well-established olefin metathesis, but instead of the metathesis of two olefin moieties, it involves one carbonyl and one alkene moiety.<sup>9,10</sup> It has received increasing attention since the discovery of iron(III) chloride as an efficient and rather broadly applicable catalyst by the Schindler group in 2016.<sup>11,12</sup> The Li group presented the first approach to synthesize 2,5-dihydropyrroles via carbonyl olefin metathesis using 20% iron(III) chloride and an excess of allyl trimethyl silane.<sup>7</sup> The allyl trimethyl silane functions as a scavenger for the formed benzaldehyde (Figure 1a), which was suggested to inhibit the reaction by catalyst binding. The first catalytic approach without a stoichiometric additive was presented in 2018 by the Schindler group with the introduction of an electron-poor protecting group.<sup>8</sup> It was found that the *p*-toluenesulfonamide group acted as a competitive catalyst binding site, preventing turn-over with substoichiometric amounts of iron(III) chloride. The use of the electron-deficient protecting group 4-trifluoromethylbenzene sulfonyl (trifluorotsyl, <sup>t</sup>F<sub>3</sub>Ts) reduced the undesired catalyst binding, enabling the use of catalytic amounts of iron(III) chloride (Figure 1b). Moreover, the Schindler group demonstrated that the use of amino acids as starting materials enables facile access to chiral, optically active, 3-aryl-2,5-dihydropyrroles. In 2020, the Schindler group was able to expand the substrate scope and access tetrahydropyrrolidines.<sup>13</sup> Recent findings in the Nguyen group demonstrated

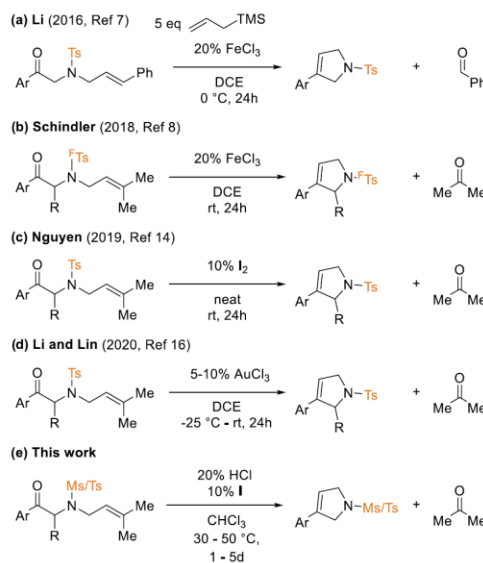


Figure 1. Synthetic routes toward 3-aryl-2,5-dihydropyrroles.

Received: October 7, 2021

Published: December 20, 2021





that other catalysts ( $I_2$ , NIS, ICl)<sup>14,15</sup> are able to convert regular tosyl-protected substrates with substoichiometric amounts of catalyst (Figure 1c). Li and Lin reported the use of  $AuCl_3$  as a catalyst for the COM approach to pyrrolidines (Figure 1d).<sup>16</sup> Lambert and co-workers demonstrated that related N-heterocycles are also accessible by COM via a [3 + 2] cycloaddition/cycloreversion mechanism.<sup>17</sup> We here present that the catalyst combination of the supramolecular capsule **I** (Figure 2) and HCl is able to tolerate not only the

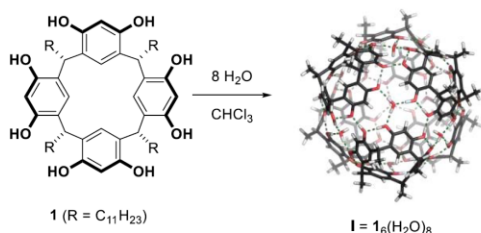


Figure 2. Structure of the self-assembled hexameric resorcinarene capsule **I** and its precursor resorcinarene **1**.

toluenesulfonyl protecting group but also the more Lewis-basic sulfonamide moiety formed from the mesyl-protecting group (Figure 1e). To our knowledge, this is the first report about the successful use of the mesyl-protected nitrogen for a COM reaction without the need for (super)stoichiometric additives.<sup>7</sup>

In 2018, we reported that the hexameric resorcinarene capsule (**I**) in the presence of HCl is a competent catalyst for the COM reaction.<sup>18</sup> In apolar solvents, resorcinarene **1** forms a dynamic hexamer interconnected via a hydrogen-bond network (Figure 2).<sup>19–22</sup> This supramolecular capsule has been successfully applied for catalysis of reactions with cationic intermediates/transition states.<sup>23–31</sup> In this work, we present the synthesis of 3-aryl-2,5-dihydropyrroles with three different sulfonamide-protecting groups (tosyl, mesyl, trifluorotolyl) catalyzed by **I**/HCl. Mesylates are more electron-rich than tosylates and trifluorotolylates and therefore not suitable for iron(III) catalysis. Moreover, the mesyl group can be removed selectively in the presence of other sulfonamide groups, which makes it suitable for the synthesis of more complex target compounds.<sup>32</sup> Therefore, establishing the mesyl group as an orthogonal protecting group for the COM reaction can be considered highly desirable.

## RESULTS AND DISCUSSION

Initially, the established reaction conditions from our previous work on the COM reaction (50 °C, 5% HCl, 10 mol % **I**) were explored.<sup>18</sup> However, these conditions that were optimized for non-nitrogen-containing substrates exclusively resulted in only 30% yield of the desired COM product **2A<sup>Ts</sup>** (Table 1, entry 1). Mainly deallylation to **2B<sup>Ts</sup>** was observed (45%). The reduction of the HCl concentration to 2.5% did not improve the outcome, as even more deallylation was observed (entry 2). Subsequently, the reaction was explored at room temperature (entries 5–9). Due to the slow conversion at 2.5 and 5% HCl loadings (entries 8–9), we explored higher concentrations (10–30%, entries 5–7). It was found that 20% HCl produced satisfactory results (85% of the desired COM product **2A<sup>Ts</sup>** and only 15% of **2B<sup>Ts</sup>**). However, the fluctuation of room temperature did lead to reproducibility issues. To establish

Table 1. Optimization of HCl Concentration and Temperature<sup>a,b</sup>

entry	T [°C]	HCl [mol%]	Conversion <sup>a</sup>	Yield <sup>b</sup> <b>2A<sup>Ts</sup></b>	Yield <sup>b</sup> <b>2B<sup>Ts</sup></b>
1	50 °C	5%	100%	30%	45%
2		2.5%	95%	37%	53%
3	30 °C	30%	100%	69%	15%
4		20%	100%	80%	20%
5		30%	100%	75%	17%
6	20%	100%	85%	15%	
7	rt	10%	89%	68%	26%
8		5%	48%	30%	4%
9		2.5%	26%	9%	0%
10	4 °C	30%	33%	27%	0%

<sup>a</sup>Conversion was determined by <sup>1</sup>H NMR, with tetraethylsilane as internal standard after 24 h. <sup>b</sup>Yields were determined by <sup>1</sup>H NMR, with tetraethylsilane as internal standard after 24 h.

reproducible reaction conditions, the reaction was carried out at 30 °C (entry 4), which resulted in a good yield of 80% of **2A<sup>Ts</sup>**. Acid concentrations above 20% lead to a decreased COM product formation, whereas the deallylation seems to be mainly dependent on the temperature.

Next, we investigated the influence of the alkene substitution. The unsubstituted olefin **2<sup>allyl</sup>** (Figure 3) did

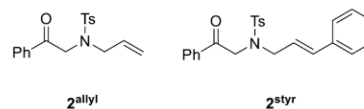


Figure 3. Substrates investigated concerning the influence of the alkene substitution.

not show any reactivity, even at an elevated temperature (50 °C) and high HCl loadings (50%; SI ch. 1). The phenyl-substituted **2<sup>styr</sup>** resulted only in deallylation. Thus, all further studies were performed with the dimethyl-substituted olefin moiety.

The main part of the investigation focused on the exploration of the substrate scope with three different protecting groups: tosyl, mesyl, and trifluorotolyl.

The smallest Ts-protected substrates **2<sup>Ts</sup>** and **3<sup>Ts</sup>** were converted to the respective COM products in good yields. Based on chiral HPLC analysis of **3<sup>Ts</sup>**, the stereoinformation of the substrate was efficiently transferred onto the product (SI,

Ch. 3, pp. 28–30). Interestingly, increasing the size of the substrate by only one methylene unit ( $4^{\text{Ts}}$ ) resulted in a greatly reduced yield of the COM product (34%). This trend continued with the largest substrate investigated, the phenylalanine-derived substrate ( $5^{\text{Ts}}$ ), which produced only 17% isolated yield. To estimate the reproducibility of this trend of decreasing yield with increasing substrate size, all reactions were run in triplicate, and the yield was determined via a  $^1\text{H}$  NMR (internal standard) to exclude an influence of the purification procedure. Indeed, the trend was confirmed by these studies. Additionally, it revealed that deallylation was the dominating reaction for larger substrates. The unsubstituted, glycine-derived substrate  $2^{\text{Ts}}$  performs slightly worse than the methyl-substituted  $3^{\text{Ts}}$ . The Thorpe-Ingold effect might be responsible for this observation, as also discussed by the Schindler group in their studies with iron(III) chloride.<sup>8</sup> This influence was even more pronounced for the other protecting group ( $2^{\text{FTs}}$  vs  $3^{\text{FTs}}$  and  $2^{\text{Ms}}$  vs  $3^{\text{Ms}}$ , see below). To demonstrate the scalability of the procedure, 1 g of substrate  $3^{\text{Ts}}$  was converted and delivered product  $3\text{ATs}$  in comparable yield to the small-scale reaction (77 vs 79%; see the end of the Experimental Section). Furthermore, more readily available HCl sources than HCl-saturated chloroform, and alternative Bronsted acids were explored with substrate  $3^{\text{Ts}}$  (SI ch. 2). Several acids can be utilized in combination with capsule I. The best alternative performance was observed with HCl (37%, aq.) that resulted in nearly the same yield as the standard condition (82% vs 84%).

Interestingly,  $^{\text{F}}$ Ts-protected substrates performed, on average, worse. They required much harsher reaction conditions (40% HCl, 50 °C vs 20% HCl, 30 °C) and still converted extremely sluggishly (14 days vs 24 h). This is in contrast to iron(III)-catalysis and is likely a result of the decreased uptake of fluorinated substrates inside capsule I that we have observed before. As a side reaction, the addition of HCl to the olefin was observed in the cyclization of  $2^{\text{FTs}}$ .

Most interestingly, Ms-protected substrates were converted efficiently inside capsule I at slightly elevated temperatures (50 °C) but with the original acid loading (20% HCl). Surprisingly, the largest substrate  $5^{\text{Ms}}$  produced the highest yield (83 ± 2% NMR-yield, 62% isolated yield) of the mesyl series. This is in contrast to the tosyl- and trifluorotolyl-protected substrates where the smaller, alanine-derived substrate displayed the highest yield.

Control experiments were carried out to learn more about the origin of the COM and deallylation reactivity (Table 3). Aliquots of the reaction mixture were analyzed by  $^1\text{H}$  NMR over time and compared with the respective reference reactions (entry 0). First, an experiment with 1.5 equiv of tetrabutylammonium bromide (TBAB) was performed (entry 1). TBAB is a strong binding ammonium guest, which can effectively prevent cationic reactions inside capsule I.<sup>23,33–35</sup> Reactivity observed under these conditions likely stems from a background reaction outside of the capsule. All substrates investigated did not show any formation of the COM product. In the case of the tosyl- and mesyl-protected derivatives, some deallylation was observed, indicating that deallylation also takes place outside of the capsule. In entry 2, the capsule was efficiently disassembled by the addition of an excess of methanol. No reactivity was observed under these conditions. Next, the catalyst components (I and HCl) were tested separately (entries 3 and 4). No product formation was observed, which indicates that the COM only takes place

inside I in the presence of HCl. Some deallylation product was observable for  $2^{\text{Ts}}$  and  $2^{\text{Ms}}$  in both cases. However, the low yield after extended reaction time (7 days) is much lower than under regular conditions (entry 0). The following conclusions can be drawn from these control experiments. (1) The deallylation seems not to depend on either I or HCl but is accelerated in the presence of the catalyst combination. (2) On the other hand, COM product formation is only observed when both catalyst components (I and HCl) are present.

What causes the observed inverse trends for the tosyl- and mesyl-protected substrates (Table 2)? As the cavity of I only

Table 2. Evaluation of the Protecting Group Influence<sup>a,b,c</sup>

10% I HCl CHCl <sub>3</sub>		A + B	
20% HCl, 30 °C, 24h	40% HCl, 50 °C, 14d	20% HCl, 50 °C, 48h	
 A: 74±2% <sup>a</sup> B: 25±3% <sup>a</sup> Iso. yield: 62% (A) <sup>b</sup>	 A: 9±1% <sup>a</sup> B: 22±0.6% <sup>a</sup> Iso. yield: 6% (A) <sup>b,c</sup>	 A: 27±2% <sup>a</sup> B: 43±5% <sup>a</sup> Iso. yield: 25% (A) <sup>b</sup>	
 A: 84±0.8% <sup>a</sup> B: 11±0.5% <sup>a</sup> Iso. yield: 79% (A) <sup>b</sup>	 A: 58±3% <sup>a</sup> B: 35±2% <sup>a</sup> Iso. yield: 50% (A) <sup>b</sup>	 A: 54±0.2% <sup>a</sup> B: 30±0.1% <sup>a</sup> Iso. yield: 55% (A) <sup>b</sup>	
 A: 31±0.8% <sup>a</sup> B: 30±5% <sup>a</sup> Iso. yield: 34% (A) <sup>b</sup>	 A: 18±0.5% <sup>a</sup> B: 52±0.9% <sup>a</sup> Iso. yield: 17% (A) <sup>b</sup>	 A: 45±0.4% <sup>a</sup> B: 38±0.3% <sup>a</sup> Iso. yield: 41% (A) <sup>b</sup>	
 A: 24±0.4% <sup>a</sup> B: 66±0.6% <sup>a</sup> Iso. yield: 17% (A) <sup>b</sup>	 A: 32±2% <sup>a</sup> B: 16±1% <sup>a</sup> Iso. yield: 35% (A) <sup>b</sup>	 A: 83±2% <sup>a</sup> B: 12±2% <sup>a</sup> Iso. yield: 62% (A) <sup>b</sup>	

<sup>a</sup>Reactions run in triplicate and analyzed by  $^1\text{H}$  NMR with tetraethylsilane as internal standard (std. deviation reported).  
<sup>b</sup>Isolated yield. <sup>c</sup>Addition of HCl to the olefin was observed.

offers limited space, we suspect that the restricted rotation of the substrate might be the key factor. Substrates that carry a large protecting group (Ts or  $^{\text{F}}$ Ts) and additionally a larger R-residue (ethyl, phenyl) might suffer from a decreased conformational freedom required for the COM reaction. In these cases, deallylation, which does not depend on large conformational changes outcompetes the COM reaction. The smaller mesyl-protecting group, on the other hand, facilitates the conversion of the substrates with the larger R-residues (ethyl, benzyl).

In summary, we demonstrated that several 3-aryl-2,5-dihydropyrroles can be synthesized efficiently with the catalyst combination I/HCl. Most interestingly, this catalyst combination is able to convert mesyl-protected substrates. To our knowledge, such substrates have not been converted in a COM reaction before, as they would suffer from catalyst inhibition due to the high Lewis basicity. As the mesyl group can be deprotected selectively in the presence of other sulfonamides, it provides an orthogonal reactivity compared to the protecting groups utilized so far for the COM reaction. Furthermore, a strong size dependence of the conversion inside capsule **I** was observed. These results combined with the performed control experiments provide very strong evidence that the COM reaction takes place inside the capsule exclusively. The results further highlight the unique reactivity observed inside the closed cavity of capsule **I** compared to reactions in solution (Table 3).

Table 3. Control Experiments<sup>a</sup>

entry	I	HCl	2 <sup>Ts</sup>		2 <sup>FTs</sup>		2 <sup>Ms</sup>	
			A <sup>a</sup>	B <sup>a</sup>	A <sup>a</sup>	B <sup>a</sup>	A <sup>a</sup>	B <sup>a</sup>
			30°C, 1d		50°C, 14d		50°C, 2d	
0	10%	20%	74%	25%	9%	22%	27%	43%
			30°C, 7d		50°C, 14d		50°C, 7d	
1	10%	20%	n.d.	14%	n.d.	n.d.	n.d.	3%
			1.5 equiv <i>n</i> Bu <sub>4</sub> NBr					
2	10%	20%	n.d.	n.d.	n.d.	n.d.	n.d.	n.d.
			60 equiv MeOH					
3	0%	20%	n.d.	15%	n.d.	n.d.	n.d.	3%
4	10%	0%	n.d.	13%	n.d.	n.d.	n.d.	2%

<sup>a</sup>Analyzed by <sup>1</sup>H NMR with tetraethylsilane as internal standard; n.d. = not detectable via <sup>1</sup>H NMR.

## EXPERIMENTAL SECTION

**General Information.** Reagents were purchased from commercial sources (Acros Organics, Alfa Aesar, Fluorochem, Sigma-Aldrich, VWR) and used without prior purification. <sup>1</sup>H NMR spectra were recorded at 298 K at 500 or 600 MHz on a Bruker UltraShield 500 spectrometer or a 600 MHz Bruker Avance III NMR spectrometer equipped with a cryogenic QCI-F probe, respectively. <sup>13</sup>C NMR spectra were recorded at 126 or 151 MHz on a Bruker UltraShield 500 spectrometer or a 600 MHz Bruker AvanceIII NMR spectrometer equipped with a cryogenic QCI-F probe, respectively. Chemical shifts of <sup>1</sup>H NMR and <sup>13</sup>C NMR spectra (measured at 298 K) are given in ppm using residual solvent signals as references (CDCl<sub>3</sub>: 7.26 and 77.16 ppm). Coupling constants (*J*) are reported in hertz (Hz). Standard abbreviations indicating multiplicity were used as follows: singlet (s), doublet (d), triplet (t), quartet (q), pentet (p), sextet (s), septet (h), multiplet (m), broad (b). High-resolution mass spectra were obtained using the electrospray ionization-time of flight (ESI-TOF) technique on a Bruker maXis 4G mass spectrometer. Analytical

thin-layer chromatography (TLC) was performed on Merck silica gel 60 F<sub>254</sub> glass-backed plates, which were analyzed by fluorescence detection with UV light ( $\lambda = 254$  nm, [UV]) and after exposure to standard staining reagents and subsequent heat treatment. The following staining solution was used: acidic cerium ammonium molybdate solution [CAM] (40 g of ammonium heptamolybdate, 1.6 g of cerium sulfate in 900 mL of H<sub>2</sub>O with 100 mL of conc. H<sub>2</sub>SO<sub>4</sub>).

**General Procedure for NMR Experiments.** A stock solution of resorcinarene (99.5 mM) was prepared by suspending resorcinarene in chloroform-d<sub>1</sub> (filtered over basic aluminum oxide) in a 4 mL screw-cap vial. The vial was heated gently in a 50 °C waterbath until the suspension turned clear. After cooling to room temperature, tetraethylsilane was added to the resorcinarene stock solution to obtain a tetraethylsilane concentration of 66.4 mM (6.64  $\mu$ mol, 0.4 equiv in the final reaction mixture). An aliquot of the resorcinarene stock solution (100  $\mu$ L, 9.95  $\mu$ mol, 0.6 equiv) was added to a 1.5 mL screw-cap vial equipped with a stirring bar. HCl (0.2 equiv) was added as HCl-saturated chloroform solution (freshly titrated). Filtered chloroform was added to receive a total volume of 400  $\mu$ L. The substrate was added as a stock solution (100  $\mu$ L, 166 mM, 16.6  $\mu$ mol, 1.0 equiv). The vial was transferred to an aluminum heating block. Aliquots of 50  $\mu$ L were dissolved in 0.5 mL of chloroform-d<sub>1</sub> and analyzed by <sup>1</sup>H NMR.

**Preparation of Starting Materials.** Substrates 3<sup>Ts</sup>, 5<sup>Ts</sup>, 5<sup>FTs</sup> were prepared according to literature procedures.<sup>5</sup>

**General Procedure A: Synthesis of 2<sup>Ms</sup>, 2<sup>FTs</sup>, 2<sup>allyl</sup>, and 2<sup>styr</sup> via Protection and *N*-Alkenylation of 2-Aminoacetophenone.** 2-Aminoacetophenone hydrochloride (1.0 equiv) was suspended in a mixture of THF:H<sub>2</sub>O (1:2) to obtain a 0.3 M solution. The solution was cooled to 0 °C with an ice bath, and sulfonyl chloride (1.2 equiv) and triethylamine (3.0 equiv) were added. The solution was stirred for 4 h at 0 °C. The reaction was quenched with HCl (1 M) and extracted three times with EtOAc. The organic phase was dried with Na<sub>2</sub>SO<sub>4</sub>, and the solvent was removed under reduced pressure. The obtained protected aminoacetophenones (PAP) were purified by flash chromatography.

PAP was dissolved in dry DMF to obtain a 0.1 M solution. The solution was cooled to 0 °C in an ice bath, NaH (60% dispersion in mineral oil, 1.2 equiv) was added, and the reaction was stirred for 15 min at 0 °C. Alkenyl bromide (1.2 equiv) was added, and the reaction was allowed to warm to room temperature overnight. The reaction was quenched by the addition of a saturated NH<sub>4</sub>Cl solution and extracted with EtOAc. The combined organic phase was dried with Na<sub>2</sub>SO<sub>4</sub>, and the solvent was removed under reduced pressure. The final compound was purified by flash chromatography (SiO<sub>2</sub> EtOAc/cHex).

**General Procedure B: Synthesis of 3<sup>Ms</sup>, 4<sup>Ms</sup>, 3<sup>FTs</sup>, and 4<sup>FTs</sup> via *N*-Prenylation and Addition of Phenyl Lithium to Amino Acid Esters.** The amino acid (1.0 equiv) was suspended in MeOH to obtain a 1 M suspension. The mixture was cooled to 0 °C in an ice bath and thionyl chloride (1.2 equiv) was added dropwise. The reaction was allowed to warm to room temperature and stirred for 2 h. The solvent and remaining thionyl chloride were removed under reduced pressure to afford the crude amino acid methyl ester. The product was used without further purification.

The amino acid methyl ester (1.0 equiv) was suspended in DCM to obtain a 0.5 M suspension. The mixture was cooled to 0 °C in an ice bath, and sulfonyl chloride (1.2 equiv) was added. Triethylamine (2.2 equiv) was added dropwise, and the mixture was stirred for 4 h at 0 °C. The reaction was quenched by the addition of water and extracted with EtOAc. The combined organic phase was dried with Na<sub>2</sub>SO<sub>4</sub>, and the solvent was removed under reduced pressure. The crude product was used without further purification.

The protected amino acid was dissolved in dry DMF to obtain a 0.1 M solution. The solution was cooled to 0 °C in an ice bath, NaH (60% dispersion in mineral oil, 1.2 equiv) was added, and the reaction was stirred for 15 min at 0 °C. Prenyl bromide (1.2 equiv) was added, and the reaction was allowed to warm to room temperature overnight. The reaction was quenched by the addition of a saturated NH<sub>4</sub>Cl solution and extracted with EtOAc. The combined organic phase was

dried with  $\text{Na}_2\text{SO}_4$ , and the solvent was removed under reduced pressure. Purification by flash chromatography ( $\text{SiO}_2$  EtOAc/cHex) afforded the desired prenylated ester (EST).

Iodobenzene (1.1 equiv) was dissolved in THF to obtain a 0.1 M solution. The solution was cooled to  $-78^\circ\text{C}$  in a dry ice/acetone cooling bath.  $n\text{BuLi}$  (2.5 M, 1.1 equiv) was added, and the mixture was stirred for 10 min. EST (1.0 equiv) was added, and the reaction was stirred for 1 h at  $-78^\circ\text{C}$ . Higher temperature or longer reaction times lead to lower yields. The reaction was quenched by the addition of a saturated  $\text{NH}_4\text{Cl}$  solution and extracted with EtOAc. The combined organic phase was dried with  $\text{Na}_2\text{SO}_4$ , and the solvent was removed under reduced pressure. The final compound was purified by flash chromatography ( $\text{SiO}_2$  EtOAc/cHex).

**General Procedure C: Synthesis of 4<sup>Ts</sup> and 5<sup>Ms</sup> via N-Protection, Weinreb-Amidation, Grignard Addition, and N-Prenylation.** The respective amino acid (1.0 equiv) was suspended in a mixture of THF/ $\text{H}_2\text{O}$  (1:2) to obtain a 0.3 M solution. The solution was cooled to  $0^\circ\text{C}$  in an ice bath, and sulfonyl chloride (1.2 equiv) and triethylamine (3.0 equiv) were added. The solution was stirred for 4 h at  $0^\circ\text{C}$ . The reaction was quenched with HCl (1 M) and extracted three times with EtOAc. The organic phase was dried with  $\text{Na}_2\text{SO}_4$ , and the solvent was removed under reduced pressure. The obtained product was used without further purification.

The protected amino acid (1.0 equiv), *N,O*-dimethylhydroxylamine hydrochloride (1.1 equiv), and morpholine (1.1 equiv) were dissolved in DCM to obtain a 0.45 M solution. The mixture was cooled to  $0^\circ\text{C}$  in an ice bath, and DCC (1.1 equiv) was added in one portion. The reaction was allowed to warm up to room temperature overnight. The reaction was quenched by the addition of HCl (1 M), and the mixture was extracted with DCM. The organic phase was washed with sat.  $\text{NaHCO}_3$  solution and brine. The organic phase was dried with  $\text{Na}_2\text{SO}_4$  and filtered through a celite pad. The solvent was removed under reduced pressure, and the residue was purified by column chromatography to obtain the Weinreb amide (WA).

Aryl magnesium bromide (2.0 equiv) was dissolved in dry THF to obtain a 0.2 M solution. The solution was cooled to  $0^\circ\text{C}$  in an ice bath, and WA (1.0 equiv) was added as a 2.5 M solution in dry THF. The reaction was allowed to warm to room temperature and stirred for 4 h or until judged complete by TLC analysis. The reaction was quenched by the addition of a saturated  $\text{NH}_4\text{Cl}$  solution and extracted with EtOAc. The combined organic phase was dried with  $\text{Na}_2\text{SO}_4$ , and the solvent was removed under reduced pressure. Purification by flash chromatography ( $\text{SiO}_2$  EtOAc/cHex) afforded the aryl ketone (AK).

AK was dissolved in dry DMF to obtain a 0.1 M solution. The solution was cooled to  $0^\circ\text{C}$  in an ice bath, NaH (60% dispersion in mineral oil, 1.2 equiv) was added, and the reaction was stirred for 15 min at  $0^\circ\text{C}$ . Prenyl bromide (1.2 equiv) was added, and the reaction was allowed to warm to room temperature overnight. The reaction was quenched by the addition of a saturated  $\text{NH}_4\text{Cl}$  solution and extracted with EtOAc. The combined organic phase was dried with  $\text{Na}_2\text{SO}_4$ , and the solvent was removed under reduced pressure. The final compound was purified by flash chromatography ( $\text{SiO}_2$  EtOAc/cHex).

**General Procedure D: Carbonyl Olefin Metathesis. Preparation and Titration of HCl-Concentrated Chloroform Solution.** The HCl-concentrated chloroform solution was prepared by passing HCl-gas (prepared by dropwise addition of concentrated  $\text{H}_2\text{SO}_4$  to dry NaCl) through chloroform for ca. 30 min. The concentration of HCl in chloroform was determined as follows: to a solution of phenol red in EtOH (0.002 wt %, 2.5 mL) was added HCl-saturated chloroform (100  $\mu\text{L}$ ) via a microman M1 pipette equipped with plastic tips. Upon addition, the solution turned from yellow (neutral) to pink (acidic). The resulting solution was then titrated with 0.1 M ethanolic solution of triethylamine ( $\text{NEt}_3$ ). At the equivalence point, the solution turned from pink to yellow.

Resorcinarene (0.6 equiv) was weighed into a pressure vial and chloroform (filtered through basic aluminum oxide) was added to reach a concentration of 25.0 mM regarding resorcinarene. The capped vial was heated gently in a  $50^\circ\text{C}$  water bath until the

suspension turned clear. After cooling to room temperature, HCl (0.2 equiv) was added in the form of HCl-saturated chloroform. The substrate was added (1.0 equiv) and filtered chloroform was added to receive a total concentration of 33.1 mM regarding the substrate. The vial was equipped with a stirring bar and transferred to an oil bath set to  $50$  or  $30^\circ\text{C}$ . The reaction mixture was transferred directly to the column ( $\text{SiO}_2$  100% pentane) and was rinsed with pentane. The eluent was gradually changed to the desired mixture.

**Synthesis of 2<sup>Ts</sup> and 2A<sup>Ts</sup>.** 4-Methyl-*N*-(2-oxo-2-phenylethyl)-benzenesulfonamide (2PAP<sup>Ts</sup>). 2-Aminoacetophenone hydrochloride (450 mg, 2.62 mmol) and tosyl chloride (599 mg, 3.14 mmol) were treated according to the general procedure A. Flash chromatography ( $\text{SiO}_2$  20% EtOAc/80% cHex) afforded 2PAP<sup>Ts</sup> (687 mg, 2.37 mmol, 90%) as a white solid.  $^1\text{H}$  NMR (600 MHz,  $\text{CDCl}_3$ )  $\delta$  7.87–7.83 (m, 2H), 7.78 (d,  $J$  = 8.0 Hz, 2H), 7.64–7.59 (m, 1H), 7.47 (t,  $J$  = 7.7 Hz, 2H), 7.29 (d,  $J$  = 8.0 Hz, 2H), 5.62 (t,  $J$  = 4.7 Hz, 1H), 4.46 (d,  $J$  = 4.5 Hz, 3H), 2.40 (s, 3H).  $^{13}\text{C}\{^1\text{H}\}$  NMR (151 MHz,  $\text{CDCl}_3$ )  $\delta$  192.6, 143.9, 136.1, 134.6, 133.8, 129.9, 129.1, 128.0, 127.3, 48.8, 21.6.

The spectroscopic data matched those reported in the literature.<sup>36</sup>

4-Methyl-*N*-(3-methylbut-2-en-1-yl)-*N*-(2-oxo-2-phenylethyl)-benzenesulfonamide (2<sup>Ts</sup>). 2PAP<sup>Ts</sup> (300 mg, 1.05 mmol) and prenyl bromide (144  $\mu\text{L}$ , 1.25 mmol) were treated according to the general procedure A. Flash chromatography ( $\text{SiO}_2$  10% EtOAc/90% cHex) afforded 2<sup>Ts</sup> (272 mg, 761  $\mu\text{mol}$ , 72%) as a colorless oil.  $^1\text{H}$  NMR (500 MHz,  $\text{CDCl}_3$ )  $\delta$  7.92 (dd,  $J$  = 8.4, 1.3 Hz, 2H), 7.75 (d,  $J$  = 8.3 Hz, 2H), 7.61–7.55 (m, 1H), 7.47 (t,  $J$  = 7.8 Hz, 2H), 7.32–7.29 (m, 2H), 5.04–4.97 (m, 1H), 4.64 (s, 2H), 3.89 (d,  $J$  = 7.5 Hz, 2H), 2.44 (s, 3H), 1.59 (d,  $J$  = 1.4 Hz, 3H), 1.45 (d,  $J$  = 1.4 Hz, 3H).  $^{13}\text{C}\{^1\text{H}\}$  NMR (151 MHz,  $\text{CDCl}_3$ )  $\delta$  194.6, 143.3, 139.2, 136.8, 135.1, 133.6, 129.6, 128.7, 128.0, 127.5, 118.3, 52.1, 45.5, 25.7, 21.6, 17.6.

The spectroscopic data matched those reported in the literature.<sup>16</sup>

3-Phenyl-1-tosyl-2,5-dihydro-1H-pyrrole (2A<sup>Ts</sup>). 2<sup>Ts</sup> (61.1 mg, 171  $\mu\text{mol}$ ) was treated according to the general procedure D. The reaction was carried out at  $30^\circ\text{C}$  for 24 h. Flash chromatography ( $\text{SiO}_2$  10% EtOAc/90% pentane) afforded 2A<sup>Ts</sup> (31.8 mg, 106  $\mu\text{mol}$ , 62%) as a colorless oil.  $^1\text{H}$  NMR (500 MHz,  $\text{CDCl}_3$ )  $\delta$  7.77 (d,  $J$  = 8.1 Hz, 2H), 7.36–7.27 (m, 7H), 6.04–5.97 (m, 1H), 4.52–4.43 (m, 2H), 4.34–4.26 (m, 2H), 2.41 (s, 3H).  $^{13}\text{C}\{^1\text{H}\}$  NMR (126 MHz,  $\text{CDCl}_3$ )  $\delta$  143.7, 137.5, 134.2, 132.6, 130.0, 128.8, 128.6, 127.6, 125.5, 119.0, 55.8, 55.0, 21.7.

The spectroscopic data matched those reported in the literature.<sup>7</sup>

*N*-Allyl-4-methyl-*N*-(2-oxo-2-phenylethyl)benzenesulfonamide (2<sup>allyl</sup>). 2PAP<sup>Ts</sup> (201 mg, 693  $\mu\text{mol}$ ) and allyl bromide (72  $\mu\text{L}$ , 832  $\mu\text{mol}$ ) were treated according to the general procedure A. Flash chromatography ( $\text{SiO}_2$  10% EtOAc/90% cHex) afforded 2<sup>allyl</sup> (186 mg, 0.565 mmol, 81%) as colorless oil.  $^1\text{H}$  NMR (500 MHz,  $\text{CDCl}_3$ )  $\delta$  7.90 (dd,  $J$  = 8.4, 1.3 Hz, 2H), 7.76 (d,  $J$  = 8.3 Hz, 2H), 7.62–7.56 (m, 1H), 7.47 (dd,  $J$  = 8.1, 7.4 Hz, 2H), 7.32–7.29 (m, 2H), 5.70 (ddt,  $J$  = 16.8, 10.3, 6.6 Hz, 1H), 5.18–5.09 (m, 2H), 4.74 (s, 2H), 3.93 (d,  $J$  = 6.6 Hz, 2H), 2.44 (s, 3H).  $^{13}\text{C}\{^1\text{H}\}$  NMR (151 MHz,  $\text{CDCl}_3$ )  $\delta$  194.0, 143.5, 137.0, 135.0, 133.8, 132.5, 129.7, 128.9, 128.0, 127.6, 120.0, 51.8, 50.8, 21.7.

The spectroscopic data matched those reported in the literature.<sup>37</sup>

*N*-Cinnamyl-4-methyl-*N*-(2-oxo-2-phenylethyl)benzenesulfonamide (2<sup>cinn</sup>). 2PAP<sup>Ts</sup> (300 mg, 1.04 mmol) and cinnamyl bromide (185  $\mu\text{L}$ , 1.25 mmol) were treated according to the general procedure A. Flash chromatography ( $\text{SiO}_2$  10% EtOAc/90% cHex) afforded 2<sup>cinn</sup> (258 mg, 0.636 mmol, 61%) as a white solid.  $^1\text{H}$  NMR (500 MHz,  $\text{CDCl}_3$ )  $\delta$  7.91–7.86 (m, 2H), 7.81–7.77 (m, 2H), 7.60–7.55 (m, 1H), 7.46–7.41 (m, 2H), 7.34–7.30 (m, 2H), 7.29–7.19 (m, 5H), 6.43–6.35 (m, 1H), 6.03 (dt,  $J$  = 15.9, 6.9 Hz, 1H), 4.76 (s, 2H), 4.08 (dd,  $J$  = 6.9, 1.3 Hz, 2H), 2.44 (s, 3H).  $^{13}\text{C}\{^1\text{H}\}$  NMR (126 MHz,  $\text{CDCl}_3$ )  $\delta$  194.3, 143.6, 137.1, 136.1, 135.1, 135.0, 133.8, 129.8, 128.9, 128.7, 128.2, 128.2, 127.7, 126.7, 123.6, 52.1, 50.5, 21.7. HRMS calcd for  $\text{C}_{24}\text{H}_{23}\text{NO}_3\text{SNa}$  [(M + Na)<sup>+</sup>]: 428.1291 found: 428.1294.

(*S*)-2-Methyl-3-phenyl-1-tosyl-2,5-dihydro-1H-pyrrole (3A<sup>Ts</sup>). 3<sup>Ts</sup> (63.5 mg, 171  $\mu\text{mol}$ ) was treated according to the general procedure D. The reaction was carried out at  $30^\circ\text{C}$  for 24 h. Flash chromatography ( $\text{SiO}_2$  10% EtOAc/90% pentane) afforded 3A<sup>Ts</sup>

(42.4 mg, 135  $\mu$ mol, 79%) as a white solid.  $^1\text{H}$  NMR (600 MHz,  $\text{CDCl}_3$ )  $\delta$  7.76 (d,  $J$  = 8.3 Hz, 2H), 7.38–7.23 (m, 7H), 5.82 (q,  $J$  = 2.0 Hz, 1H), 5.05–4.95 (m, 1H), 4.34–4.21 (m, 2H), 2.40 (s, 3H), 1.47 (d,  $J$  = 6.4 Hz, 3H).  $^{13}\text{C}$  NMR (151 MHz,  $\text{CDCl}_3$ )  $\delta$  143.6, 143.5, 135.1, 133.1, 129.9, 128.8, 128.3, 127.4, 126.4, 118.9, 63.0, 54.9, 22.2, 21.6.

The spectroscopic data matched those reported in the literature.<sup>8</sup>

**Synthesis of 4<sup>TS</sup> and 4A<sup>TS</sup>.** (S)-N-Methoxy-N-methyl-2-((4-methylphenyl)sulfonamido)butanamide (4WA<sup>TS</sup>). L-2-Aminobutyric acid (425 mg, 4.12 mmol, 1.0 equiv) was treated according to the general procedure C. Purification by flash chromatography ( $\text{SiO}_2$ , 30% EtOAc/70% cHex) yielded product 4WA<sup>TS</sup> (895 mg, 2.98 mmol, 72%) as a white solid.  $^1\text{H}$  NMR (500 MHz,  $\text{CDCl}_3$ )  $\delta$  7.73–7.69 (m, 2H), 7.27 (d,  $J$  = 7.9 Hz, 2H), 5.44 (d,  $J$  = 9.9 Hz, 1H), 4.17 (td,  $J$  = 9.5, 9.0, 4.4 Hz, 1H), 3.53 (s, 3H), 2.96 (s, 3H), 2.40 (s, 3H), 1.69 (dtd,  $J$  = 14.7, 7.3, 4.5 Hz, 1H), 1.53 (dt,  $J$  = 13.8, 7.5 Hz, 1H), 0.99–0.89 (m, 3H).  $^{13}\text{C}$  NMR (126 MHz,  $\text{CDCl}_3$ )  $\delta$  143.5, 137.1, 129.6, 127.5, 61.4, 54.3, 32.2, 26.9, 21.6, 9.8. HRMS calcd for  $\text{C}_{13}\text{H}_{23}\text{N}_2\text{O}_5\text{SNa}$  [(M + Na)]<sup>+</sup>: 323.1036 found 323.1038.

(S)-4-Methyl-N-(1-oxo-1-phenylbutan-2-yl)benzenesulfonamide (4AK<sup>TS</sup>). 4WA<sup>TS</sup> (1.00 g, 3.33 mmol, 1.0 equiv) was treated according to the general procedure C. Purification by flash chromatography ( $\text{SiO}_2$ , 20% EtOAc/80% cHex) yielded product 4AK<sup>TS</sup> (426 mg, 1.34 mmol, 40%) as a white solid.  $^1\text{H}$  NMR (500 MHz,  $\text{CDCl}_3$ )  $\delta$  7.72 (d,  $J$  = 8.4 Hz, 2H), 7.66 (d,  $J$  = 8.5 Hz, 2H), 7.61–7.55 (m, 1H), 7.47–7.40 (m, 2H), 7.13 (d,  $J$  = 7.6 Hz, 2H), 5.70 (d,  $J$  = 8.5 Hz, 1H), 4.84–4.77 (m, 1H), 2.29 (s, 3H), 1.93–1.82 (m, 1H), 1.65–1.55 (m, 1H), 0.94–0.87 (m, 3H).  $^{13}\text{C}$  NMR (126 MHz,  $\text{CDCl}_3$ )  $\delta$  198.1, 143.6, 137.0, 134.13, 134.0, 129.7, 128.9, 128.4, 127.2, 58.7, 27.6, 21.5, 9.3.

The spectroscopic data matched those reported in the literature.<sup>38</sup>

(S)-4-Methyl-N-(3-methylbut-2-en-1-yl)-N-(1-oxo-1-phenylbutan-2-yl)benzenesulfonamide (4<sup>TS</sup>). 4AK<sup>TS</sup> (549 mg, 1.73 mmol, 1.0 equiv) was treated according to the general procedure C. Purification by flash chromatography ( $\text{SiO}_2$ , 10% EtOAc/90% cHex) yielded product 4<sup>TS</sup> as a white solid (551 mg, 1.43 mmol, 83%).  $^1\text{H}$  NMR (500 MHz,  $\text{CDCl}_3$ )  $\delta$  8.00 (dd,  $J$  = 8.4, 1.3 Hz, 2H), 7.57 (dd,  $J$  = 8.0, 6.5 Hz, 3H), 7.47 (dd,  $J$  = 8.4, 7.1 Hz, 2H), 7.18 (d,  $J$  = 8.0 Hz, 2H), 5.35 (dd,  $J$  = 7.8, 6.2 Hz, 1H), 4.92 (ddt,  $J$  = 6.9, 5.4, 1.4 Hz, 1H), 3.94 (ddt,  $J$  = 16.1, 6.9, 1.2 Hz, 1H), 3.77–3.69 (m, 1H), 2.37 (s, 3H), 2.08–1.95 (m, 1H), 1.53 (d,  $J$  = 1.3 Hz, 6H), 1.44 (tt,  $J$  = 13.5, 7.4 Hz, 1H), 0.95 (t,  $J$  = 7.3 Hz, 3H).  $^{13}\text{C}$  NMR (126 MHz,  $\text{CDCl}_3$ )  $\delta$  197.9, 143.4, 137.6, 136.4, 135.4, 133.3, 129.6, 128.8, 128.7, 127.6, 121.3, 61.5, 43.1, 25.7, 22.0, 21.6, 17.8, 11.5. HRMS calcd for  $\text{C}_{22}\text{H}_{32}\text{N}_2\text{O}_5\text{SNa}$  [(M + Na)]<sup>+</sup>: 408.1604 found 408.1609.

(S)-2-Ethyl-3-phenyl-1-tosyl-2,5-dihydro-1H-pyrrole (4A<sup>TS</sup>). 4<sup>TS</sup> (140 mg, 364  $\mu$ mol) was treated according to the general procedure D. The reaction was carried out at 30  $^\circ\text{C}$  for 24 h. Flash chromatography ( $\text{SiO}_2$ , 10% EtOAc/90% pentane) afforded 4A<sup>TS</sup> (41.0 mg, 125  $\mu$ mol, 34%) as a white solid.  $^1\text{H}$  NMR (500 MHz,  $\text{CDCl}_3$ )  $\delta$  7.77–7.73 (m, 2H), 7.36–7.24 (m, 7H), 5.85 (q,  $J$  = 2.0 Hz, 1H), 5.09 (dtd,  $J$  = 5.5, 3.7, 1.7 Hz, 1H), 4.32–4.18 (m, 2H), 2.39 (s, 3H), 2.04 (dq,  $J$  = 14.7, 7.4, 4.0 Hz, 1H), 1.70 (dq,  $J$  = 14.5, 7.3, 3.6 Hz, 1H), 0.78 (t,  $J$  = 7.4 Hz, 3H).  $^{13}\text{C}$  NMR (126 MHz,  $\text{CDCl}_3$ )  $\delta$  143.5, 141.4, 135.2, 133.4, 129.9, 128.8, 128.3, 127.4, 126.5, 120.2, 67.7, 55.9, 26.5, 21.6, 7.4. HRMS calcd for  $\text{C}_{19}\text{H}_{21}\text{NO}_5\text{SNa}$  [(M + Na)]<sup>+</sup>: 350.1185 found 350.1188.

(S)-2-Benzyl-3-phenyl-1-tosyl-2,5-dihydro-1H-pyrrole (5A<sup>TS</sup>). 5<sup>TS</sup> (38.8 mg, 86.6  $\mu$ mol) was treated according to the general procedure D. The reaction was carried out at 30  $^\circ\text{C}$  for 24 h. Flash chromatography ( $\text{SiO}_2$ , 10% EtOAc/90% pentane) afforded 5A<sup>TS</sup> (5.80 mg, 14.9  $\mu$ mol, 17%) as a white solid.

$^1\text{H}$  NMR (500 MHz,  $\text{CDCl}_3$ )  $\delta$  7.79–7.74 (m, 2H), 7.36 (dd,  $J$  = 8.3, 6.6 Hz, 2H), 7.33–7.27 (m, 3H), 7.26–7.23 (m, 2H), 7.15 (dd,  $J$  = 4.8, 1.9 Hz, 3H), 7.03–6.98 (m, 2H), 5.62 (dt,  $J$  = 2.9, 1.6 Hz, 1H), 5.30 (dtd,  $J$  = 4.9, 2.9, 1.3 Hz, 1H), 4.04 (ddd,  $J$  = 15.7, 2.6, 1.5 Hz, 1H), 3.55 (ddd,  $J$  = 15.7, 5.2, 1.9 Hz, 1H), 3.36 (dd,  $J$  = 13.7, 4.8 Hz, 1H), 3.01 (dd,  $J$  = 13.7, 2.7 Hz, 1H), 2.39 (s, 3H).  $^{13}\text{C}$  NMR (126 MHz,  $\text{CDCl}_3$ )  $\delta$  143.6, 140.7, 136.3, 135.2, 133.4, 130.8, 129.9, 129.0, 128.4, 127.7, 127.3, 126.6, 126.4, 121.3, 67.4, 55.67, 39.8, 21.6.

The spectroscopic data matched those reported in the literature.<sup>8</sup>

**Synthesis of 2<sup>FTS</sup> and 2A<sup>FTS</sup>.** N-(2-Oxo-2-phenylethyl)-4-(trifluoromethyl)benzenesulfonamide (2PAP<sup>FTS</sup>). 2-Aminoacetophenone hydrochloride (1.00 g, 5.83 mmol) and 4-trifluoromethylbenzenesulfonyl chloride (1.71 g, 6.98 mmol) were treated according to the general procedure A. Flash chromatography ( $\text{SiO}_2$ , 20% EtOAc/80% cHex) afforded 2PAP<sup>FTS</sup> (1.76 g, 5.14 mmol, 88%) as a white solid.  $^1\text{H}$  NMR (600 MHz,  $\text{CDCl}_3$ )  $\delta$  8.04 (d,  $J$  = 8.1 Hz, 2H), 7.85 (dd,  $J$  = 8.5, 1.3 Hz, 2H), 7.77 (d,  $J$  = 8.2 Hz, 2H), 7.63 (t,  $J$  = 7.5 Hz, 1H), 7.52–7.45 (m, 2H), 5.77 (s, 1H), 4.51 (s, 2H).  $^{13}\text{C}$  NMR (151 MHz,  $\text{CDCl}_3$ )  $\delta$  192.2, 143.0, 134.8, 134.8 (q,  $J$  = 33.1), 133.6, 129.2, 128.0, 127.8, 126.5 (q,  $J$  = 3.8 Hz), 123.3 (q,  $J$  = 273.1 Hz), 48.7.

The spectroscopic data matched those reported in the literature.<sup>39</sup>

N-(3-Methylbut-2-en-1-yl)-N-(2-oxo-2-phenylethyl)-4-(trifluoromethyl)benzenesulfonamide (2<sup>FTS</sup>). 2PAP<sup>FTS</sup> (700 mg, 2.04 mmol) and prenyl bromide (283  $\mu$ L, 2.45 mmol) were treated according to the general procedure A. Flash chromatography ( $\text{SiO}_2$ , 10% EtOAc/90% cHex) afforded 2<sup>FTS</sup> (603 mg, 1.47 mmol, 72%) as a pale yellow solid.  $^1\text{H}$  NMR (500 MHz,  $\text{CDCl}_3$ )  $\delta$  8.01 (d,  $J$  = 8.0 Hz, 2H), 7.88 (dd,  $J$  = 8.4, 1.3 Hz, 2H), 7.78 (d,  $J$  = 8.3 Hz, 2H), 7.63–7.57 (m, 1H), 7.48 (dd,  $J$  = 8.2, 7.4 Hz, 2H), 5.07 (dddd,  $J$  = 7.5, 6.1, 2.8, 1.5 Hz, 1H), 4.76 (s, 2H), 3.95 (d,  $J$  = 7.5 Hz, 2H), 1.64 (d,  $J$  = 1.4 Hz, 3H), 1.46 (d,  $J$  = 1.3 Hz, 3H).  $^{13}\text{C}$  NMR (151 MHz,  $\text{CDCl}_3$ )  $\delta$  194.1, 143.89, 143.88, 143.87, 143.86, 139.83, 134.87, 134.19 (q,  $J$  = 32.9 Hz), 134.00, 128.99, 128.09, 127.97, 126.10 (q,  $J$  = 3.7 Hz), 123.46 (q,  $J$  = 272.9 Hz), 117.98, 51.67, 45.56, 25.84, 17.70.

The spectroscopic data matched those reported in the literature.<sup>8</sup>

3-Phenyl-1-((4-(trifluoromethyl)phenyl)sulfonyl)-2,5-dihydro-1H-pyrrole (2A<sup>FTS</sup>). 2<sup>FTS</sup> (70.0 mg, 170  $\mu$ mol) was treated according to the general procedure D. The reaction was carried out at 50  $^\circ\text{C}$  for 14 days with 0.4 equiv of HCl. Flash chromatography ( $\text{SiO}_2$ , 10% EtOAc/90% pentane) afforded 2A<sup>FTS</sup> (3.40 mg, 9.62  $\mu$ mol, 6%) as a colorless oil. Yield:  $^1\text{H}$  NMR (500 MHz,  $\text{CDCl}_3$ )  $\delta$  8.05–7.98 (m, 2H), 7.81 (dt,  $J$  = 8.2, 0.7 Hz, 2H), 7.35–7.27 (m, 5H), 6.03 (p,  $J$  = 2.1 Hz, 1H), 4.55–4.50 (m, 2H), 4.34 (td,  $J$  = 4.4, 2.3 Hz, 2H).  $^{13}\text{C}$  NMR (126 MHz,  $\text{CDCl}_3$ )  $\delta$  141.0, 137.5, 134.6 (q,  $J$  = 33.1 Hz), 132.3, 128.9, 128.8, 128.0, 126.6 (q,  $J$  = 3.7 Hz), 125.5, 124.4 (m), 118.7, 55.7, 55.1.

The spectroscopic data matched those reported in the literature.<sup>8</sup>

**Synthesis of 3<sup>FTS</sup> and 3A<sup>FTS</sup>.** Methyl-N-(3-methylbut-2-en-1-yl)-N-((4-(trifluoromethyl)phenyl)sulfonyl)-L-alanine (3EST<sup>FTS</sup>). L-Alanine (286 g, 3.21 mmol) was treated according to the general procedure B. Flash chromatography ( $\text{SiO}_2$ , 10% EtOAc/90% cHex) afforded 3EST<sup>FTS</sup> (934 mg, 2.46 mmol, 77%) as a colorless oil.  $^1\text{H}$  NMR (500 MHz,  $\text{CDCl}_3$ )  $\delta$  7.98–7.93 (m, 2H), 7.79–7.72 (m, 2H), 5.04 (tdd,  $J$  = 5.5, 2.9, 1.4 Hz, 1H), 4.69 (q,  $J$  = 7.3 Hz, 1H), 3.95–3.88 (m, 1H), 3.86–3.78 (m, 1H), 3.58 (s, 3H), 1.63 (dd,  $J$  = 10.5, 1.3 Hz, 6H), 1.44 (d,  $J$  = 7.3 Hz, 3H).  $^{13}\text{C}$  NMR (126 MHz,  $\text{CDCl}_3$ )  $\delta$  171.8, 144.4 (m), 136.4, 134.2 (q,  $J$  = 33.0 Hz), 128.0, 126.0 (q,  $J$  = 3.7 Hz), 123.4 (q,  $J$  = 272.8 Hz), 120.2, 55.1, 52.3, 43.7, 25.8, 17.7, 16.6.  $\text{C}_{16}\text{H}_{20}\text{F}_3\text{NO}_4\text{SNa}$  [(M + Na)]<sup>+</sup>: 402.0957 found 402.0964.

(S)-N-(3-Methylbut-2-en-1-yl)-N-(1-oxo-1-phenylpropan-2-yl)-4-(trifluoromethyl)benzenesulfonamide (3<sup>FTS</sup>). 3EST<sup>FTS</sup> (934 mg, 2.46 mmol) was treated according to the general procedure B. Flash chromatography ( $\text{SiO}_2$ , 5% EtOAc; 95% Pentane) afforded 3<sup>FTS</sup> (108 mg, 254  $\mu$ mol, 10%) as a white solid.  $^1\text{H}$  NMR (500 MHz,  $\text{CDCl}_3$ )  $\delta$  8.02–7.97 (m, 2H), 7.89–7.85 (m, 2H), 7.72–7.68 (m, 2H), 7.60–7.55 (m, 1H), 7.50–7.44 (m, 2H), 5.59 (q,  $J$  = 7.0 Hz, 1H), 4.84 (tdd,  $J$  = 6.5, 2.8, 1.4 Hz, 1H), 3.91 (dd,  $J$  = 15.7, 6.4 Hz, 1H), 3.79–3.70 (m, 1H), 1.52–1.50 (m, 6H), 1.32 (d,  $J$  = 7.0 Hz, 3H).  $^{13}\text{C}$  NMR (151 MHz,  $\text{CDCl}_3$ )  $\delta$  197.9, 143.9, 137.0, 135.6, 134.4 (q,  $J$  = 33.2 Hz), 133.5, 128.8, 128.8, 128.1, 126.2 (q,  $J$  = 3.6 Hz), 124.2 (q,  $J$  = 272.9 Hz), 120.4, 56.3, 43.2, 25.7, 17.8, 14.3. HRMS calcd for  $\text{C}_{21}\text{H}_{23}\text{F}_3\text{NO}_5\text{SNa}$  [(M + Na)]<sup>+</sup>: 448.1165 found 448.1172.

(+S)-2-Methyl-3-phenyl-1-((4-(trifluoromethyl)phenyl)sulfonyl)-2,5-dihydro-1H-pyrrole (3A<sup>FTS</sup>). 3<sup>FTS</sup> (71.2 mg, 167  $\mu$ mol) was treated according to the general procedure D. The reaction was carried out at 50  $^\circ\text{C}$  for 14 days with 0.4 equiv of HCl. Flash

chromatography (SiO<sub>2</sub> 10% EtOAc/90% pentane) afforded **3A<sup>FTS</sup>** (31.0 mg, 84.4 μmol, 50%) as a white solid. <sup>1</sup>H NMR (500 MHz, CDCl<sub>3</sub>) δ 8.03–7.99 (m, 2H), 7.80–7.75 (m, 2H), 7.37–7.26 (m, 5H), 5.86 (q, *J* = 2.0 Hz, 1H), 5.12–5.00 (m, 1H), 4.39–4.24 (m, 2H), 1.49 (d, *J* = 6.3 Hz, 3H). <sup>13</sup>C{<sup>1</sup>H} NMR (126 MHz, CDCl<sub>3</sub>) δ 143.6, 142.1 (q, *J* = 1.3 Hz), 134.5 (q, *J* = 33.0 Hz), 132.7, 128.9, 128.6, 127.8, 126.5 (m, 2C), 123.4 (q, *J* = 272.9), 118.6, 63.3, 54.9, 22.0. HRMS calcd for C<sub>18</sub>H<sub>16</sub>F<sub>3</sub>NO<sub>2</sub>SNa [(M + Na)<sup>+</sup>]: 390.0746 found 390.0742.

(*S*)-*N*-(1-*Oxo-1-phenylpropan-2-yl*)-4-(trifluoromethyl)benzenesulfonamide (**3B<sup>FTS</sup>**). Isolated as a white solid (28.0 mg, 78.3 μmol, 47%). <sup>1</sup>H NMR (500 MHz, CDCl<sub>3</sub>) δ 7.95–7.92 (m, 2H), 7.78–7.74 (m, 2H), 7.68–7.57 (m, 3H), 7.50–7.43 (m, 2H), 5.87 (d, *J* = 8.1 Hz, 1H), 4.98 (dq, *J* = 8.2, 7.2 Hz, 1H), 1.44 (d, *J* = 7.2 Hz, 3H). <sup>13</sup>C{<sup>1</sup>H} NMR (151 MHz, CDCl<sub>3</sub>) δ 197.7, 143.8, 134.6, 134.5 (q, *J* = 33.1 Hz), 133.2, 129.2, 128.6, 127.7, 126.4 (q, *J* = 3.7 Hz), 123.21 (q, *J* = 273.0 Hz), 53.6, 21.3. HRMS calcd for C<sub>16</sub>H<sub>14</sub>F<sub>3</sub>NO<sub>2</sub>SNa [(M + Na)<sup>+</sup>]: 380.0539 found 380.0540.

**Synthesis of 4<sup>FTS</sup> and 4A<sup>FTS</sup>.** Methyl-(*S*)-2-((*N*-(3-methylbut-2-en-1-yl)-4-(trifluoromethyl)phenyl)sulfonamido)butanoate (**4EST<sup>FTS</sup>**). L-2-Aminobutyric acid (316 mg, 3.07 mmol) was treated according to the general procedure B. Flash chromatography (SiO<sub>2</sub> 10% EtOAc/90% cHex) afforded **4EST<sup>FTS</sup>** (857 g, 2.18 mmol, 71%) as a colorless oil. <sup>1</sup>H NMR (500 MHz, CDCl<sub>3</sub>) δ 7.98–7.93 (m, 2H), 7.77–7.71 (m, 2H), 5.06 (dddd, *J* = 8.4, 5.6, 2.8, 1.4 Hz, 1H), 4.48 (dd, *J* = 9.6, 5.8 Hz, 1H), 3.87 (dt, *J* = 7.0, 1.1 Hz, 2H), 3.51 (s, 3H), 1.97 (dq, *J* = 14.8, 7.4, 5.9 Hz, 1H), 1.70 (ddq, *J* = 14.6, 9.6, 7.3 Hz, 1H), 1.63 (s, 6H), 0.99 (t, *J* = 7.4 Hz, 3H). <sup>13</sup>C{<sup>1</sup>H} NMR (126 MHz, CDCl<sub>3</sub>) δ 171.4, 144.4 (d, *J* = 1.4 Hz), 136.0, 134.2 (q, *J* = 32.9 Hz), 128.1, 125.9 (q, *J* = 3.7 Hz), 123.5 (q, *J* = 272.9 Hz), 61.3, 52.1, 43.6, 25.8, 23.3, 17.8, 11.0. HRMS calcd for C<sub>17</sub>H<sub>22</sub>F<sub>3</sub>NO<sub>2</sub>SNa [(M + Na)<sup>+</sup>]: 416.1114 found: 416.1117.

(*S*)-*N*-(3-Methylbut-2-en-1-yl)-*N*-(1-oxo-1-phenylbutan-2-yl)-4-(trifluoromethyl)benzenesulfonamide (**4F<sup>FTS</sup>**). **4EST<sup>FTS</sup>** (857 mg, 2.18 mmol) was treated according to the general procedure B. Flash chromatography (SiO<sub>2</sub> 5% EtOAc/95% Pentane) afforded **4F<sup>FTS</sup>** (98.0 mg, 22.3 μmol, 10%) as a white solid. <sup>1</sup>H NMR (500 MHz, CDCl<sub>3</sub>) δ 7.93 (dd, *J* = 8.4, 1.3 Hz, 2H), 7.79–7.75 (m, 2H), 7.62–7.56 (m, 3H), 7.47 (dd, *J* = 8.3, 7.3 Hz, 2H), 5.41 (t, *J* = 7.1 Hz, 1H), 4.96 (dddd, *J* = 7.7, 6.0, 2.9, 1.4 Hz, 1H), 4.03 (ddt, *J* = 16.2, 7.4, 1.0 Hz, 1H), 3.86 (ddt, *J* = 16.1, 6.3, 1.2 Hz, 1H), 2.04 (dt, *J* = 14.2, 7.2 Hz, 1H), 1.60–1.54 (m, 7H), 1.01 (t, *J* = 7.3 Hz, 3H). <sup>13</sup>C{<sup>1</sup>H} NMR (151 MHz, CDCl<sub>3</sub>) δ 197.8, 144.2, 136.1, 135.8, 134.2 (q, *J* = 33.1 Hz), 133.7, 128.9, 128.6, 128.0, 126.0 (q, *J* = 3.7 Hz), 123.3 (q, *J* = 272.9 Hz), 120.6, 61.7, 43.4, 25.7, 22.7, 17.9, 11.5. HRMS calcd for C<sub>22</sub>H<sub>24</sub>F<sub>3</sub>NO<sub>2</sub>SNa [(M + Na)<sup>+</sup>]: 462.1321 found 462.1326.

(*S*)-2-Ethyl-3-phenyl-1-((4-(trifluoromethyl)phenyl)sulfonyl)-2,5-dihydro-1H-pyrrole (**4A<sup>FTS</sup>**). **4F<sup>FTS</sup>** (59.6 mg, 136 μmol) was treated according to the general procedure D. The reaction was carried out at 50 °C for 14 days with 0.4 equiv of HCl. Flash chromatography (SiO<sub>2</sub> 10% EtOAc/90% pentane) afforded **4A<sup>FTS</sup>** (9.0 mg, 23.6 μmol, 17%) as a white solid. <sup>1</sup>H NMR (500 MHz, CDCl<sub>3</sub>) δ 8.00 (d, *J* = 8.2 Hz, 2H), 7.77 (d, *J* = 8.3 Hz, 2H), 7.36–7.24 (m, 5H), 5.89 (q, *J* = 2.0 Hz, 1H), 5.13 (tq, *J* = 4.1, 1.9 Hz, 1H), 4.44–4.16 (m, 2H), 2.05 (dtd, *J* = 14.7, 7.4, 4.2 Hz, 1H), 1.79–1.66 (m, 1H), 0.77 (t, *J* = 7.3 Hz, 3H). <sup>13</sup>C{<sup>1</sup>H} NMR (151 MHz, CDCl<sub>3</sub>) δ 141.9, 141.3, 134.6 (q, *J* = 33.1 Hz), 132.9, 128.9, 128.59, 127.8, 126.4 (m), 123.3 (q, *J* = 272.9 Hz), 119.9, 67.9, 56.0, 26.4, 7.3. HRMS calcd for C<sub>19</sub>H<sub>18</sub>F<sub>3</sub>NO<sub>2</sub>SNa [(M + Na)<sup>+</sup>]: 404.0903 found 404.0900.

(*S*)-*N*-(1-*Oxo-1-phenylbutan-2-yl*)-4-(trifluoromethyl)benzenesulfonamide (**4B<sup>FTS</sup>**). Isolated as a white solid (26.0 mg, 70.0 μmol, 51%). <sup>1</sup>H NMR (500 MHz, CDCl<sub>3</sub>) δ 7.93–7.88 (m, 2H), 7.74–7.70 (m, 2H), 7.62–7.57 (m, 3H), 7.45 (dd, *J* = 8.3, 7.4 Hz, 2H), 5.80 (d, *J* = 8.6 Hz, 1H), 4.86 (ddd, *J* = 8.7, 7.2, 4.4 Hz, 1H), 1.92 (dq, *J* = 14.8, 7.4, 4.4 Hz, 1H), 1.63 (dp, *J* = 14.6, 7.3 Hz, 1H), 0.93 (t, *J* = 7.4 Hz, 3H). <sup>13</sup>C{<sup>1</sup>H} NMR (151 MHz, CDCl<sub>3</sub>) δ 197.6, 143.6, 134.5, 134.5 (q, *J* = 33.0 Hz), 134.2, 133.7, 129.1, 128.4, 127.7, 126.3 (q, *J* = 3.8 Hz), 123.2 (q, *J* = 273.0 Hz) 58.8, 27.6, 9.3. HRMS calcd for C<sub>17</sub>H<sub>16</sub>F<sub>3</sub>NO<sub>2</sub>SNa [(M + Na)<sup>+</sup>]: 394.0695 found 394.0695.

1(*S*)-2-Benzyl-3-phenyl-1-((4-(trifluoromethyl)phenyl)sulfonyl)-2,5-dihydro-1H-pyrrole (**5A<sup>FTS</sup>**). **5F<sup>FTS</sup>** (51.6 mg, 103 μmol) was treated according to the general procedure D. The reaction was carried out at 50 °C for 14 days with 0.4 equiv of HCl. Flash chromatography (SiO<sub>2</sub> 10% EtOAc/90% pentane) afforded **5A<sup>FTS</sup>** (16.0 mg, 36.1 μmol, 35%) as a white solid. <sup>1</sup>H NMR (600 MHz, CDCl<sub>3</sub>) δ 8.01–7.97 (m, 2H), 7.80–7.75 (m, 2H), 7.40–7.33 (m, 3H), 7.28–7.25 (m, 2H), 7.17 (dd, *J* = 5.0, 1.9 Hz, 3H), 7.01–6.98 (m, 2H), 5.67 (dt, *J* = 2.9, 1.6 Hz, 1H), 5.32 (tdt, *J* = 5.1, 2.7, 1.3 Hz, 1H), 4.04 (ddd, *J* = 15.6, 2.6, 1.4 Hz, 1H), 3.58 (ddd, *J* = 15.7, 5.1, 1.9 Hz, 1H), 3.36 (dd, *J* = 13.8, 4.8 Hz, 1H), 3.03 (dd, *J* = 13.8, 2.7 Hz, 1H). <sup>13</sup>C{<sup>1</sup>H} NMR (151 MHz, CDCl<sub>3</sub>) δ 141.8, 140.7, 135.9, 134.5 (q, *J* = 33.0 Hz), 132.9, 130.7, 129.1, 128.6, 126.5 (m), 123.3 (q, *J* = 273.0 Hz), 121.0, 67.6, 55.7, 39.7.

The spectroscopic data matched those reported in the literature.<sup>8</sup>  
**Synthesis of 2<sup>Ms</sup> and 2A<sup>Ms</sup>.** *N*-(2-*Oxo-2-phenylethyl*)-methanesulfonamide (**2PAP<sup>Ms</sup>**). 2-Aminoacetophenone hydrochloride (1.00 g, 5.83 mmol) and mesyl chloride (540 μL, 6.98 mmol) were treated according to the general procedure A. Flash chromatography (SiO<sub>2</sub> 30% EtOAc/70% cHex) afforded **2PAP<sup>Ms</sup>** (800 mg, 3.75 mmol, 64%) as a white solid. <sup>1</sup>H NMR (500 MHz, CDCl<sub>3</sub>) δ 8.00–7.91 (m, 2H), 7.68–7.63 (m, 1H), 7.55–7.49 (m, 2H), 5.34 (s, 1H), 4.68 (d, *J* = 4.8 Hz, 2H), 3.01 (s, 3H). <sup>13</sup>C{<sup>1</sup>H} NMR (126 MHz, CDCl<sub>3</sub>) δ 193.4, 134.7, 133.9, 129.2, 128.1, 49.3, 41.0.

The spectroscopic data matched those reported in the literature.<sup>40</sup>  
*N*-(3-Methylbut-2-en-1-yl)-*N*-(2-*oxo-2-phenylethyl*)-methanesulfonamide (**2M<sup>Ms</sup>**). **2PAP<sup>Ms</sup>** (400 mg, 1.88 mmol) and prenyl bromide (260 μL, 2.25 mmol) were treated according to the general procedure A. Flash chromatography (SiO<sub>2</sub> 20% EtOAc/80% cHex) afforded **2M<sup>Ms</sup>** (296 mg, 1.05 mmol, 56%) as a pale yellow solid. <sup>1</sup>H NMR (500 MHz, CDCl<sub>3</sub>) δ 7.93–7.89 (m, 2H), 7.64–7.59 (m, 1H), 7.52–7.47 (m, 2H), 5.20 (tdt, *J* = 7.5, 2.9, 1.4 Hz, 1H), 4.76 (s, 2H), 4.02–3.96 (m, 2H), 3.09 (s, 3H), 1.70 (q, *J* = 1.1 Hz, 3H), 1.53 (d, *J* = 1.4 Hz, 3H). <sup>13</sup>C{<sup>1</sup>H} NMR (126 MHz, CDCl<sub>3</sub>) δ 195.6, 139.2, 134.9, 134.1, 129.1, 128.0, 118.8, 51.9, 45.1, 40.3, 25.9, 17.8. HRMS calcd For C<sub>14</sub>H<sub>19</sub>NO<sub>2</sub>SNa [(M + Na)<sup>+</sup>]: 304.0978 found 304.0979.

1-(Methylsulfonyl)-3-phenyl-2,5-dihydro-1H-pyrrole (**2A<sup>Ms</sup>**). **2M<sup>Ms</sup>** (45.5 mg, 162 μmol) was treated according to the general procedure D. The reaction was carried out at 50 °C for 48 h. Flash chromatography (SiO<sub>2</sub> 10% EtOAc/90% pentane) afforded **2A<sup>Ms</sup>** (9.00 mg, 40.3 μmol, 25%) as a colorless oil. <sup>1</sup>H NMR (500 MHz, CDCl<sub>3</sub>) δ 7.41–7.29 (m, 5H), 6.14 (p, *J* = 2.1 Hz, 1H), 4.56 (ddd, *J* = 4.6, 4.0, 2.0 Hz, 2H), 4.39–4.34 (m, 2H), 2.89 (s, 3H). <sup>13</sup>C{<sup>1</sup>H} NMR (126 MHz, CDCl<sub>3</sub>) δ 137.8, 132.5, 128.9, 128.8, 125.6, 119.1, 55.9, 55.2, 34.8.

The spectroscopic data matched those reported in the literature.<sup>7</sup>  
**Synthesis of 3<sup>Ms</sup> and 3A<sup>Ms</sup>.** Methyl-*N*-(3-methylbut-2-en-1-yl)-*N*-(methylsulfonyl)-L-alanine (**3EST<sup>Ms</sup>**). L-Alanine (1.33 g, 14.9 mmol) was treated according to the general procedure B. Flash chromatography (SiO<sub>2</sub> 20% EtOAc/80% cHex) afforded **3EST<sup>Ms</sup>** (2.55 g, 10.2 mmol, 68%) as a colorless oil. <sup>1</sup>H NMR (500 MHz, CDCl<sub>3</sub>) δ 5.24–5.17 (m, 1H), 4.61 (q, *J* = 7.3 Hz, 1H), 3.93–3.81 (m, 2H), 3.74 (s, 3H), 2.95 (s, 3H), 1.71 (q, *J* = 1.3 Hz, 3H), 1.66 (d, *J* = 1.4 Hz, 3H), 1.47 (d, *J* = 7.3 Hz, 3H). <sup>13</sup>C{<sup>1</sup>H} NMR (126 MHz, CDCl<sub>3</sub>) δ 172.6, 136.0, 120.9, 55.4, 52.5, 43.5, 40.5, 25.9, 17.9, 16.9. HRMS calcd For C<sub>10</sub>H<sub>19</sub>NO<sub>4</sub>SNa [(M + Na)<sup>+</sup>]: 272.0927 found 272.0929.

(*S*)-*N*-(3-Methylbut-2-en-1-yl)-*N*-(1-*oxo-1-phenylpropan-2-yl*)-methanesulfonamide (**3M<sup>Ms</sup>**). **3EST<sup>Ms</sup>** (1.00 g, 4.01 mmol) was treated according to the general procedure B. Flash chromatography (SiO<sub>2</sub> 5% EtOAc/95% pentane) afforded **3M<sup>Ms</sup>** (172 mg, 582 μmol, 14%) as a colorless oil. <sup>1</sup>H NMR (500 MHz, CDCl<sub>3</sub>) δ 8.02–7.97 (m, 2H), 7.60–7.55 (m, 1H), 7.51–7.44 (m, 2H), 5.55 (q, *J* = 7.1 Hz, 1H), 5.03 (ddq, *J* = 8.3, 5.6, 1.4 Hz, 1H), 3.94–3.78 (m, 2H), 2.84 (s, 3H), 1.63–1.57 (m, 6H), 1.49 (d, *J* = 7.1 Hz, 3H). <sup>13</sup>C{<sup>1</sup>H} NMR (126 MHz, CDCl<sub>3</sub>) δ 198.8, 136.4, 135.6, 133.5, 128.8, 128.8, 121.1, 56.6, 43.0, 40.6, 25.8, 17.7, 15.4. HRMS calcd for C<sub>15</sub>H<sub>21</sub>NO<sub>2</sub>SNa [(M + Na)<sup>+</sup>]: 318.1134 found 318.1139.

(*S*)-2-Methyl-1-(methylsulfonyl)-3-phenyl-2,5-dihydro-1H-pyrrole (**3A<sup>Ms</sup>**). **3A<sup>Ms</sup>** (50.0 mg, 169  $\mu$ mol) was treated according to the general procedure D. The reaction was carried out at 50 °C for 48 h. Flash chromatography (SiO<sub>2</sub> 10% EtOAc/90% pentane) afforded **3A<sup>Ms</sup>** (22.0 mg, 92.7  $\mu$ mol, 55%) as a colorless oil. <sup>1</sup>H NMR (500 MHz, CDCl<sub>3</sub>)  $\delta$  7.41–7.28 (m, 5H), 6.05–5.98 (m, 1H), 5.08–5.00 (m, 1H), 4.39–4.25 (m, 2H), 2.86 (s, 3H), 1.45 (d, *J* = 6.4 Hz, 3H). <sup>13</sup>C{<sup>1</sup>H} NMR (126 MHz, CDCl<sub>3</sub>)  $\delta$  143.9, 132.9, 129.0, 128.6, 126.5, 118.9, 62.9, 54.7, 35.6, 21.7. HRMS calcd for C<sub>12</sub>H<sub>13</sub>NO<sub>2</sub>SNa [(M + Na)]<sup>+</sup>: 260.0717 found 260.0716.

(*S*)-*N*-(1-Oxo-1-phenylpropan-2-yl)methanesulfonamide (**3B<sup>Ms</sup>**). Isolated as a white solid (9.00 mg, 39.6  $\mu$ mol, 23%) <sup>1</sup>H NMR (500 MHz, CDCl<sub>3</sub>)  $\delta$  7.99–7.95 (m, 2H), 7.65 (ddt, *J* = 7.8, 7.0, 1.3 Hz, 1H), 7.53 (ddd, *J* = 7.7, 6.9, 1.1 Hz, 2H), 5.45 (d, *J* = 8.1 Hz, 1H), 5.15 (dq, *J* = 8.2, 7.2 Hz, 1H), 2.92 (s, 3H), 1.51 (d, *J* = 7.2 Hz, 3H). <sup>13</sup>C{<sup>1</sup>H} NMR (126 MHz, CDCl<sub>3</sub>)  $\delta$  198.6, 134.6, 133.5, 129.3, 128.9, 54.0, 41.9, 21.5. HRMS calcd for C<sub>10</sub>H<sub>13</sub>NO<sub>3</sub>SNa<sup>+</sup>: 250.0508 found 250.0513.

**Synthesis of 4<sup>Ms</sup> and 4A<sup>Ms</sup>. Methyl (S)-2-(*N*-(3-methylbut-2-en-1-yl)methylsulfonamido)butanoate (**4EST<sup>Ms</sup>**). L-2-Aminobutyric acid (533 mg, 5.17 mmol) was treated according to the general procedure B. Flash chromatography (SiO<sub>2</sub> 20% EtOAc/80% cHex) afforded **4EST<sup>Ms</sup>** (879 mg, 3.34 mmol, 65%) as a colorless oil. <sup>1</sup>H NMR (500 MHz, CDCl<sub>3</sub>)  $\delta$  5.23 (ddp, *J* = 9.3, 6.4, 1.5 Hz, 1H), 4.39 (dd, *J* = 10.1, 5.5 Hz, 1H), 3.94–3.79 (m, 2H), 3.74 (s, 3H), 2.96 (s, 3H), 1.99 (dq, *J* = 14.7, 7.4, 5.5 Hz, 1H), 1.78–1.69 (m, 4H), 1.66 (d, *J* = 1.3 Hz, 3H), 1.01 (t, *J* = 7.4 Hz, 3H). <sup>13</sup>C{<sup>1</sup>H} NMR (126 MHz, CDCl<sub>3</sub>)  $\delta$  172.2, 136.1, 120.5, 61.4, 52.4, 43.3, 40.5, 25.9, 23.0, 17.9, 11.0. HRMS calcd for C<sub>11</sub>H<sub>21</sub>NO<sub>3</sub>SNa [(M + Na)]<sup>+</sup>: 286.1083 found 286.1085.**

(*S*)-*N*-(3-Methylbut-2-en-1-yl)-*N*-(1-oxo-1-phenylbutan-2-yl)methanesulfonamide (**4<sup>Ms</sup>**). **4EST<sup>Ms</sup>** (879 mg, 3.34 mmol) was treated according to the general procedure B. Flash chromatography (SiO<sub>2</sub> 5% EtOAc/95% pentane) afforded **4<sup>Ms</sup>** (81.0 mg, 262  $\mu$ mol, 8%) as a colorless oil. <sup>1</sup>H NMR (500 MHz, CDCl<sub>3</sub>)  $\delta$  8.00–7.96 (m, 2H), 7.62–7.57 (m, 1H), 7.52–7.46 (m, 2H), 5.35 (dd, *J* = 8.4, 6.2 Hz, 1H), 5.11 (ddp, *J* = 7.6, 6.0, 1.4 Hz, 1H), 3.99 (ddt, *J* = 16.3, 7.8, 0.9 Hz, 1H), 3.87–3.78 (m, 1H), 2.76 (s, 3H), 2.02 (dtd, *J* = 14.6, 7.3, 6.2 Hz, 1H), 1.75 (ddq, *J* = 14.5, 8.4, 7.3 Hz, 1H), 1.67–1.62 (m, 6H), 1.05 (t, *J* = 7.3 Hz, 3H). <sup>13</sup>C{<sup>1</sup>H} NMR (126 MHz, CDCl<sub>3</sub>)  $\delta$  198.7, 136.2, 135.9, 133.7, 129.0, 128.7, 121.15, 61.9, 42.7, 41.0, 25.8, 22.7, 17.9, 11.2. HRMS calcd for C<sub>16</sub>H<sub>23</sub>NO<sub>3</sub>SNa [(M + Na)]<sup>+</sup>: 332.1291 found 332.1294.

(*S*)-2-Ethyl-1-(methylsulfonyl)-3-phenyl-2,5-dihydro-1H-pyrrole (**4A<sup>Ms</sup>**). **4<sup>Ms</sup>** (81.0 mg, 262  $\mu$ mol) was treated according to the general procedure D. The reaction was carried out at 50 °C for 48 h. Flash chromatography (SiO<sub>2</sub> 10% EtOAc/90% pentane) afforded **4A<sup>Ms</sup>** (27.0 mg, 107  $\mu$ mol, 41%) as a colorless oil. Yield: <sup>1</sup>H NMR (500 MHz, CDCl<sub>3</sub>)  $\delta$  7.39–7.29 (m, 5H), 6.07 (dd, *J* = 2.5, 1.5 Hz, 1H), 5.10–5.06 (m, 1H), 4.36 (ddd, *J* = 16.0, 2.6, 1.7 Hz, 1H), 4.25 (ddd, *J* = 16.0, 5.1, 1.9 Hz, 1H), 2.83 (s, 3H), 1.97 (dq, *J* = 14.8, 7.4, 4.1 Hz, 1H), 1.72 (dq, *J* = 14.6, 7.3, 4.0 Hz, 1H), 0.83 (t, *J* = 7.4 Hz, 3H). <sup>13</sup>C{<sup>1</sup>H} NMR (126 MHz, CDCl<sub>3</sub>)  $\delta$  141.7, 132.9, 128.8, 128.5, 126.4, 120.1, 67.4, 55.7, 34.8, 26.3, 7.4. HRMS calcd for C<sub>13</sub>H<sub>17</sub>NO<sub>2</sub>SNa [(M + Na)]<sup>+</sup>: 274.0872 found 274.0873.

(*S*)-*N*-(1-Oxo-1-phenylbutan-2-yl)methanesulfonamide (**4B<sup>Ms</sup>**). Isolated as a white solid (16.0 mg, 66.3  $\mu$ mol, 25%) <sup>1</sup>H NMR (500 MHz, CDCl<sub>3</sub>)  $\delta$  7.98–7.94 (m, 2H), 7.68–7.63 (m, 1H), 7.56–7.51 (m, 2H), 5.41 (d, *J* = 8.6 Hz, 1H), 5.02 (ddd, *J* = 8.6, 7.4, 4.2 Hz, 1H), 2.88 (s, 3H), 1.99 (ddd, *J* = 14.4, 7.3, 4.2 Hz, 1H), 1.66 (dt, *J* = 14.5, 7.3 Hz, 1H), 0.99 (t, *J* = 7.4 Hz, 3H). <sup>13</sup>C{<sup>1</sup>H} NMR (126 MHz, CDCl<sub>3</sub>)  $\delta$  198.5, 134.5, 134.0, 129.3, 128.8, 59.4, 41.5, 27.7, 9.5. HRMS calcd for C<sub>11</sub>H<sub>13</sub>NO<sub>3</sub>SNa [(M + Na)]<sup>+</sup>: 264.0665 found 264.0669.

**Synthesis of 5<sup>Ms</sup> and 5A<sup>Ms</sup>. (S)-*N*-Methoxy-*N*-methyl-2-(methylsulfonamido)-3-phenylpropanamide (**5WA<sup>Ms</sup>**). L-Phenylalanine (2.03 g, 12.3 mmol, 1.0 equiv) was treated according to the general procedure C. Purification by flash chromatography (SiO<sub>2</sub> 40% EtOAc/60% cHex) yielded product **5WA<sup>Ms</sup>** as a colorless oil (1.40 g, 4.89 mmol, 40%) <sup>1</sup>H NMR (500 MHz, CDCl<sub>3</sub>)  $\delta$  7.38–7.21 (m, 5H),**

5.25 (d, *J* = 9.6 Hz, 1H), 4.67 (td, *J* = 9.3, 4.7 Hz, 1H), 3.76 (s, 3H), 3.26 (s, 3H), 3.11 (dd, *J* = 13.5, 4.7 Hz, 1H), 2.79 (dd, *J* = 13.5, 9.1 Hz, 1H), 2.49 (s, 3H). <sup>13</sup>C{<sup>1</sup>H} NMR (126 MHz, CDCl<sub>3</sub>)  $\delta$  171.7, 136.7, 129.8, 128.8, 128.8, 127.4, 61.9, 55.4, 41.4, 39.6, 32.4. HRMS calcd C<sub>12</sub>H<sub>18</sub>N<sub>2</sub>O<sub>4</sub>SNa [(M + Na)]<sup>+</sup>: 309.0879 found 309.0885.

(*S*)-*N*-(1-Oxo-1,3-diphenylpropan-2-yl)methanesulfonamide (**5AK<sup>Ms</sup>**). **5WA<sup>Ms</sup>** (1.40 g, 4.89 mmol, 1.0 equiv) was treated according to the general procedure C. Purification by flash chromatography (SiO<sub>2</sub> 20% EtOAc/80% cHex) yielded product **5AK<sup>Ms</sup>** (700 mg, 2.31 mmol, 47%) as a white solid. <sup>1</sup>H NMR (500 MHz, CDCl<sub>3</sub>)  $\delta$  8.03–7.98 (m, 2H), 7.69–7.63 (m, 1H), 7.57–7.52 (m, 2H), 7.31–7.21 (m, 3H), 7.17–7.12 (m, 2H), 5.38–5.29 (m, 2H), 3.26–3.18 (m, 1H), 2.94–2.84 (m, 1H), 2.58 (s, 3H). <sup>13</sup>C{<sup>1</sup>H} NMR (126 MHz, CDCl<sub>3</sub>)  $\delta$  197.7, 135.6, 134.5, 134.2, 129.8, 129.3, 128.9, 128.8, 127.6, 59.3, 41.6, 40.5. HRMS calcd C<sub>16</sub>H<sub>17</sub>NO<sub>3</sub>SNa [(M + Na)]<sup>+</sup>: 326.0821 found 326.0825.

(*S*)-*N*-(3-Methylbut-2-en-1-yl)-*N*-(1-oxo-1,3-diphenylpropan-2-yl)methanesulfonamide (**5<sup>Ms</sup>**). **5AK<sup>Ms</sup>** (700 mg, 2.31 mmol, 1.0 equiv) was treated according to the general procedure C. Purification by flash chromatography (SiO<sub>2</sub> 10% EtOAc/90% cHex) yielded product **5<sup>Ms</sup>** as a white solid (453 mg, 1.22 mmol, 53%) <sup>1</sup>H NMR (500 MHz, CDCl<sub>3</sub>)  $\delta$  8.03–7.97 (m, 2H), 7.58–7.51 (m, 1H), 7.47–7.41 (m, 2H), 7.34–7.27 (m, 4H), 7.20 (ddt, *J* = 8.6, 6.3, 1.7 Hz, 1H), 5.81 (t, *J* = 7.4 Hz, 1H), 4.96 (dddd, *J* = 8.5, 5.6, 2.8, 1.4 Hz, 1H), 3.87 (dt, *J* = 7.1, 1.1 Hz, 2H), 3.42 (dd, *J* = 14.2, 7.1 Hz, 1H), 3.06 (dd, *J* = 14.2, 7.7 Hz, 1H), 2.43 (s, 3H), 1.67–1.58 (m, 6H). <sup>13</sup>C{<sup>1</sup>H} NMR (126 MHz, CDCl<sub>3</sub>)  $\delta$  197.5, 137.4, 136.7, 135.9, 133.6, 129.7, 128.9, 128.8, 127.0, 120.6, 61.4, 42.8, 41.0, 35.5, 25.8, 17.9. HRMS calcd for C<sub>21</sub>H<sub>25</sub>NO<sub>3</sub>SNa [(M + Na)]<sup>+</sup>: 394.1447 found 394.1455.

(*S*)-2-Benzyl-1-(methylsulfonyl)-3-phenyl-2,5-dihydro-1H-pyrrole (**5A<sup>Ms</sup>**). **5<sup>Ms</sup>** (62.5 mg, 168  $\mu$ mol) was treated according to the general procedure D. The reaction was carried out at 50 °C for 48 h. Flash chromatography (SiO<sub>2</sub> 10% EtOAc/90% pentane) afforded **5A<sup>Ms</sup>** (33.0 mg, 105  $\mu$ mol, 62%) as a colorless oil. <sup>1</sup>H NMR (500 MHz, CDCl<sub>3</sub>)  $\delta$  7.47–7.33 (m, 5H), 7.18–7.13 (m, 3H), 7.04–6.98 (m, 2H), 5.86 (q, *J* = 2.5, 2.0 Hz, 1H), 5.31 (dd, *J* = 4.8, 3.2 Hz, 1H), 4.10 (ddd, *J* = 16.0, 2.7, 1.3 Hz, 1H), 3.55 (ddd, *J* = 16.0, 5.1, 1.8 Hz, 1H), 3.26 (dd, *J* = 13.8, 4.8 Hz, 1H), 3.01 (dd, *J* = 13.7, 3.1 Hz, 1H), 2.81 (s, 3H). <sup>13</sup>C{<sup>1</sup>H} NMR (126 MHz, CDCl<sub>3</sub>)  $\delta$  141.2, 136.1, 133.1, 130.8, 129.1, 128.6, 127.8, 126.6, 126.5, 121.4, 67.3, 55.5, 39.7, 34.8. HRMS calcd for C<sub>18</sub>H<sub>19</sub>NO<sub>2</sub>SNa [(M + Na)]<sup>+</sup>: 336.1029 found 336.1033.

**Large-Scale Synthesis of 3A<sup>Ts</sup>**. Resorcinarene (1.78 g, 1.61 mmol, 0.6 equiv) was weighed into a pressure vial, and chloroform (filtered through basic aluminum oxide) was added to reach a concentration of 25.0 mM regarding resorcinarene. The capped vial was heated gently with a heatgun until the suspension turned clear. After cooling to room temperature, HCl (3.85 mL, 0.14 M, 538  $\mu$ mol, 0.2 equiv) was added in the form of HCl-saturated chloroform. The substrate **3<sup>Ts</sup>** (1.00 g, 2.69 mmol, 1.0 equiv) and filtered chloroform were added to receive a total concentration of 33.1 mM regarding the substrate. The vial was equipped with a stirring bar and transferred to an oil bath set to 30 °C. After 24 h, the reaction mixture was transferred directly to the column (SiO<sub>2</sub>, 100% cHex) and rinsed with cHex. The eluent was gradually changed to a mixture of 90% cHex and 10% EtOAc. **3A<sup>Ts</sup>** (646 mg, 2.06 mmol, 77%) was obtained as a white solid.

## ASSOCIATED CONTENT

### Supporting Information

The Supporting Information is available free of charge at <https://pubs.acs.org/doi/10.1021/acs.joc.1c02447>.

Experimental details and NMR spectra of new compounds (PDF)

## AUTHOR INFORMATION

## Corresponding Author

Konrad Tiefenbacher – Department of Chemistry, University of Basel, CH-4058 Basel, Switzerland; Department of Biosystems Science and Engineering, ETH Zurich, CH-4058 Basel, Switzerland; [orcid.org/0000-0002-3351-6121](https://orcid.org/0000-0002-3351-6121); Email: [konrad.tiefenbacher@unibas.ch](mailto:konrad.tiefenbacher@unibas.ch), [tkonrad@ethz.ch](mailto:tkonrad@ethz.ch)

## Authors

Fabian Huck – Department of Chemistry, University of Basel, CH-4058 Basel, Switzerland

Lorenzo Catti – Laboratory for Chemistry and Life Science Institute of Innovative Research, Tokyo Institute of Technology, Yokohama 226-8503, Japan

Gian Lino Reber – Department of Chemistry, University of Basel, CH-4058 Basel, Switzerland

Complete contact information is available at: <https://pubs.acs.org/10.1021/acs.joc.1c02447>

## Author Contributions

K.T. conceived and supervised the project. K.T., L.C., and F.H. planned the project. F.H. carried out all of the experiments besides the synthesis of substrates 4<sup>FTs</sup> and 5<sup>FTs</sup>, which were prepared by G.L.R. F.H. analyzed the data. K.T. and F.H. compiled a first version of the manuscript. All authors contributed to the final version of the manuscript.

## Notes

The authors declare no competing financial interest.

## ACKNOWLEDGMENTS

The authors thank Dr. Michael Pfeffer for the HRMS analysis.

## REFERENCES

- Groso, E. J.; Schindler, C. S. Recent Advances in the Application of Ring-Closing Metathesis for the Synthesis of Unsaturated Nitrogen Heterocycles. *Synthesis* **2019**, *51*, 1100–1114.
- Li, X.; Li, J. Recent Advances in the Development of MMPs and APNs Based on the Pyrrolidine Platforms. *Mini-Rev. Med. Chem.* **2010**, *10*, 794–805.
- Liddell, J. R.; et al. Pyrrolizidine alkaloids. *Nat. Prod. Rep.* **1999**, *16*, 499–507.
- O'Hagan, D. Pyrrole, pyrrolidine, pyridine, piperidine and tropine alkaloids. *Nat. Prod. Rep.* **2000**, *17*, 435–446.
- Huang, P.-Q. Asymmetric Synthesis of Five-Membered Ring Heterocycles. In *Asymmetric Synthesis of Nitrogen Heterocycles*; Wiley, 2009; pp 51–94.
- Schultz, D. M.; Wolfe, J. P. Recent Developments in Palladium-Catalyzed Alkene Aminoarylation Reactions for the Synthesis of Nitrogen Heterocycles. *Synthesis* **2012**, *44*, 351–361.
- Ma, L.; Li, W.; Xi, H.; Bai, X.; Ma, E.; Yan, X.; Li, Z. FeCl<sub>3</sub>-Catalyzed Ring-Closing Carbonyl–Olefin Metathesis. *Angew. Chem., Int. Ed.* **2016**, *55*, 10410–10413.
- Groso, E. J.; Golonka, A. N.; Harding, R. A.; Alexander, B. W.; Sodano, T. M.; Schindler, C. S. 3-Aryl-2,5-Dihydropyrroles via Catalytic Carbonyl–Olefin Metathesis. *ACS Catal.* **2018**, *8*, 2006–2011.
- Becker, M. R.; Watson, R. B.; Schindler, C. S. Beyond olefins: new metathesis directions for synthesis. *Chem. Soc. Rev.* **2018**, *47*, 7867–7881.
- Albright, H.; Davis, A. J.; Gomez-Lopez, J. L.; Vonesh, H. L.; Quach, P. K.; Lambert, T. H.; Schindler, C. S. Carbonyl–Olefin Metathesis. *Chem. Rev.* **2021**, *121*, 9359–9406.
- Ludwig, J. R.; Zimmerman, P. M.; Gianino, J. B.; Schindler, C. S. Iron(III)-catalyzed carbonyl–olefin metathesis. *Nature* **2016**, *533*, 374–379.
- Ludwig, J. R.; Phan, S.; McAtee, C. C.; Zimmerman, P. M.; Devery, J. J.; Schindler, C. S. Mechanistic Investigations of the Iron(III)-Catalyzed Carbonyl–Olefin Metathesis Reaction. *J. Am. Chem. Soc.* **2017**, *139*, 10832–10842.
- Ryakaczewski, K. A.; Groso, E. J.; Vonesh, H. L.; Gaviria, M. A.; Richardson, A. D.; Zehnder, T. E.; Schindler, C. S. Tetrahydropyridines via FeCl<sub>3</sub>-Catalyzed Carbonyl–Olefin Metathesis. *Org. Lett.* **2020**, *22*, 2844–2848.
- Tran, U. P. N.; Oss, G.; Breugst, M.; Detmar, E.; Pace, D. P.; Liyanto, K.; Nguyen, T. V. Carbonyl–Olefin Metathesis Catalyzed by Molecular Iodine. *ACS Catal.* **2019**, *9*, 912–919.
- Oss, G.; Nguyen, T. V. Iodonium-Catalyzed Carbonyl–Olefin Metathesis Reactions. *Synlett* **2019**, *30*, 1966–1970.
- Wang, R.; Chen, Y.; Shu, M.; Zhao, W.; Tao, M.; Du, C.; Fu, X.; Li, A.; Lin, Z. AuCl<sub>3</sub>-Catalyzed Ring-Closing Carbonyl–Olefin Metathesis. *Chem. - Eur. J.* **2020**, *26*, 1941–1946.
- Zhang, Y.; Sim, J. H.; MacMillan, S. N.; Lambert, T. H. Synthesis of 1,2-Dihydroquinolines via Hydrazine-Catalyzed Ring-Closing Carbonyl–Olefin Metathesis. *Org. Lett.* **2020**, *22*, 6026–6030.
- Catti, L.; Tiefenbacher, K. Bronsted Acid-Catalyzed Carbonyl–Olefin Metathesis inside a Self-Assembled Supramolecular Host. *Angew. Chem., Int. Ed.* **2018**, *57*, 14589–14592.
- MacGillivray, L. R.; Atwood, J. L. A chiral spherical molecular assembly held together by 60 hydrogen bonds. *Nature* **1997**, *389*, 469–472.
- Avram, L.; Cohen, Y. The Role of Water Molecules in a Resorcinarene Capsule As Probed by NMR Diffusion Measurements. *Org. Lett.* **2002**, *4*, 4365–4368.
- Avram, L.; Cohen, Y. Spontaneous Formation of Hexameric Resorcinarene Capsule in Chloroform Solution as Detected by Diffusion NMR. *J. Am. Chem. Soc.* **2002**, *124*, 15148–15149.
- Avram, L.; Cohen, Y.; Rebek, J., Jr. Recent advances in hydrogen-bonded hexameric encapsulation complexes. *Chem. Commun.* **2011**, *47*, 5368–5375.
- Cavarzan, A.; Scarso, A.; Sgarbossa, P.; Strukul, G.; Reek, J. N. H. Supramolecular Control on Chemo- and Regioselectivity via Encapsulation of (NHC)-Au Catalyst within a Hexameric Self-Assembled Host. *J. Am. Chem. Soc.* **2011**, *133*, 2848–2851.
- Bianchini, G.; Sorella, G. L.; Canever, N.; Scarso, A.; Strukul, G. Efficient isonitrile hydration through encapsulation within a hexameric self-assembled capsule and selective inhibition by a photo-controllable competitive guest. *Chem. Commun.* **2013**, *49*, 5322–5324.
- Giust, S.; La Sorella, G.; Sperti, L.; Fabris, F.; Strukul, G.; Scarso, A. Supramolecular Catalysis in the Synthesis of Substituted 1 H-Tetrazoles from Isonitriles by a Self-Assembled Hexameric Capsule. *Asian J. Org. Chem.* **2015**, *4*, 217–220.
- Caneva, T.; Sperti, L.; Strukul, G.; Scarso, A. Efficient epoxide isomerization within a self-assembled hexameric organic capsule. *RSC Adv.* **2016**, *6*, 83505–83509.
- Zhang, Q.; Catti, L.; Tiefenbacher, K. Catalysis inside the Hexameric Resorcinarene Capsule. *Acc. Chem. Res.* **2018**, *51*, 2107–2114.
- La Manna, P.; Talotta, C.; Floresta, G.; De Rosa, M.; Soriente, A.; Rescifina, A.; Gaeta, C.; Neri, P. Mild Friedel–Crafts Reactions inside a Hexameric Resorcinarene Capsule: C–Cl Bond Activation through Hydrogen Bonding to Bridging Water Molecules. *Angew. Chem., Int. Ed.* **2018**, *57*, 5423–5428.
- Gaeta, C.; Talotta, C.; De Rosa, M.; La Manna, P.; Soriente, A.; Neri, P. The Hexameric Resorcinarene Capsule at Work: Supramolecular Catalysis in Confined Spaces. *Chem. - Eur. J.* **2019**, *25*, 4899–4913.
- Zhu, Y.; Rebek, J., Jr.; Yu, Y. Cyclizations catalyzed inside a hexameric resorcinarene capsule. *Chem. Commun.* **2019**, *55*, 3573–3577.
- Gaeta, C.; La Manna, P.; De Rosa, M.; Soriente, A.; Talotta, C.; Neri, P. Supramolecular Catalysis with Self-Assembled Capsules and Cages: What Happens in Confined Spaces. *ChemCatChem* **2021**, *13*, 1638–1658.



(32) Naito, H.; Hata, T.; Urabe, H. Selective Deprotection of Methanesulfonamides to Amines. *Org. Lett.* **2010**, *12*, 1228–1230.

(33) Shivanyuk, A.; Rebek, J. Reversible encapsulation by self-assembling resorcinarene subunits. *Proc. Natl. Acad. Sci. U.S.A.* **2001**, *98*, 7662–7665.

(34) Zhang, Q.; Tiefenbacher, K. Hexameric Resorcinarene Capsule is a Bronsted Acid: Investigation and Application to Synthesis and Catalysis. *J. Am. Chem. Soc.* **2013**, *135*, 16213–16219.

(35) La Sorella, G.; Sporni, L.; Strukul, G.; Scarso, A. Supramolecular Encapsulation of Neutral Diazoacetate Esters and Catalyzed 1,3-Dipolar Cycloaddition Reaction by a Self-Assembled Hexameric Capsule. *ChemCatChem* **2015**, *7*, 291–296.

(36) Li, X.; Chen, M.; Xie, X.; Sun, N.; Li, S.; Liu, Y. Synthesis of Multiple-Substituted Pyrroles via Gold(I)-Catalyzed Hydroamination/Cyclization Cascade. *Org. Lett.* **2015**, *17*, 2984–2987.

(37) Tarantino, K. T.; Liu, P.; Knowles, R. R. Catalytic Ketyl-Olefin Cyclizations Enabled by Proton-Coupled Electron Transfer. *J. Am. Chem. Soc.* **2013**, *135*, 10022–10025.

(38) Rao, W.; Koh, M. J.; Kothandaraman, P.; Chan, P. W. H. Gold-Catalyzed Cycloisomerization of 1,7-Diyne Benzoates to Indeno[1,2-c]azepines and Azabicyclo[4.2.0]octa-1(8),5-dienes. *J. Am. Chem. Soc.* **2012**, *134*, 10811–10814.

(39) Zhang, X.; Li, S.-S.; Wang, L.; Xu, L.; Xiao, J.; Liu, Z.-J. 2-Methylquinoline promoted oxidative ring-opening of N-sulfonyl aziridines with DMSO: facile synthesis of  $\alpha$ -amino aryl ketones. *Tetrahedron* **2016**, *72*, 8073–8077.

(40) Miura, T.; Biyajima, T.; Fujii, T.; Murakami, M. Synthesis of  $\alpha$ -Amino Ketones from Terminal Alkynes via Rhodium-Catalyzed Denitrogenative Hydration of N-Sulfonyl-1,2,3-triazoles. *J. Am. Chem. Soc.* **2012**, *134*, 194–196.

**HAZARD AWARENESS  
REDUCES LAB INCIDENTS**

**ACS Essentials of  
Lab Safety for  
General Chemistry**

A new course from the  
American Chemical Society

ACS Institute  
Learn. Develop. Excel.

EXPLORE  
ORGANIZATIONAL  
SALES  
solutions.acs.org/essentials-of-lab-safety

REGISTER FOR  
INDIVIDUAL ACCESS  
institute.acs.org/courses/essentials-lab-safety/html

## 7. Experimental Part

### 7.1 General Information

#### Experimental

All reactions were carried out using standard Schlenk techniques with argon (Ar 4.6) as an inert gas. Unless indicated otherwise, glass equipment was dried under a high vacuum ( $10^{-2}$  mbar) at 500-600 °C using a heat gun. Reactions at low temperatures were performed using cooling baths (-78 °C using dry ice/acetone, 0 °C using ice/water).

#### Solvents

Anhydrous solvents were purchased from Acros and were used without prior purification. Solvents for extractions, chromatography, filtrations and non-anhydrous reactions were purchased from VWR as HPLC grade solvents and were used without prior purification. NMR solvents were purchased from Cambridge Isotope Laboratories and were used without prior purification.

#### Thin-Layer Chromatography (TLC)

Analytical thin-layer chromatography (TLC) was performed on Merck silica gel 60 F254 glass-baked plates, which were analyzed by fluorescence detection with UV-light ( $\lambda = 254$  nm, [UV]) and after exposure to standard staining reagents and subsequent heat treatment. The following staining solution was used: acidic cerium ammonium molybdate solution [CAM] (40 g ammonium heptamolybdate, 1.6 g cerium sulfate in 900 mL H<sub>2</sub>O with 100 mL conc. H<sub>2</sub>SO<sub>4</sub>).

#### Sources of chemicals

Sources of Chemicals: Reagents (Acros, Alfa Aesar, Fluorochem, Sigmar-Aldrich, VWR) were used without prior purification

#### High-Pressure Liquid Chromatography (HPLC)

HPLC was performed on an LC Prominence Liquid Chromatograph system by Shimadzu equipped with a UV-Vis detector and an ELSD unit. For analytical analysis, a Shim-pack GIS CN 5  $\mu$ m column (250  $\times$  4.6 mm) by Shimadzu was used. For preparative separation, a Shim-pack GIS CN 5  $\mu$ m column (250  $\times$  30 mm) by SHIMADZU was used.

#### NMR-Spectroscopy

$^1\text{H}$  NMR spectra were recorded at 500 MHz on a Bruker UltraShield 500 spectrometer.  $^{13}\text{C}$  NMR spectra were recorded at 126 MHz on a Bruker UltraShield 500 spectrometer. Chemical shifts of  $^1\text{H}$  NMR and  $^{13}\text{C}$  NMR spectra (measured at 298 K) are given in ppm by using residual solvent signals as references ( $\text{CDCl}_3$ : 7.26 ppm and 77.16 ppm, respectively; Acetone- $d_6$ : 2.05 ppm and 29.84 ppm). Coupling constants (J) are reported in Hertz (Hz). Standard abbreviations indicating multiplicity were used as follows: s (singlet), d (doublet), t (triplet), q (quartet), p (pentet), s (sextet), h (septet), m (multiplet), b (broad).

### **IR-Spectroscopy**

Infrared spectra were recorded on a Bruker ALPHA spectrometer (attenuated total reflection, ATR). Only selected absorbances ( $\nu_{\text{max}}$ ) are reported. Standard abbreviations indicating signal intensity were used as follows: s (strong), m (medium), w (weak), b (broad).

### ***In Situ* IR-Spectroscopy**

*In situ* infrared spectra were recorded on a Mettler-Toledo React IR 15 equipped with a DiComp (Diamond) probe and a silver halide fiber (6 mm x 1.5 m).

### **ESI-HRMS**

High resolution mass spectra were obtained using the electrospray ionization-time of flight (ESI-TOF) technique on a Bruker maXis 4G mass spectrometer.

### **Preparation and titration of HCl-concentrated chloroform solution**

HCl-concentrated chloroform solution was prepared by passing HCl-gas (prepared by dropwise addition of concentrated  $\text{H}_2\text{SO}_4$  to dry NaCl) through chloroform for ca. 30 min. The concentration of HCl in chloroform was determined as follows: to a solution of phenol red in EtOH (0.002wt %, 2.5 mL) was added HCl-saturated chloroform (100  $\mu\text{L}$ ) via a microman M1 pipette equipped with plastic tips. Upon addition, the solution turned from yellow (neutral) to pink (acidic). The resulting solution was then titrated with 0.1 M ethanolic solution of triethylamine ( $\text{NEt}_3$ ). At the equivalence point, the solution turned from pink to yellow.

## 7.2 Carbonyl-Olefin Metathesis

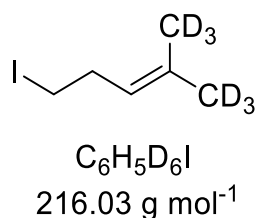
### 7.2.1 Mechanistic investigation

#### 7.2.1.1 Synthetic Procedures and Analytical Data

##### 7.2.1.1.1 General procedures

The alkylating agents 5-bromo-2-methyl-2-pentene (homoprenyl bromide),<sup>131</sup> 5-iodo-2methyl-2-pentene (homoprenyl iodide),<sup>131</sup> and 1-bromo-3-(methyl-d3)but-2-ene-4,4,4-d3 (prenyl bromide d<sub>6</sub>)<sup>109</sup> were prepared according to published procedures. Their spectroscopic data matched those reported in the literature. Resorcinarene was prepared according to published procedures.<sup>98</sup>

##### 7.2.1.1.2 Homoprenyl iodide (d<sub>6</sub>) (334)



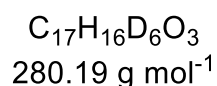
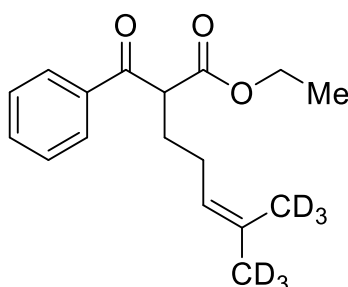
A flask was charged with magnesium shavings (252 mg, 10.4 mmol, 2.1 eq.) Diethyl ether (10.0 mL) was added. Methyl iodide-d<sub>3</sub> (0.64 mL, 10 mmol, 2.1 eq.) was added dropwise to the suspension in a way, that constant reflux was maintained. After complete addition, the reaction mixture was stirred for 1.5 h. Methyl cyclopropanecarboxylate (0.50 mL, 4.9 mmol, 1 eq.) in diethyl ether (10 mL) was added dropwise to the solution. The reaction was stirred at 50 °C for 1 h and then cooled to room temperature. The solution was added dropwise to an aqueous solution of sulphuric acid (30 vol %) at 0 °C and stirred for 4 h at room temperature. The organic phase was separated from the aqueous one. The aqueous phase was extracted with diethyl ether (3 x 100 mL). The combined organic phases were washed with brine. During these washing steps, several drops of aqueous sodium thiosulfate solution were added, until the intensive yellow color disappeared. The organic phase was dried over Na<sub>2</sub>SO<sub>4</sub> and concentrated under reduced pressure. The crude product was distilled with a Kugelrohr distillation (170 °C, 100 mbar). The product was received as a pale yellow oil (760 mg, 3.52 mmol, 71 %)

<sup>1</sup>H NMR (500 MHz, CDCl<sub>3</sub>): δ [ppm] = 5.09 (t, *J* = 7.2 Hz, 1H), 3.11 (t, *J* = 7.4 Hz, 2H), 2.57 (q, *J* = 7.3 Hz, 2H).

<sup>13</sup>C NMR (126 MHz, CDCl<sub>3</sub>) δ [ppm] 134.5, 123.3, 32.7, 22.5, 14.2, 6.3.

The spectroscopic data matched those reported in the literature<sup>132</sup>

7.2.1.1.3 Ethyl 2-benzoyl-6-methyl(d<sub>3</sub>) hept-5-enoate-7,7,7-(d<sub>3</sub>) (**87D**)



A flask was charged with NaH (60 % suspension in paraffin oil, 40.5 mg, 1.01 mmol, 1.3 eq.). THF (4 mL) was added and the suspension was cooled to 0 °C. Ethyl benzoylacetate (0.18 mL, 1.04 mmol, 1.3 eq.) was added dropwise and the solution was stirred for 10 min at 0 °C. **334** (168 mg, 777 μmol, 1 eq.) in THF (1 mL) was added and the reaction was stirred at 50 °C for 3 days. After cooling to room temperature, the reaction was quenched by the addition of saturated aqueous NH<sub>4</sub>Cl. The mixture was extracted with EtOAc (3 x 30 mL). The combined organic phases were dried over Na<sub>2</sub>SO<sub>4</sub> and concentrated under reduced pressure. Purification by column chromatography (SiO<sub>2</sub>: 95 % pentane: 5 % Et<sub>2</sub>O) yielded ethyl 2-benzoyl-6-methyl(d<sub>3</sub>) hept-5-enoate-7,7,7-(d<sub>3</sub>) (62.8 mg, 224 μmol, 29 %) as colorless oil.

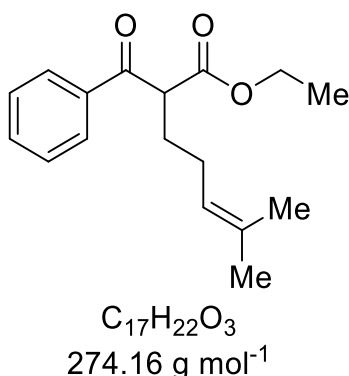
**<sup>1</sup>H NMR** (500 MHz, CDCl<sub>3</sub>) δ [ppm] 7.98 – 7.96 (m, 2H), 7.60 – 7.55 (m, 1H), 7.47 (t, *J* = 8.4, 7.0 Hz, 2H), 5.12 – 5.08 (m, 1H), 4.33 – 4.28 (m, 1H), 4.14 (qd, *J* = 7.1, 1.1 Hz, 2H), 2.10 – 1.99 (m, 5H), 1.17 (t, *J* = 7.1 Hz, 3H).

**<sup>13</sup>C NMR** (126 MHz, CDCl<sub>3</sub>) δ [ppm] 195.7, 170.2, 136.5, 133.5, 128.8, 128.7, 123.2, 61.4, 53.6, 29.2, 26.0, 14.2. (CD<sub>3</sub>-Signals not observable, the number of signals deviates from the theoretical value due to signal overlap)

**HRMS** calcd for C<sub>17</sub>H<sub>16</sub>D<sub>6</sub>O<sub>3</sub>Na<sup>+</sup> 303.1838 found: 303.1839

**IR (ATR):**  $\tilde{\nu}$  [cm<sup>-1</sup>] 2980.72 (w), 2931.90 (w), 1734.04 (s), 1683.40 (s), 1596.84 (w), 1580.22 (w), 1467.11 (w), 1447.49 (m), 1368.48 (m), 1251.18 (s), 1181.24 (s), 1149.15 (s), 1109.59 (m), 1094.92 (m), 1045.29 (m), 1026.03 (m), 1001.85 (m), 979.05 (m), 873.54 (m), 820.83 (m), 775.60 (m), 733.14 (m), 690.12 (s) 660.45 (m), 603.37 (m), 493.81 (w), 470.69 (w), 446.27 (w)

#### 7.2.1.1.4 Ethyl 2-benzoyl-6-methyl hept-5-enoate (**87**)



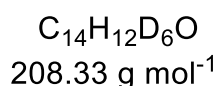
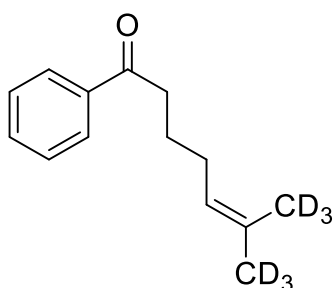
A flask was charged with NaH (60 % suspension in paraffin oil, 492 mg, 12.3 mmol, 1.3 eq.). THF (100 mL) was added and the suspension was cooled to 0 °C. Ethyl benzoylacetate (1.8 mL, 10.4 mmol, 1.1 eq.) was added dropwise and the solution was stirred for 10 min at 0 °C. Homoprenyl iodide (1.99 g, 9.46 mmol, 1 eq.) in THF (5 mL) was added and the reaction was stirred at 50 °C for 16 h. After cooling to room temperature, the reaction was quenched by the addition of saturated aqueous NH<sub>4</sub>Cl. The mixture was extracted with EtOAc (3 x 100 mL). The combined organic phases were dried over Na<sub>2</sub>SO<sub>4</sub> and concentrated under reduced pressure. Purification by column chromatography (SiO<sub>2</sub>: 95 % pentane: 5 % Et<sub>2</sub>O) yielded Ethyl 2-benzoyl-6-methyl hept-5-enoate (702 mg, 2.56 mmol, 27 %) as a colorless oil.

**<sup>1</sup>H NMR** (500 MHz, CDCl<sub>3</sub>) δ [ppm] 7.97 (d, *J* = 7.5 Hz, 2H), 7.60 – 7.55 (m, 1H), 7.47 (t, *J* = 7.7 Hz, 2H), 5.10 (t, *J* = 6.3 Hz, 1H), 4.33 – 4.28 (m, 1H), 4.14 (q, *J* = 7.1 Hz, 2H), 2.05 (tq, *J* = 6.1, 3.3, 2.4 Hz, 4H), 1.67 (s, 3H), 1.52 (s, 3H), 1.17 (t, *J* = 7.1 Hz, 3H).

**<sup>13</sup>C NMR** (126 MHz, CDCl<sub>3</sub>) δ [ppm] 195.7, 170.2, 136.5, 133.5, 133.5, 128.8, 128.7, 123.2, 61.4, 53.6, 29.2, 26.1, 25.8, 17.8, 14.2.

The spectroscopic data matched those reported in the literature<sup>63</sup>

7.2.1.1.5 6-methyl-1-phenylhept-5-en-1-one-(d<sub>6</sub>) (**281D**)



**87D** (519 mg, 1.85 mmol, 1 eq.) was dissolved in ethanol (6 mL). Potassium hydroxide (311 mg, 5.54 mmol, 3 eq.) was dissolved in water (2 mL) and added to the solution of **87D**. The mixture was heated to reflux for 3 h. After cooling to room temperature, 2 M HCl was added until CO<sub>2</sub> development stopped. The aqueous phase was extracted with Et<sub>2</sub>O and dried over Na<sub>2</sub>SO<sub>4</sub>. The solvent was removed under reduced pressure and the residue was purified by column chromatography (SiO<sub>2</sub>: 95 % pentane: 5 % Et<sub>2</sub>O). **281D** was received as a colorless oil (292 mg, 1.40 mmol, 76 %)

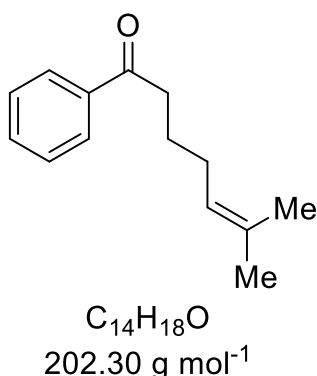
<sup>1</sup>H NMR (500 MHz, CDCl<sub>3</sub>) δ [ppm] 7.97 – 7.93 (m, 2H), 7.58 – 7.51 (m, 1H), 7.50 – 7.41 (m, 2H), 5.14 (t, *J* = 7.2 Hz, 1H), 3.04 – 2.82 (m, 2H), 2.08 (q, *J* = 7.3 Hz, 2H), 1.79 (p, *J* = 7.4 Hz, 2H).

<sup>13</sup>C NMR (126 MHz, CDCl<sub>3</sub>) δ [ppm] 200.7, 137.3, 133.0, 132.6, 128.7, 128.2, 124.0, 38.1, 27.7, 25.9, 24.6, 17.9. (the number of signals deviates from the theoretical value due to signal overlap)

HRMS calcd for C<sub>14</sub>H<sub>12</sub>D<sub>6</sub>ONa<sup>+</sup> 231.1626 found: 231.1626

IR (ATR):  $\tilde{\nu}$  [cm<sup>-1</sup>] 2936.08(w), 2860.30 (w), 1682.74 (s), 1597.47 (w), 1580.52 (w), 1448.26 (m), 1409.01 (w), 1366.13 (w), 1318.39 (w), 1257.88 (m), 1219.39 (m), 1196.71 (m), 1179.73 (m), 1158.09 (m), 1048.03 (m), 1026.99 (m), 1001.48 (m), 977.84 (m), 928.15 (m), 872.49 (m), 825.74 (m), 741.83 (s), 689.01 (s), 656.40 (m), 599.69 (m), 569.42 (m), 485.29 (w)

7.2.1.1.6 6-methyl-1-phenylhept-5-en-1-one (**281**)



**87** (300 mg, 1.09 mmol, 1 eq.) was dissolved in ethanol (4 mL). Potassium hydroxide (183 mg, 3.27 mmol, 3 eq.) was dissolved in water (1 mL) and added to the solution of **87**. The mixture was heated to reflux for 3 h. After cooling to room temperature, 2 M HCl was added until CO<sub>2</sub> development stopped. The aqueous phase was extracted with Et<sub>2</sub>O and dried over Na<sub>2</sub>SO<sub>4</sub>. The solvent was removed under reduced pressure and the residue was purified by column chromatography (SiO<sub>2</sub>: 95 % pentane: 5 % Et<sub>2</sub>O). **281** was received as a colorless oil (183 mg, 904 μmol, 83 %)

**<sup>1</sup>H NMR** (500 MHz, CDCl<sub>3</sub>) δ [ppm] 7.98 – 7.91 (m, 2H), 7.58 – 7.53 (m, 1H), 7.48 – 7.42 (m, 2H), 5.14 (ddt, *J* = 8.7, 5.8, 1.5 Hz, 1H), 3.01 – 2.91 (m, 2H), 2.13 – 2.04 (m, 2H), 1.79 (p, *J* = 7.4 Hz, 2H), 1.69 (d, *J* = 1.3 Hz, 3H), 1.60 (d, *J* = 1.4 Hz, 3H).

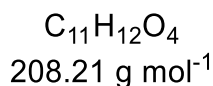
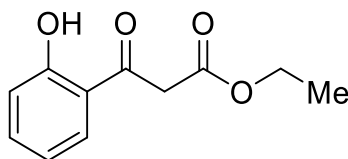
**<sup>13</sup>C NMR** (126 MHz, CDCl<sub>3</sub>) δ [ppm] 200.7, 137.3, 133.0, 132.6, 128.7, 128.2, 124.0, 38.1, 27.6, 25.9, 24.6, 17.9 (the number of signals deviates from the theoretical value due to signal overlap)

**HRMS** calcd for C<sub>14</sub>H<sub>18</sub>ONa<sup>+</sup>: 225.1250 found: 225.1246

**IR (ATR):**  $\tilde{\nu}$  [cm<sup>-1</sup>] 2926.66 (w), 2858.12 (w), 1683.12 (s), 1597.48 (w) 1580.55 (w), 1448.03 (m), 1408.63 (w), 1366.27 (w), 1318.93 (w), 1256.94 (m), 1213.67 (m), 1179.47 (m), 1158.39 (m) 1106.83 (m) 1069.14 (m) 1000.95 (m), 986.90 (m), 870.50 (m), 830.27 (m), 751.02 (m), 730.11 (m), 689.06 (s), 657.06 (w), 600.06 (w), 570.06 (w), 427.41 (w)



7.2.1.1.7 Ethyl 3-(2-hydroxyphenyl)-3-oxopropanoate (**335**)



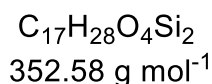
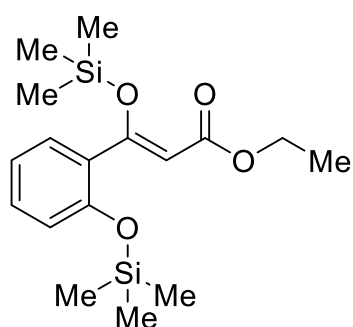
HMDS (14 mL, 67 mmol, 3 eq.) was dissolved in THF (66.0 mL) and cooled to -78°C. *n*-BuLi in hexane (26 mL, 2.5 M, 65 mmol 3 eq.) was added and the mixture was stirred for 30 min at -78°C and 30 min at 0 °C. The thereby obtained solution of LiHMDS was cooled to -78°C and 2-hydroxyacetophenone (2.65 mL, 22.0 mmol, 1 eq.) dissolved in THF (14 mL) was added dropwise. The reaction was stirred for 60 min at -78°C and 60 min at 0°C. Diethyl carbonate (2.93 mL, 24.2 mmol, 1.1 eq.) was added dropwise and the reaction was allowed to warm up to room temperature overnight. NH<sub>4</sub>Cl solution was added and the mixture was extracted with EtOAc and dried with Na<sub>2</sub>SO<sub>4</sub>. The solvent was removed under reduced pressure and the residue was purified by column chromatography (SiO<sub>2</sub>: 90 % cHex: 10 % EtOAc). **335** was received as a yellow oil (3.77 g, 18.1 mmol, 82 %)

<sup>1</sup>H NMR (500 MHz, CDCl<sub>3</sub>) δ [ppm] 11.85 (d, *J* = 0.4 Hz, 1H), 7.67 (dd, *J* = 8.1, 1.6 Hz, 1H), 7.50 (ddd, *J* = 8.6, 7.1, 1.6 Hz, 1H), 7.00 (dd, *J* = 8.4, 1.2 Hz, 1H), 6.92 (ddd, *J* = 8.2, 7.2, 1.2 Hz, 1H), 4.23 (q, *J* = 7.1 Hz, 2H), 4.00 (s, 2H), 1.27 (t, *J* = 7.1 Hz, 3H).

<sup>13</sup>C NMR (126 MHz, CDCl<sub>3</sub>) δ [ppm] 198.6, 167.0, 162.9, 137.2, 130.4, 119.4, 119.1, 118.8, 61.9, 46.0, 14.2.

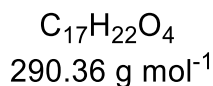
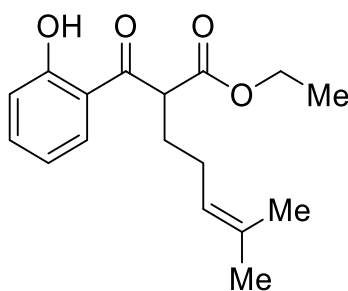
The spectroscopic data matched those reported in the literature<sup>133</sup>

7.2.1.1.8 Ethyl (Z)-3-((trimethylsilyloxy)-3-(2-((trimethylsilyloxy)phenyl)acrylate (**336**)



HMDS (11.5 mL, 54.3 mmol, 3 eq.) was dissolved in THF (66 mL) and cooled to  $-78^\circ\text{C}$ . *n*-BuLi in hexane (21.7 mL, 2.5 M, 54.2 mmol, 3 eq.) was added and the mixture was stirred for 30 min at  $-78^\circ\text{C}$  and another 30 min at  $0^\circ\text{C}$ . The thereby obtained solution of LiHMDS was cooled to  $-78^\circ\text{C}$  and **335** (3.77 g, 18.1 mmol, 1 eq.) dissolved in THF (7 mL) was added. The solution was stirred for 60 min and trimethylchlorosilane (6.94 mL, 54.3 mmol, 3 eq.) was added. The reaction was allowed to warm to room temperature overnight.  $\text{NaHCO}_3$  solution was added and the mixture was extracted with EtOAc. The solvent was removed under reduced pressure, the received colorless oil was used without further purification.

7.2.1.1.9 Ethyl 2-(2-hydroxybenzoyl)-6-methylhept-5-enoate (**282**)



**336** (1.00 g, 2.84 mmol, 1 eq.) was dissolved in THF (10 mL). Tetrakis(triphenylphosphine)-Pd(0) (328 mg, 0.28 mmol, 0.1 eq.) and  $\text{K}_2\text{CO}_3$  (393 mg, 2.84 mmol, 1 eq.) were added and the suspension was heated to  $50^\circ\text{C}$ . Homoprenyl iodide (506  $\mu\text{L}$ , 3.61 mmol, 1.3 eq.) was added and the reaction was stirred for 48 h at  $50^\circ\text{C}$ . The starting material was not consumed completely, but longer reaction times lead to a reduced yield.  $\text{NH}_4\text{Cl}$  solution is added and the mixture is extracted with EtOAc. The solvent was removed under reduced pressure and the

residue was purified by column chromatography (SiO<sub>2</sub>: 95 % cHex: 5 % EtOAc) and HPLC. **282** was received as a colorless oil (90.0 mg, 310 μmol, 11 %)

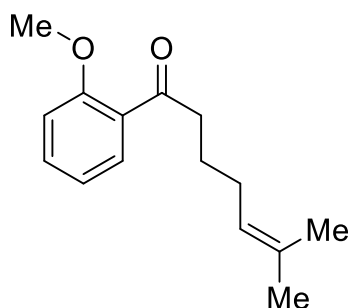
<sup>1</sup>H NMR (500 MHz, CDCl<sub>3</sub>) δ [ppm] 12.07 (s, 1H), 7.78 (dd, J = 8.1, 1.6 Hz, 1H), 7.49 (ddd, J = 8.6, 7.2, 1.6 Hz, 1H), 7.00 (dd, J = 8.5, 1.2 Hz, 1H), 6.92 (ddd, J = 8.2, 7.2, 1.2 Hz, 1H), 5.10 (dq, J = 2.8, 1.4 Hz, 1H), 4.37 – 4.29 (m, 1H), 4.17 (qd, J = 7.1, 2.0 Hz, 2H), 2.17 – 2.00 (m, 4H), 1.67 (d, J = 1.4 Hz, 3H), 1.52 (d, J = 1.4 Hz, 3H), 1.21 (t, J = 7.1 Hz, 3H)

<sup>13</sup>C NMR (126 MHz, CDCl<sub>3</sub>) δ [ppm] 201.5, 169.7, 163.2, 136.9, 133.9, 130.3, 122.9, 119.2, 119.1, 118.9, 61.7, 53.1, 29.3, 26.0, 25.8, 17.8, 14.2.

HRMS calcd for C<sub>17</sub>H<sub>22</sub>O<sub>4</sub>Na<sup>+</sup>: 313.1410 found: 313.1414

IR (ATR):  $\tilde{\nu}$  [cm<sup>-1</sup>] 2979.78 (w), 2928.76 (w), 2360.12 (m), 2341.79 (m), 1734.59 (s), 1637.14 (s), 1613.84 (m), 1579.06 (m), 1486.78 (m), 1445.81 (s), 1368.64 (m), 1342.07 (m), 1304.24 (m), 1241.37 (m), 1178.88 (m), 1148.51 (s), 1033.76 (m), 975.31 (w), 753.43 (s), 692.99 (w), 667.75 (w), 661.17 (w), 618.91 (w), 526.15 (w), 428.14 (w)

7.2.1.1.10 1-(2-methoxyphenyl)-6-methylhept-5-en-1-one (**284**)



C<sub>15</sub>H<sub>20</sub>O<sub>2</sub>  
232.32 g mol<sup>-1</sup>

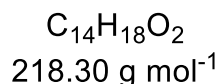
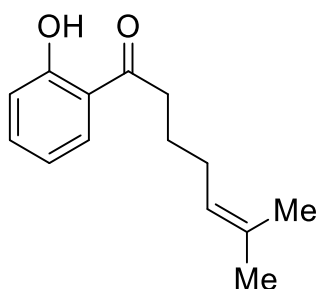
LiHMDS (4.36 mL, 1.0 M, 4.36 mmol 1.1 eq.) was dissolved in THF (12 mL) at -78 °C. 2'-Methoxyacetophenone (595 mg, 3.96 mmol, 1 eq.) was added dropwise to the solution. The reaction was stirred for 1 h at -78 °C and 1 h at 0 °C. The mixture was cooled again to -78 °C and homoprenyliodide (915 mg, 4.36 mmol, 1.1 mmol) was added to the solution and the reaction was allowed to warm to room temperature overnight. NH<sub>4</sub>Cl solution was added and the mixture was extracted with EtOAc and dried with Na<sub>2</sub>SO<sub>4</sub>. The solvent was removed under

reduced pressure and the residue was purified by column chromatography (SiO<sub>2</sub>: 95 % Pentane: 5 % EtOAc). **284** was received as a colorless oil (111 mg, 478 μmol, 12 %)

<sup>1</sup>H NMR (500 MHz, CDCl<sub>3</sub>) δ [ppm] 7.64 (dd, *J* = 7.6, 1.8 Hz, 1H), 7.44 (ddd, *J* = 9.0, 7.5, 1.9 Hz, 1H), 7.01 – 6.92 (m, 2H), 5.13 (ddt, *J* = 8.7, 7.2, 1.5 Hz, 1H), 3.89 (s, 3H), 2.95 (t, *J* = 7.4 Hz, 2H), 2.04 (q, *J* = 7.4 Hz, 2H), 1.72 (q, *J* = 7.5 Hz, 2H), 1.68 (s, 3H), 1.59 (s, 3H).

The spectroscopic data matched those reported in the literature<sup>98</sup>

#### 7.2.1.1.11 1-(2-hydroxyphenyl)-6-methylhept-5-en-1-one (**261**)

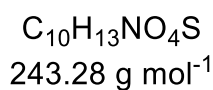
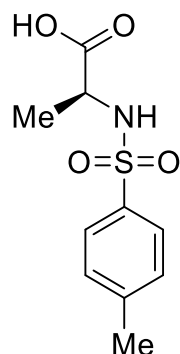


A pressure tube, sealed with a septum, was charged with NaH (60 % suspension in paraffin oil, 95 mg, 2.39 mmol, 5.0 eq.) and anhydrous DMF (3.5 mL). Ethanethiol (0.18 mL, 2.39 mmol, 5.0 eq.) was added dropwise to this suspension at room temperature. To the yellow solution was added a solution of **23** (111 mg, 0.48 mmol, 1.0 eq.) in anhydrous DMF (1.0 mL) and the septum was replaced by a PTFE front-seal plug. The reaction mixture was then stirred for 4 h at 130 °C. After cooling to room temperature, the reaction was quenched by the addition of saturated aqueous NH<sub>4</sub>Cl, and this mixture was extracted with Et<sub>2</sub>O (3 × 30 mL). The combined organic phases were washed with water (5 × 50 mL), dried over Na<sub>2</sub>SO<sub>4</sub>, filtered and concentrated under reduced pressure. Purification by flash column chromatography SiO<sub>2</sub>: 95 % pentane: 5 % EtOAc yielded the product as a colorless oil (85.0 mg, 389 μmol, 81 %).

<sup>1</sup>H NMR (500 MHz, CDCl<sub>3</sub>) δ [ppm] 12.40 (s, 1H), 7.76 (dd, *J* = 8.0, 1.7 Hz, 1H), 7.46 (ddd, *J* = 8.6, 7.1, 1.7 Hz, 1H), 6.98 (dd, *J* = 8.4, 1.1 Hz, 1H), 6.89 (ddd, *J* = 8.3, 7.2, 1.2 Hz, 1H), 5.13 (dddd, *J* = 7.2, 5.7, 3.0, 1.5 Hz, 1H), 2.98 (t, *J* = 7.4 Hz, 2H), 2.10 (q, *J* = 7.3 Hz, 2H), 1.80 (p, *J* = 7.3 Hz, 2H), 1.70 (d, *J* = 1.4 Hz, 3H), 1.60 (s, 3H).

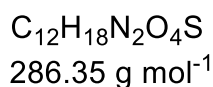
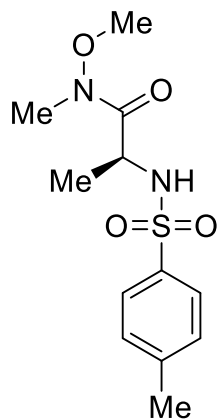
The spectroscopic data matched those reported in the literature<sup>98</sup>

#### 7.2.1.1.12 Tosyl-L-alanine (**337**)



Alanine (2.00 g, 22.4 mmol, 1 eq.) was dissolved in a 1:2 mixture of THF and water (60 mL). The solution was cooled to 0 °C and triethylamine (9.5 mL, 67.5 mmol, 3 eq.) and tosyl chloride (5.15 g, 27.0 mmol, 1.2 eq.). The solution was stirred for 4 h at 0 °C. HCl (1 M) was added until a white precipitate formed. The mixture was extracted with Et<sub>2</sub>O. The solvent was removed under reduced pressure and the residue was used without further purification.

#### 7.2.1.1.13 (S)-N-methoxy-N-methyl-2-((4-methylphenyl)sulfonamido)propanamide(**338**)



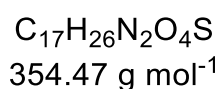
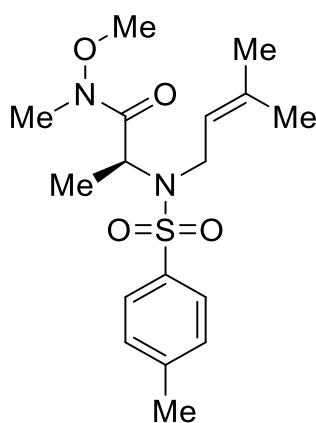
**337** (2.00 g, 8.22 mmol, 1 eq.), N,O-dimethylhydroxylamine hydrochloride (884 mg, 9.06 mmol, 1.1 eq.) and morpholine (1.00 mL, 9.09 mmol, 1.1 eq.) were dissolved in DCM (10 mL). The mixture was cooled to 0 °C and DCC (1.87 g, 9.06 mmol, 1.1 eq.) was added in one portion. The reaction was allowed to warm up to room temperature overnight. The reaction was

quenched by the addition of HCl (1 M) and the mixture was extracted with DCM. The organic phase was washed with sat. NaHCO<sub>3</sub> solution and brine. The organic phase was dried with Na<sub>2</sub>SO<sub>4</sub> and filtered through a celite<sup>®</sup> pad. The solvent was removed under reduced pressure and the residue was purified by column chromatography (SiO<sub>2</sub>, 70 % cHex: 30 % EtOAc). The product was obtained as a colorless oil (1.45 g, 5.05 mmol, 61 %)

<sup>1</sup>H NMR (500 MHz, CDCl<sub>3</sub>) δ [ppm] 7.72 (d, *J* = 8.3 Hz, 2H), 7.29 – 7.26 (m, 2H), 5.50 (d, *J* = 9.3 Hz, 1H), 4.34 (t, *J* = 8.0 Hz, 1H), 3.56 (s, 3H), 2.99 (s, 3H), 2.41 (s, 3H), 1.30 (d, *J* = 7.0 Hz, 3H).

The spectroscopic data matched those reported in the literature<sup>66</sup>

7.2.1.1.14 (S)-N-methoxy-N-methyl-2-((4-methyl-N-(3-methylbut-2-en-1-yl)phenyl)sulfonamido)propanamide (**339**)



**338** (2.50 g, 8.74 mmol, 1 eq.) was dissolved in DMF (82 mL). The solution was cooled to 0 °C and NaH (60 % suspension in paraffin oil, 420 mg, 10.5 mmol, 1.2 eq.) was added. The mixture was continued to stir for 15 min. Prenyl bromide (1.21 mL, 10.5 mmol, 1.2 eq.) was added and the solution was allowed to warm up to room temperature overnight. NH<sub>4</sub>Cl solution was added and the mixture was extracted with EtOAc and dried with Na<sub>2</sub>SO<sub>4</sub>. The solvent was removed under reduced pressure and the residue was purified by column chromatography (SiO<sub>2</sub>, 80 % cHex: 20 % EtOAc). The product was received as a colorless oil (2.13 g, 6.00 mmol, 69 %)

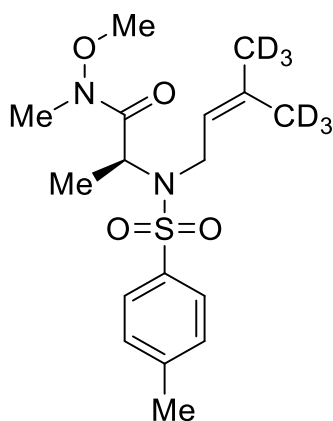
<sup>1</sup>H NMR (500 MHz, CDCl<sub>3</sub>) δ [ppm] 7.68 (d, *J* = 8.1 Hz, 2H), 7.27 – 7.24 (m, 2H), 5.19 – 5.05 (m, 2H), 4.10 (dd, *J* = 16.8, 6.6 Hz, 1H), 3.99 – 3.90 (m, 1H), 3.77 (s, 3H), 3.09 (s, 3H), 2.41 (s, 3H), 1.63 (d, *J* = 12.0 Hz, 6H), 1.27 (d, *J* = 7.2 Hz, 3H).

$^{13}\text{C}$  NMR (151 MHz,  $\text{CDCl}_3$ )  $\delta$  [ppm] 172.5, 143.2, 137.9, 133.8, 129.5, 127.5, 127.4, 122.8, 61.8, 51.2, 42.9, 32.2, 25.8, 21.6, 17.9, 16.0. (the number of signals deviates from the theoretical value due to signal overlap)

HRMS calcd for  $\text{C}_{17}\text{H}_{26}\text{N}_2\text{O}_4\text{SNa}^+$ : 377.1505 found: 377.1511

IR (ATR):  $\tilde{\nu}$  [ $\text{cm}^{-1}$ ]: 2975.27 (w), 2935.67 (w), 1666.48 (s), 1597.89 (w), 1493.80 (m), 1446.65 (m), 1377.51 (m), 1336.29 (s), 1305.06 (m), 1288.51 (m), 1152.15 (s), 1110.86 (m), 1090.76 (s), 1066.56 (m), 988.56 (s), 917.10 (m), 889.31 (m), 843.64 (m), 814.80 (m), 769.76 (m), 745.74 (s), 708.69 (m), 687.78 (m), 657.16 (s), 618.98 (m), 566.07 (s), 544.46 (s), 491.54 (m), 468.39 (m), 430.67 (m)

7.2.1.1.15 (S)-N-methoxy-N-methyl-2-((4-methyl-N-(3-(methyl-d3)but-2-en-1-yl)-4,4,4-d3phenyl)sulfonamido)propanamide (**339D**)



$\text{C}_{17}\text{H}_{20}\text{D}_6\text{N}_2\text{O}_4\text{S}$   
360.50  $\text{g mol}^{-1}$

**338** (701 mg, 2.45 mmol, 1 eq.) was dissolved in DMF (40 mL). The solution was cooled to 0 °C and NaH (60 % suspension in paraffin oil, 118 mg, 2.94 mmol, 1.2 eq.) was added. The mixture was continued to stir for 15 min.  $\text{D}_6$ -prenyl bromide (0.35 mL, 2.94 mmol, 1.2 eq.) was added and the solution was allowed to warm up to room temperature overnight.  $\text{NH}_4\text{Cl}$  solution was added and the mixture was extracted with EtOAc and dried with  $\text{Na}_2\text{SO}_4$ . The solvent was removed under reduced pressure and the residue was purified by column chromatography. ( $\text{SiO}_2$ , 80 % cHex : 20 % EtOAc). The product was received as a colorless oil (747 mg, 2.07 mmol, 84 %)

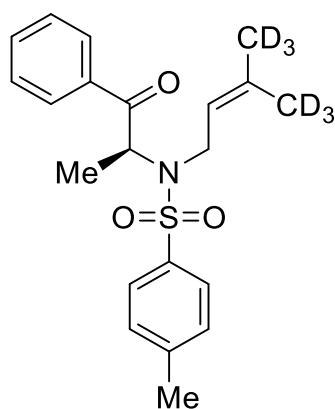
**<sup>1</sup>H NMR** (500 MHz, CDCl<sub>3</sub>) δ [ppm] 7.68 (d, *J* = 8.3 Hz, 2H), 7.26 (d, *J* = 8.1 Hz, 2H), 5.16 (t, *J* = 6.6 Hz, 1H), 5.11 (s, 1H), 4.10 (dd, *J* = 16.7, 6.7 Hz, 1H), 3.95 (dd, *J* = 16.8, 6.3 Hz, 1H), 3.76 (s, 3H), 3.09 (s, 3H), 2.40 (s, 3H), 1.27 (d, *J* = 7.2 Hz, 3H).

**<sup>13</sup>C NMR** (151 MHz, CDCl<sub>3</sub>) δ [ppm] 172.5, 143.2, 137.9, 133.7, 129.5, 127.5, 122.8, 61.8, 51.2, 42.9, 32.2, 21.7, 16.0. (CD<sub>3</sub>-Signals not observable, the number of signals deviates from the theoretical value due to signal overlap)

**HRMS** calcd for C<sub>17</sub>H<sub>20</sub>D<sub>6</sub>N<sub>2</sub>O<sub>4</sub>SNa<sup>+</sup>: 383.1882 found: 383.1889

**IR (ATR):**  $\tilde{\nu}$  [cm<sup>-1</sup>]: 2979.47 (w), 2940.10 (w), 1665.90 (s), 1597.84 (w), 1493.68 (m), 1449.36 (m), 1387.50 (m), 1337.28 (s), 1304.99 (m), 1288.93 (m), 1216.97 (m), 1152.51 (s), 1116.69 (m), 1091.07 (m), 1047.33 (m), 1031.16 (m), 1018.74 (m), 989.72 (s), 923.24 (m), 894.94 (m), 815.10 (m), 801.88 (m), 750.95 (m), 730.10 (m), 708.11 (m), 685.42 (m), 656.69 (s), 618.40 (m), 565.27 (s), 544.21 (s), 470.69 (m), 433.33 (m), 410.81 (m)

7.2.1.1.16 (S)-4-methyl-N-(3-(methyl-d<sub>3</sub>)but-2-en-1-yl-4,4-d<sub>3</sub>)-N-(1-oxo-1-phenylpropan-2-yl)benzenesulfonamide (**283D**)



C<sub>21</sub>H<sub>19</sub>D<sub>6</sub>NO<sub>3</sub>S  
377.53 g mol<sup>-1</sup>

Phenylmagnesium bromide was added as a 3 M solution in Et<sub>2</sub>O (1.38 mL, 4.14 mmol, 2 eq.) to THF (10 mL) at 0 °C. **339D** (746 mg, 2.07 mmol, 1 eq.) was dissolved in THF (1 mL) and added dropwise to the Grignard solution. The ice bath was removed and the reaction was allowed to warm up to room temperature. The reaction was stirred for 4 h followed by the addition of saturated NH<sub>4</sub>Cl solution. The mixture was extracted with EtOAc and dried with Na<sub>2</sub>SO<sub>4</sub>. The solvent was removed under reduced pressure and the residue was purified by column chromatography (SiO<sub>2</sub>, 90 % cHex : 10 % EtOAc,). The product was received as a colorless oil (608 mg, 1.61 mmol, 78 %)



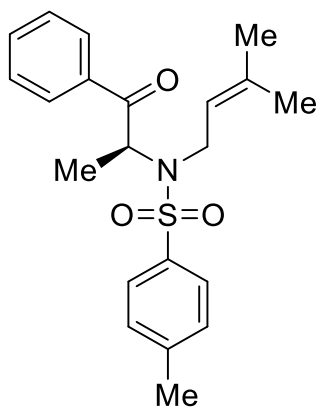
**<sup>1</sup>H NMR** (500 MHz, CDCl<sub>3</sub>) δ [ppm] 8.06 (dd, *J* = 8.4, 1.4 Hz, 2H), 7.66 (d, *J* = 8.3 Hz, 2H), 7.58 – 7.53 (m, 1H), 7.46 (ddd, *J* = 8.1, 7.1, 1.2 Hz, 2H), 7.28 – 7.23 (m, 2H), 5.54 (q, *J* = 6.9 Hz, 1H), 4.78 (dd, *J* = 7.7, 6.2 Hz, 1H), 3.86 (dd, *J* = 15.5, 6.2 Hz, 1H), 3.60 (dd, *J* = 15.5, 7.7 Hz, 1H), 2.41 (s, 3H), 1.24 (d, *J* = 6.9 Hz, 3H).

**<sup>13</sup>C NMR** (126 MHz, CDCl<sub>3</sub>) δ [ppm] 198.3, 143.7, 137.2, 135.9, 133.1, 129.8, 129.8, 128.9, 128.6, 127.7, 120.5, 115.4, 56.1, 42.7, 21.7, 13.3. (CD<sub>3</sub>-Signals not observable, the number of signals deviates from the theoretical value due to signal overlap)

**HRMS** calcd for C<sub>21</sub>H<sub>19</sub>D<sub>6</sub>NO<sub>3</sub>SNa<sup>+</sup>: 400.1824 found 400.1830

**IR (ATR):**  $\tilde{\nu}$  [cm<sup>-1</sup>] 2980.71 (w), 1686.56 (m), 1596.34 (w), 1493.87 (w), 1448.07 (w), 1378.66 (m), 1341.01 (m), 1305.12 (m), 1288.88 (m), 1228.20 (m), 1154.51 (s), 1119.23 (m), 1088.94 (m), 1060.62 (m), 1046.09 (m), 1018.20 (m), 1001.12 (m), 983.18 (m), 953.89 (m), 899.63 (m), 813.86 (m), 747.31 (s), 723.80 (s), 692.38 (s), 673.56 (s), 650.58 (s), 595.11 (s), 550.65 (s)

7.2.1.1.17 (S)-4-methyl-N-(3-methylbut-2-en-1-yl)-N-(1-oxo-1-phenylpropan-2-yl)benzenesulfonamide (**283**)



C<sub>21</sub>H<sub>25</sub>NO<sub>3</sub>S  
371.50 g mol<sup>-1</sup>

Phenylmagnesium bromide was added as 3 M solution in Et<sub>2</sub>O (1.88 mL, 5.64 mmol, 2 eq.) to THF (14 mL) at 0 °C. **339** (1.00 g, 2.82 mmol, 1 eq.) was dissolved in THF (3 mL) and added dropwise to the Grignard solution. The ice bath was removed and the reaction was allowed to warm up to room temperature. The reaction was stirred for 4 h followed by the addition of saturated NH<sub>4</sub>Cl solution. The mixture was extracted with EtOAc and dried with Na<sub>2</sub>SO<sub>4</sub>. The solvent was removed under reduced pressure and the residue was purified by column

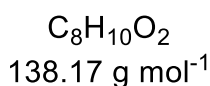
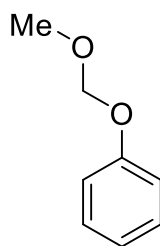
chromatography (SiO<sub>2</sub>, 10 % EtOAc, 90 % cHex). The product was received as a colorless oil (638 mg, 1.71 mmol, 61 %)

<sup>1</sup>H NMR (500 MHz, C<sub>6</sub>D<sub>6</sub>) δ [ppm] 8.32 – 8.29 (m, 2H), 7.67 (d, *J* = 8.3 Hz, 2H), 7.14 – 7.10 (m, 3H), 6.75 (s, 2H), 5.58 (q, *J* = 6.8 Hz, 1H), 4.98 (ddt, *J* = 7.6, 6.1, 1.4 Hz, 1H), 4.01 – 3.92 (m, 1H), 3.56 (dd, *J* = 15.4, 8.0 Hz, 1H), 1.87 (s, 3H), 1.34 – 1.31 (m, 6H), 1.09 (d, *J* = 6.8 Hz, 3H).

<sup>1</sup>H NMR (500 MHz, CDCl<sub>3</sub>) δ [ppm] 8.06 (dd, *J* = 8.4, 1.4 Hz, 2H), 7.66 (d, *J* = 8.3 Hz, 2H), 7.58 – 7.53 (m, 1H), 7.46 (ddd, *J* = 8.1, 6.7, 1.2 Hz, 2H), 7.28 – 7.24 (m, 2H), 5.54 (q, *J* = 6.9 Hz, 1H), 4.78 (dddd, *J* = 7.6, 6.2, 2.8, 1.4 Hz, 1H), 3.86 (dd, *J* = 15.5, 6.2 Hz, 1H), 3.60 (dd, *J* = 15.5, 7.8 Hz, 1H), 2.41 (s, 3H), 1.49 – 1.44 (m, 6H), 1.24 (d, *J* = 6.9 Hz, 3H).

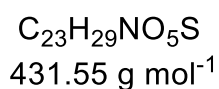
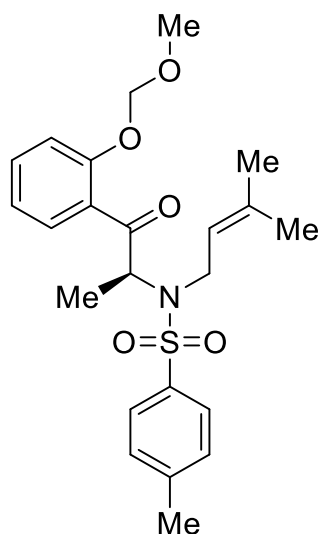
The spectroscopic data matched those reported in the literature<sup>66</sup>

#### 7.2.1.1.18 (Methoxymethoxy)benzene (340)



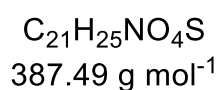
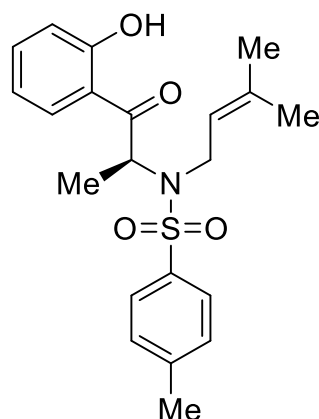
NaH (60 % suspension in paraffin oil, 274 mg, 6.84 mmol, 1.3 eq.) was suspended in THF (12 mL) and cooled to 0 °C. Phenol (500 mg, 5.26 mmol, 1 eq.) was added and the mixture was stirred for 15 min. Bromomethyl methyl ether (0.56 mL, 6.84 mmol, 1.3 eq.) was added dropwise and the reaction was stirred for 30 min at 0 °C. The solvent was removed under reduced pressure and the residue was diluted with water and extracted with DCM. The organic phase was dried over MgSO<sub>4</sub> and the solvent was removed under reduced pressure. The product was used without further purification.

7.2.1.1.19 (S)-N-(1-(2-(methoxymethoxy)phenyl)-1-oxopropan-2-yl)-4-methyl-N-(3-methylbut-2-en-1-yl)benzenesulfonamide (**341**)



**340** (484 mg, 3.50 mmol, 2.4 eq.) was dissolved in THF (23 mL) and cooled to -78°C. *t*-BuLi (2.06 mL, 1.7 M, 3.50 mmol, 2.4 eq.) was added dropwise and the reaction was stirred for 1 h at -78°C and 3 h at room temperature. The mixture was cannulated to a solution of **339** (524 mg, 1.48 mmol, 1 eq.) in THF (17.5 mL) at 0 °C. The reaction was allowed to room temperature and tracked by TLC till completion. NH<sub>4</sub>Cl solution was added and the mixture was extracted with EtOAc and dried with Na<sub>2</sub>SO<sub>4</sub>. The solvent was removed under reduced pressure and the residue was used without further purification.

7.2.1.1.20 (S)-N-(1-(2-hydroxyphenyl)-1-oxopropan-2-yl)-4-methyl-N-(3-methylbut-2-en-1-yl)benzenesulfonamide (**283**)



**341** (496 mg, 1.15 mmol, 1 eq.) was dissolved in a 1:1 mixture of methanol and water (5.8 mL) and cooled to 0 °C. 37 % Hydrochloric acid (0.6 mL, 6.6 mmol, 5.7 eq.) was added dropwise to the solution. The reaction was warmed to room temperature and stirred for 30 min. The solvent was removed under reduced pressure without any further workup. The crude mixture was directly loaded to a column (SiO<sub>2</sub>, 20 % EtOAc, 80 % cHex). The product was obtained as a white solid (309 mg, 797 μmol, 69 %)

**<sup>1</sup>H NMR** (500 MHz, CDCl<sub>3</sub>) δ [ppm] 11.72 (s, 1H), 8.23 (dd, *J* = 8.6, 1.6 Hz, 1H), 7.71 – 7.65 (m, 2H), 7.48 (ddd, *J* = 8.6, 7.4, 1.6 Hz, 1H), 7.27 (dd, *J* = 8.5, 0.9 Hz, 2H), 6.99 – 6.91 (m, 2H), 5.64 (q, *J* = 6.9 Hz, 1H), 4.81 (ddq, *J* = 7.4, 4.3, 1.4 Hz, 1H), 3.92 (ddt, *J* = 15.8, 5.7, 1.3 Hz, 1H), 3.70 – 3.61 (m, 1H), 2.42 (s, 3H), 1.48 (dd, *J* = 2.7, 1.2 Hz, 6H), 1.25 (d, *J* = 6.9 Hz, 3H).

**<sup>13</sup>C NMR** (126 MHz, CDCl<sub>3</sub>) δ [ppm] 203.3, 162.9, 143.8, 137.2, 136.8, 136.7, 130.7, 129.8, 127.6, 120.8, 119.3, 118.4, 118.3, 55.3, 42.7, 25.6, 21.7, 17.8, 13.3. (the number of signals deviates from the theoretical value due to signal overlap)

**HRMS** calcd for C<sub>21</sub>H<sub>25</sub>NO<sub>4</sub>SNa<sup>+</sup>: 410.1397 found: 410.1405

**IR (ATR):**  $\tilde{\nu}$  [cm<sup>-1</sup>] 2972.19 (w), 2943.75 (w), 2914.67 (w), 1643.73 (m), 1334.60 (s), 1268.74 (s), 1203.45 (m), 1155.05 (s), 1086.49 (m), 887.61 (m), 818.80 (m), 754.83 (m), 745.81 (m), 718.95 (m), 708.05 (m), 672.83 (m), 651.86 (m), 569.68 (m), 559.67 (m), 546.00 (s), 532.30 (m), 518.27 (m)

### 7.2.1.2 Cyclization Experiments

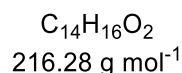
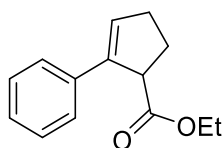
#### 7.2.1.2.1 General Procedure for the cyclisation with FeCl<sub>3</sub>

A two-neck flask was heated out under reduced pressure and transferred to an N<sub>2</sub> glove box. FeCl<sub>3</sub> (0.2 eq.) was weighed precisely so that the amount ranged between 5 – 10 mg. The sealed flask was transferred to a Schlenk line and, anhydrous 1,2-dichloroethane (**87**/ **281**) or toluene (**270**) was added to reach a concentration of 5 μM. The substrate was added (1 eq.) and the reaction was stirred at room temperature and tracked by TLC. The reaction mixture was transferred directly to the column (SiO<sub>2</sub> 100 % pentane) and was rinsed with pentane. The eluent was gradually changed to the desired mixture.

#### 7.2.1.2.2 General Procedure for the cyclization with II and HCl

Resorcinarene (0.6 eq.) was weighed into a pressure vial and chloroform (filtered through basic aluminum oxide) was added. The capped vial was heated gently until the suspension turned clear. After cooling to room temperature, HCl (0.05 eq. (**281**)/ 0.2 eq. (**270**)) was added in the form of HCl-saturated chloroform. The substrate was added (**281**/ **270** 1 eq.) and filtered chloroform was added to receive a total concentration of 33.1 mM. The vial was equipped with a stirring bar and transferred to an oil bath set to 50°C (**281**) or 30°C (**270**). The reaction mixture was transferred directly to the column (SiO<sub>2</sub> 100 % pentane) and was rinsed with pentane. The eluent was gradually changed to the desired mixture.

#### 7.2.1.2.3 Ethyl 2-phenylcyclopent-2-ene-1-carboxylate (**342**)



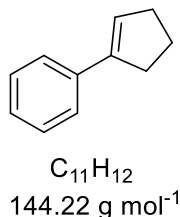
<sup>1</sup>H NMR (500 MHz, CDCl<sub>3</sub>) δ [ppm] 7.44 – 7.41 (m, 2H), 7.32 – 7.27 (m, 2H), 7.24 – 7.19 (m, 1H), 6.34 (td, *J* = 2.7, 1.6 Hz, 1H), 4.15 – 4.02 (m, 2H), 3.98 – 3.94 (m, 1H), 2.72 (dddt, *J* = 17.8, 9.1, 6.7, 2.6 Hz, 1H), 2.58 – 2.49 (m, 1H), 2.36 (dtd, *J* = 13.0, 9.1, 6.6 Hz, 1H), 2.25 (ddt, *J* = 13.1, 8.8, 4.4 Hz, 1H), 1.14 (t, *J* = 7.1 Hz, 3H).

The spectroscopic data matched those reported in the literature<sup>98</sup>

**FeCl<sub>3</sub> catalysis:** According to the general procedure, **87** (108 mg, 395 μmol, 1 eq.) was used. Column chromatography (SiO<sub>2</sub>, 100 % pentane) provided **342** as colorless oil (65.6 mg, 303 μmol, 77 %) <sup>63</sup>

**Capsule (II)/HCl-catalysis:** was reported in a previous publication<sup>98</sup>

#### 7.2.1.2.4 Cyclopent-1-en-1-ylbenzene (**343**)



<sup>1</sup>H NMR (500 MHz, CDCl<sub>3</sub>) δ [ppm] 7.47 – 7.43 (m, 2H), 7.32 (dd, *J* = 8.4, 7.0 Hz, 2H), 7.24 – 7.19 (m, 1H), 6.19 (p, *J* = 2.3 Hz, 1H), 2.76 – 2.68 (m, 2H), 2.54 (tq, *J* = 7.5, 2.5 Hz, 2H), 2.03 (p, *J* = 7.6 Hz, 2H).

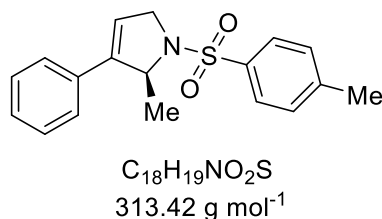
<sup>13</sup>C NMR (126 MHz, CDCl<sub>3</sub>) δ [ppm] 142.6, 137.0, 128.4, 127.0, 126.3, 125.7, 33.5, 33.3, 23.5.

The spectroscopic data matched those reported in the literature<sup>134</sup>

**FeCl<sub>3</sub> catalysis:** According to the general procedure, **281** (46.1 mg, 228 μmol, 1eq.) was used. Column chromatography (SiO<sub>2</sub>, 100 % pentane) provided **343** as colorless oil (26.6 mg, 184 μmol, 81 %)

**Capsule (II)/HCl-catalysis:** According to the general procedure, **281** (30.1 mg, 149 μmol, 1eq.) was used. Column chromatography (SiO<sub>2</sub>, 100 % pentane) provided **343** as colorless oil (15.6 mg, 108 μmol, 72 %)

#### 7.2.1.2.5 (S)-2-methyl-3-phenyl-1-tosyl-2,5-dihydro-1H-pyrrole (**344**)



$^1\text{H}$  NMR (500 MHz,  $\text{CDCl}_3$ )  $\delta$  [ppm] 7.76 (d,  $J = 8.3$  Hz, 2H), 7.38 – 7.23 (m, 7H), 5.82 (q,  $J = 2.0$  Hz, 1H), 5.05 – 4.95 (m, 1H), 4.34 – 4.21 (m, 2H), 2.40 (s, 3H), 1.47 (d,  $J = 6.4$  Hz, 3H).

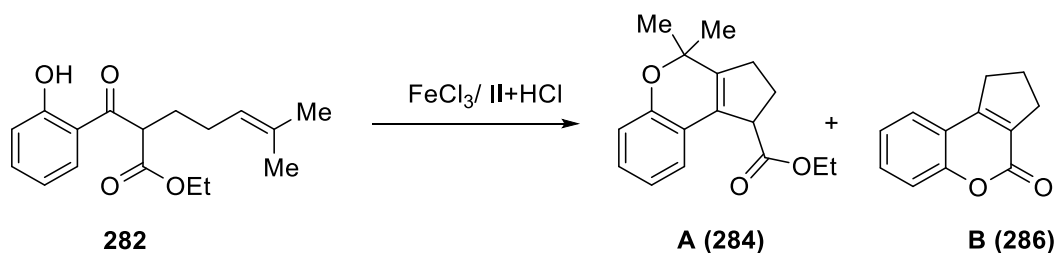
The spectroscopic data matched those reported in the literature<sup>66, 105</sup>

**$\text{FeCl}_3$  catalysis** According to the general procedure, **270** (55.0 mg, 148  $\mu\text{mol}$ , 1 eq.) was used. Column chromatography ( $\text{SiO}_2$ , 90 % pentane: 10 % EtOAc) provided **344** as white solid (40.0 mg, 128  $\mu\text{mol}$ , 86 %)

**Capsule (II)/HCl-catalysis:** According to the general procedure, **270** (61.7 mg, 166  $\mu\text{mol}$ , 1 eq.) was used. Column chromatography ( $\text{SiO}_2$ , 90 % pentane: 10 % EtOAc) provided **344** as white solid (42.9 mg, 137  $\mu\text{mol}$ , 82 %)

### 7.2.1.3 Cation Trapping Experiments

#### 7.2.1.3.1 Mechanistic Probe **282**



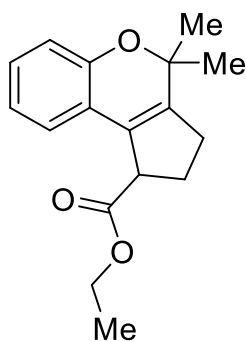
**$\text{FeCl}_3$  catalysis:** A 15 mL pressure vial was heated out under reduced pressure and transferred to an  $\text{N}_2$  glovebox and  $\text{FeCl}_3$  (1.90 mg, 11.7  $\mu\text{mol}$ , 0.2 eq.) was added. The pressure vial was transported back to the fume hood and DCE (4.9 mL) was added. **282** (17.0 mg, 58.5  $\mu\text{mol}$ , 1 eq.) was dissolved in DCE (1 mL) and added to the suspension. The reaction turned black after the addition of **282**. After 5 min the suspension turned clear and yellow. The reaction was stirred for 6 d at 50  $^\circ\text{C}$ , however, no conversion was observed. The reaction volume was split in half, whereas one half was transferred to another pressure vial with additional  $\text{FeCl}_3$  (4.75 mg, 29.3  $\mu\text{mol}$ , 1 eq.). The rest of the reaction volume was evaporated under reduced pressure and loaded onto the column.

The concentration of the reaction mixture under reduced pressure led to decomposition of the material and neither product nor starting material was obtained.

Excess of  $\text{FeCl}_3$  led to fast conversion within 4 h and two products were isolated. The reaction mixture was loaded onto the column and rinsed with pentane to remove DCE. The solvent was changed to 2.5 % EtOAc in pentane, to obtain products **284** and **286** (see below for details).

**Capsule (II)/HCl-catalysis:** Resorcinarene (242 mg, 0.219 mmol, 1.2 eq.) was suspended in 8 mL chloroform (filtered through basic aluminum oxide) in a 15 mL pressure tube. The capped vial was heated gently until the suspension turned clear. After cooling to room temperature, HCl was added in the form of HCl-saturated chloroform (263  $\mu$ L, 18.0  $\mu$ mol, 0.1 eq.). Chloroform (filtered through basic aluminum oxide) was added to obtain a total volume of 11.2 mL and **282** (53.1 mg, 183  $\mu$ mol, 1 eq.) was added. The vial was placed in a 400 mL oil bath to ensure a constant temperature of 50  $^{\circ}$ C over the reaction period. The reaction mixture was directly loaded onto the column and rinsed with pentane to remove chloroform. The solvent was changed to 2.5 % EtOAc in pentane, to obtain product **284** (see below for details).

#### 7.2.1.3.2 Ethyl 4,4-dimethyl-1,2,3,4-tetrahydrocyclopenta[c]chromene-1-carboxylate (**284**)



Chemical Formula:  $C_{17}H_{20}O_3$   
 $272.34 \text{ g mol}^{-1}$

The Product was obtained as a white solid.

**$^1\text{H NMR}$**  (500 MHz,  $\text{CDCl}_3$ )  $\delta$  [ppm] 7.09 – 7.03 (m, 2H), 6.85 – 6.76 (m, 2H), 4.13 (qd,  $J = 7.1, 3.7$  Hz, 2H), 3.89 – 3.82 (m, 1H), 2.74 (dtd,  $J = 16.1, 7.9, 2.6$  Hz, 1H), 2.52 – 2.40 (m, 1H), 2.32 – 2.20 (m, 2H), 1.48 (s, 3H), 1.44 (s, 3H), 1.21 (t,  $J = 7.1$  Hz, 3H).

**$^{13}\text{C NMR}$**  (126 MHz,  $\text{CDCl}_3$ )  $\delta$  [ppm] 174.8, 152.7, 143.5, 128.6, 128.5, 123.3, 120.7, 120.7, 116.2, 78.4, 60.8, 49.8, 32.0, 28.3, 26.5, 26.4, 14.3.

**HRMS** calcd for  $C_{17}H_{20}O_3\text{Na}^+$ : 295.1305 found: 295.1310

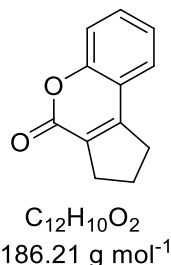
**IR (ATR):**  $\tilde{\nu}$  [ $\text{cm}^{-1}$ ]: 2979.11 (w), 2935.88 (w), 1726.07 (s), 1605.52 (w), 1487.91 (m), 1447.46 (m), 1377.54 (m), 1359.74 (m), 1332.14 (w), 1299.32 (m), 1288.12 (m), 1274.21 (m), 1234.68 (m), 1207.49 (m), 1150.12 (s), 1121.05 (m), 1084.12 (m), 1019.60 (m), 950.84 (m), 929.95 (m), 904.28 (m), 879.24 (w), 849.69 (w), 805.20 (w), 760.34 (s), 658.53 (w), 629.55 (w), 612.40 (w), 566.94 (w), 546.58 (w), 534.44 (w), 479.77 (w), 423.00 (w), 415.63 (w)



**FeCl<sub>3</sub> catalysis:** 2.00mg, 7.34 μmol, 25 %

**Capsule (I)/HCl-catalysis:** 40.0 mg, 0.147 μmol, 80 %

#### 7.2.1.3.3 2,3-dihydrocyclopenta[c]chromen-4(1H)-one (**286**)



The product was obtained as a white solid.

**<sup>1</sup>H NMR** (500 MHz, CDCl<sub>3</sub>) δ [ppm] 7.49 (ddd, *J* = 8.6, 7.2, 1.6 Hz, 1H), 7.45 (dd, *J* = 7.8, 1.6 Hz, 1H), 7.37 (dd, *J* = 8.2, 1.1 Hz, 1H), 7.30 – 7.26 (m, 1H), 3.10 (ddt, *J* = 8.3, 7.0, 1.9 Hz, 2H), 2.94 (tt, *J* = 7.6, 1.9 Hz, 2H), 2.23 (ddd, *J* = 15.3, 8.0, 7.1 Hz, 2H).

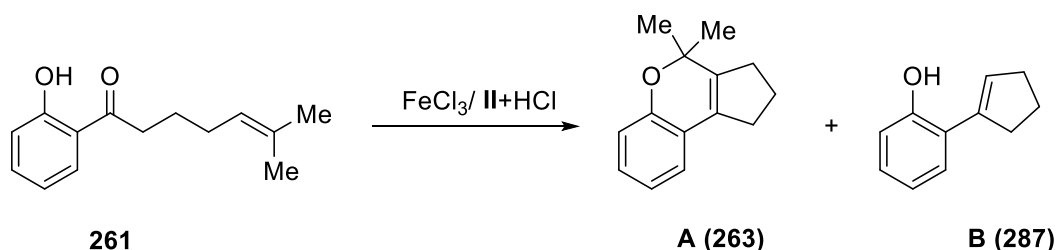
**<sup>13</sup>C NMR** (151 MHz, CDCl<sub>3</sub>) δ [ppm] 160.4, 156.2, 154.3, 131.0, 128.2, 124.9, 124.2, 118.9, 116.9, 32.2, 30.8, 22.6.

**HRMS** calcd for C<sub>12</sub>H<sub>10</sub>O<sub>2</sub>Na<sup>+</sup>: 209.0573 found: 209.0572

**IR (ATR):**  $\tilde{\nu}$  [cm<sup>-1</sup>]: 2969.83 (w), 2919.55 (w), 2854.43 (w), 2360.65 (s), 2342.51 (s), 1720.14 (s)

**FeCl<sub>3</sub> catalysis:** 2.00 mg, 10.7 μmol, 37 %

#### 7.2.1.3.4 Mechanistic Probe **261**

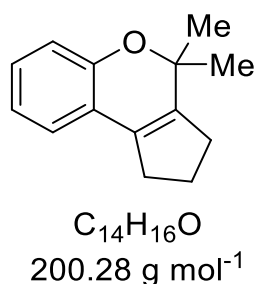


**FeCl<sub>3</sub> catalysis:** A two-neck flask was heated out under reduced pressure and transported to an N<sub>2</sub> glovebox and FeCl<sub>3</sub> (5.06 mg, 31.2 μmol, 0.2 eq.) was added. The flask was transported to a Schlenk line and dry DCE (14.6 mL) was added. **261** (34.1 mg, 156 μmol, 1 eq.) was

dissolved in dry DCE (1 mL) and added to the suspension. The reaction was stirred at room temperature and tracked by TLC. Upon completion, the reaction mixture was directly loaded onto the column and rinsed with pentane to remove DCE. The eluent was then changed to 2.5 % EtOAc in pentane.

**Capsule (II)/HCl-catalysis:** The experiment was performed as described in our previous publication yielding **263** exclusively.<sup>98</sup>

#### 7.2.1.3.5 4,4-dimethyl-1,2,3,4-tetrahydrocyclopenta[c]chromene (**263**)



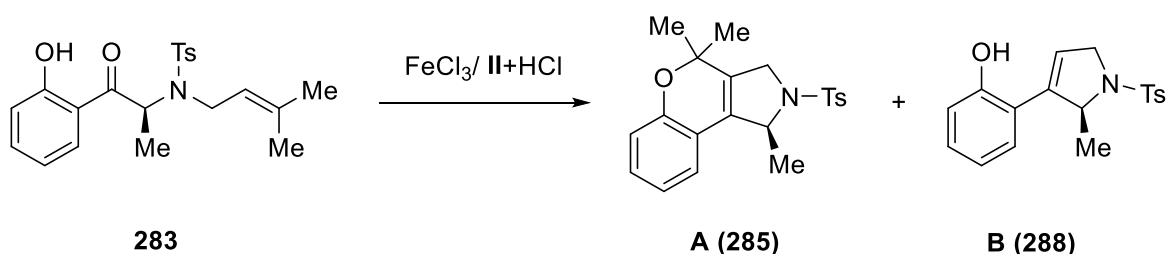
**<sup>1</sup>H NMR** (600 MHz, CDCl<sub>3</sub>)  $\delta$  [ppm] 7.06 (td,  $J = 7.7, 1.7$  Hz, 1H), 6.94 (dd,  $J = 7.4, 1.7$  Hz, 1H), 6.84 (td,  $J = 7.4, 1.2$  Hz, 1H), 6.79 (dd,  $J = 8.0, 1.1$  Hz, 1H), 2.65 (ddd,  $J = 9.8, 4.7, 2.3$  Hz, 2H), 2.50 (tt,  $J = 8.0, 2.4$  Hz, 2H), 2.04 (p,  $J = 7.5$  Hz, 2H), 1.43 (s, 6H).

**<sup>13</sup>C NMR** (151 MHz, CDCl<sub>3</sub>)  $\delta$  [ppm] 152.6, 139.9, 130.0, 128.1, 123.1, 121.9, 120.6, 115.9, 78.8, 32.7, 30.9, 26.7, 22.5.

The spectroscopic data matched those reported in the literature<sup>98</sup>

**FeCl<sub>3</sub> catalysis:** The product **263** was obtained as a colorless oil (28.0 mg, 0.140 mmol, 90 %)

#### 7.2.1.3.6 Mechanistic Probe **283**

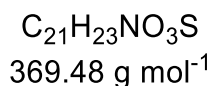
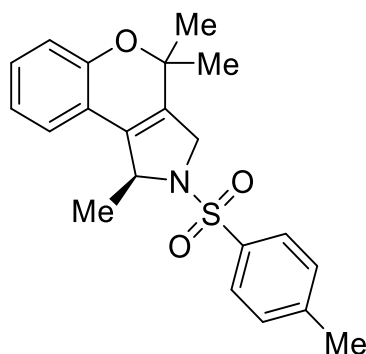


**FeCl<sub>3</sub> catalysis:** A 5 mL Kugelrohr was heated out under reduced pressure and transferred to N<sub>2</sub> glovebox. FeCl<sub>3</sub> (5.39 mg, 33.2  $\mu$ mol, 0.2 eq.) was added. A 15 mL two-neck flask was heated out under reduced pressure and anhydrous toluene (7.3 mL) was added. **283** (64.3 mg, 166  $\mu$ mol, 1 eq.) was added in toluene (1 mL). The Kugelrohr was mounted to the two-neck

flask and FeCl<sub>3</sub> was flushed down with the reaction mixture. The reaction was stirred at room temperature and was tracked by TLC. After completion, the reaction mixture was loaded directly onto the column and rinsed with pentane to remove toluene. The solvent was changed to 10 % EtOAc in pentane and was subsequently increased to 30 % EtOAc to obtain products **285** and **288** (see below for details).

**Capsule (II)/HCl-catalysis:** Resorcinarene (85.4 mg, 77.3 μmol, 0.6 eq.) was suspended in 2 mL chloroform (filtered through basic aluminum oxide) in a 15 mL pressure tube. The capped vial was heated gently until the suspension turned clear. After cooling to room temperature, HCl was added in the form of HCl-saturated chloroform (766 μL, 25.8 μmol, 0.2 eq.). Chloroform (filtered through basic aluminum oxide) was added to obtain a total volume of 3.88 mL and **283** (50.0 mg, 0.129 mmol, 1 eq.) was added. The vial was placed in a 400 mL oil bath to ensure a constant temperature of 30 °C, over the reaction period. The reaction mixture was loaded onto the column and rinsed with pentane. The solvent was changed to 10 % EtOAc in pentane and was subsequently increased to 30 % EtOAc, to obtain products **285** and **288** (see below for details).

#### 7.2.1.3.7 4,4-dimethyl-2-tosyl-1,2,3,4-tetrahydrochromeno[3,4-c]pyrrole (**285**)



The product was obtained as white solid:

**<sup>1</sup>H NMR** (500 MHz, CDCl<sub>3</sub>) δ [ppm] 7.72 (d, J = 8.3 Hz, 2H), 7.28 (d, J = 8.0 Hz, 2H), 7.11 (td, J = 7.7, 1.8 Hz, 1H), 6.90 (dd, J = 7.6, 1.8 Hz, 1H), 6.86 (td, J = 7.4, 1.2 Hz, 1H), 6.80 (dd, J = 8.1, 1.1 Hz, 1H), 4.94 (qdd, J = 6.4, 4.6, 1.6 Hz, 1H), 4.26 (dd, J = 15.3, 4.7 Hz, 1H), 4.16 (dd, J = 15.3, 1.6 Hz, 1H), 2.39 (s, 3H), 1.56 (d, J = 6.5 Hz, 3H), 1.46 (s, 3H), 1.16 (s, 3H).

$^{13}\text{C}$  NMR (126 MHz,  $\text{CDCl}_3$ )  $\delta$  [ppm] 152.9, 143.8, 135.2, 132.7, 130.7, 129.9, 129.5, 127.3, 123.1, 121.1, 118.0, 116.9, 76.4, 62.7, 53.5, 26.8, 25.9, 22.2, 21.7 (the number of signals deviates from the theoretical value due to signal overlap)

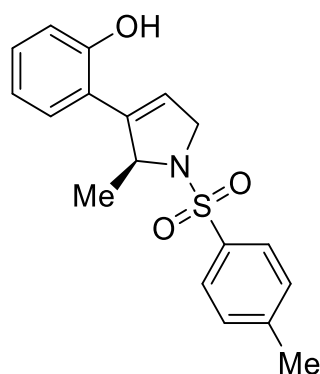
HRMS calcd for  $\text{C}_{21}\text{H}_{23}\text{NO}_3\text{SNa}^+$ :392.1291 found: 392.1293

IR (ATR):  $\tilde{\nu}$  [ $\text{cm}^{-1}$ ]: 2980.46 (w), 1597.86 (w), 1572.59 (w), 1491.42 (w), 1451.52 (w), 1341.18 (s), 1292.66 (w), 1281.13 (w), 1266.97 (w), 1240.61 (w), 1162.24 (s), 1132.28 (w), 1119.82 (m) 1094.94 (s), 1054.92 (m), 1035.15 (m), 1014.96 (w), 969.92 (m), 921.90 (m), 813.12 (m), 769.46 (m), 754.14 (m), 710.46 (m), 689.71 (m), 661.58 (s), 607.52 (m), 582.58 (m), 550.11 (s), 517.58 (w), 460.86 (w)

**$\text{FeCl}_3$  catalysis:** (17.0 mg, 46.0  $\mu\text{mol}$ , 27 %)

**Capsule (II)/HCl-catalysis:** (10.0 mg, 27.1  $\mu\text{mol}$ , 21 %)

7.2.1.3.8 2-(1-tosyl-2,5-dihydro-1H-pyrrol-3-yl)phenol (**288**)



$\text{C}_{18}\text{H}_{19}\text{NO}_3\text{S}$   
329.41  $\text{g mol}^{-1}$

The product was obtained as white solid:

$^1\text{H}$  NMR (500 MHz,  $\text{CDCl}_3$ )  $\delta$  [ppm] 7.80 – 7.76 (m, 2H), 7.31 (d,  $J = 8.0$  Hz, 2H), 7.16 (td,  $J = 7.7, 1.7$  Hz, 1H), 7.06 (dd,  $J = 7.7, 1.7$  Hz, 1H), 6.88 (td,  $J = 7.5, 1.2$  Hz, 1H), 6.82 (dd,  $J = 8.1, 1.1$  Hz, 1H), 5.83 (q,  $J = 2.0$  Hz, 1H), 5.25 (s, 1H), 5.14 – 5.09 (m, 1H), 4.43 – 4.11 (m, 2H), 2.41 (s, 3H), 1.38 (d,  $J = 6.4$  Hz, 3H).

$^{13}\text{C}$  NMR (151 MHz,  $\text{CDCl}_3$ )  $\delta$  [ppm] 153.3, 143.7, 141.1, 134.9, 129.9, 129.6, 129.2, 127.5, 121.7, 120.9, 120.9, 120.3, 116.2, 64.3, 54.9, 22.1, 21.7 (the number of signals deviates from the theoretical value due to signal overlap)

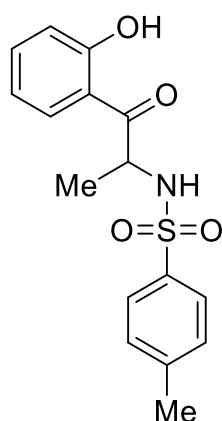
**HRMS** calcd for  $C_{18}H_{19}NO_3SNa^+$ : 352.0978 found: 352.0978

**IR (ATR):**  $\tilde{\nu}$  [ $cm^{-1}$ ]: 3312.61 (w), 2980.86 (w), 2919.33 (w), 2851.88 (w), 1627.08 (s), 1612.15 (s), 1596.99 (m), 1576.24 (m), 1490.85 (m), 1449.00 (m), 1426.28 (m), 1378.29 (m), 1342.94 (m), 1305.71 (m), 1260.50 (m), 1236.27 (m), 1205.93 (m), 1162.75 (s), 1141.53 (m), 1118.72 (m), 1088.77 (m), 1075.43 (m), 1052.29 (m), 1035.90 (m), 969.71 (m), 941.41 (m), 867.31 (m), 818.22 (m), 754.64 (s), 670.00 (s), 566.66 (s), 555.74 (s), 512.16 (m), 486.46 (m), 465.12 (m), 442.76 (m)

**FeCl<sub>3</sub> catalysis:** (16.0 mg, 48.6  $\mu$ mol, 29 %)

**Capsule (II)/HCl-catalysis:** (20.0 mg, 60.7  $\mu$ mol, 47 %)

7.2.1.3.9 N-(1-(2-hydroxyphenyl)-1-oxopropan-2-yl)-4-methylbenzenesulfonamide (**345**)



$C_{16}H_{17}NO_4S$   
319.38  $g\ mol^{-1}$

**<sup>1</sup>H NMR** (500 MHz,  $CDCl_3$ )  $\delta$  [ppm] 11.43 (s, 1H), 7.64 (d,  $J = 8.3$  Hz, 2H), 7.56 (dd,  $J = 8.1$ , 1.6 Hz, 1H), 7.49 (ddd,  $J = 8.6$ , 7.2, 1.6 Hz, 1H), 7.15 – 7.11 (m, 2H), 6.94 (dd,  $J = 8.4$ , 1.1 Hz, 1H), 6.90 (ddd,  $J = 8.2$ , 7.2, 1.2 Hz, 1H), 5.62 (d,  $J = 9.2$  Hz, 1H), 4.98 (dd,  $J = 9.2$ , 7.1 Hz, 1H), 2.31 (s, 3H), 1.44 (d,  $J = 7.1$  Hz, 3H).

**<sup>13</sup>C NMR** (126 MHz,  $CDCl_3$ )  $\delta$  [ppm] 203.5, 163.2, 144.0, 137.6, 136.8, 129.8, 129.5, 127.3, 119.5, 118.9, 116.4, 52.6, 21.6, 21.5 (the number of signals deviates from the theoretical value due to signal overlap)

**HRMS** calcd for  $C_{16}H_{17}NO_4SNa^+$ : 342.0777 found: 342.0770

**IR (ATR):**  $\tilde{\nu}$  [ $\text{cm}^{-1}$ ]: 3417.18 (w), 2980.14 (m), 2922.04 (m), 1597.54 (w), 1494.28 (w), 1451.63 (s), 1374.00 (s), 1322.54 (m), 1291.13 (m), 1255.57 (m), 1195.73 (m), 1151.21 (s), 1089.64 (m), 1038.72 (m), 949.73 (m), 815.97 (m), 755.27 (m), 668.88 (s), 625.60 (s), 595.49 (s), 548.11 (s), 515.02 (s)

**FeCl<sub>3</sub> catalysis:** (4.0 mg, 12  $\mu\text{mol}$ , 7 %)

**Capsule (II)/HCl-catalysis:** (12.0 mg, 37.6  $\mu\text{mol}$ , 29 %)

## 7.2.2 Kinetic Analysis

7.2.2.1.1 General Procedure for the kinetic experiments with FeCl<sub>3</sub>

7.2.2.1.1.1 Substrate **87** and **281**

A 15 mL two-neck flask was heated out under reduced pressure and transferred to an N<sub>2</sub> glovebox. FeCl<sub>3</sub> (0.2 eq.) was weighed precisely so that the amount ranged between 3 – 5 mg. The sealed flask was transferred to a Schlenk line, the react IR probe head was inserted and a background measurement of the gas phase was performed. Afterward, anhydrous 1,2-dichloroethane was added to reach a concentration of 5  $\mu\text{M}$ . The sample was stirred for 15 min to reach the respective temperature and a new reference IR spectra of 1,2-dichloroethane was measured. Substrate (1 eq.) was added and the conversion was tracked by 15 s measurements of the carbonyl vibration (**281**: 1685.6  $\text{cm}^{-1}$  Figure 67; **87**: 1687.2  $\text{cm}^{-1}$  Figure 68)

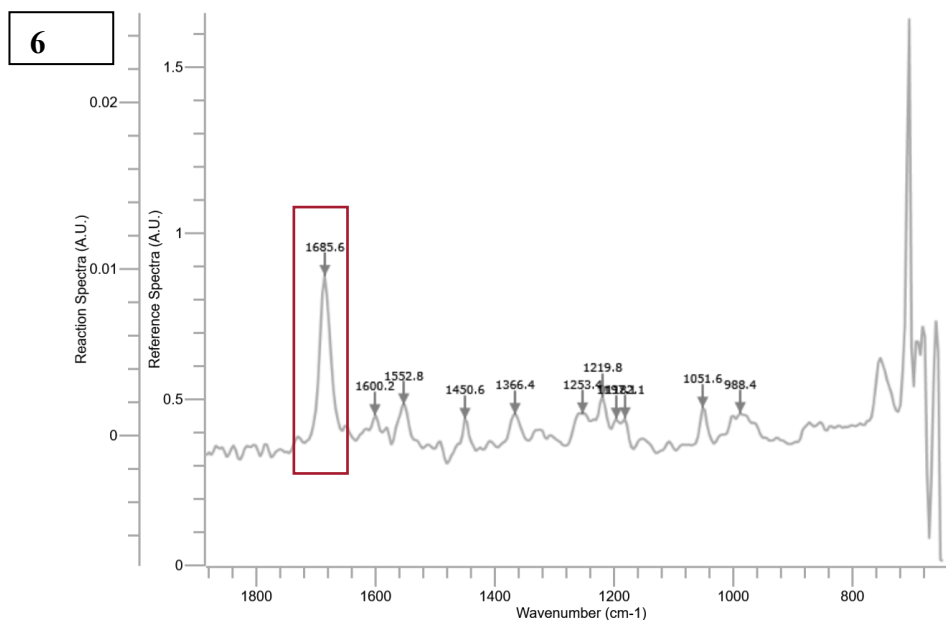


Figure 67 *In situ* infrared spectra of **281** in DCE

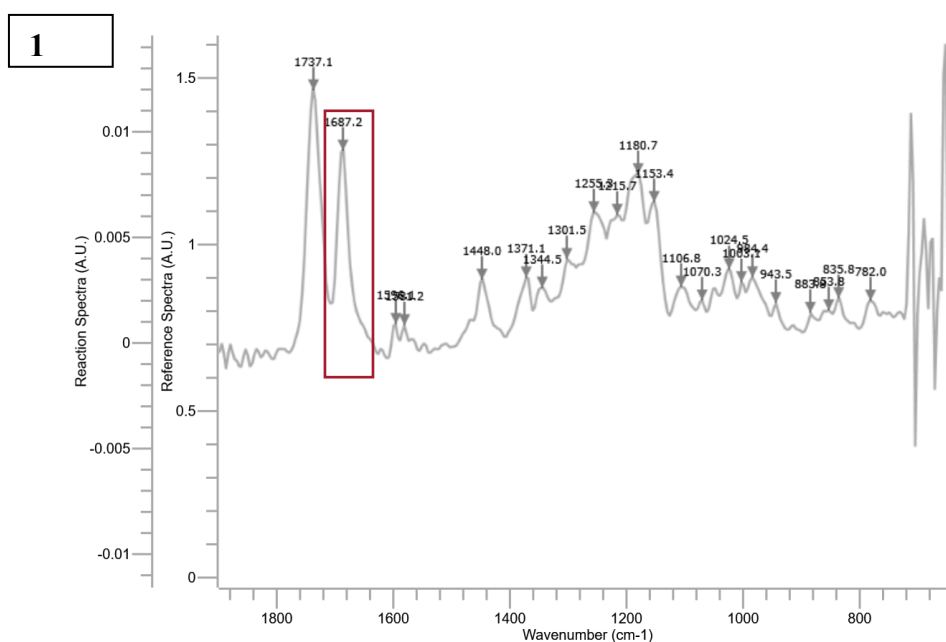


Figure 68 *In situ* infrared spectra of **87** in DCE

#### 7.2.2.1.1.2 Substrate **270**

A 5 mL Kugelrohr was heated out under reduced pressure and transferred to an N<sub>2</sub> glovebox. FeCl<sub>3</sub> (0.2 eq.) was weighed precisely so that the amount ranged between 3 – 7 mg (Figure 70). A 15 mL two-neck flask was heated out under reduced pressure and the react IR probe was inserted (Figure 70). A background measurement of the gas phase was performed and afterward, anhydrous toluene was added. The sample was stirred for 15 min to reach the respective temperature. A new reference IR spectrum of toluene was measured at the respective

temperature. Substrate **270** (1 eq.) was added in 100  $\mu\text{L}$  toluene and the IR measurement (15 s) was started. The Kugelrohr was mounted to the two-neck flask and  $\text{FeCl}_3$  was flushed down with the reaction mixture (Figure 71). Temperatures below 30  $^\circ\text{C}$  were achieved by placing the reaction setup in a 7  $^\circ\text{C}$  cooling chamber. The reaction was tracked by the vibration at 1230.6  $\text{cm}^{-1}$ . Toluene proved to be a superior solvent compared to DCE due to a better signal-to-noise ratio. Adding **270** to a suspension of  $\text{FeCl}_3$  in toluene or DCE led to instant consumption of the starting material. The problem was solved by adding  $\text{FeCl}_3$  after the substrate.

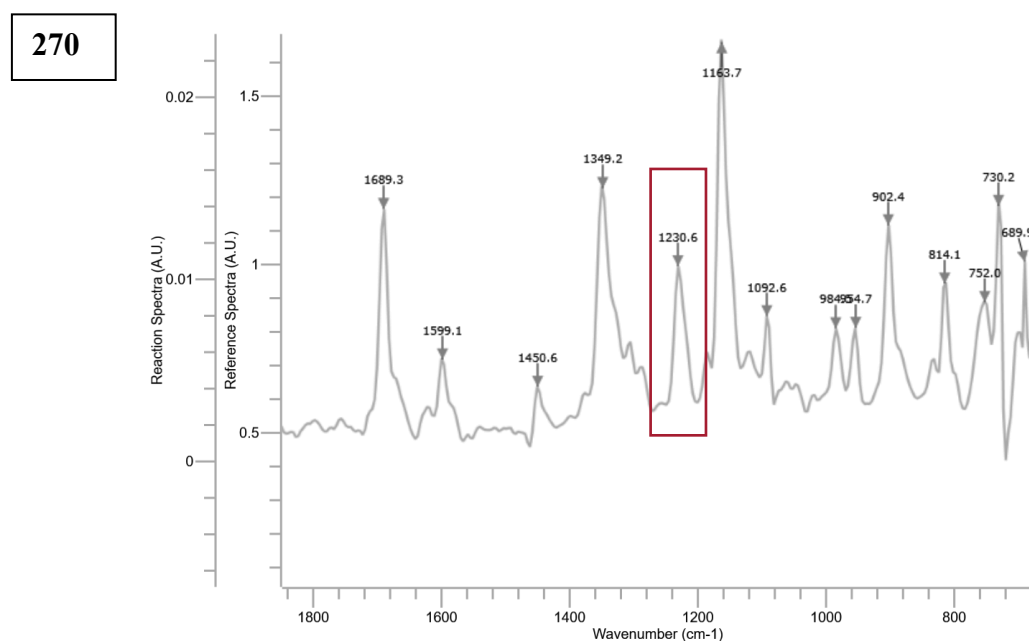


Figure 69 *In situ* infrared spectra of **270** in toluene



Figure 70 (Left) Kugelrohr with  $\text{FeCl}_3$ ; (Right) Two-neck flask with inserted IR-probe head





Figure 71 (Left) Reaction setup; (Right) Mounted Kugelrohr with  $\text{FeCl}_3$

#### 7.2.2.1.2 General procedure for the kinetic experiments with **II**

Resorcinarene (22.0 mg, 19.9  $\mu\text{mol}$ , 0.6 eq.) was suspended in 0.5 mL chloroform-d (filtered through basic aluminum oxide) into a 4 mL screw-cap vial. The capped vial was heated gently until the suspension turned clear. After cooling to room temperature, HCl (0.05 eq. (**87**, **281**)/ 0.2 eq. (**270**)) was added in the form of HCl-saturated chloroform. Chloroform (filtered through basic aluminum oxide) was added to receive a total volume of 1 mL. Tetraethylsilane (2.52  $\mu\text{L}$ , 13.3  $\mu\text{mol}$ , 0.4 eq.) and the substrate (33.2  $\mu\text{mol}$  (**87**, **281**, **270**), 1 eq.) were added. The vial was equipped with a stirring bar and transferred to an aluminum heating block. Aliquots of 50  $\mu\text{L}$  were dissolved in 0.5 mL of acetone- $\text{d}_6$  and analyzed by  $^1\text{H}$  NMR (Figure 72). Acetone leads to the disassembly of the hydrogen bond network of the capsule and therefore stops the reaction and liberates all encapsulated guest molecules. Temperatures below 30  $^\circ\text{C}$  were achieved by placing the reaction setup in a 7  $^\circ\text{C}$  cooling chamber.

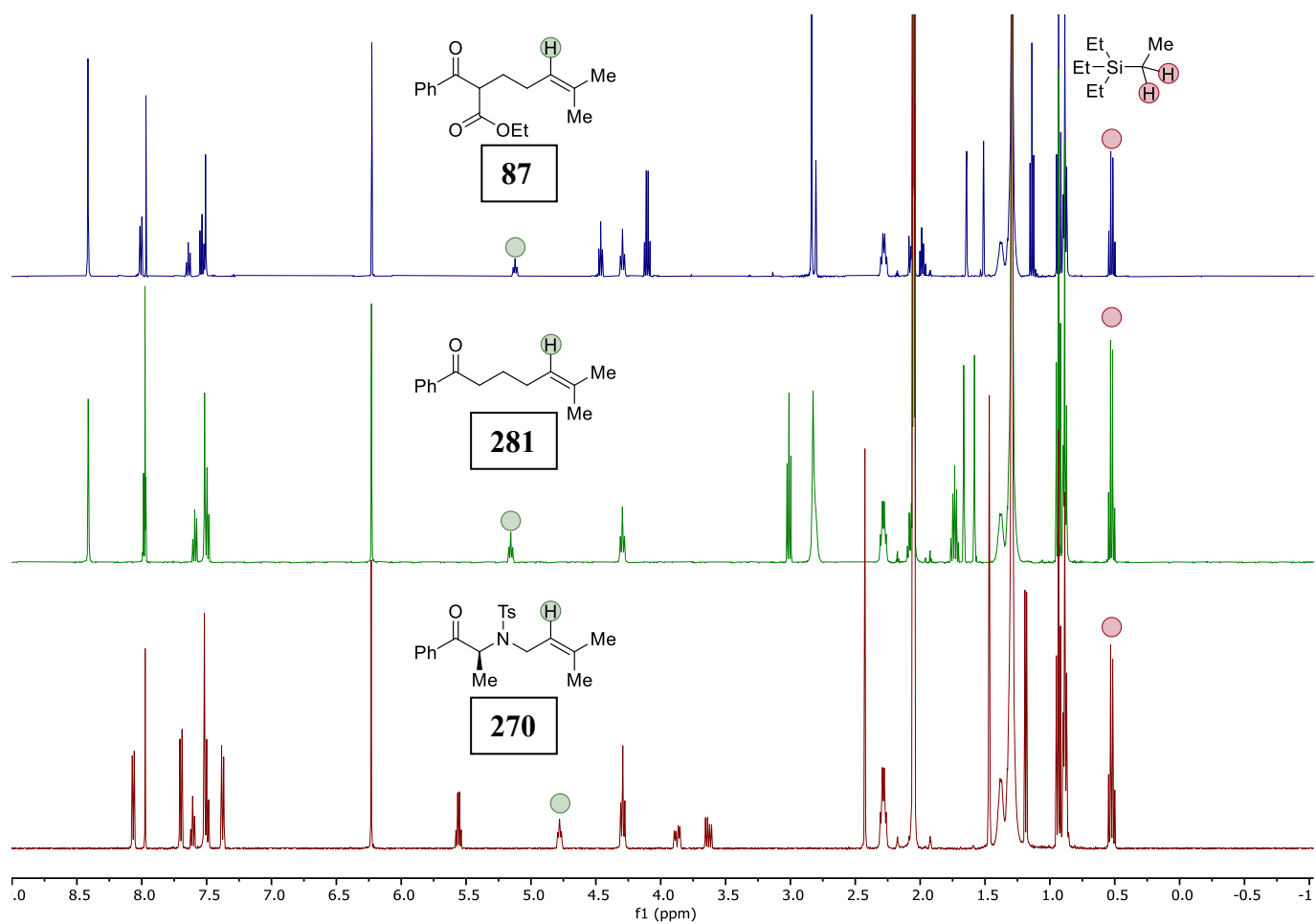


Figure 72  $^1\text{H}$  NMR Spectra of **II** and substrates **87**, **281**, **270** in acetone- $d_6$ . To track the consumption of the starting material, the olefinic H-signal (green) was integrated. Tetraethylsilane (red) was used as an internal standard.

7.2.2.1.3 Rate order determination of **87** at standard conditions

1 eq. **87**, 50°C, 0.1 eq. Capsule (**II**), 0.05 eq. HCl

	Time [min]	C [mmol mL <sup>-1</sup> ]		
	60	0.0268588	0.0262944	0.0276556
	120	0.02573	0.0254312	0.0266596
	180	0.0249664	0.0246012	0.02573
	240	0.024236	0.023738	0.0250992
	300	0.0234724	0.0232732	0.0244352
	360	0.022742	0.0226756	0.023738
Slope			-1.21101E-05	
		-1.33749E-05	05	-1.28057E-05
R <sup>2</sup>		0.994	0.988	0.990858109
Average				-1.27636E-05
Stdev				6.33434E-07

2 eq. **87**, 0.1 eq. Capsule (**II**), 0.05 eq. HCl,

	Time [min]	C [mmol mL <sup>-1</sup> ]		
	30	0.0624824	0.065902	0.065072
	60	0.0622832	0.0654372	0.064574
	90	0.0617188	0.0651716	0.064408
	120	0.0614532	0.0648064	0.0640096
	150	0.0610216	0.064408	0.0636112
	180	0.0606564	0.0638768	0.0629804
Slope			-1.29322E-05	
		-1.25528E-05	05	-1.30903E-05
R <sup>2</sup>		0.990	0.991	0.976281613
Average				-1.28584E-05
Stdev				2.76252E-07

The reaction order was determined with Equation 2

$$\ln \left( \frac{\text{slope}_a}{\text{slope}_b} \right) = y \ln \left( \frac{\text{concentration}_a}{\text{concentration}_b} \right)$$

Equation 2

$$\ln \left( \frac{\text{slope}_a}{\text{slope}_b} \right) = y \ln \left( \frac{\text{concentration}_a}{\text{concentration}_b} \right)$$

y = order

LN (AVG <sub>1eq.</sub> /AVG <sub>2eq.</sub> )	LN (c <sub>1eq.</sub> /c <sub>2eq.</sub> )	order
-0.0074	-0.69315	0.11

As the reaction was determined to be zero-order in the concentration of the substrate under the standard conditions, the rate constant **k** can be derived from the slope of the plot [**Substrate**] against **time**.

### 7.2.2.2 Eyring Analysis

#### 7.2.2.2.1 Eyring equation

$$\ln\left(\frac{k}{T}\right) = \frac{-\Delta H^\ddagger}{R} \cdot \frac{1}{T} + \frac{\Delta S^\ddagger}{R} + \ln\left(\frac{k_B}{h}\right)$$

$$\Delta H^\ddagger = -R \cdot (\text{slope Eyring plot}) \quad \Delta S^\ddagger = R \cdot \left(\text{interception Eyring plot} - \ln\left(\frac{k_B}{h}\right)\right)$$

#### 7.2.2.2.2 FeCl<sub>3</sub> catalysis: Substrate **281**

<b>303 K</b>		<b>C [mmol mL<sup>-1</sup>]</b>		
	<b>Time [s]</b>			
	0.00	0.025	0.025	0.025
	15.00	0.024198	0.02413	0.024524485
	30.00	0.022889		0.022776787
	45.00	0.021789	0.023759	0.022949778
	60.00	0.022944	0.023775	0.022451988
	75.00	0.022282	0.022873	0.021640341
	90.00	0.022007	0.022392	0.02141706
	105.00	0.020916	0.022179	0.021476992
	120.00	0.020081	0.022302	0.020658691
	135.00	0.019567	0.021443	0.02050274
	150.00	0.019825	0.021542	0.019487375
	165.00	0.020538	0.020533	0.019900144
	180.00	0.019232	0.020603	0.019305445
	195.00	0.01905	0.019764	0.018526497
	210.00	0.018797	0.01938	0.018481115
	225.00	0.018919	0.018461	0.01763254
	240.00	0.0181	0.01852	0.018473352
	255.00	0.01777	0.017271	0.018120844
Slope			-2.77155E-05	-2.67717E-05
		-2.52E-05	05	
R <sup>2</sup>		0.883	0.965	0.959
Average				-2.65663E-05
Stdev				1.264E-06

313 K	Time [s]	C [mmol mL <sup>-1</sup> ]		
	0.00	0.025	0.025	0.025
	15.00	0.024111	0.023336	0.023211
	30.00	0.022818	0.022922	0.021737
	45.00	0.02081	0.023033	0.022311
	60.00	0.021639	0.021493	0.021639
	75.00	0.020504	0.019263	0.020448
	90.00	0.019441	0.019204	0.019856
Slope			-6.42002E-05	-5.01387E-05
R <sup>2</sup>		-5.96872E-05	05	
Average		0.918	0.919	0.891
Stdev				-5.80087E-05
				7.17942E-06

323 K	Time [s]	C [mmol mL <sup>-1</sup> ]		
	0.00	0.025	0.025	0.025
	15.00	0.022946	0.023892	0.021818
	30.00	0.020656	0.02235	0.023114
	45.00	0.020667	0.020662	0.020069
	60.00	0.018254	0.019072	0.019277
Slope		-0.000105132	-1.005795E-04	-8.88737E-05
R <sup>2</sup>		0.946274752	0.994910626	0.823132147
Average				-9.81949E-05
Stdev				8.38712E-06

### Eyring-Plot

T [K]	Ln(k T <sup>-1</sup> )		Average	Stdev
303	-16.3024	-16.2077	-16.2424	
313	-15.4731	-15.4002	-15.6474	
323	-14.9384	-14.9827	-15.1064	

---

$\Delta H$	13.30205	11.96003	11.05845	<b>12.10684</b>	1.128983
$\Delta S$	-35.6479	-39.8547	-43.0043	<b>-39.5023</b>	3.690875
$\Delta G$	23.93046	23.8427	23.8802	<b>23.88445</b>	0.044037

---

7.2.2.2.3 FeCl<sub>3</sub> catalysis: Substrate 270

284 K	Time [s]	C [mmol mL <sup>-1</sup> ]		
	0.00	0.02	0.02	0.02
	15.00	0.019924474	0.01973821	0.019621251
	30.00	0.019906658	0.01993237	0.019397339
	45.00	0.019201872	0.01955484	0.019558391
	60.00	0.018819372	0.01951364	0.019512276
	75.00	0.018847647	0.01998951	0.019680899
	90.00	0.018472378	0.01972248	0.0194105
	105.00	0.018275981	0.01992277	0.019654731
	120.00	0.018068571	0.01983774	0.019411698
	135.00	0.018032761	0.01982922	0.019548734
	150.00	0.01772415	0.01949931	0.019397451
	165.00	0.01774661	0.01956801	0.018786981
	180.00	0.017662932	0.01870118	0.018552417
	195.00	0.017151858	0.0185255	0.018153291
	210.00	0.017011898	0.01839257	0.018092802
	225.00	0.016794195	0.01816464	0.01806552
	240.00	0.01691556	0.01787964	0.017601521
	255.00	0.016828531	0.01775022	0.017139419
	270.00	0.016528713	0.01737612	0.017253397
	285.00	0.016257074	0.01708284	0.016851276
	300.00	0.016090954	0.01703843	0.016791821
	315.00	0.016206154	0.01666991	0.016400338
	330.00	0.016212493	0.01677962	0.01627074
	345.00	0.015958866	0.01603904	0.016052193
	360.00	0.016160418	0.01614974	0.015766894
	Slope	-1.14281E-05	-1.1567E-05	-1.18856E-05
	R <sup>2</sup>	0.95820843	0.89425518	0.922816775
	Average			-1.16269E-05
	Stdev			2.34533E-07



293 K	Time [s]	C [mmol mL <sup>-1</sup> ]		
	0.00	0.02	0.02	0.02
	15.00	0.019998873	0.019756	0.019436
	30.00	0.019635636	0.019322	0.019142
	45.00	0.019928156	0.01899	0.018988
	60.00	0.019276631	0.018461	0.01863
	75.00	0.018902803	0.018023	0.018006
	91.00	0.018053955	0.017345	0.01791
	105.00	0.017421454	0.017112	0.017573
	120.00	0.016947397	0.016829	0.016987
	135.00	0.016623381	0.016271	0.016735
	150.00	0.015953675	0.016147	0.016343
	165.00	0.0157112	0.015615	0.015792
Slope		-2.93579E-05	-2.74134E-05	-2.43013E-05
R <sup>2</sup>		0.953476025	0.993115678	0.991605375
Average				-2.70242E-05
Stdev				2.55068E-06

303 K	Time [s]	C [mmol mL <sup>-1</sup> ]		
	0.00	0.02	0.02	0.02
	15.00	0.018288671	0.019099	0.019146985
	30.00	0.01743144	0.018421	0.017971459
	45.00	0.016772426	0.017234	0.017647998
	60.00	0.016151531	0.016939	0.01645262
	75.00	0.016025637	0.015886	0.015653238
	0.00			
Slope		-5.13186E-05	-5.37901E-05	-5.74102E-05
R <sup>2</sup>		0.911228762	0.987282	0.988401994

Average	-5.4173E-05
Stdev	3.06382E-06

### Eyring-Plot

T [K]		Ln(k T <sup>-1</sup> )		Average	Stdev
303	-17.0289	-17.0169	-16.9897		
313	-16.1166	-16.1852	-16.3057		
323	-15.5917	-15.5446	-15.4795		
$\Delta H$	12.92258	13.24941	13.61172	<b>13.26123</b>	0.344723
$\Delta S$	-35.4327	-34.3245	-33.1078	<b>-34.2883</b>	1.162858
$\Delta G$	23.664	23.65488	23.64835	<b>23.65574</b>	0.007857

## 7.2.2.2.4 Capsule (II)/HCl-catalysis: Substrate 87

<b>323 K</b>	Time [min]	C [mmol mL <sup>-1</sup> ]		
	60	0.0266928	0.029714	0.027722
	120	0.0261284	0.0292492	0.0271576
	180	0.0252652	0.02905	0.026726
	240	0.025066	0.0281204	0.0259956
	300	0.0243688	0.0271244	0.025398
	360	0.0234392	0.026726	0.0249
Slope		-1.03552E-05	-1.05924E-05	-9.58057E-06
R <sup>2</sup>		0.980	0.961	0.996
Average				-1.01761E-05
Stdev				4.32063E-07

<b>313 K</b>	Time [min]	C [mmol mL <sup>-1</sup> ]	Time [min]	C [mmol mL <sup>-1</sup> ]	
	60	0.033432	60	0.034096	0.032536
	120	0.032868	120	0.033333	0.031972
	180	0.032636	180	0.0331	0.031507
	240	0.03237	300	0.032503	0.030743
	300	0.031806	350	0.032038	0.030478
	360	0.031573	470	0.031474	0.030146
Slope		-6.1E-06		-6.1E-06	-5.9E-06
R <sup>2</sup>		0.981905		0.977176	0.962911
Average					-6.01688E-06
Stdev					7.34765E-08

<b>303 K</b>	Time [min]	C [mmol mL <sup>-1</sup> ]		
	100	0.032883	0.036638	0.032666
	200	0.031946	0.035843	0.032083
	300	0.031768	0.035825	0.031636
	400	0.031571	0.035467	0.031308

	500	0.031395	0.035219	0.031222	
	600	0.030996	0.03504	0.031088	
Slope		-3.2E-06	-2.9E-06	-3.1E-06	
R <sup>2</sup>		0.888266	0.914154	0.908513	
Average					-3.07729E-06
Stdev					1.24521E-07

---

### Eyring-Plot

T [K]		Ln(k T <sup>-1</sup> )		Average	Stdev
303	-1.84E+01	-1.85E+01	-1.84E+01		
313	-1.78E+01	-1.78E+01	-1.78E+01		
323	-1.73E+01	-1.72E+01	-1.73E+01		
$\Delta H$	1.07E+01	1.19E+01	1.04E+01	<b>11.03</b>	0.796735825
$\Delta S$	-4.83E+01	-4.45E+01	-4.94E+01	<b>-47.37</b>	2.555124126
$\Delta G$	2.51E+01	2.52E+01	2.51E+01	<b>25.15</b>	0.037917712

---

## 7.2.2.2.5 Capsule (II)/HCl-catalysis: 281

<b>323 K</b>	Time [min]	C [mmol mL <sup>-1</sup> ]		
	60	0.030776	0.030743	0.030577
	120	0.029581	0.029581	0.029183
	180	0.029017	0.028552	0.028519
	240	0.028054	0.028154	0.027755
	300	0.027755	0.027523	0.027257
	360	0.026958	0.026925	0.026792
Slope		-1.21575E-05	-1.2221E-05	-1.21259E-05
R <sup>2</sup>		0.977006721	0.967943066	0.959284152
Average				-1.21681E-05
Stdev				3.94359E-08

<b>313 K</b>	Time [min]	C [mmol mL <sup>-1</sup> ]		
	90	0.032968	0.033897	0.032436
	180	0.032602	0.033167	0.031673
	270	0.03164	0.032569	0.031009
	360	0.031507	0.031972	0.03081
	450	0.030776	0.031772	0.030179
	540	0.030544	0.031374	0.029714
Slope		-5.6282E-06	-5.52279E-06	-5.80737E-06
R <sup>2</sup>		0.966237463	0.967725564	0.980628664
Average				-5.65278E-06
Stdev				1.1747E-07

<b>303 K</b>	Time [min]	C [mmol mL <sup>-1</sup> ]		
	120	0.033897	0.033964	0.033798
	240	0.033698	0.033665	0.033532
	360	0.033432	0.033432	0.033167
	480	0.0331	0.033266	0.032968

	600	0.033034	0.033067	0.032835	
	720	0.032702	0.032735	0.032702	
Slope			-1.92876E-	-1.84971E-06	
		-1.97619E-06	06		
R <sup>2</sup>		0.984045345	0.989737338	0.960968761	
Average					-1.91822E-06
Stdev					6.38934E-08

### Eyring-Plot

T [K]		Ln(k T <sup>-1</sup> )		Average	Stdev
303	-1.89E+01	-1.88E+01	-1.89E+01		
313	-1.78E+01	-1.78E+01	-1.79E+01		
323	-1.71E+01	-1.71E+01	-1.71E+01		
$\Delta H$	1.77E+01	1.71E+01	1.74E+01	<b>17.39</b>	0.316
$\Delta S$	-2.62E+01	-2.82E+01	-2.74E+01	<b>-27.28</b>	0.999
$\Delta G$	2.55E+01	2.55E+01	2.55E+01	<b>25.52</b>	0.0187

## 7.2.2.2.6 Capsule (II)/HCl-catalysis: 270

<b>303 K</b>	Time [min]	C [mmol mL <sup>-1</sup> ]		
	10	0.02739	0.0272904	0.0280208
	20	0.025996	0.026394	0.0267924
	30	0.025033	0.025066	0.0255308
	40	0.023506	0.0240368	0.0244684
	50	0.02251	0.0227088	0.0232732
	60	0.021846	0.0216464	0.0225428
Slope		-1.1345E-04	-1.1516E-04	-1.1146E-04
R <sup>2</sup>		9.89E-01	9.98E-01	9.95E-01
Average				-1.1335E-04
Stdev				1.5118E-06

<b>293 K</b>	Time [min]	C [mmol mL <sup>-1</sup> ]		
	0	0.029548	0.0281868	0.0279212
	20	0.0289504	0.027556	0.0272904
	40		0.0268256	0.0268588
	60	0.0277552	0.0263276	0.026228
	80	0.027224	0.0257632	0.0255972
	100	0.02656	0.0252984	0.0250992
Slope		-2.9610E-05	-2.9026E-05	-2.8315E-05
R <sup>2</sup>		9.99E-01	9.95E-01	9.98E-01
Average				-2.8984E-05
Stdev				5.295E-07

<b>283 K</b>	Time [min]	C [mmol mL <sup>-1</sup> ]		
	40	0.029913	0.029614	0.028419
	80	0.029448	0.029382	0.027954
	120	0.028818	0.028386	0.027689
	160	0.02812	0.028021	0.027058
	200	0.027822	0.027689	0.026361

	240	0.027324	0.026958	0.026128	
Slope		-1.3233E-05	-1.3375E-05	-1.2047E-05	
R <sup>2</sup>		9.90E-01	9.73E-01	9.82E-01	
Average					-1.2885E-05
Stdev					5.9533E-07

### Eyring-Plot

T [K]		Ln(k T <sup>-1</sup> )		Average	Stdev
283	1.32E-05	1.34E-05	1.20E-05		
293	2.96E-05	2.90E-05	2.83E-05		
303	1.13E-04	1.15E-04	1.11E-04		
$\Delta H$	1.7683E+01	1.7713E+01	1.8335E+01	<b>17.9104</b>	0.3678
$\Delta S$	-1.8496E+01	-1.8390E+01	-1.6376E+01	<b>-17.7540</b>	1.194885
$\Delta G$	2.3198E+01	2.3196E+01	2.3217E+01	<b>23.2038</b>	0.01162



7.2.2.3 Secondary Kinetic Isotope Effect

7.2.2.3.1 FeCl<sub>3</sub> catalysis: Substrate **87/87D**

**303 K**

<b>(87)</b>			
Time [s]	C [mmol mL <sup>-1</sup> ]		
15.00	0.020773	0.023256	0.022563
30.00	0.021306	0.018856	0.021942
45.00	0.021154	0.02007	0.020779
60.00	0.020067	0.020217	0.021082
75.00	0.01859	0.017793	0.017953
90.00	0.01647	0.016676	0.018548
105.00	0.017537	0.01642	0.018233
120.00	0.018712	0.014586	0.017076
135.00	0.017592	0.016162	0.016515
150.00	0.016111	0.015108	0.013994
165.00	0.01476	0.013953	0.014675
180.00	0.0158	0.013434	0.013643
196.00	0.013485	0.012528	0.010816
210.00	0.013917	0.011933	0.010029
225.00	0.012448	0.01161	0.012805
240.00	0.012274	0.00905	0.011286
255.00	0.009838	0.010787	0.01079
270.00	0.010136	0.009436	0.009727
285.00	0.010879	0.009394	0.007561
k	-4.28073E-05	-4.65713E-05	-5.28892E-05
R <sup>2</sup>	0.939592183	0.941358485	0.950434929
Average			-4.74226E-05
Stdev			5.09457E-06
<b>(87D)</b>			

Time [s]	C [mmol mL <sup>-1</sup> ]		
15.00	0.022878	0.024683	0.023393
30.00	0.023198	0.022925	0.022336
45.00	0.02	0.022462	0.021825
60.00	0.018671	0.02034	0.020151
75.00	0.018204	0.019951	0.019857
90.00	0.015498	0.018178	0.017527
105.00	0.015762	0.016989	0.016038
120.00	0.01528	0.017248	0.014883
135.00	0.012434	0.015523	0.013811
150.00	0.013728	0.015594	0.01279
165.00	0.011088	0.014908	0.01251
180.00	0.009941	0.013007	0.011101
k	-7.8065E-05	-6.5462E-05	-7.809E-05
R <sup>2</sup>	0.957257757	0.970971574	0.986707337
Average			-7.38723E-05
StDev			7.28357E-06

### **β-SKIE**

	β-SKIE		
	0.653926571	0.596571	0.677286
Average			0.642594454
StDev			0.041533259

7.2.2.3.2 FeCl<sub>3</sub> catalysis: Substrate 281/281D

303 K

<b>(281)</b>				
	Time [s]		C [mmol mL <sup>-1</sup> ]	
	0.00	0.025	0.025	0.025
	15.00	0.024198	0.02413	0.024524485
	30.00	0.022889		0.022776787
	45.00	0.021789	0.023759	0.022949778
	60.00	0.022944	0.023775	0.022451988
	75.00	0.022282	0.022873	0.021640341
	90.00	0.022007	0.022392	0.02141706
	105.00	0.020916	0.022179	0.021476992
	120.00	0.020081	0.022302	0.020658691
	135.00	0.019567	0.021443	0.02050274
	150.00	0.019825	0.021542	0.019487375
	165.00	0.020538	0.020533	0.019900144
	180.00	0.019232	0.020603	0.019305445
	195.00	0.01905	0.019764	0.018526497
	210.00	0.018797	0.01938	0.018481115
	225.00	0.018919	0.018461	0.01763254
	240.00	0.0181	0.01852	0.018473352
	255.00	0.01777	0.017271	0.018120844
Slope		-2.52118E-05	-2.77155E-05	-2.67717E-05
R <sup>2</sup>		0.882996914	0.964703614	0.959083435
Average				-2.65663E-05
Stdev				1.26444E-06

<b>(281D)</b>				
	Time [s]		C [mmol mL <sup>-1</sup> ]	

	0.00	0.025	0.025	0.025
	15.00	0.024588	0.023206	0.024003
	30.00	0.024446	0.023586	0.024067
	45.00	0.024086	0.023243	0.024188
	60.00	0.022333	0.022012	0.022486
	75.00	0.022148	0.022019	0.022476
	90.00	0.022163	0.021522	0.021595
	105.00	0.021395	0.021345	0.020626
	121.00	0.021125	0.021204	0.021768
	135.00	0.021266	0.020727	0.021763
	150.00	0.02031	0.019808	0.020778
	165.00	0.019605	0.01951	0.020305
	180.00	0.0194	0.018566	0.01908
	196.00	0.019	0.018824	0.018863
	210.00	0.018913	0.018978	0.019372
	225.00	0.018678	0.018226	0.018403
	241.00	0.01823	0.01817	0.017674
	255.00	0.019031	0.017455	0.018438
Slope		-2.70585E-05	-2.67538E-05	-2.7199E-05
R <sup>2</sup>		0.947970926	0.966480372	0.915491499
Average				-2.70037E-05
Stdev				2.27595E-07

### **β-SKIE**

	β-SKIE		
	0.931749967	1.035947	0.98429
Average			0.983996
StDev			0.052099

7.2.2.3.3 FeCl<sub>3</sub> catalysis: Substrate 270/270D

284 K

(270)			
Time [s]	C [mmol mL <sup>-1</sup> ]		
0.00	0.02	0.02	0.02
15.00	0.019924474	0.01973821	0.019621251
30.00	0.019906658	0.01993237	0.019397339
45.00	0.019201872	0.01955484	0.019558391
60.00	0.018819372	0.01951364	0.019512276
75.00	0.018847647	0.01998951	0.019680899
90.00	0.018472378	0.01972248	0.0194105
105.00	0.018275981	0.01992277	0.019654731
120.00	0.018068571	0.01983774	0.019411698
135.00	0.018032761	0.01982922	0.019548734
150.00	0.01772415	0.01949931	0.019397451
165.00	0.01774661	0.01956801	0.018786981
180.00	0.017662932	0.01870118	0.018552417
195.00	0.017151858	0.0185255	0.018153291
210.00	0.017011898	0.01839257	0.018092802
225.00	0.016794195	0.01816464	0.01806552
240.00	0.01691556	0.01787964	0.017601521
255.00	0.016828531	0.01775022	0.017139419
270.00	0.016528713	0.01737612	0.017253397
285.00	0.016257074	0.01708284	0.016851276
300.00	0.016090954	0.01703843	0.016791821
315.00	0.016206154	0.01666991	0.016400338
330.00	0.016212493	0.01677962	0.01627074
345.00	0.015958866	0.01603904	0.016052193
360.00	0.016160418	0.01614974	0.015766894
Slope	-1.14281E-05	-1.1567E-05	-1.18856E-05
R <sup>2</sup>	0.95820843	0.89425518	0.922816775

Average	-1.16269E-05
Stdev	2.34533E-07

**(270D)**

Time [s]	C [mmol mL <sup>-1</sup> ]		
0.00	0.02	0.02	0.02
15.00	0.019686386		0.019980911
30.00	0.019755347	0.018981536	0.019679203
45.00	0.018896366	0.018388313	0.019742055
60.00	0.018897916	0.01861991	0.019987275
75.00	0.018406165	0.018291884	0.019843944
90.00	0.018737215	0.017824302	0.019938077
105.00	0.018125693	0.01792072	0.019826862
120.00	0.017563764	0.017622558	0.019780717
135.00	0.017522745	0.017579578	0.019030868
150.00	0.017107875	0.017263869	0.018587449
165.00	0.016986302	0.017348105	0.018686728
180.00	0.016962476	0.016663017	0.018467537
195.00	0.016757901	0.016539896	0.018120676
210.00	0.016617836	0.016504218	0.018086145
225.00	0.016265966	0.016472462	0.017730115
240.00	0.016484687	0.016182919	0.01773988
255.00	0.015747058	0.016175744	0.017343963
270.00	0.015708222	0.015778963	0.017049801
285.00	0.015492101	0.015406342	0.016615902
300.00	0.015252826	0.015411446	0.01670483
315.00	0.015270915	0.015183078	0.016285565
330.00	0.015260437	0.014807773	0.015896725
345.00	0.014745973	0.014845371	0.015998503
360.00	0.014925849	0.014952862	0.015667417
Slope	-1.44479E-05	-1.33186E-05	-1.31777E-05

R <sup>2</sup>	0.974472866	0.977195585	0.948613921
Average			-1.36481E-05
Stdev			6.96252E-07

**β-SKIE**

β-SKIE			
	0.822651617	0.868487845	0.867233116
Average			0.852791
StDev			0.026109

## 7.2.2.3.4 Capsule (II)/HCl-catalysis: Substrate 87/87D

**323 K**


---

<b>87</b>				
	Time [min]		C [mmol mL <sup>-1</sup> ]	
	60	0.0266928	0.029714	0.027722
	120	0.0261284	0.0292492	0.0271576
	180	0.0252652	0.02905	0.026726
	240	0.025066	0.0281204	0.0259956
	300	0.0243688	0.0271244	0.025398
	360	0.0234392	0.026726	0.0249
Slope		-1.03552E-05	-1.05924E-05	-9.58057E-06
R <sup>2</sup>		0.980	0.961	0.996
Average				1.01761E-05
Stdev				4.32063E-07

---

<b>87D</b>				
	Time [min]		C [mmol mL <sup>-1</sup> ]	
	60	0.029183	0.0289504	0.0291164
	120	0.027954	0.0280208	0.028054
	180	0.027423	0.0277884	0.0272904
	240	0.027158	0.0270912	0.0271908
	300	0.026394	0.026394	0.0266264
	360	0.026228	0.0256636	0.0256304
Slope		-9.4E-06	-1.04817E-05	-1.03869E-05
R <sup>2</sup>		0.936	0.985	0.954
Average				1.00865E-05
Stdev				4.93399E-07

---



**$\beta$ -SKIE**

$\beta$ -SKIE			
	1.02020202	1.010558	0.996956
Average			<b>1.009239</b>
StDev			0.011679

## 7.2.2.3.5 Capsule (II)/HCl-catalysis: 281/281D

323 K

<b>(281D)</b>				
	Time [min]	C [mmol mL <sup>-1</sup> ]		
	60	0.030776	0.030743	0.030577
	120	0.029581	0.029581	0.029183
	180	0.029017	0.028552	0.028519
	240	0.028054	0.028154	0.027755
	300	0.027755	0.027523	0.027257
	360	0.026958	0.026925	0.026792
Slope		-1.21575E-05	-1.2221E-05	-1.21259E-05
R <sup>2</sup>		0.977006721	0.967943066	0.959284152
Average				-1.21681E-05
Stdev				3.94359E-08

<b>(281D)</b>				
	Time [min]	C [mmol mL <sup>-1</sup> ]		
	60	0.032171	0.0367524	0.032005
	120	0.031208	0.0357896	0.031374
	180	0.03071	0.035358	0.030577
	240	0.030212	0.0346608	0.029913
	300	0.029814	0.0341296	0.029515
	360	0.02915	0.033864	0.02905
Slope		-9.42248E-06	-9.58057E-06	-1.00074E-05
R <sup>2</sup>		0.977006721	0.967943066	0.959284152
Average				-9.67016E-06
Stdev				2.47065E-07

**β-SKIE**

β-SKIE

---

	1.290268	1.275578E+00	1.21169E+00	
Average				<b>1.25918E+00</b>
StDev				0.04177701

---

## 7.2.2.3.6 Capsule (II)/HCl-catalysis: 270/270D

**303 K**

<b>(270)</b>				
	Time [min]	C [mmol mL <sup>-1</sup> ]		
	10	0.02739	0.0272904	0.0280208
	20	0.025996	0.026394	0.0267924
	30	0.025033	0.025066	0.0255308
	40	0.023506	0.0240368	0.0244684
	50	0.02251	0.0227088	0.0232732
	60	0.021846	0.0216464	0.0225428
Slope		-1.1345E-04	-1.1516E-04	-1.1146E-04
R <sup>2</sup>		9.89E-01	9.98E-01	9.95E-01
Average				-1.1335E-04
Stdev				1.5118E-06

<b>(270D)</b>				
	Time [min]	C [mmol mL <sup>-1</sup> ]		
	10	0.0277884	0.0320048	0.0254312
	20	0.0265268	0.031163733	0.0243688
	30	0.025564	0.0300128	0.023406
	40	0.0243688	0.0289504	0.0223768
	50	0.023572	0.0280208	0.02158
	60	0.022742	0.026604267	0.0206504
Slope		-1.0083E-04	-1.0713E-04	-9.5142E-05
R <sup>2</sup>		9.94E-01	9.96E-01	9.98E-01
Average				-1.0103E-04
Stdev				4.8943E-06

**β-SKIE**

β-SKIE
--------

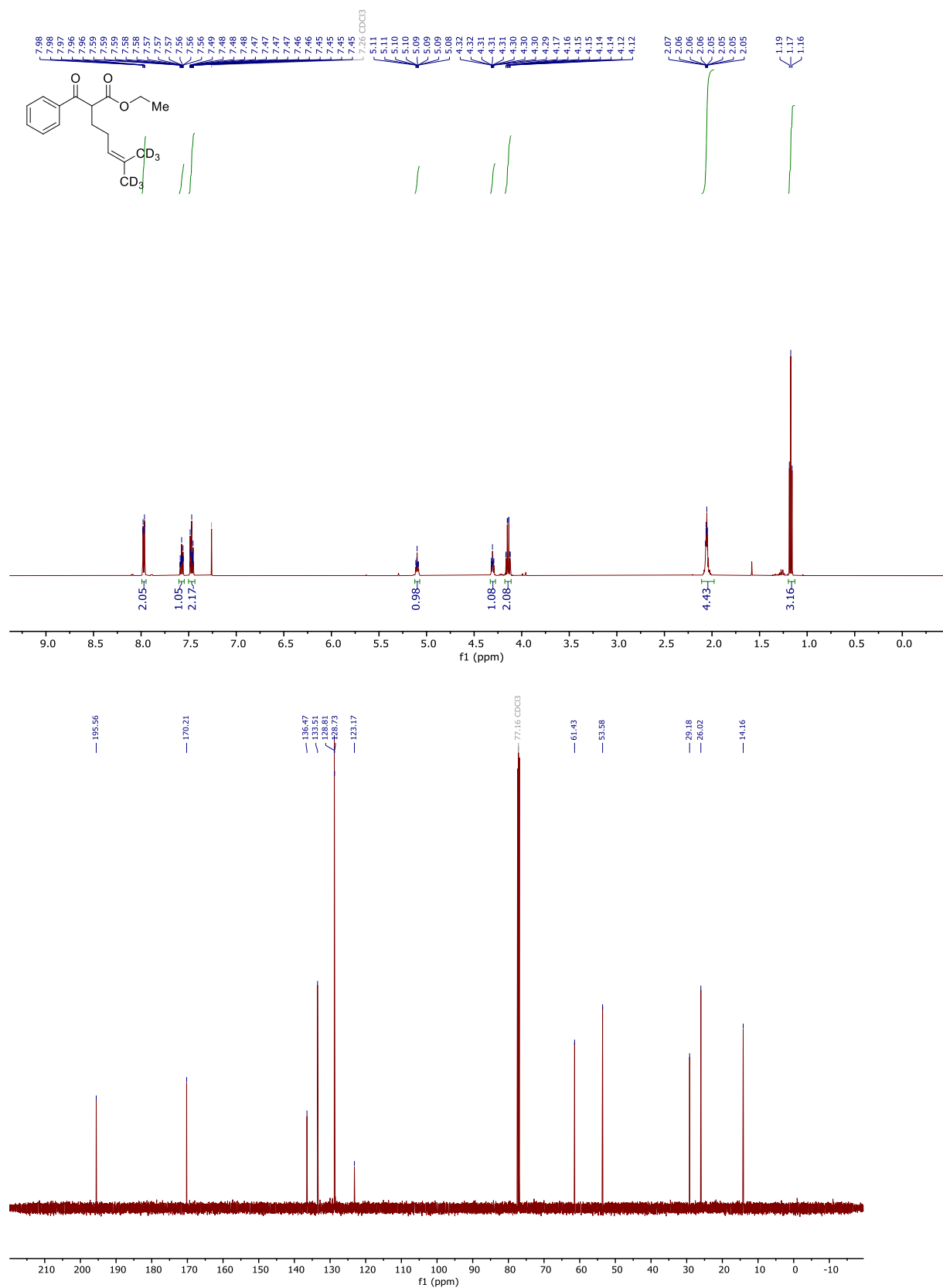
---

	1.1251E+00	1.0750E+00	1.1715E+00	
Average				<b>1.1239E+00</b>
StDev				0.0482699

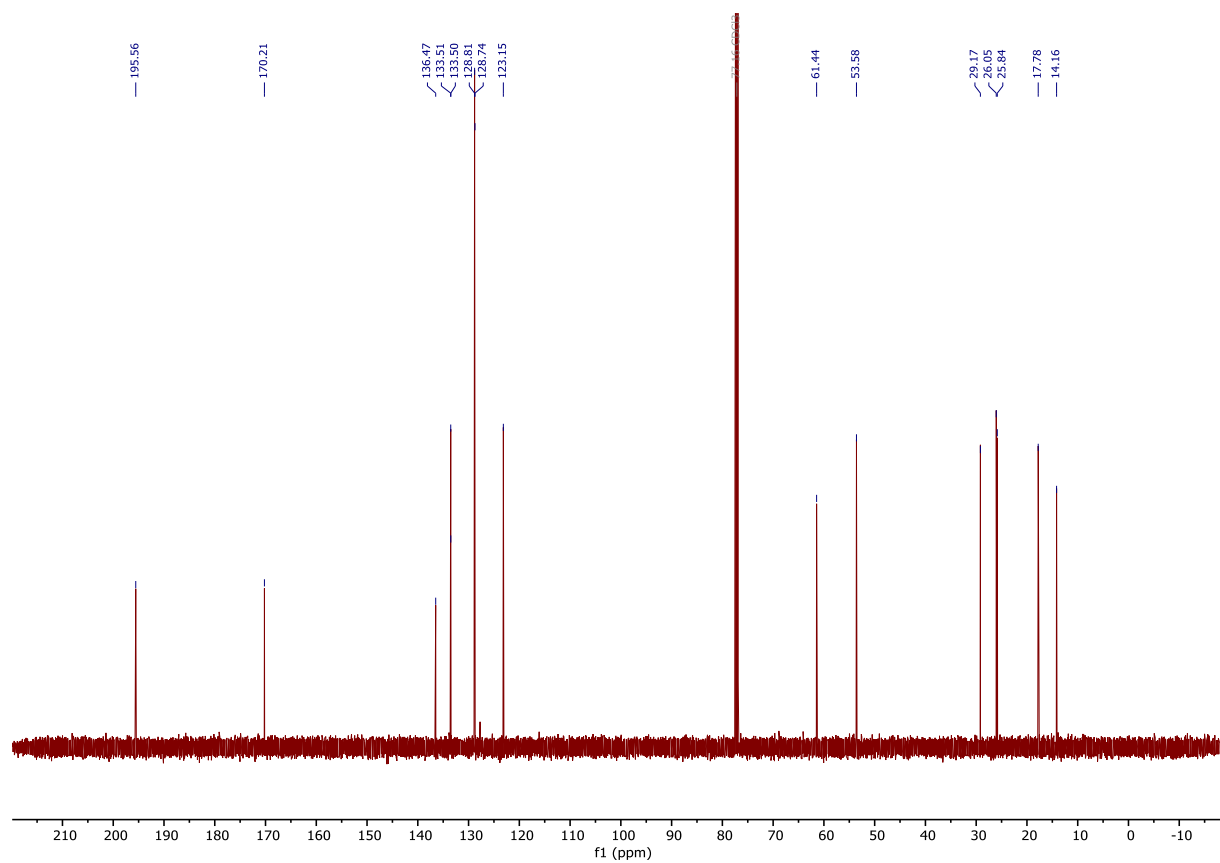
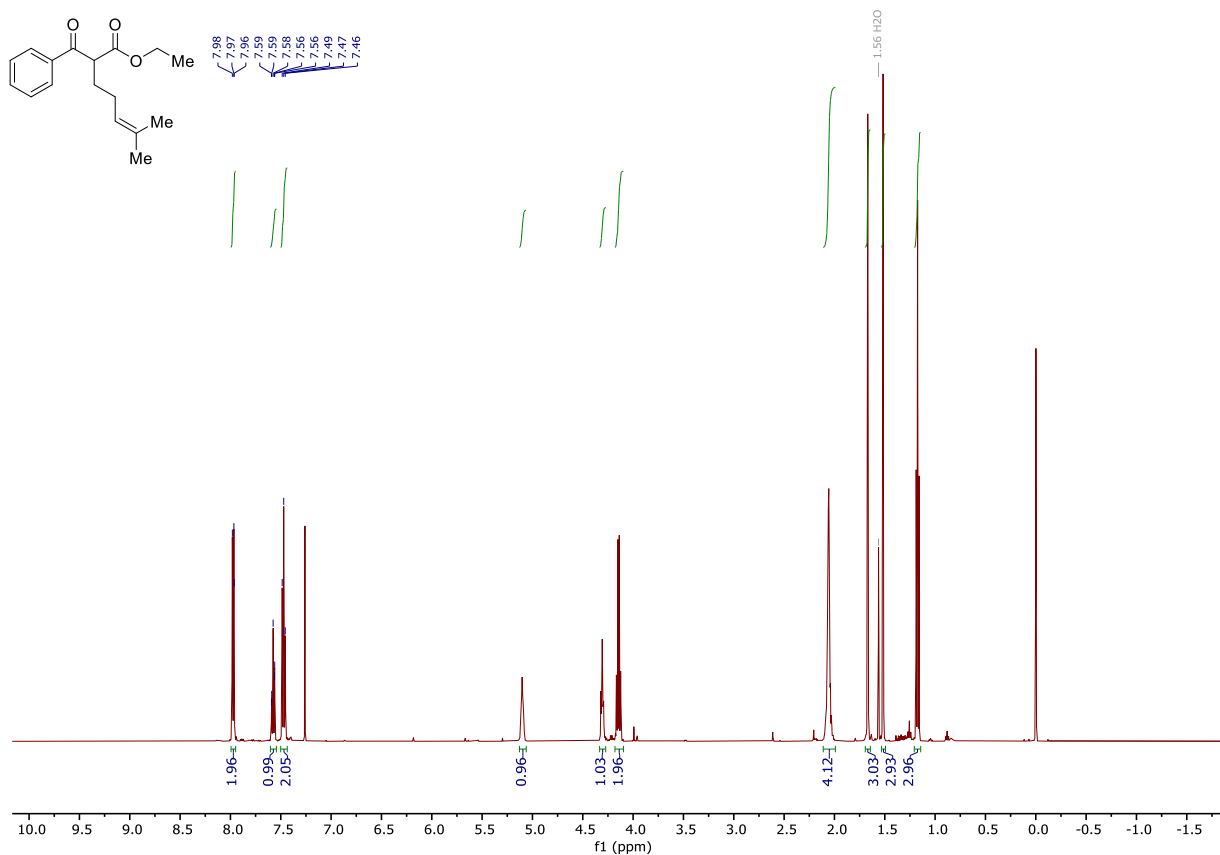
---

7.2.2.4  $^1\text{H}$  NMR and  $^{13}\text{C}$  NMR

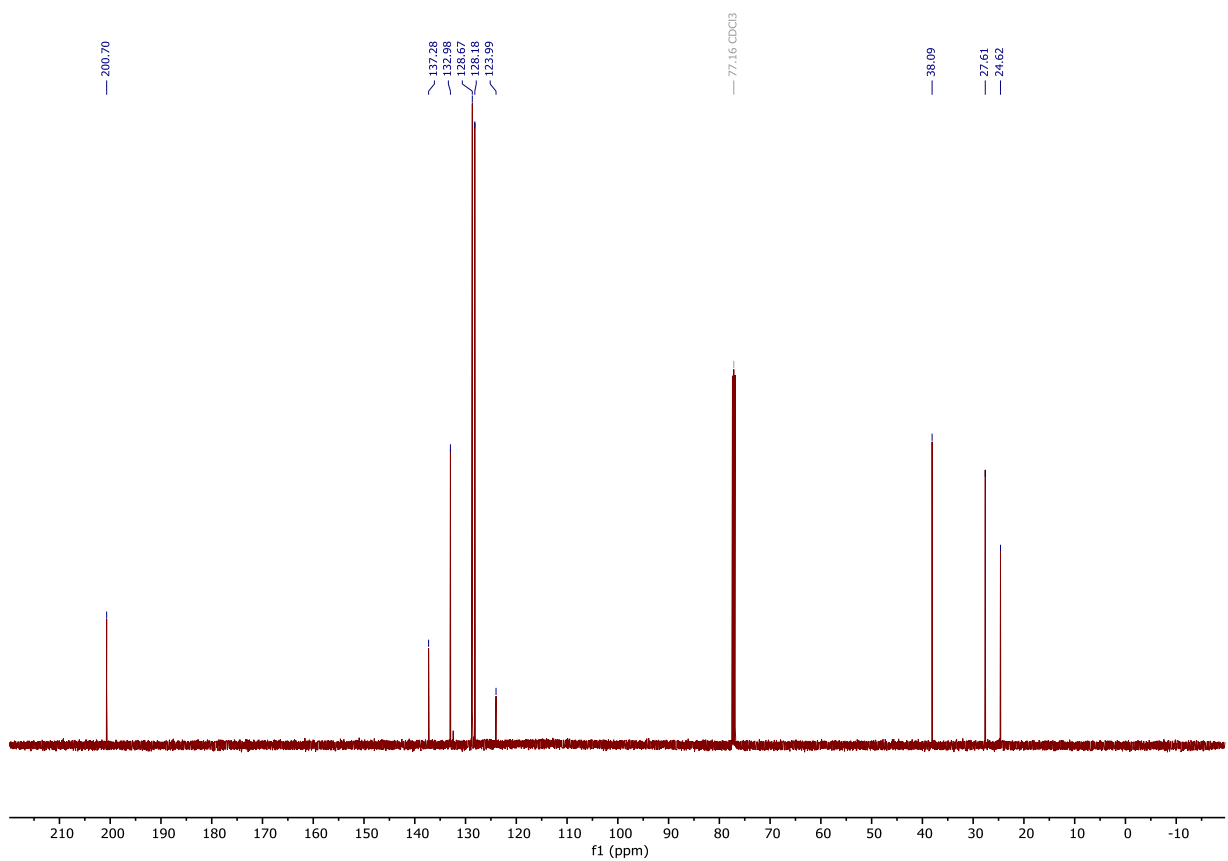
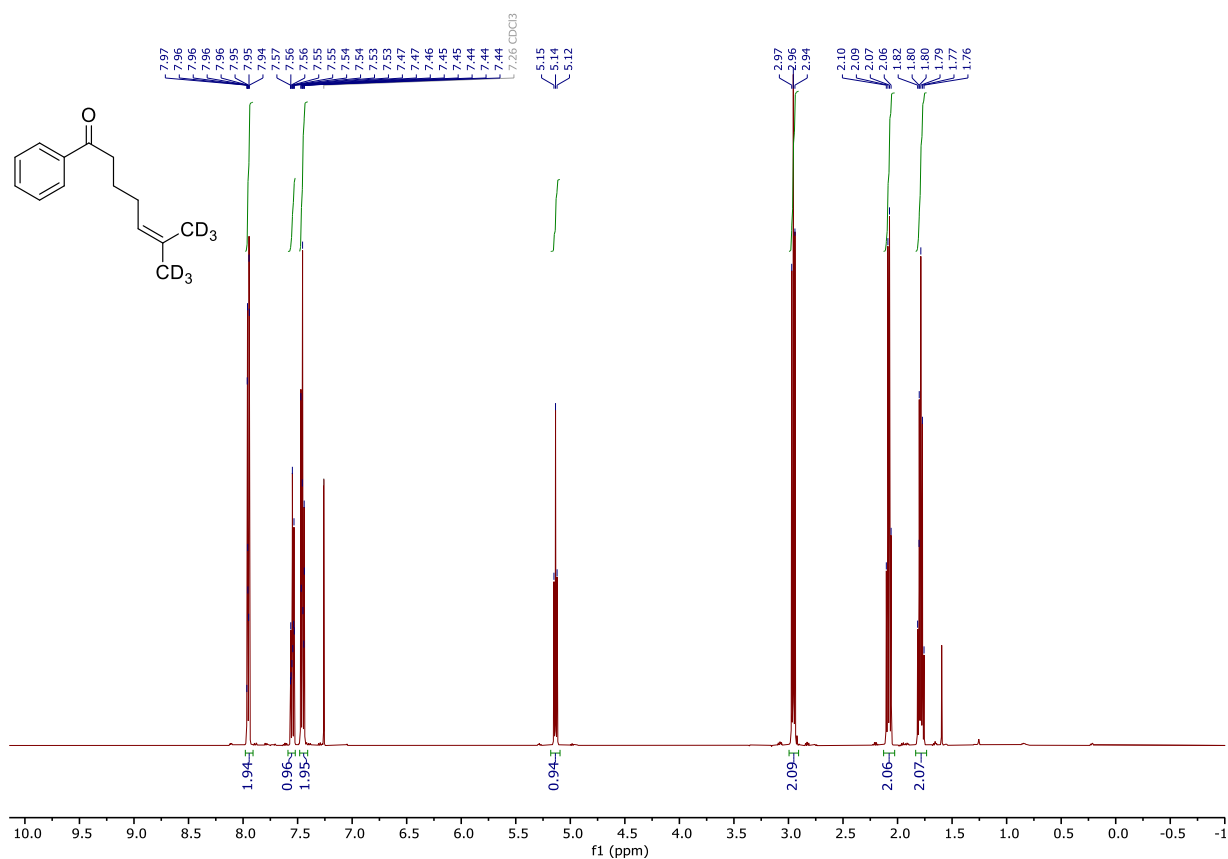
7.2.2.4.1 Ethyl 2-benzoyl-6-methyl( $\text{d}_3$ ) hept-5-enoate-7,7,7-( $\text{d}_3$ )



7.2.2.4.2 Ethyl 2-benzoyl-6-methyl hept-5-enoate

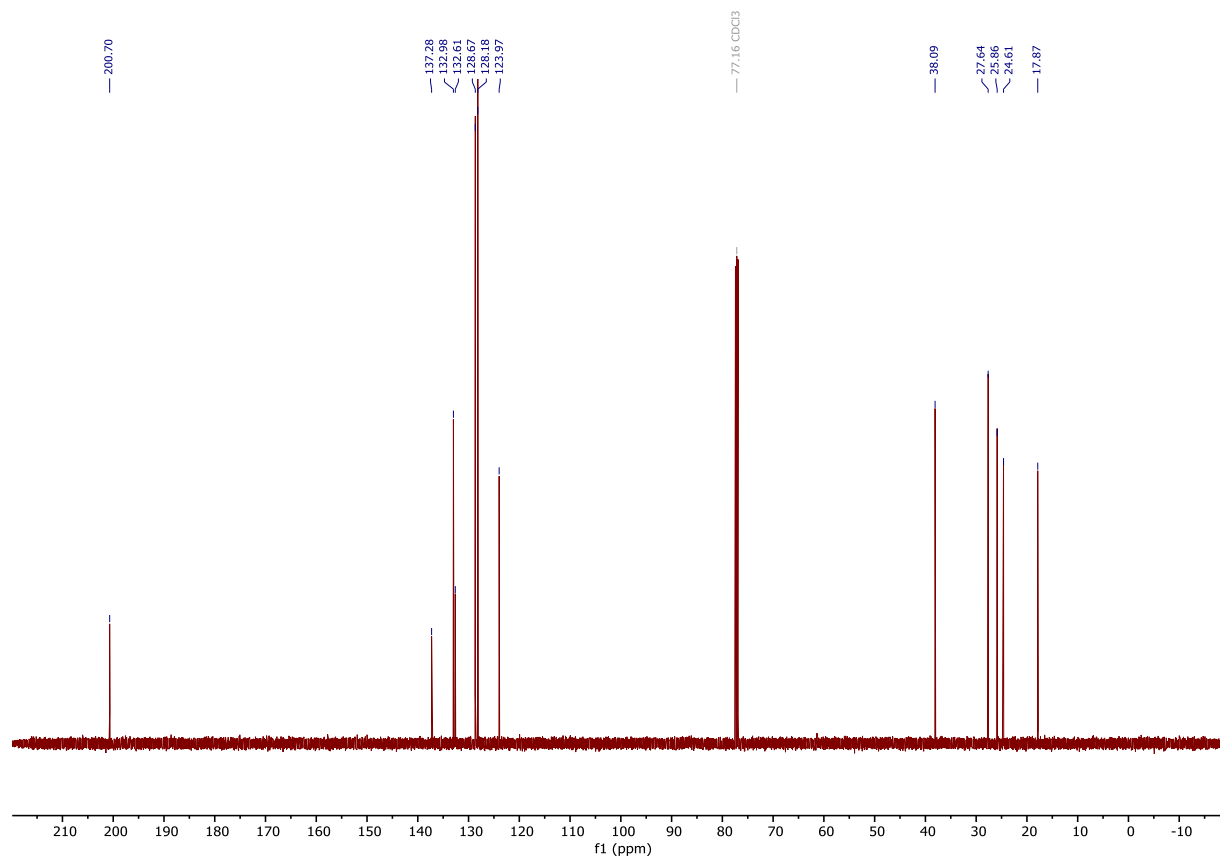
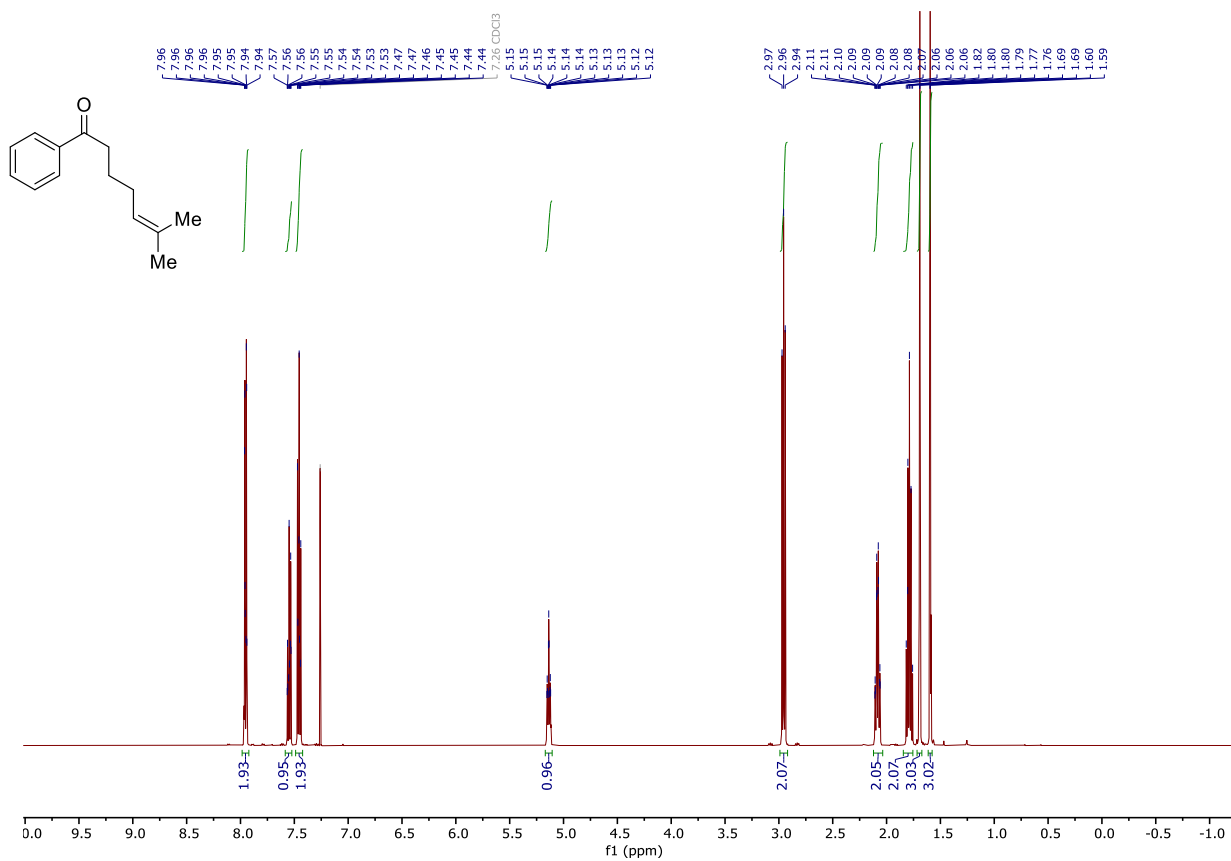


7.2.2.4.3 6-methyl-1-phenylhept-5-en-1-one-(d<sub>6</sub>)

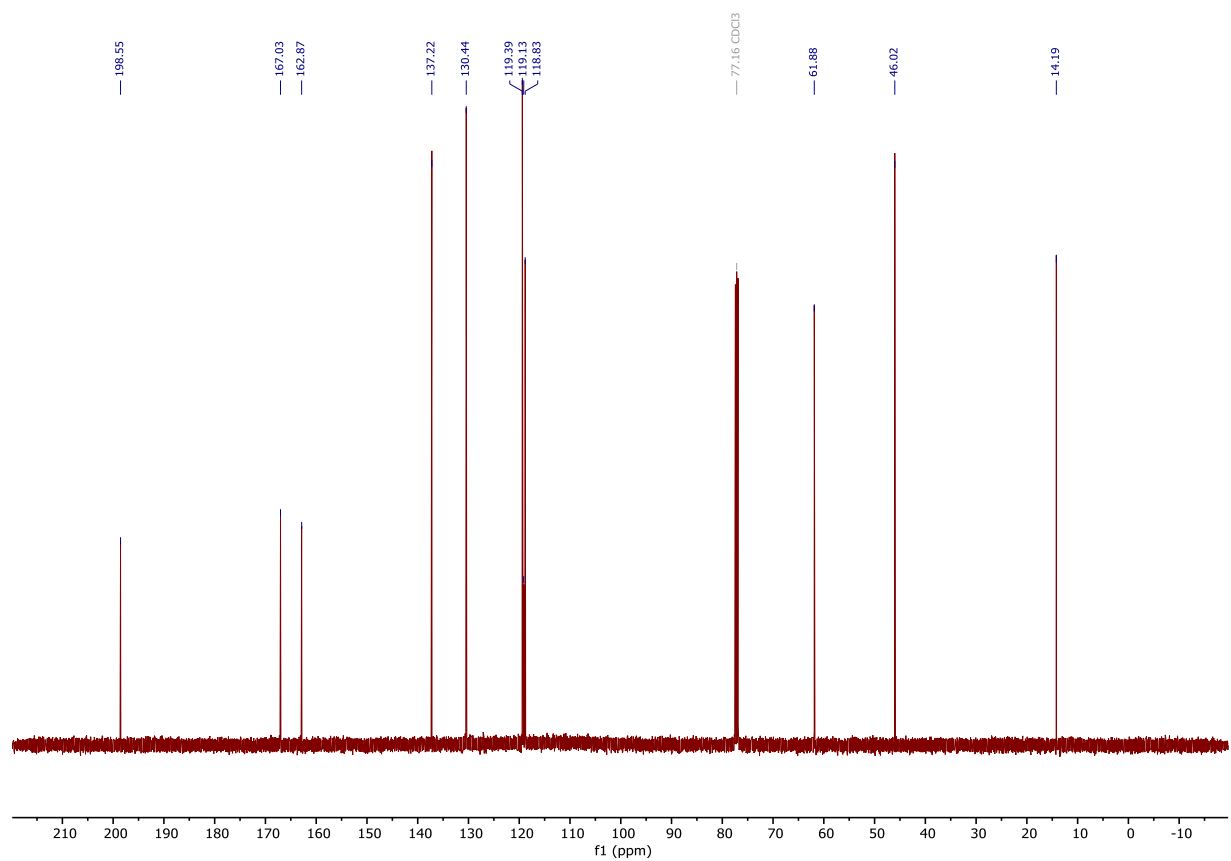
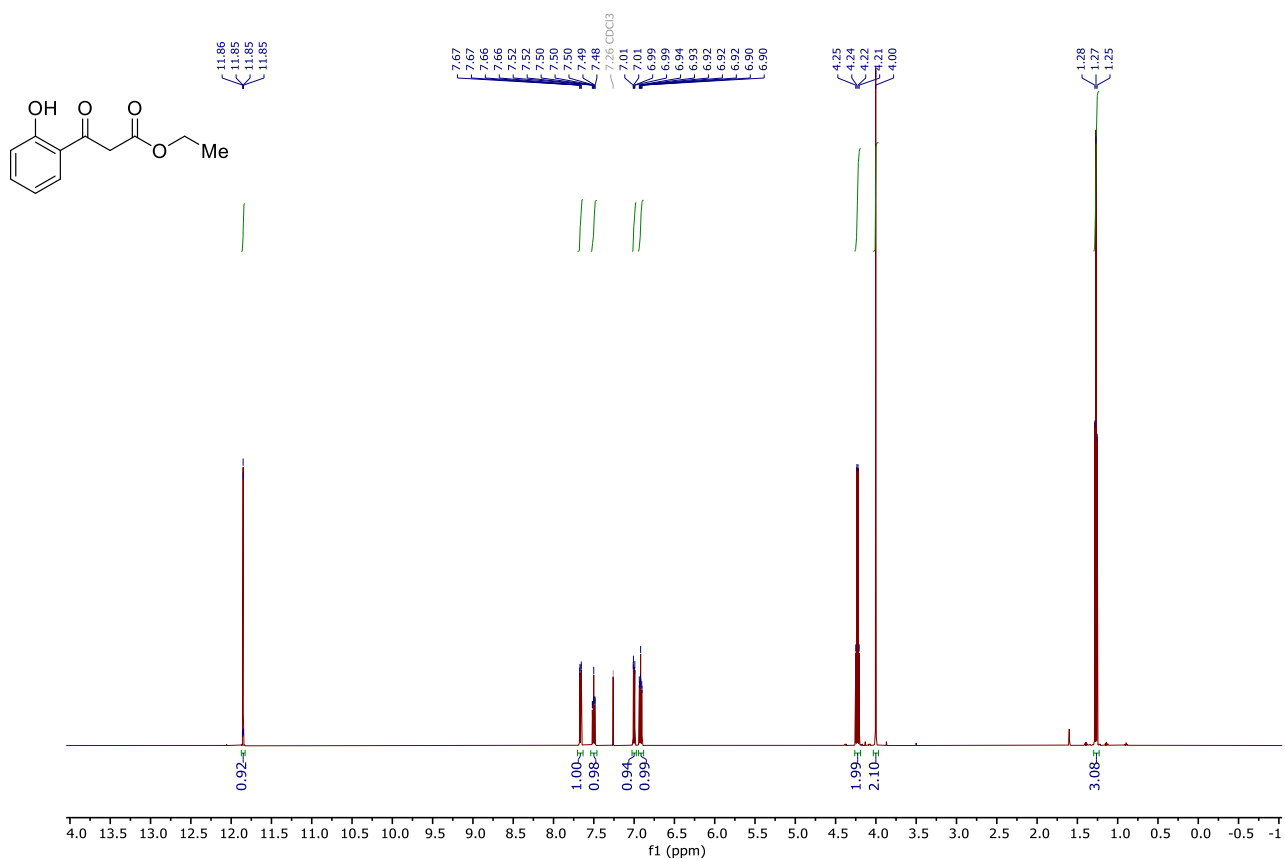




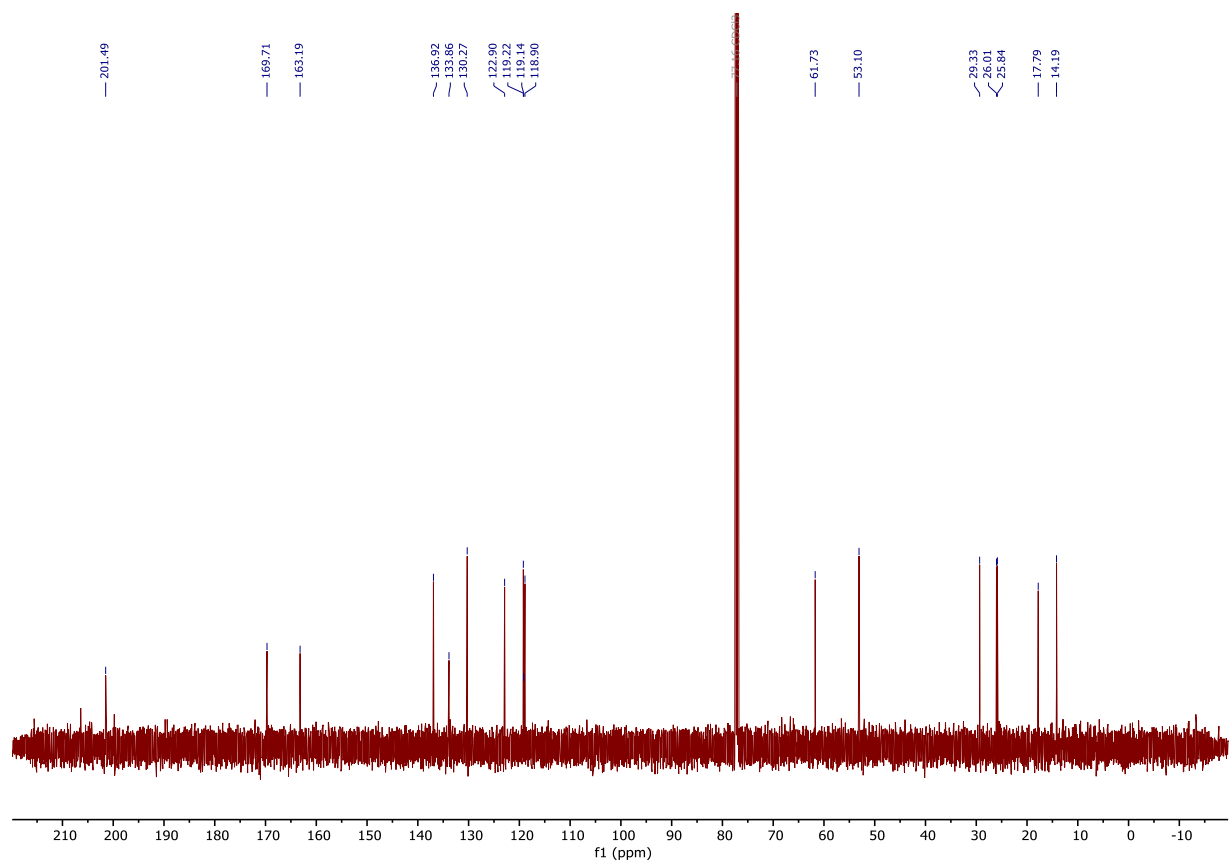
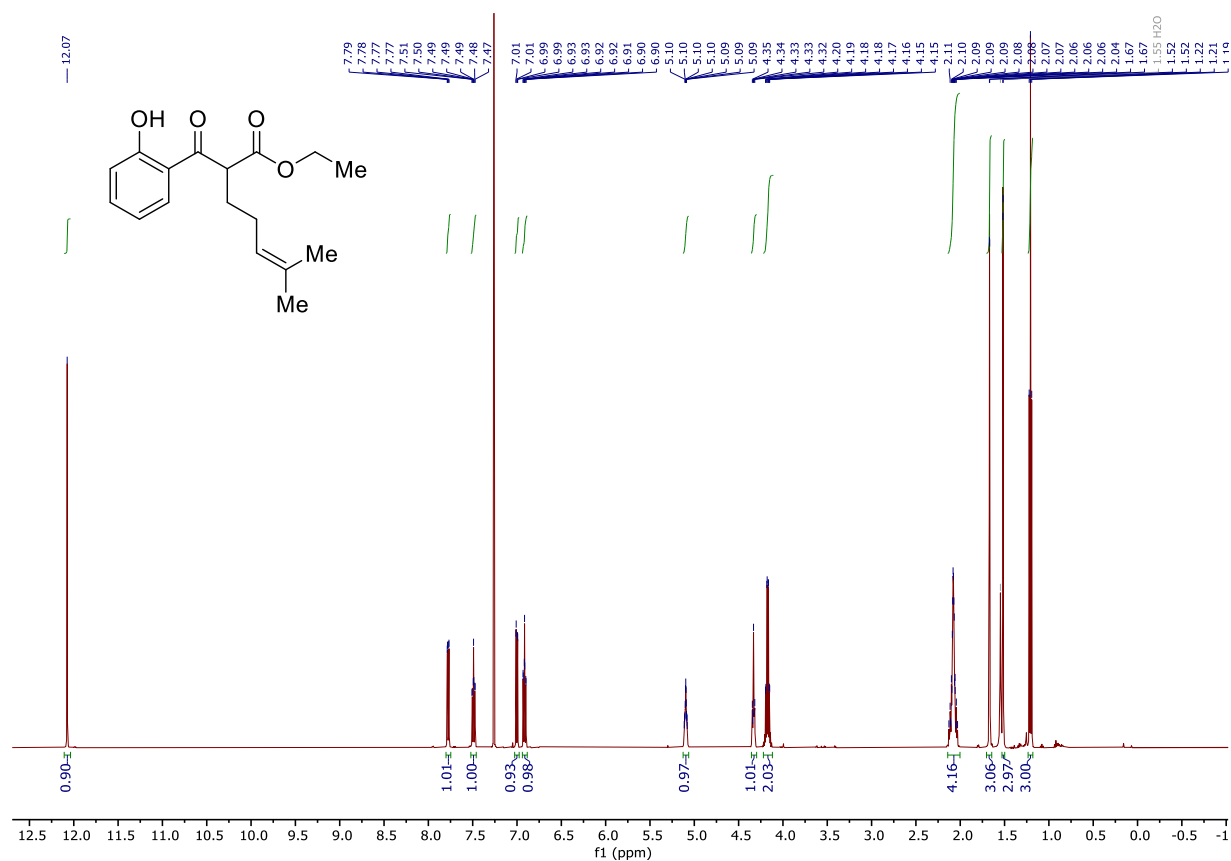
### 7.2.2.4.4 6-methyl-1-phenylhept-5-en-1-one



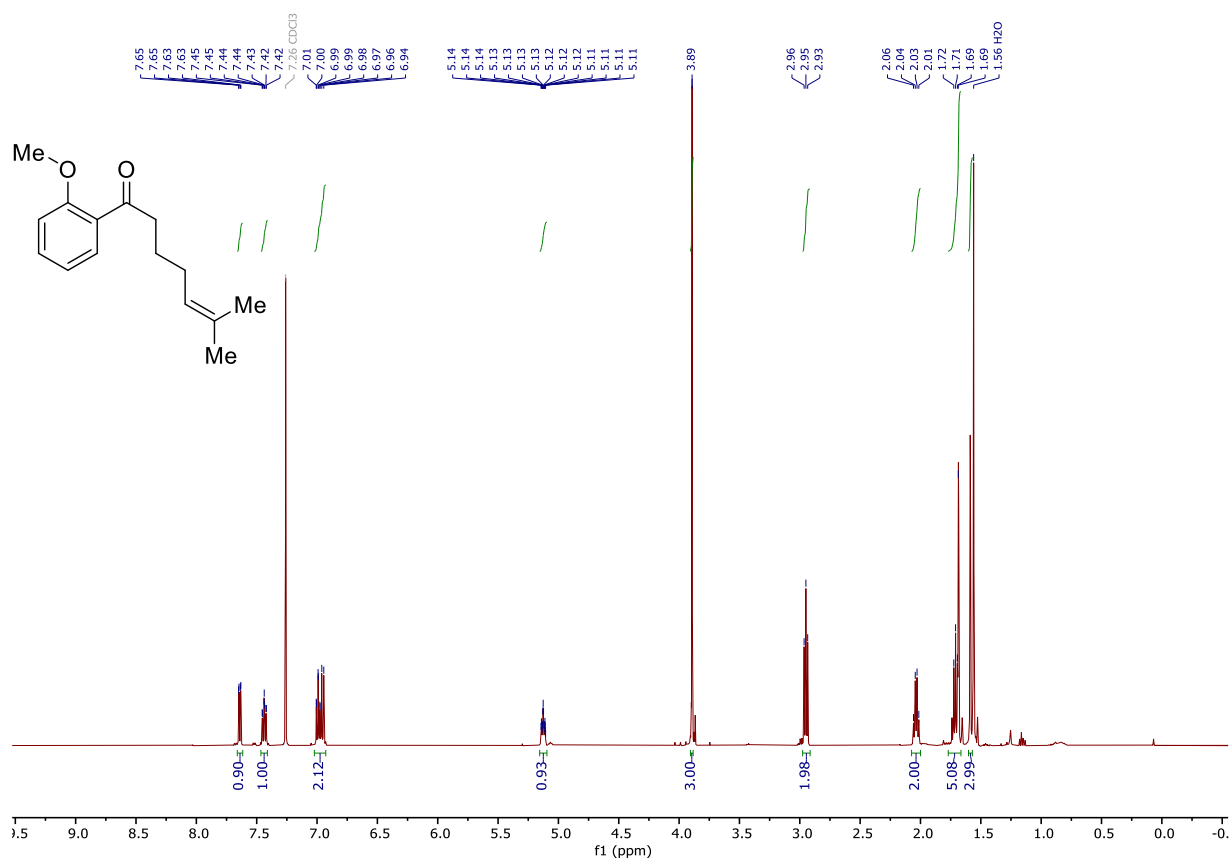
### 7.2.2.4.5 Ethyl 3-(2-hydroxyphenyl)-3-oxopropanoate



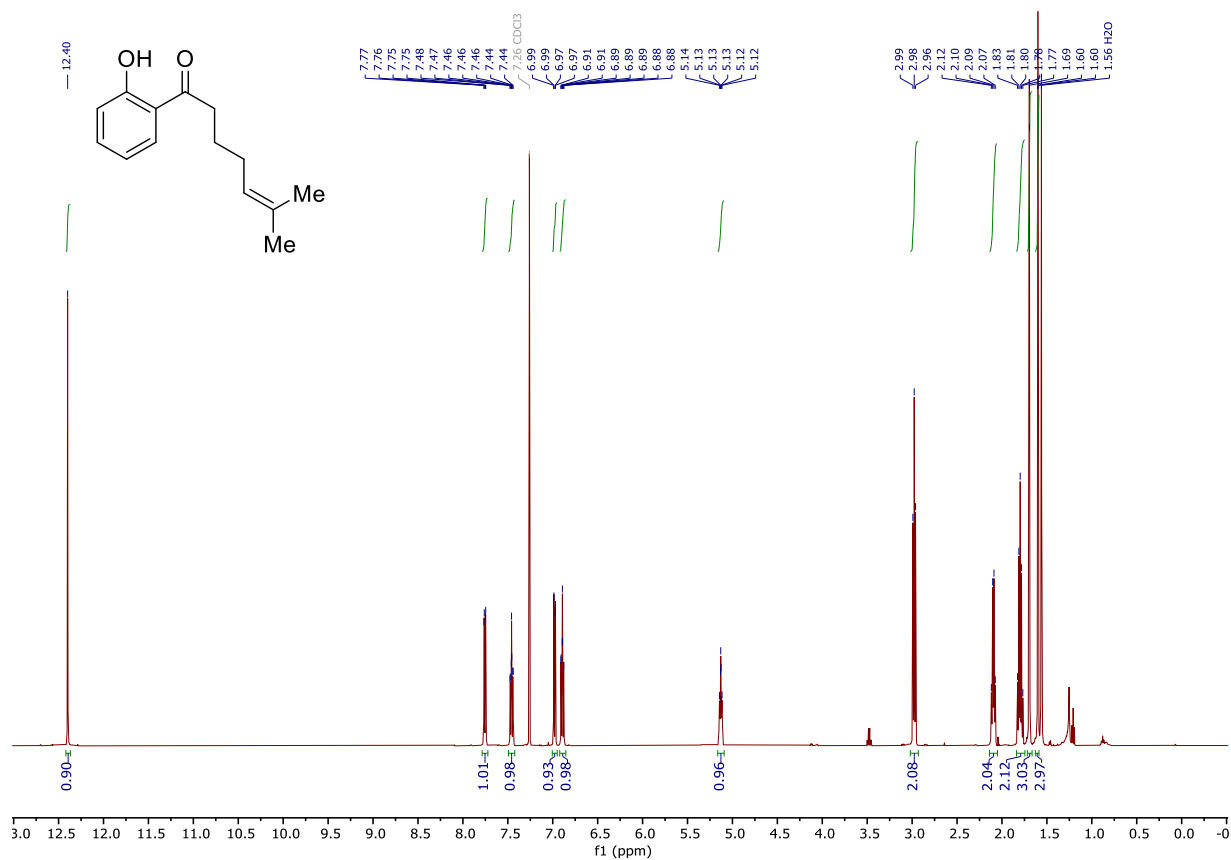
### 7.2.2.4.6 Ethyl 2-(2-hydroxybenzoyl)-6-methylhept-5-enoate



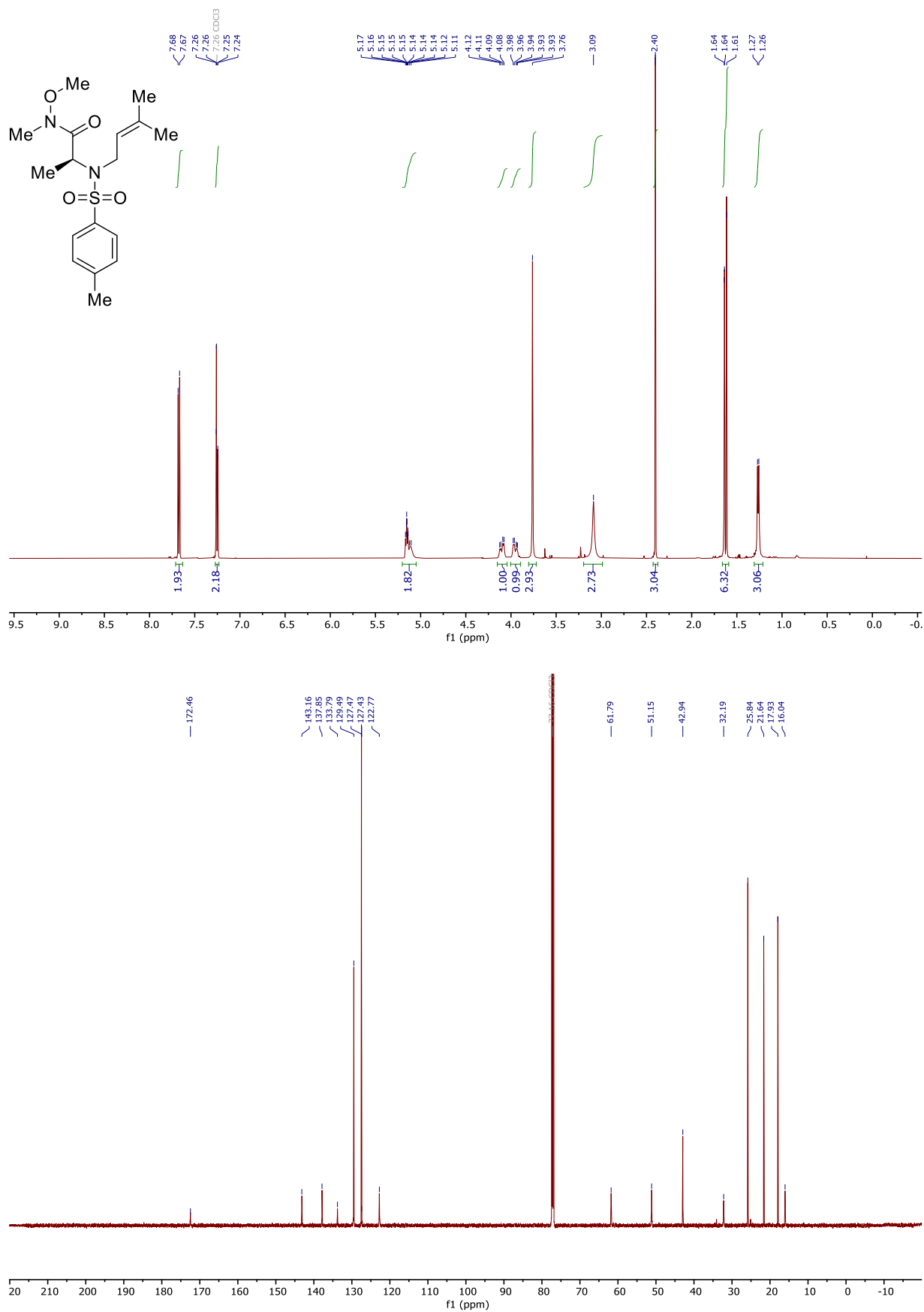
7.2.2.4.7 1-(2-methoxyphenyl)-6-methylhept-5-en-1-one



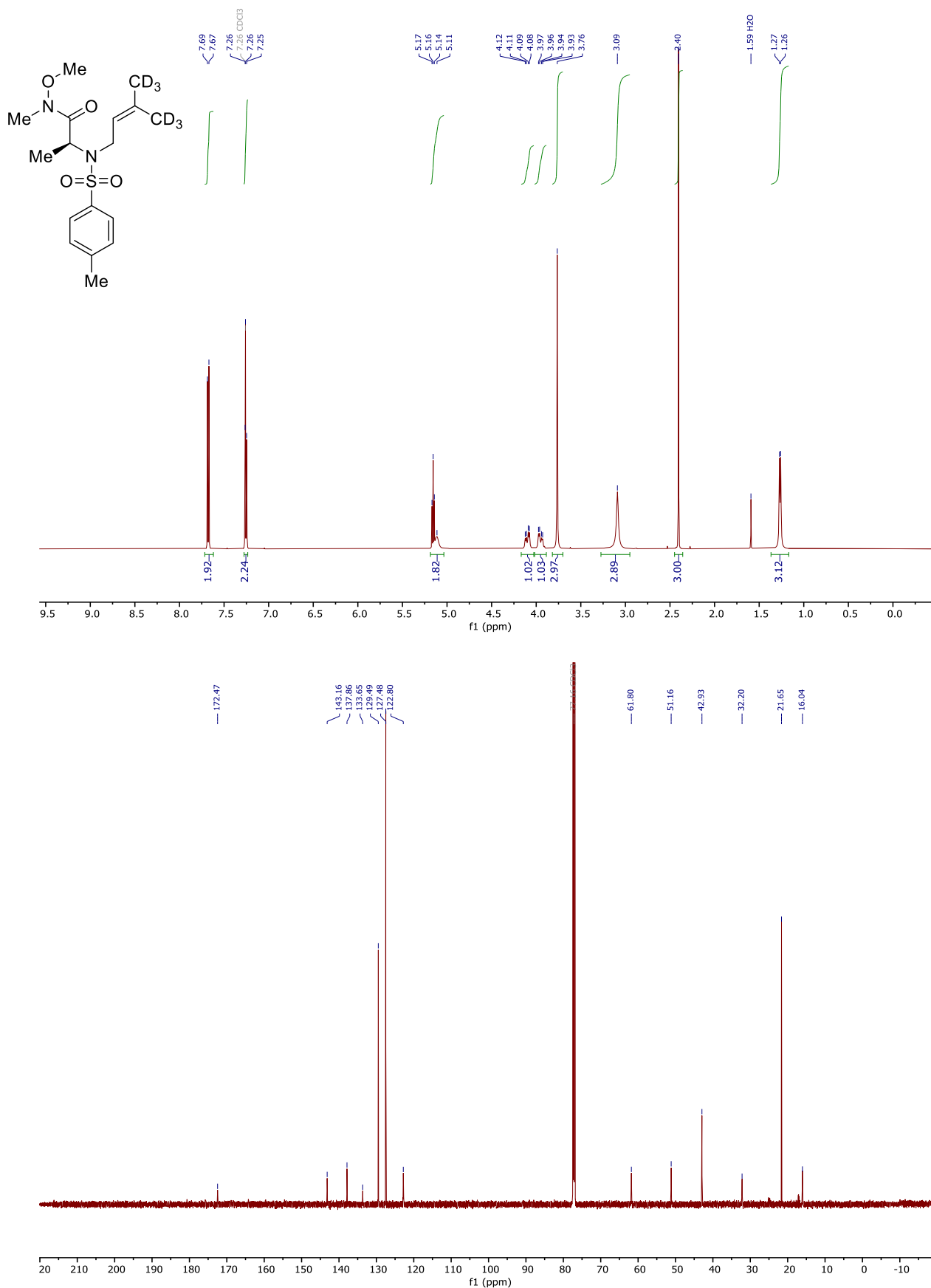
7.2.2.4.8 1-(2-hydroxyphenyl)-6-methylhept-5-en-1-one



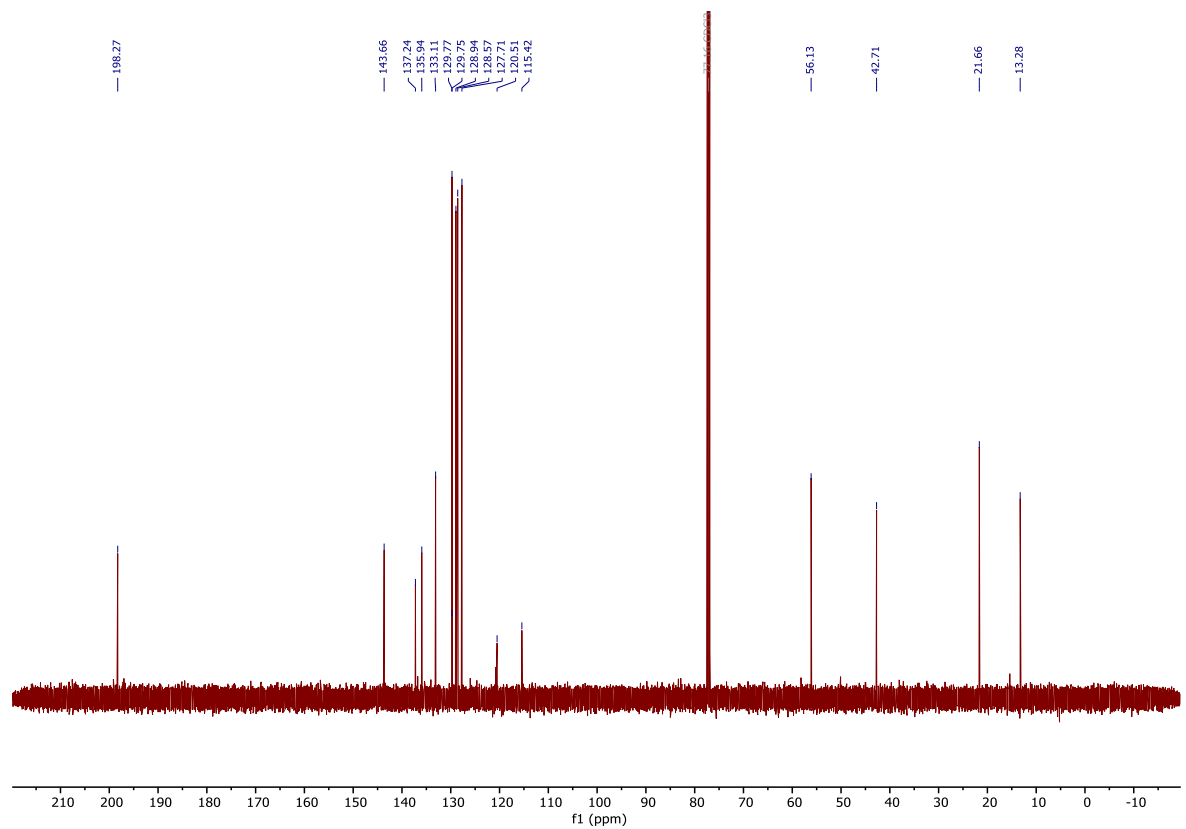
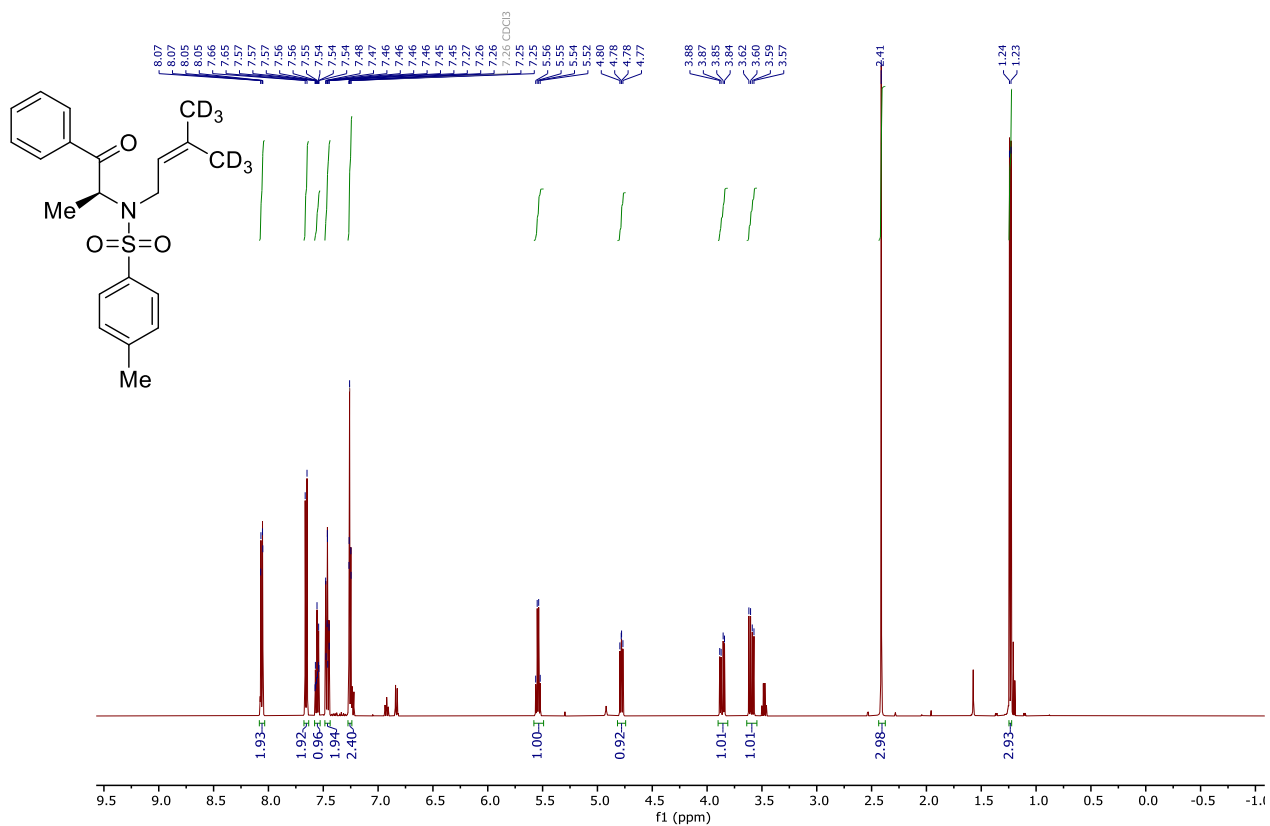
7.2.2.4.9 (S)-N-methoxy-N-methyl-2-((4-methyl-N-(3-methylbut-2-en-1-yl)phenyl)sulfonamido)propanamide



7.2.2.4.10 (S)-N-methoxy-N-methyl-2-((4-methyl-N-(3-(methyl-d3)but-2-en-1-yl)-4,4,4-d3)phenyl)sulfonamido)propanamide

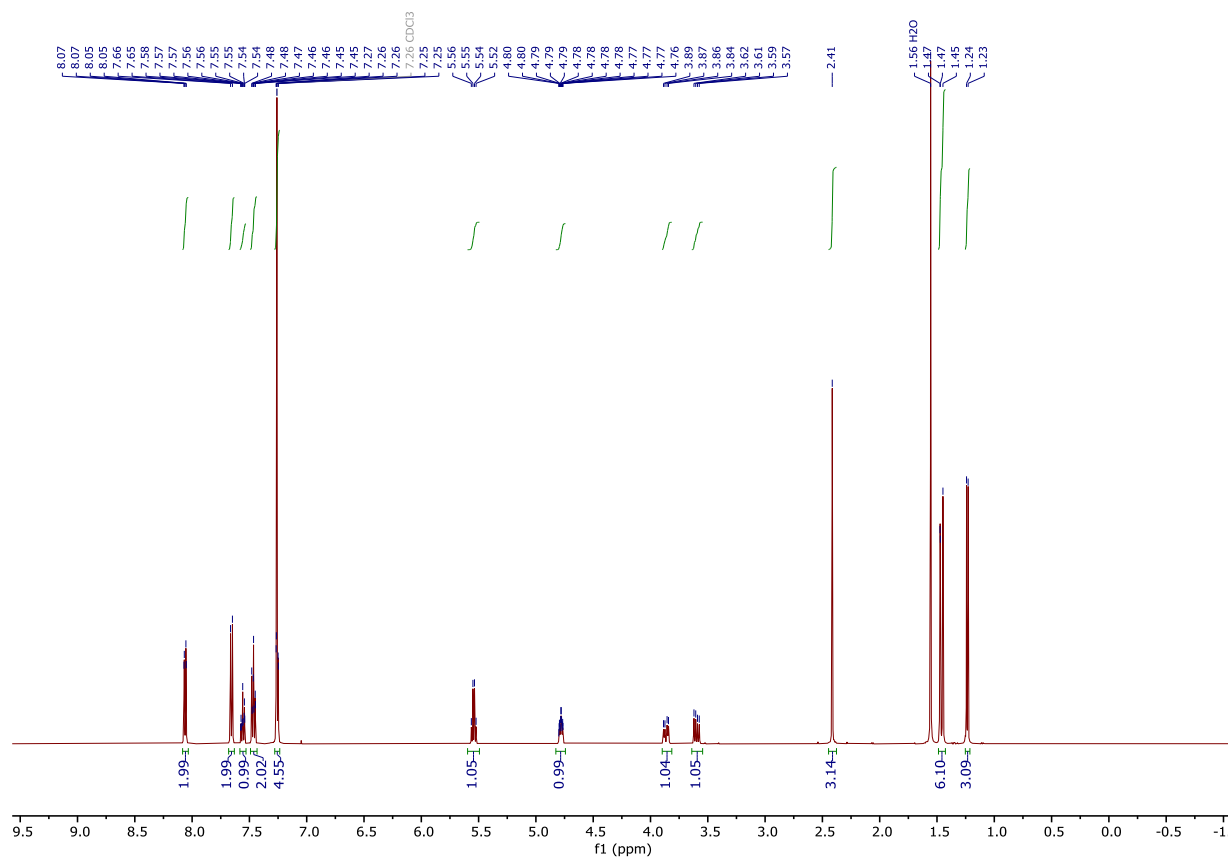
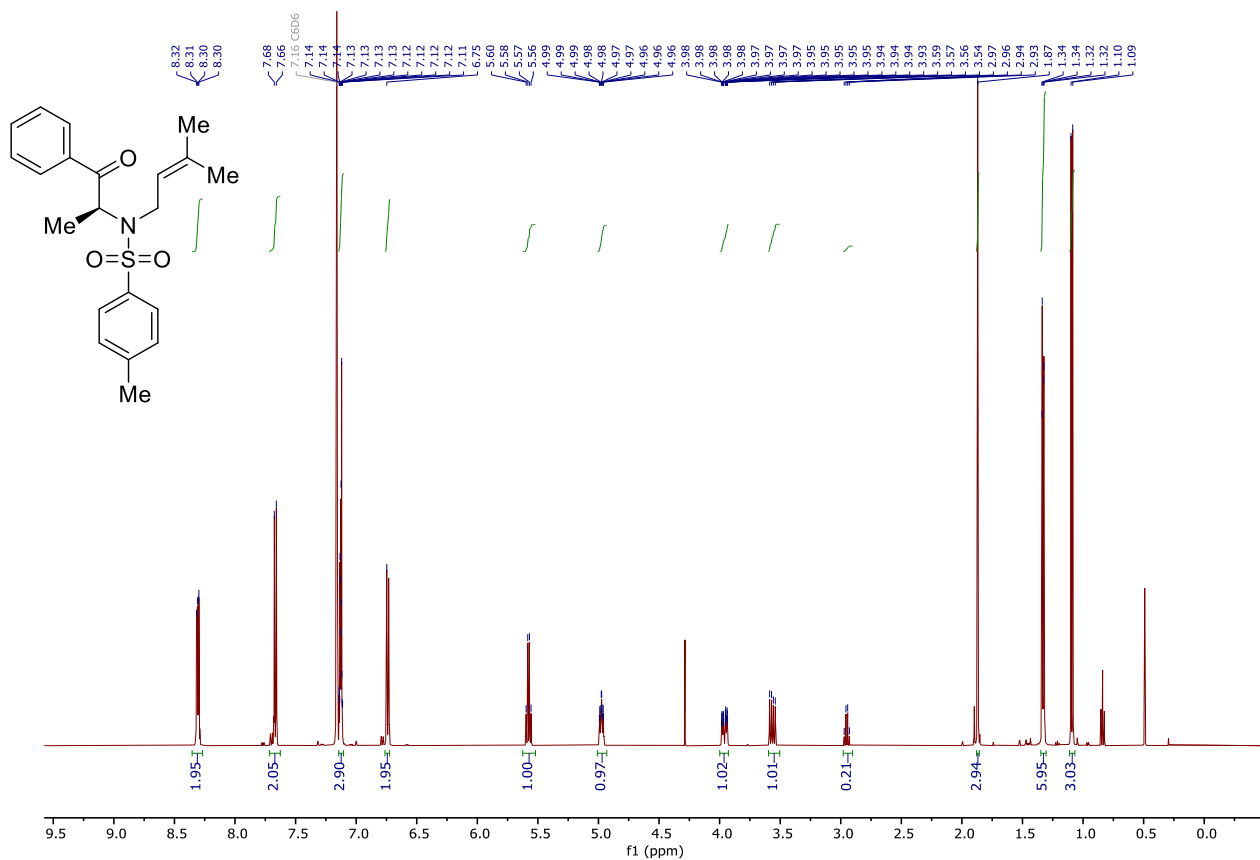


7.2.2.4.11 (S)-4-methyl-N-(3-(methyl-d3)but-2-en-1-yl)-4,4,4-d3-N-(1-oxo-1-phenylpropan-2-yl)benzenesulfonamide



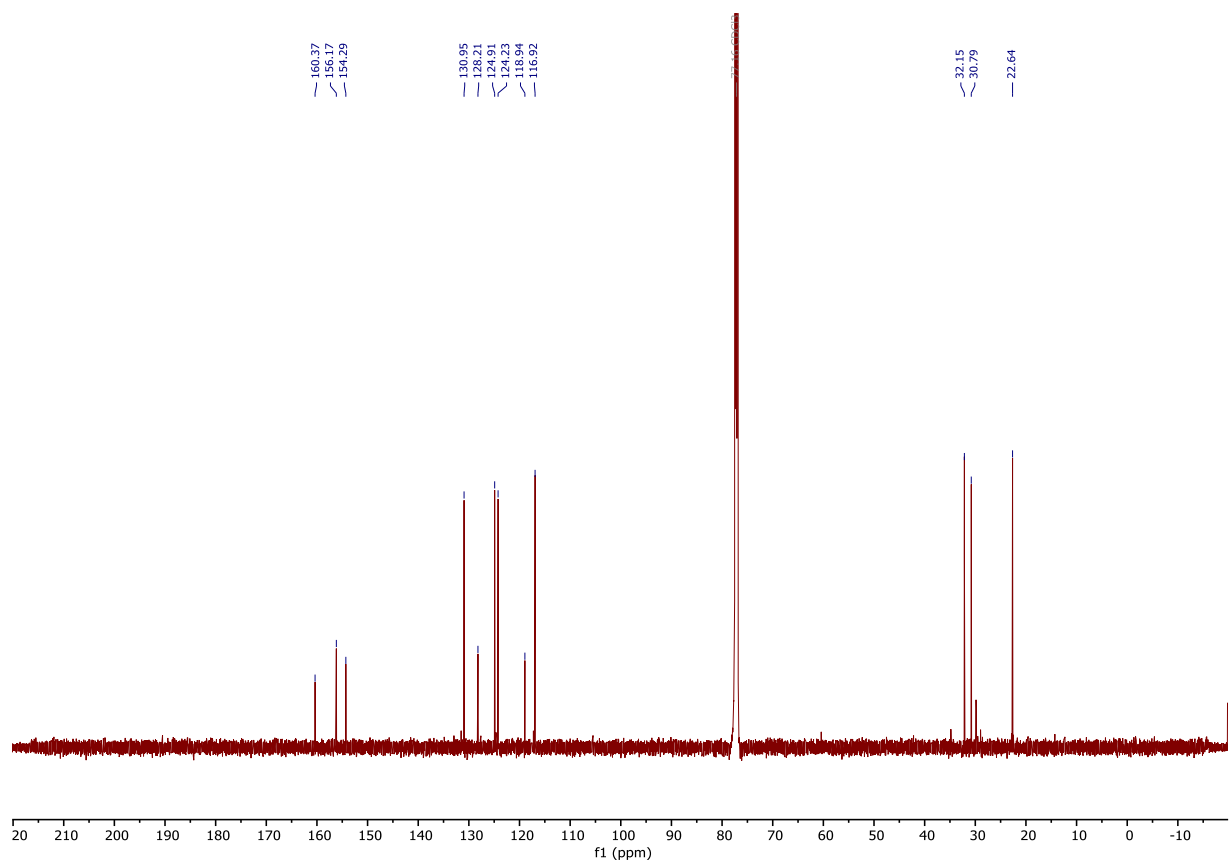
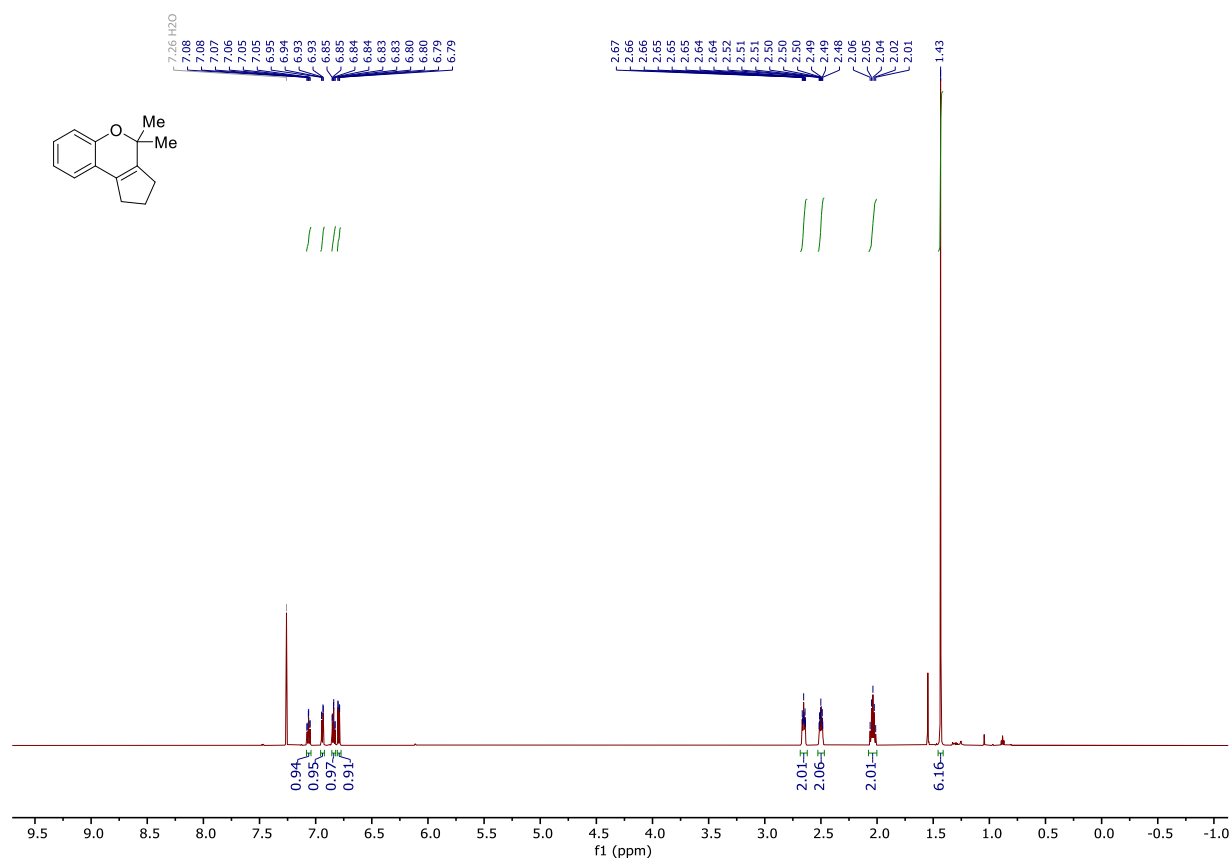


7.2.2.4.12 (S)-4-methyl-N-(3-methylbut-2-en-1-yl)-N-(1-oxo-1-phenylpropan-2-yl)benzenesulfonamide

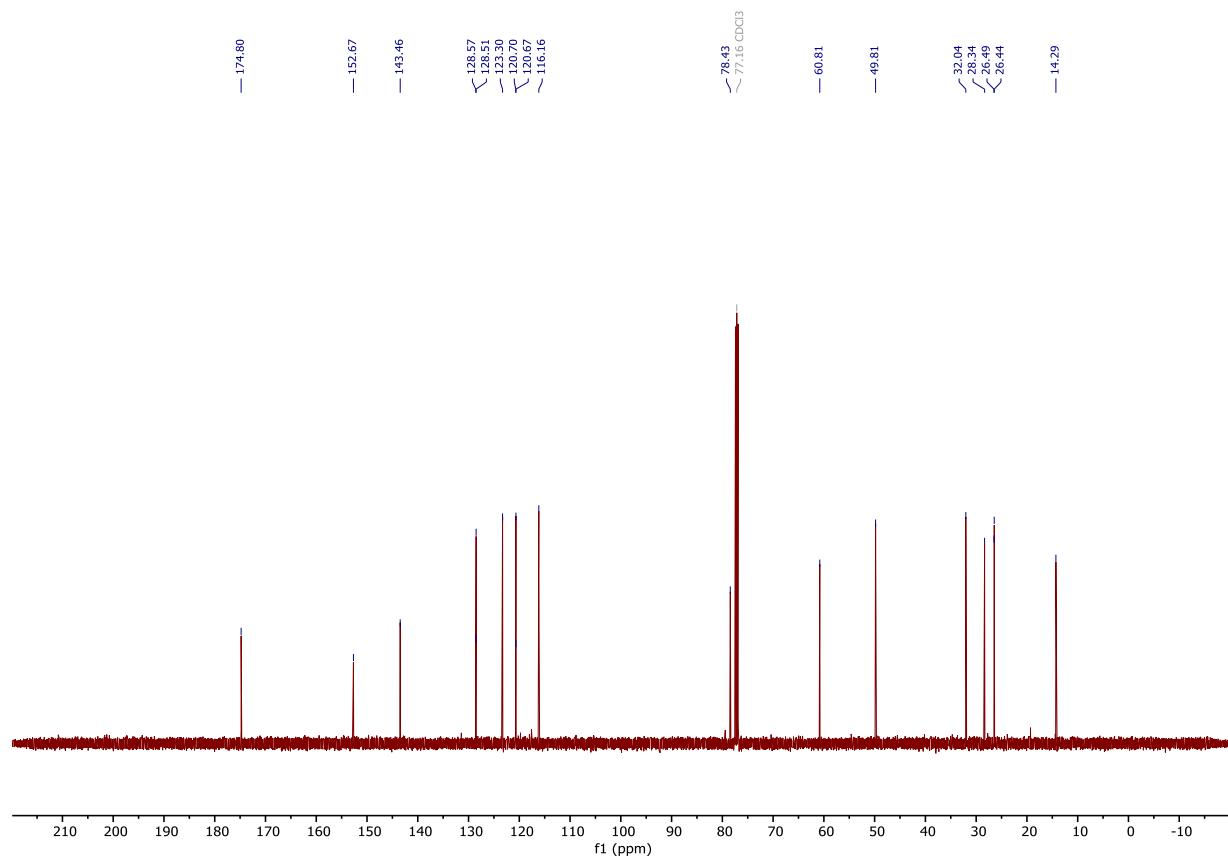
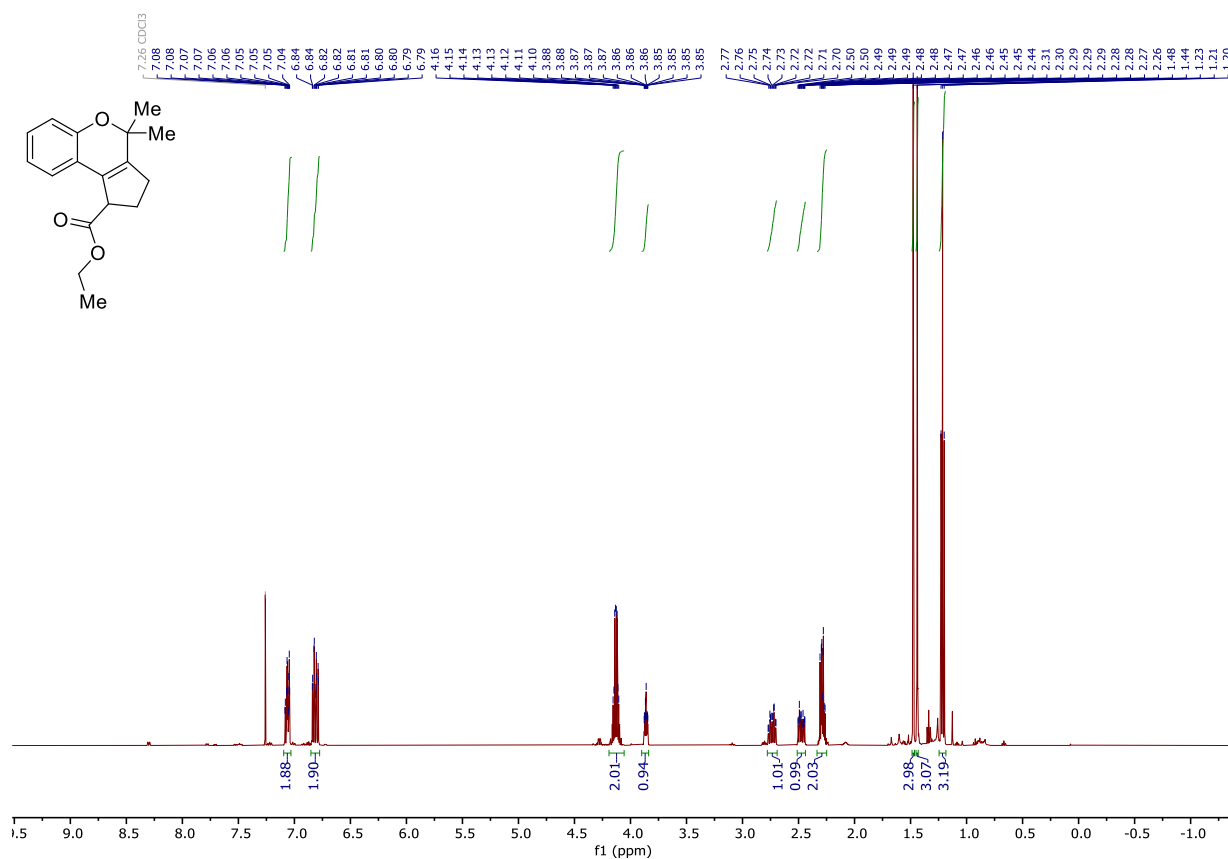




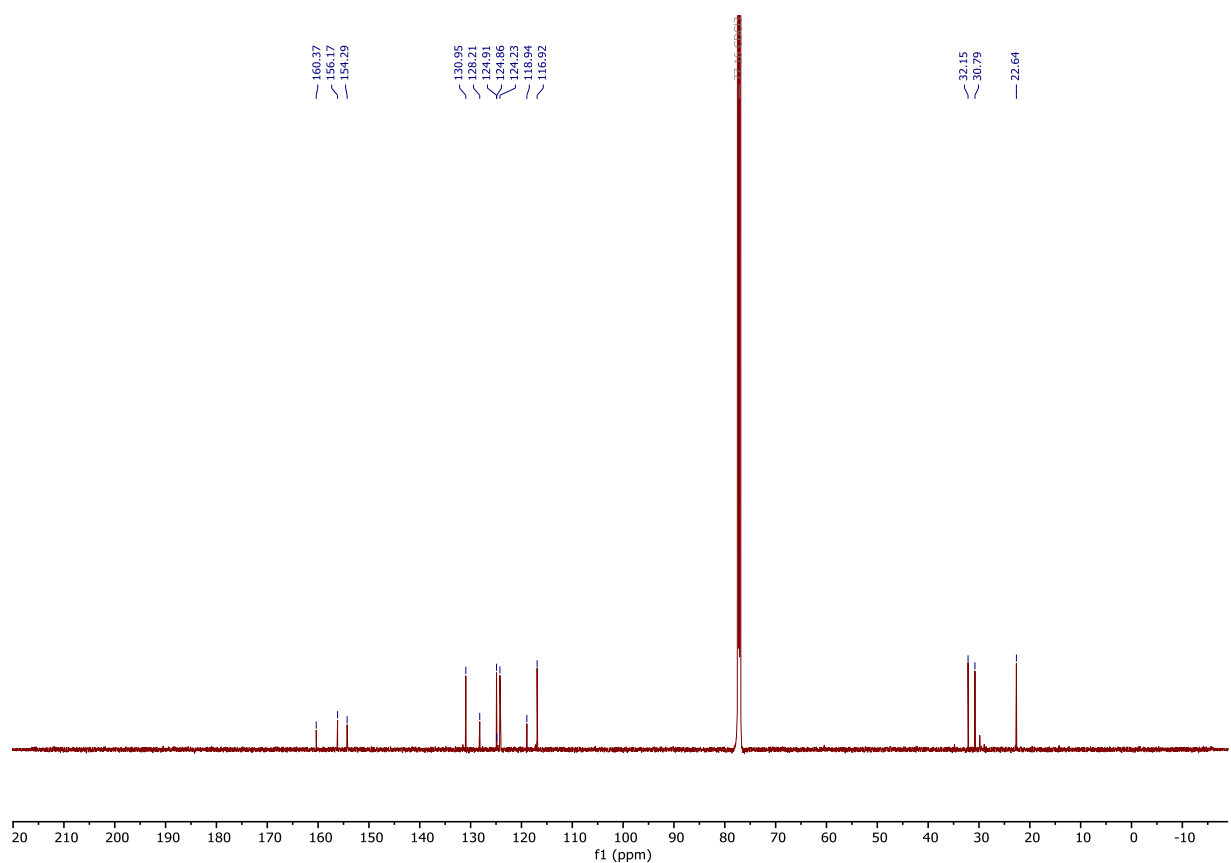
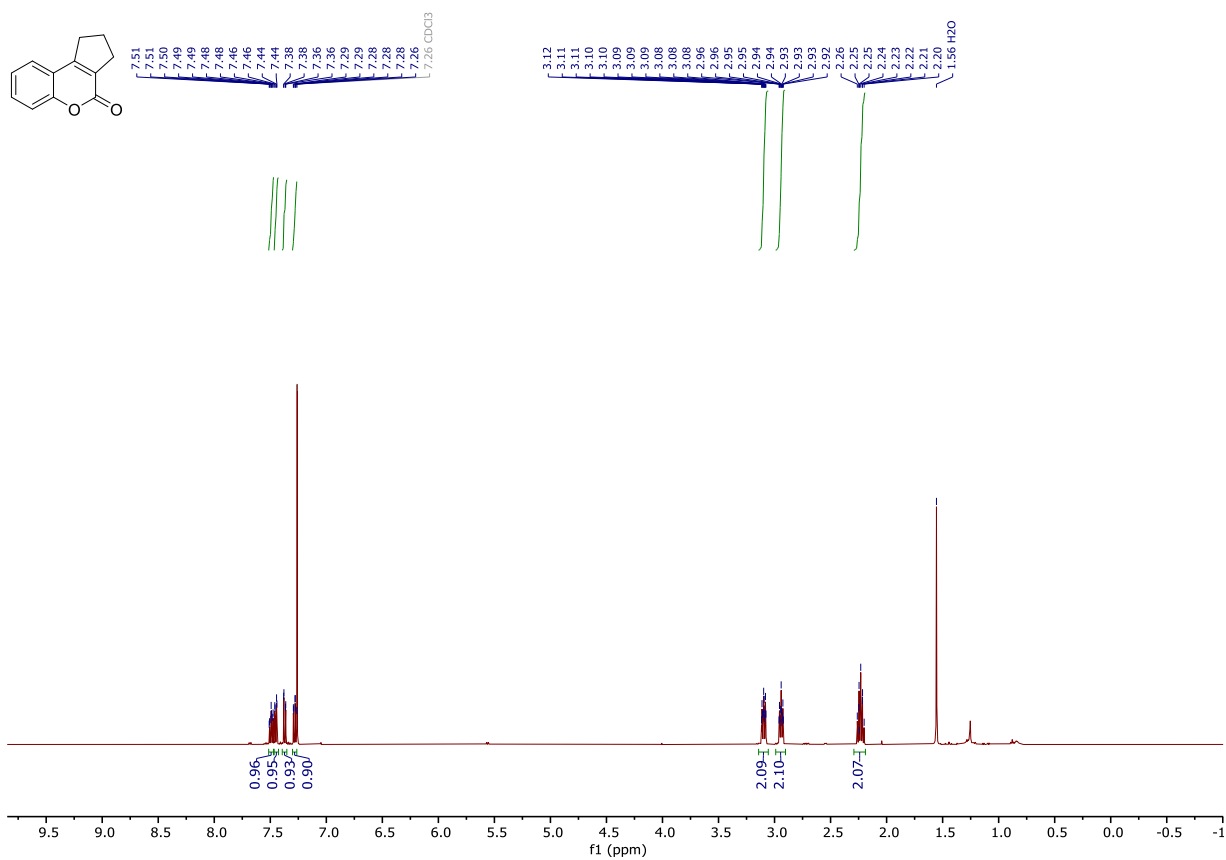
### 7.2.2.4.14 4,4-dimethyl-1,2,3,4-tetrahydrocyclopenta[c]chromene



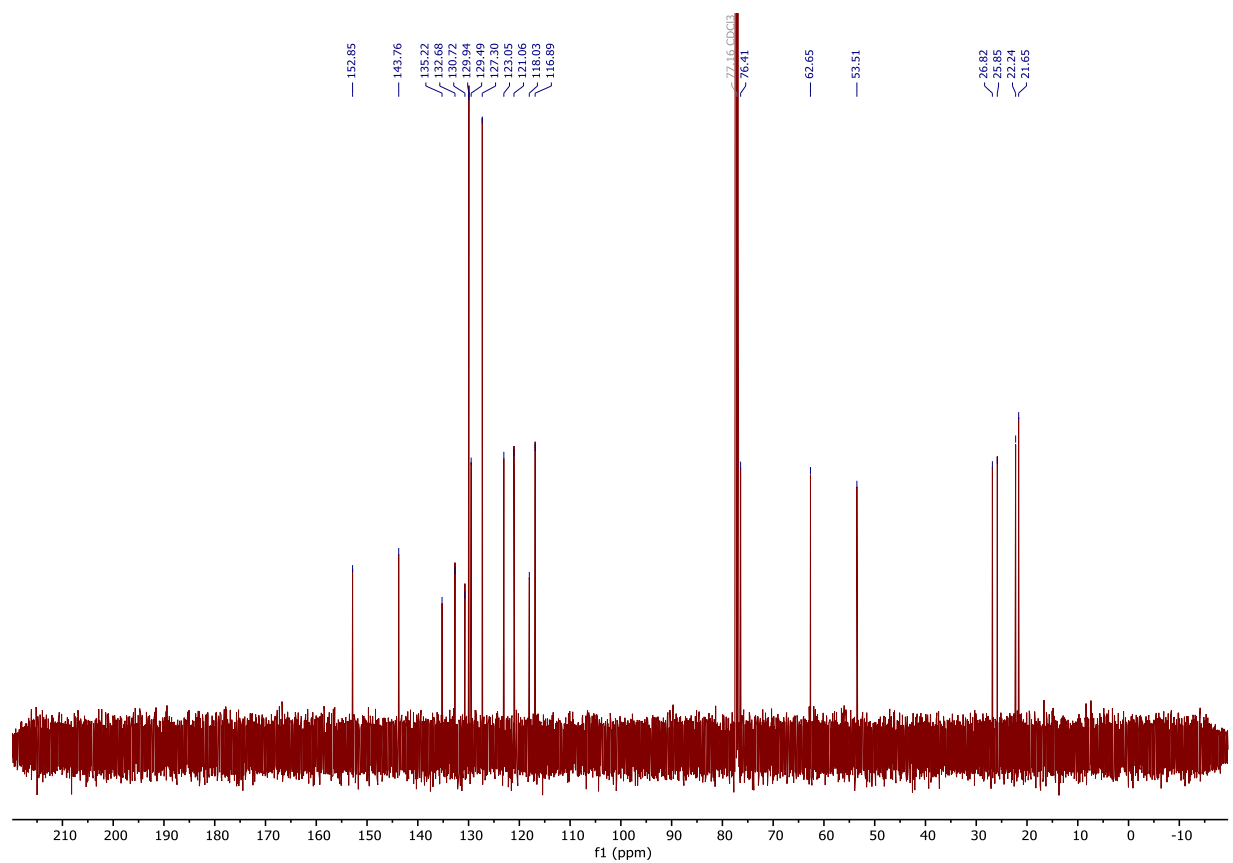
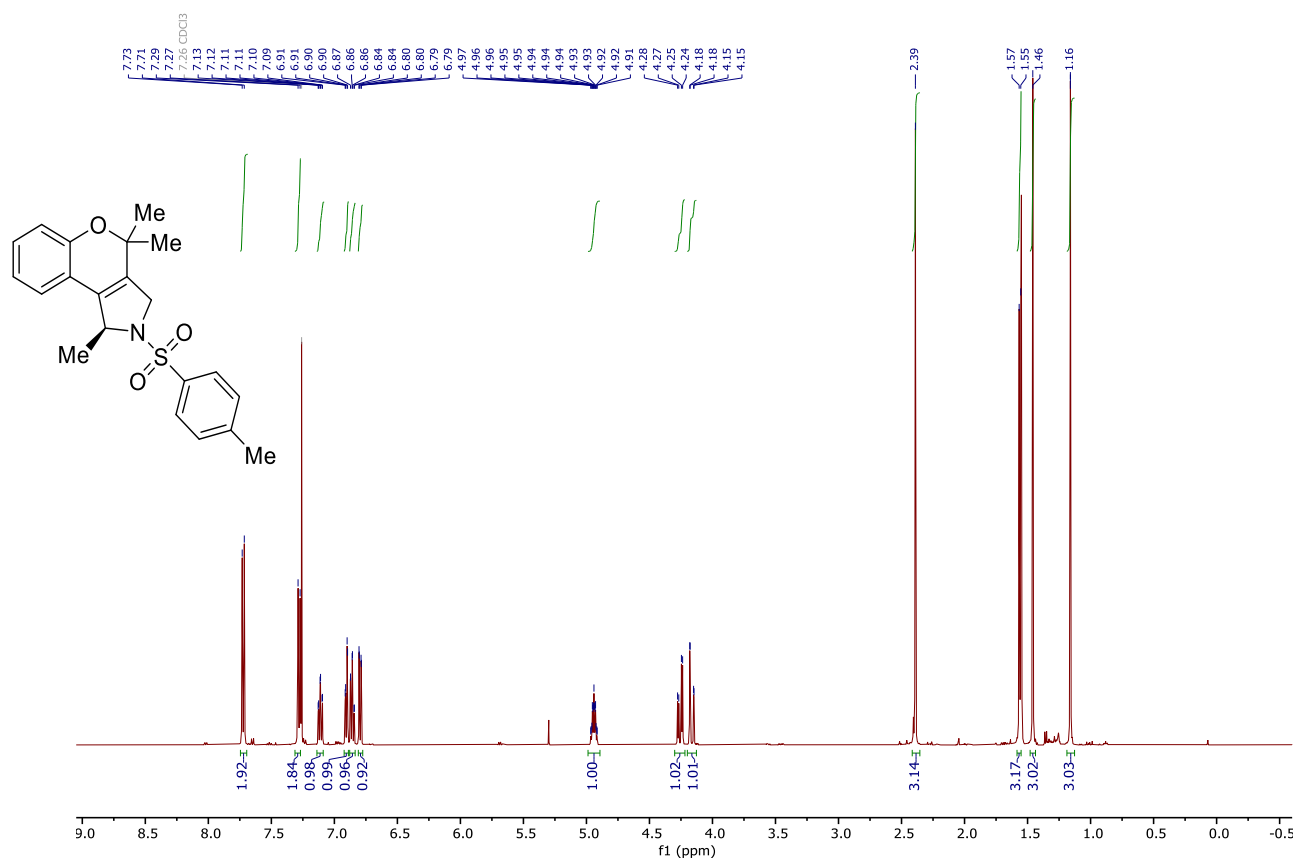
7.2.2.4.15 Ethyl 4,4-dimethyl-1,2,3,4-tetrahydrocyclopenta[c]chromene-1-carboxylate



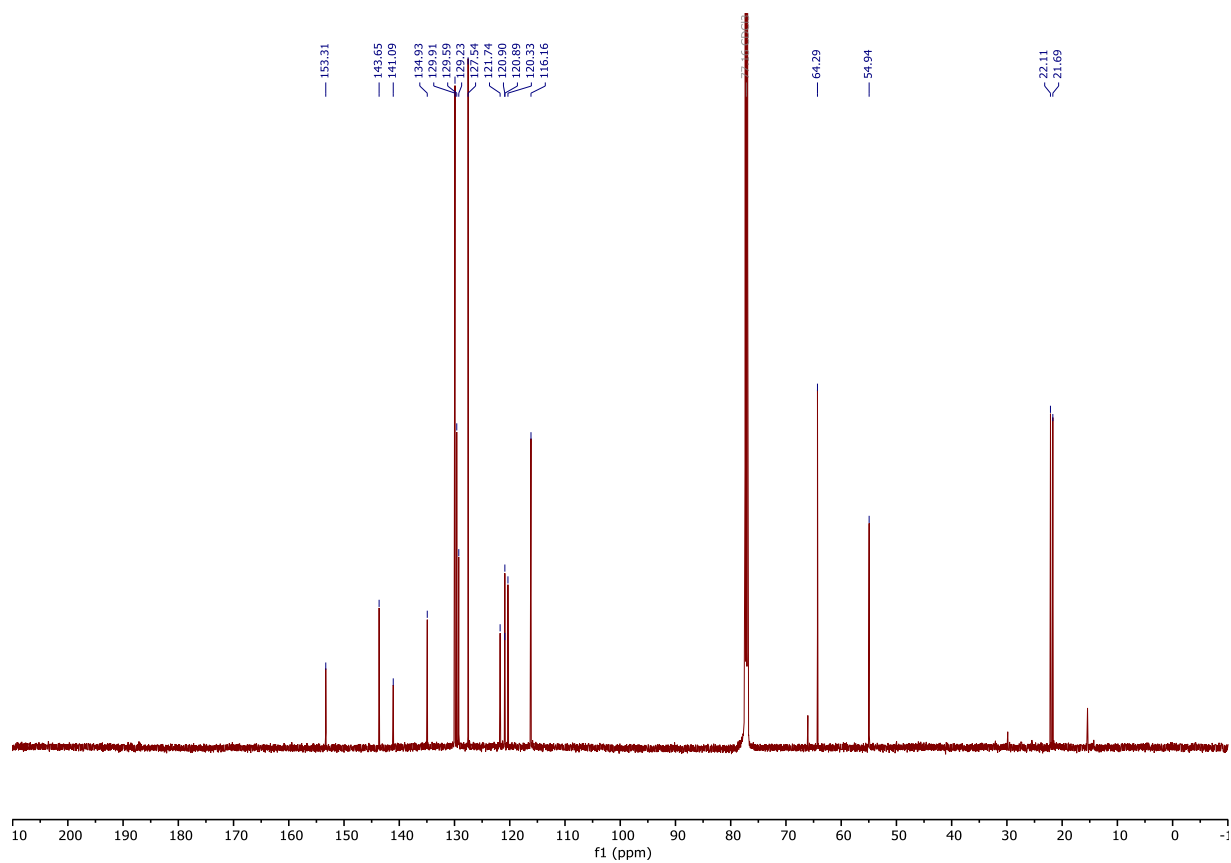
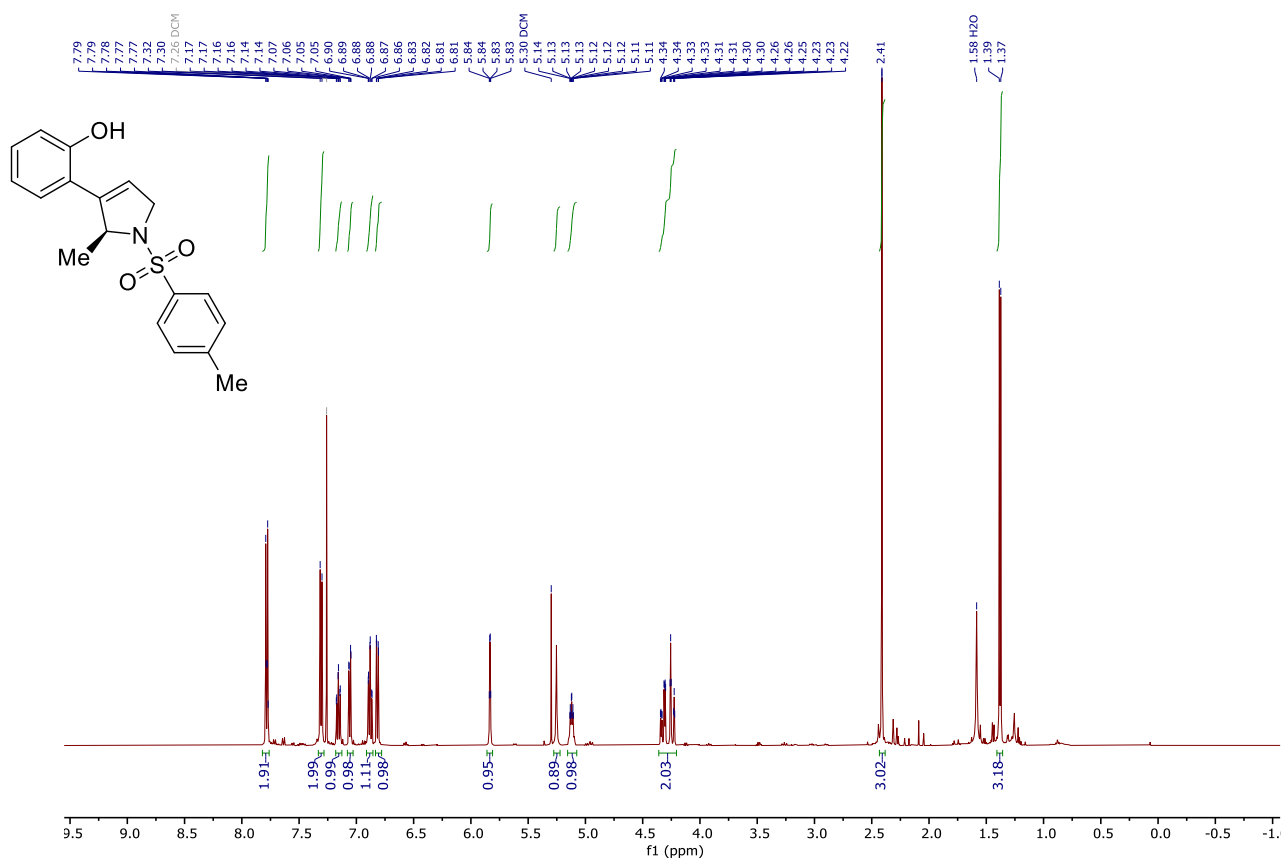
7.2.2.4.16 2,3-dihydrocyclopenta[c]chromen-4(1H)-one



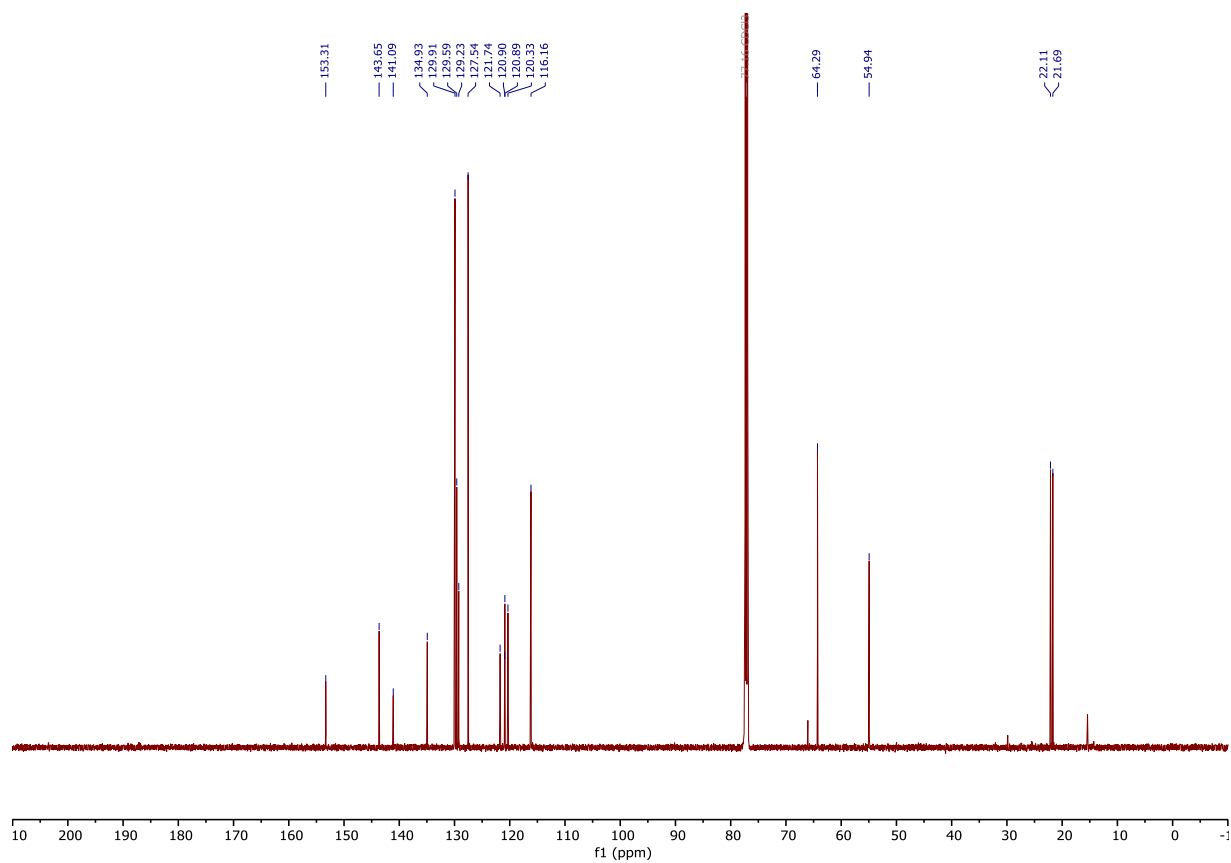
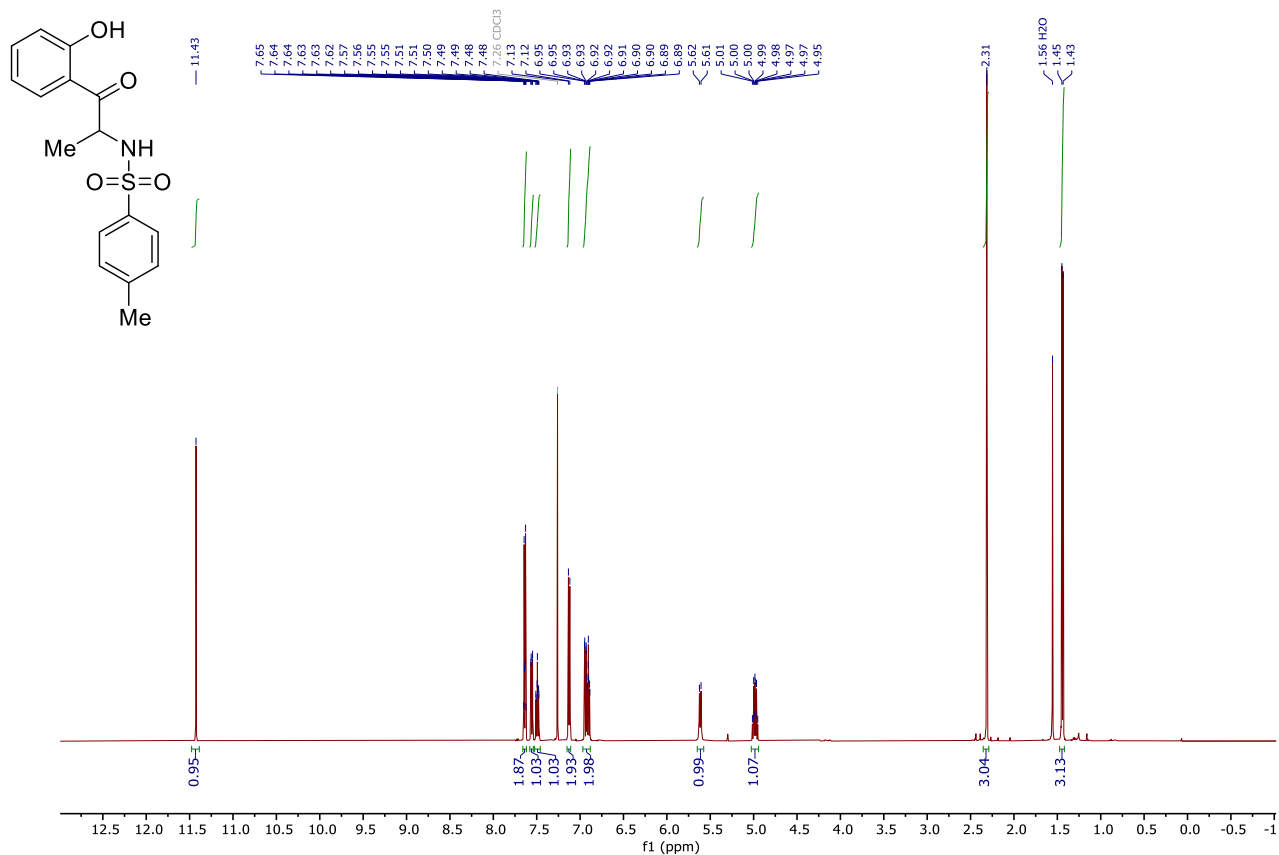
7.2.2.4.17 4,4-dimethyl-2-tosyl-1,2,3,4-tetrahydrochromeno[3,4-c]pyrrole



### 7.2.2.4.18 2-(1-tosyl-2,5-dihydro-1H-pyrrol-3-yl)phenol



7.2.2.4.19 N-(1-(2-hydroxyphenyl)-1-oxopropan-2-yl)-4-methylbenzenesulfonamide





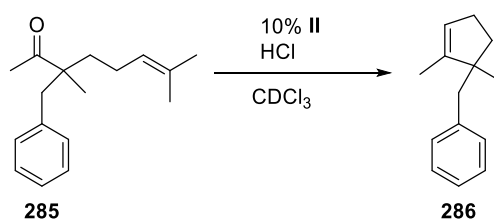
### 7.2.3 Alkyl-Ketones

Substrates **285** and **287** were prepared according to published procedures.<sup>69</sup> Their spectroscopic data matched those reported in the literature. Resorcinarene was prepared according to published procedures.<sup>98</sup>

#### 7.2.3.1.1 General Procedure for the cyclization of **285/287** with **II** and HCl

Resorcinarene (11.0 mg, 9.95  $\mu\text{mol}$ , 0.6 eq.) was suspended in 0.4 mL chloroform-d (filtered through basic aluminum oxide) into a 1.5 mL screw cap vial. The capped vial was heated gently until the suspension turned clear. After cooling to room temperature, HCl was added in the form of HCl-saturated chloroform. Chloroform (filtered through basic aluminum oxide) was added to receive a total volume of 0.5 mL. Decane (2.59  $\mu\text{L}$ , 13.3  $\mu\text{mol}$ , 0.8 eq.) and the substrate (16.6  $\mu\text{mol}$ , 1 eq.) were added. The vial was equipped with a stirring bar and transferred to an aluminum heating block. Aliquots of 50  $\mu\text{L}$  were dissolved in hexane with 0.02 % DMSO (1 mL) and stored at -20 °C for 30 min. The received suspension was centrifuged and the liquid phase was transferred and analyzed by GC.

### 7.2.3.1.2 Screening Substrate **285**



substrate	entry	HCl	time	T	Conversion
<b>285</b>	1	10%	7d	25 °C	42%
	2	20%	7d	25 °C	65%
	3	5%	2d	50 °C	100%
	4	10%	2d	50 °C	100%

7.2.3.1.2.1 10 % HCl, 25 °C

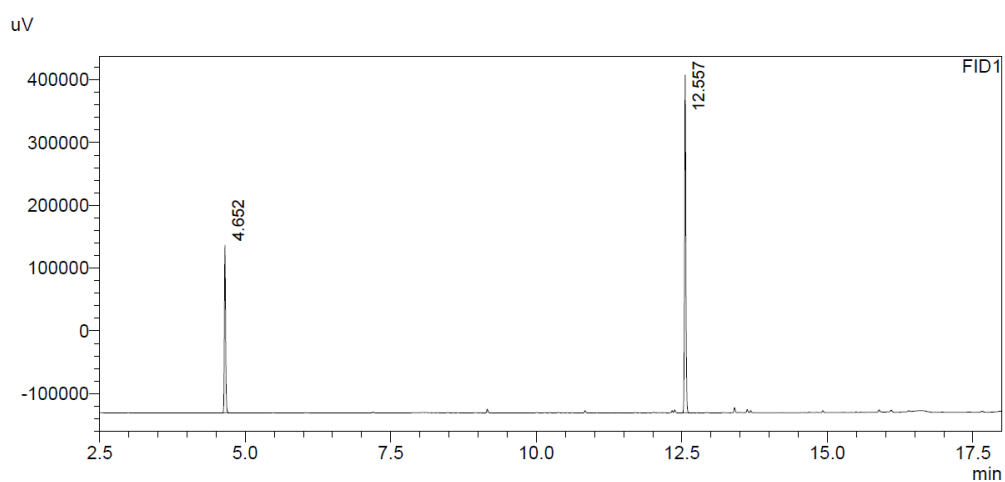


Figure 73 GC: start point 0 d, 10 % HCl, 25 °C

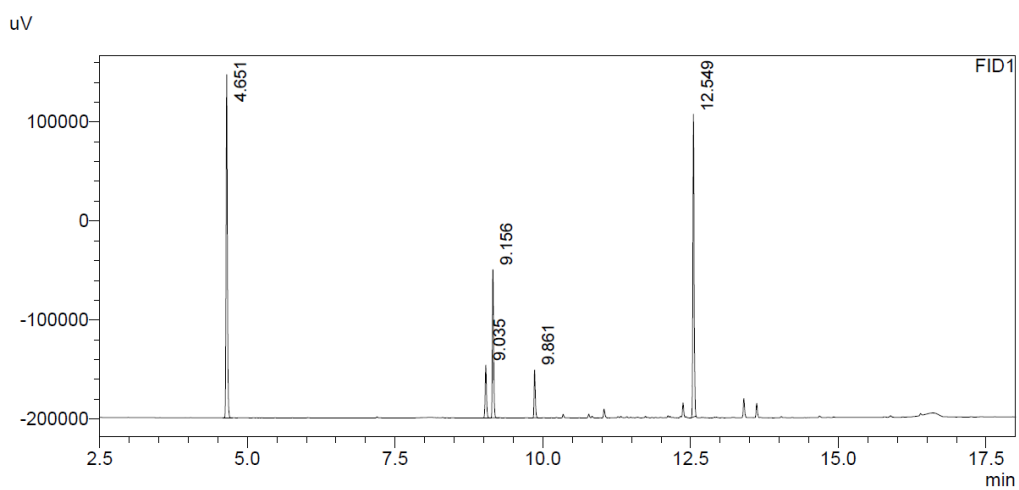


Figure 74 GC: conversion after 3 d, 10 % HCl, 25 °C

7.2.3.1.2.2 20 % HCl 25 °C

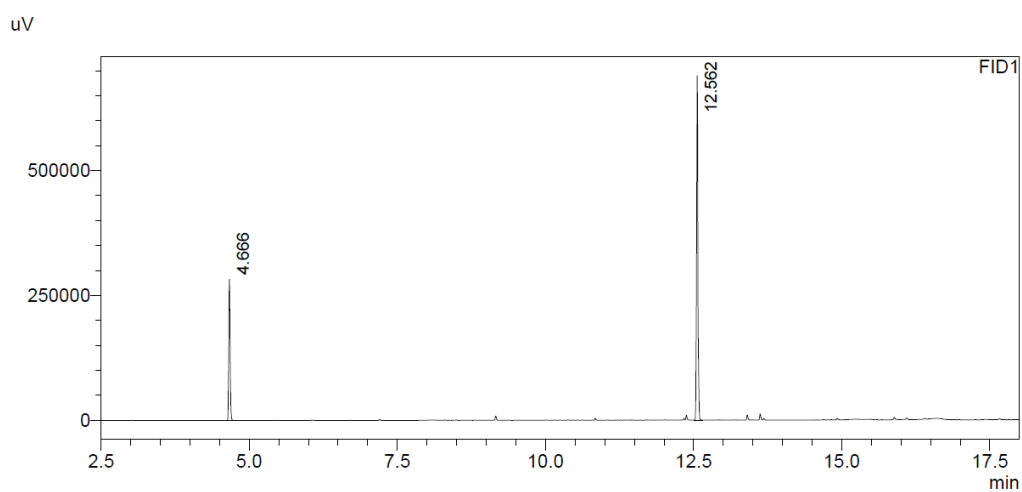


Figure 75 GC: start point 0 d, 20 % HCl, 25 °C

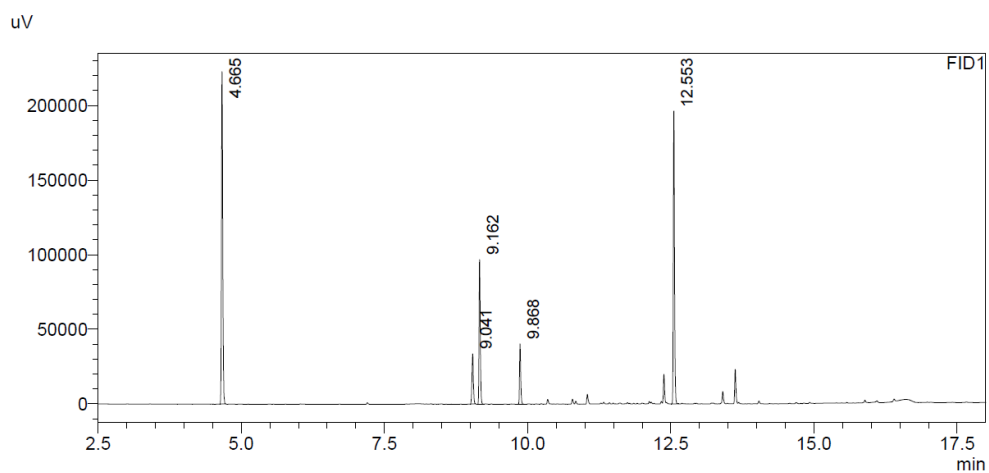


Figure 76 GC: conversion after 7 d, 20 % HCl, 25 °C

7.2.3.1.2.3 5 % HCl, 50 °C

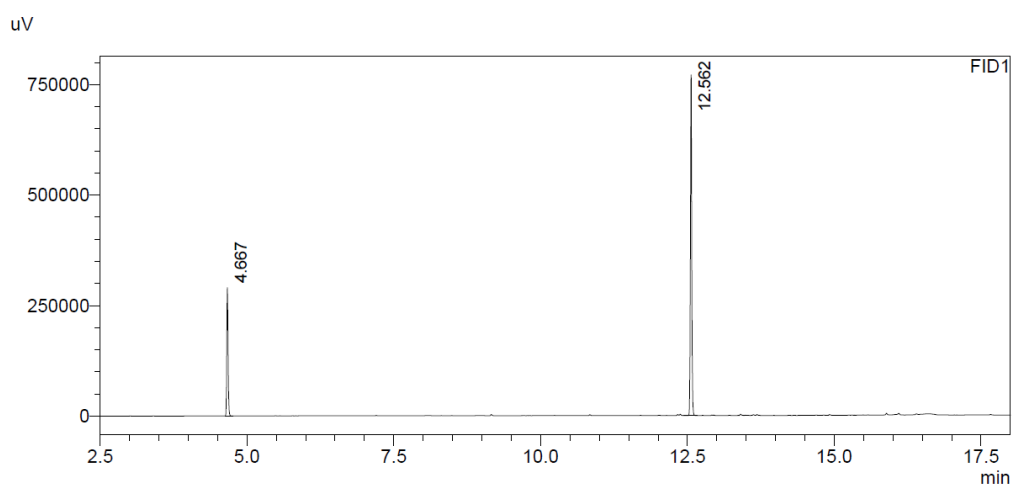


Figure 77 GC: start point 0 d, 5 % HCl, 50 °C

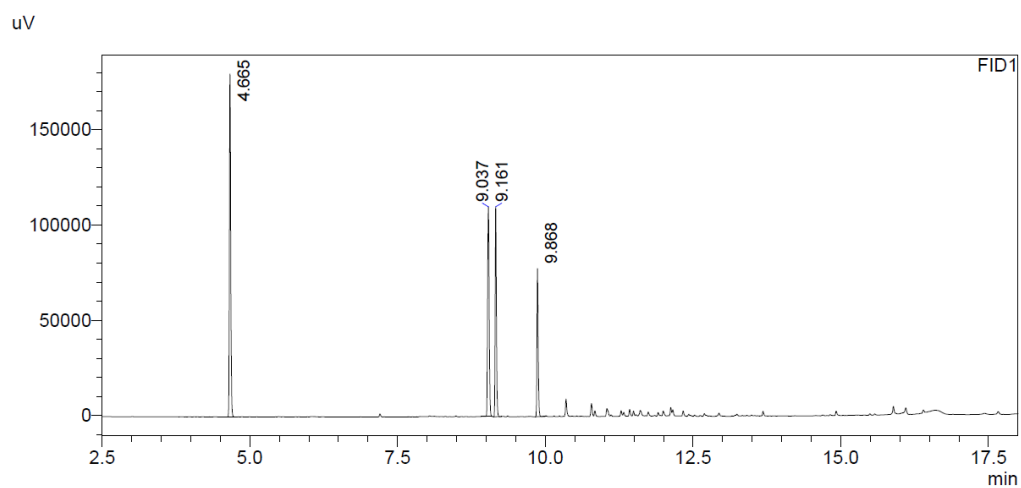
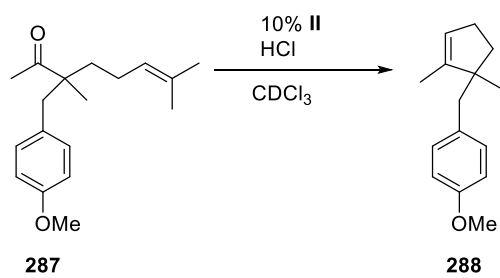


Figure 78 GC: conversion after 2 d, 5 % HCl, 50 °C

### 7.2.3.1.3 Screening of Substrate **287**



substrate	entry	HCl	time	T	Conversion
<b>287</b>	1	20%	6d	30 °C	70%
	2	40%	7d	25 °C	100%

7.2.3.1.3.1 20 % HCl 30 °C

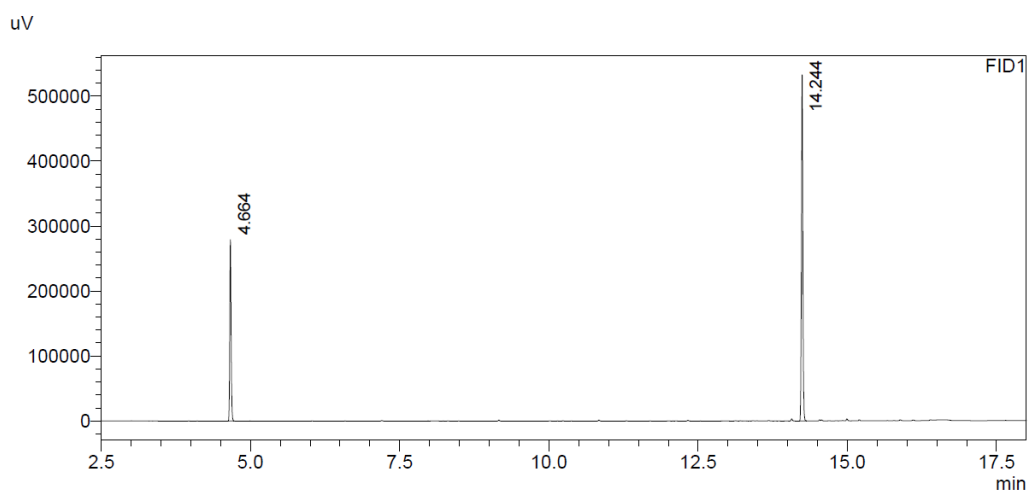


Figure 79 GC: start point 0 d, 20 % HCl, 30 °C

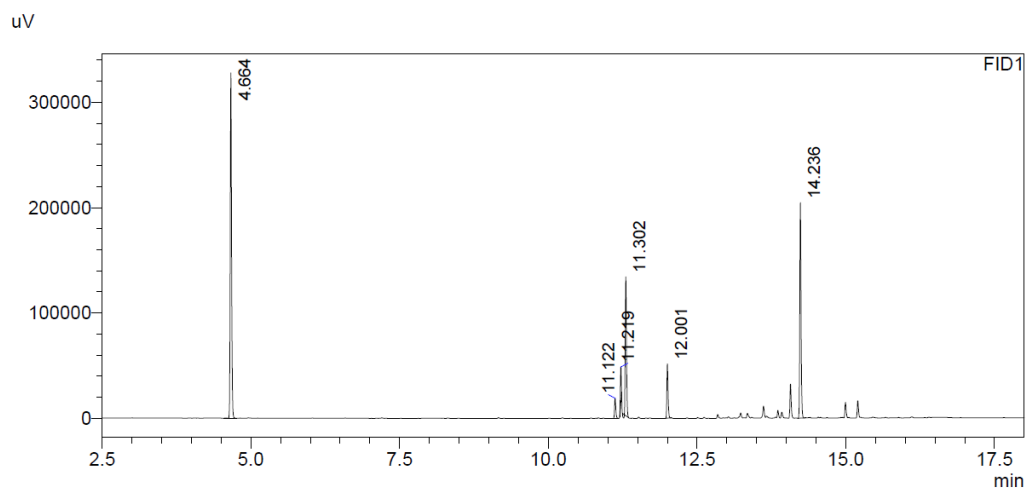


Figure 80: GC: conversion 6 d, 20 % HCl, 30 °C

7.2.3.1.3.2 40 % HCl 25 °C

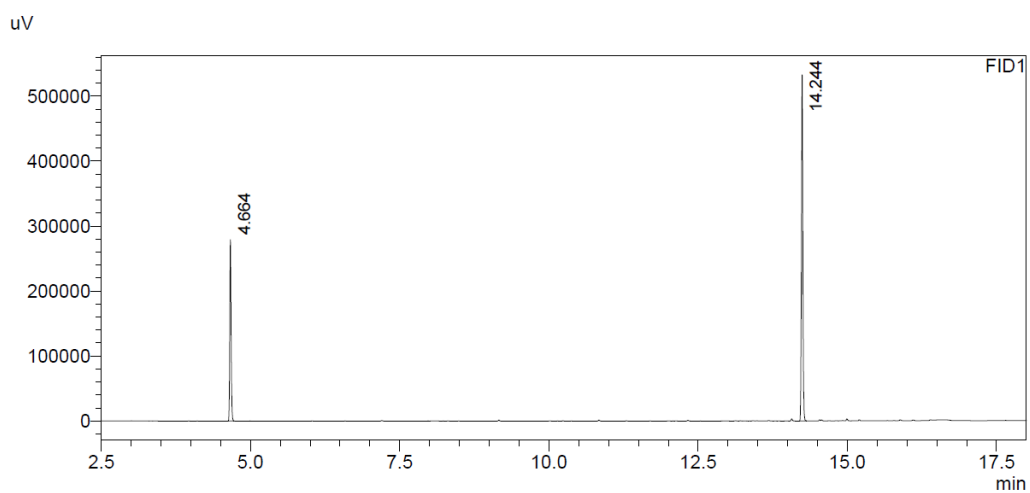


Figure 81 GC: start point 0 d, 40 % HCl, 25 °C

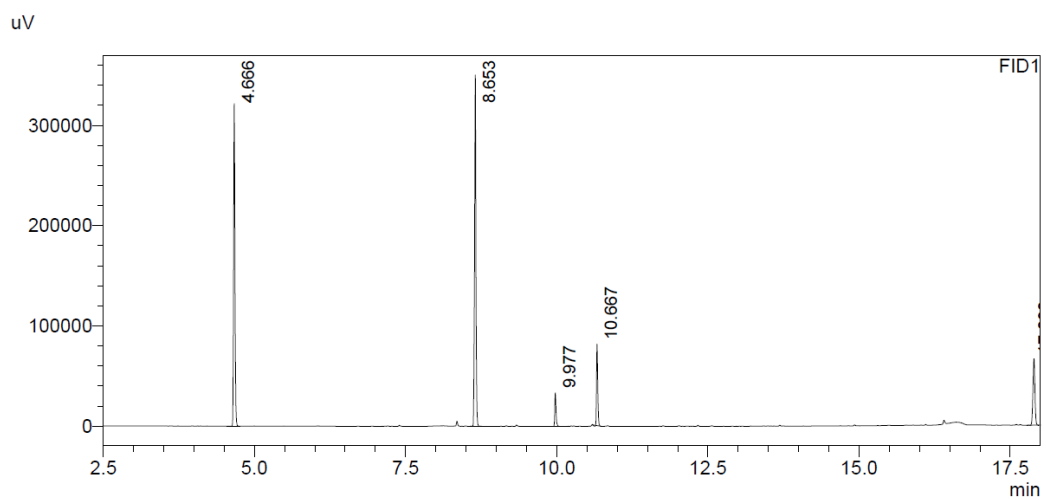


Figure 82 GC: Conversion after 7 d, 40 % HCl, 25 °C



#### 7.2.3.1.4 Isolation of products from the conversion of **287**

Resorcinarene (110 mg, 99.5  $\mu\text{mol}$ , 0.6 eq.) was suspended in 4.00 mL chloroform-d (filtered through basic aluminum oxide) into a pressure vial. The capped vial was heated gently until the suspension turned clear. After cooling to room temperature, HCl (307  $\mu\text{L}$ , 162 mM, 49.8  $\mu\text{mol}$ , 0.3 eq.) was added in the form of HCl-saturated chloroform. Chloroform (filtered through basic aluminum oxide) was added to receive a total volume of 4.77 mL. Afterward, **287** (45.6 mg, 16.6 mmol, 1 eq.) was added and the vial was equipped with a stirring bar and transferred to an aluminum heating block. Aliquots of 50  $\mu\text{L}$  were dissolved in a mixture (1 mL) of hexane and DMSO (0.02 %) and stored at -20 °C for 30 min. The received suspension was centrifuged, and the liquid phase was transferred and analyzed by GC. After 5 d, the crude mixture was transferred directly onto column ( $\text{SiO}_2$ ) and rinsed with pentane to remove the residual  $\text{CDCl}_3$ . The eluent was then changed to a mixture of pentane with 5 %  $\text{Et}_2\text{O}$ .

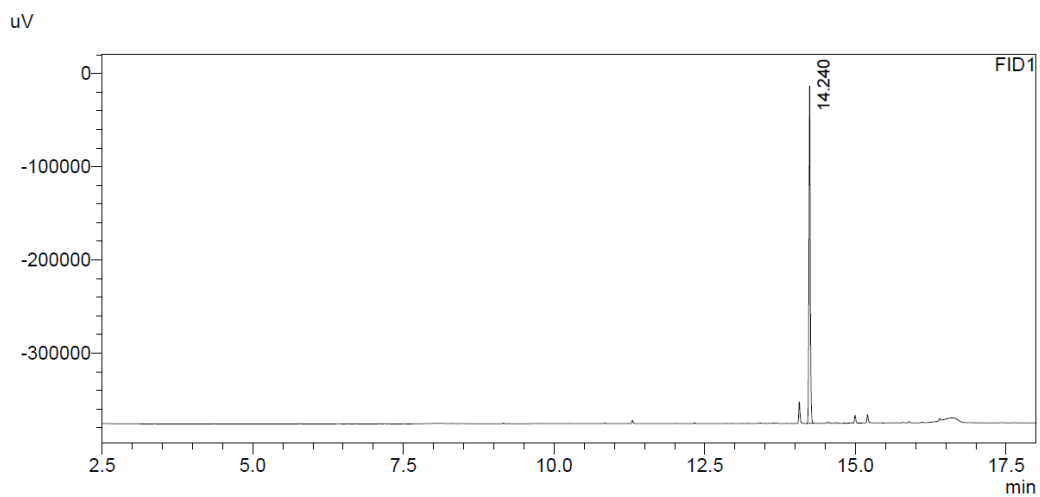


Figure 83 GC: Start point 0 d

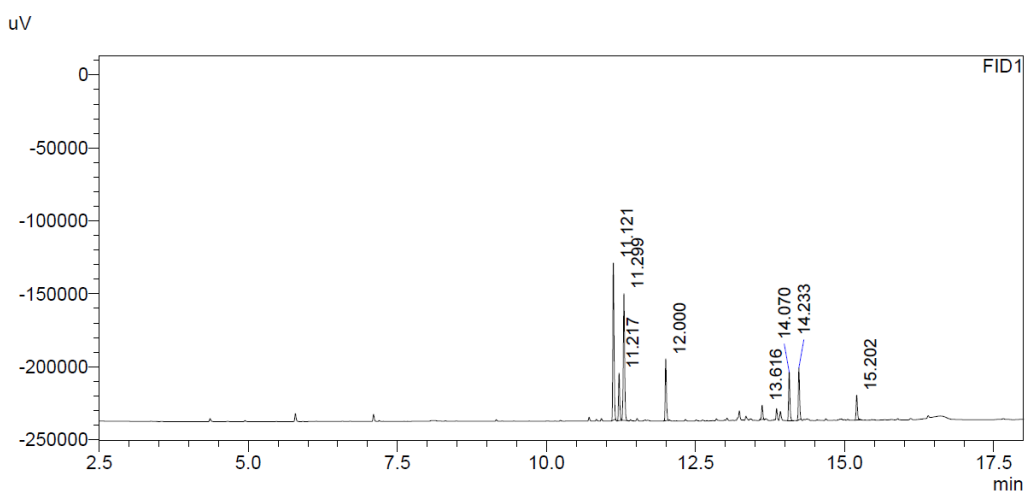


Figure 84 GC: crude mixture after 5 d

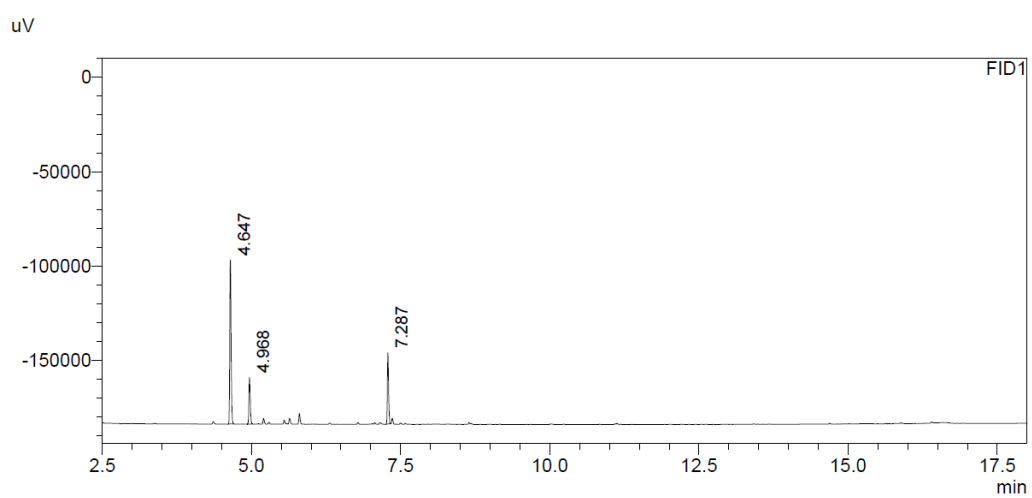
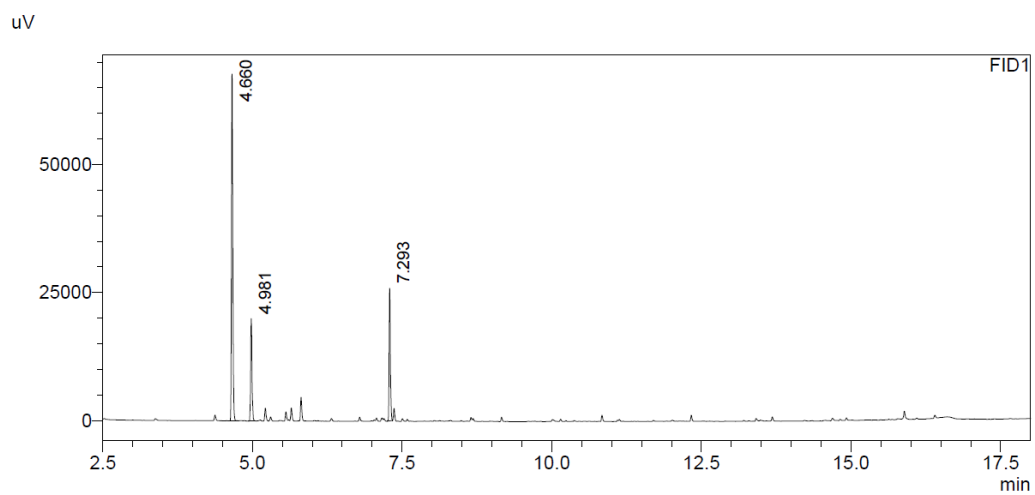


Figure 85 GC: fractions received after column

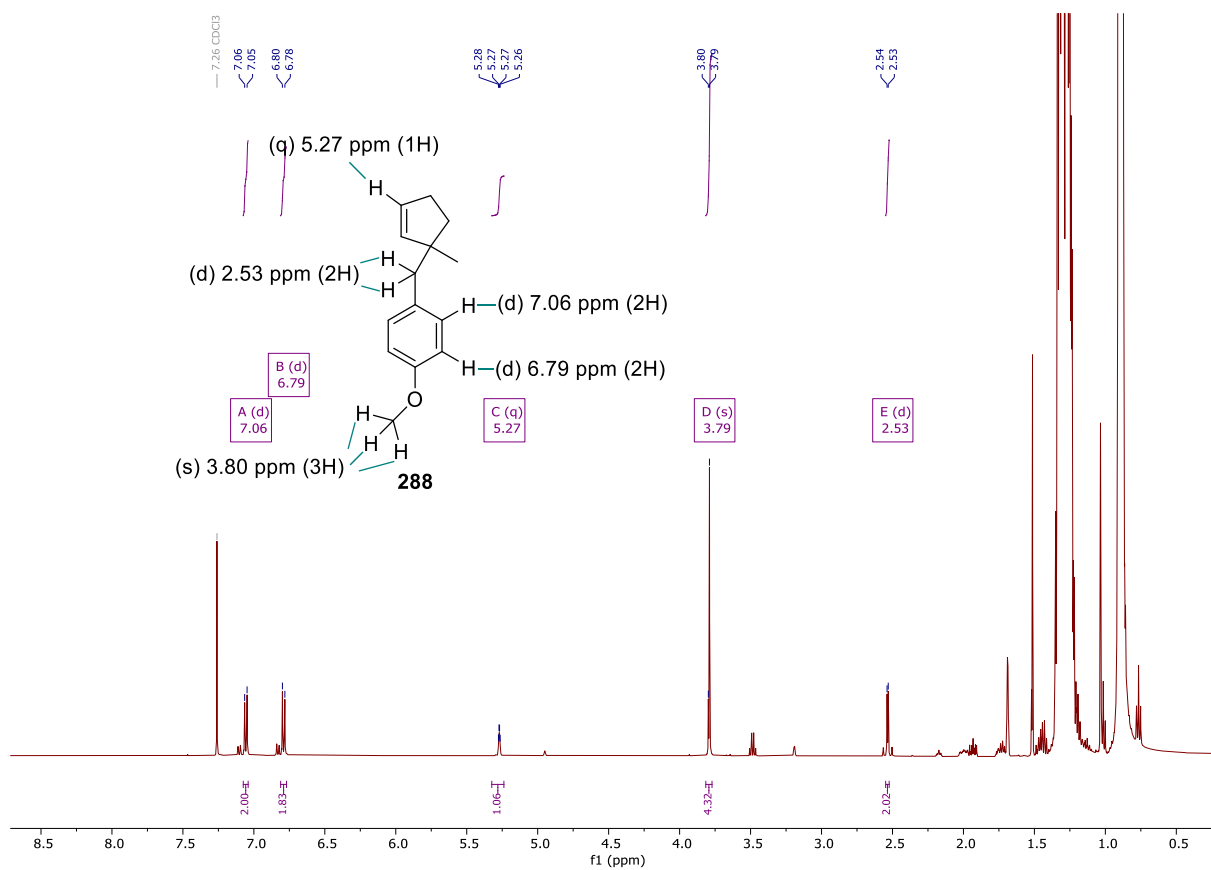


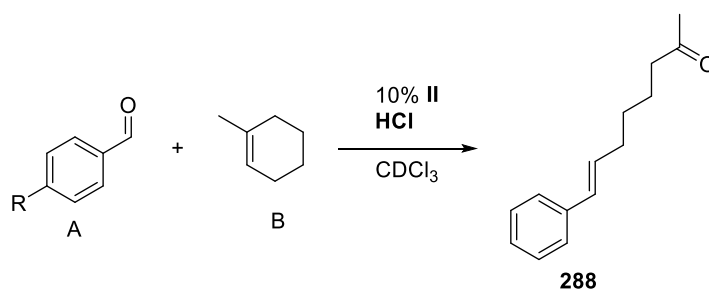
Figure 86  $^1\text{H}$  NMR of the received fractions. Highlighted signals belong to **288** according to literature<sup>69</sup>

## 7.2.4 Intermolecular Ring-opening cross carbonyl-olefin Metathesis

Resorcinarene (11.0 mg, 9.95  $\mu\text{mol}$ , 0.6 eq.) was suspended in 0.4 mL chloroform-d (filtered through basic aluminum oxide) into a 1.5 mL screw cap vial. The capped vial was heated gently until the suspension turned clear. After cooling to room temperature, HCl was added in the form of HCl-saturated chloroform. Chloroform (filtered through basic aluminum oxide) was added to receive a total volume of 0.5 mL. Decane (2.59  $\mu\text{L}$ , 13.3  $\mu\text{mol}$ , 0.8 eq.) and the aldehyde A and alkene B (16.6  $\mu\text{mol}$ , 1 eq.) were added. The vial was equipped with a stirring bar and transferred to an aluminum heating block. Aliquots of 50  $\mu\text{L}$  were dissolved in a mixture (1 mL) of hexane with 0.02 % DMSO and stored at  $-20\text{ }^{\circ}\text{C}$  for 30 min. The received suspension was centrifuged and the liquid phase was transferred and analyzed by GC.

### 7.2.4.1 Screening 1-methylcyclohexene

Table 18 Screening for reaction conditions for 1-methylcyclohexene with benzaldehyde and 4-nitrobenzaldehyde



entry	R	ratio A:B	HCl	time	T	Consumption A
1	H	1:1	10%	3 d	60 $^{\circ}\text{C}$	20%*
2	NO <sub>2</sub>	1:4	30%	5 d	30 $^{\circ}\text{C}$	11%
3	NO <sub>2</sub>	1:4	30%	5 d	60 $^{\circ}\text{C}$	23%
4	NO <sub>2</sub>	1:4	40%	5 d	30 $^{\circ}\text{C}$	3%
5	NO <sub>2</sub>	1:4	40%	5 d	60 $^{\circ}\text{C}$	27%

\*6 d decomposition

GC-data with a similar signal pattern will be summarized by one representative chromatogram

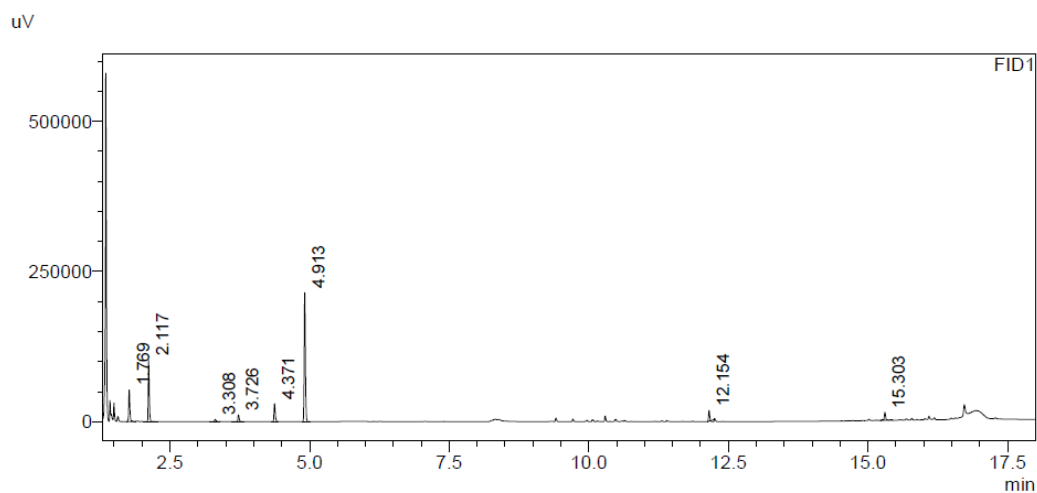


Figure 87 GC: Start point 0 d, 10 % HCl, 60 °C for aldehyde (A) and 1-methylcyclohexene (B) 1:4 (entry 1, Table 18)

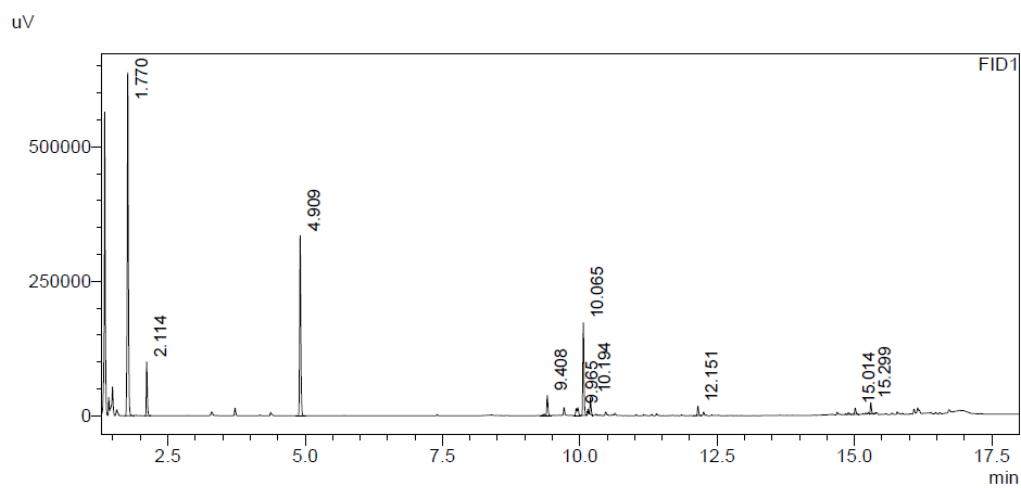


Figure 88 GC: conversion after 7 d, 10 % HCl, 60 °C for aldehyde (A) and 1-methylcyclohexene (B) 1:4 (entry 1, Table 18)

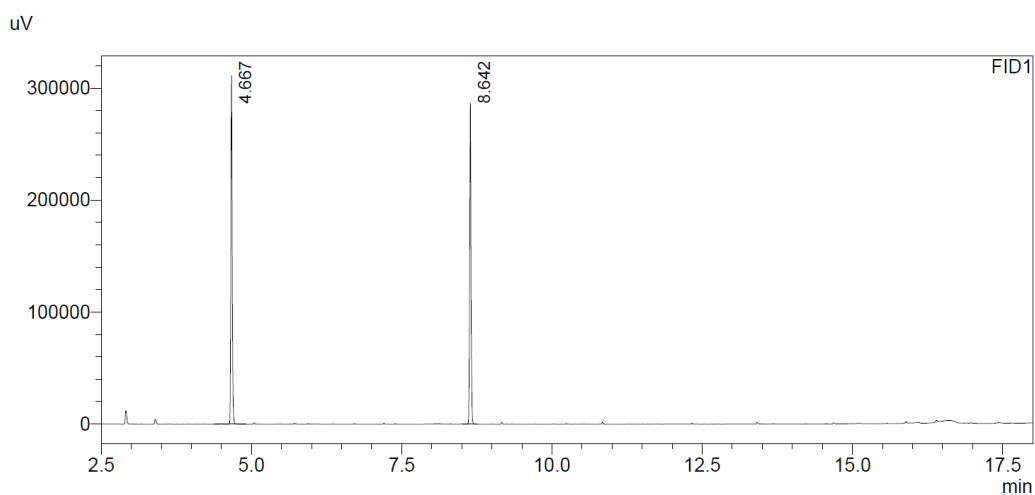


Figure 89 GC: start point 0 d, 40 % HCl, 60 °C for aldehyde (A) and 1-methylcyclohexene (B) 1:4 (entry 5, similar signal pattern for entry 3, Table 18)

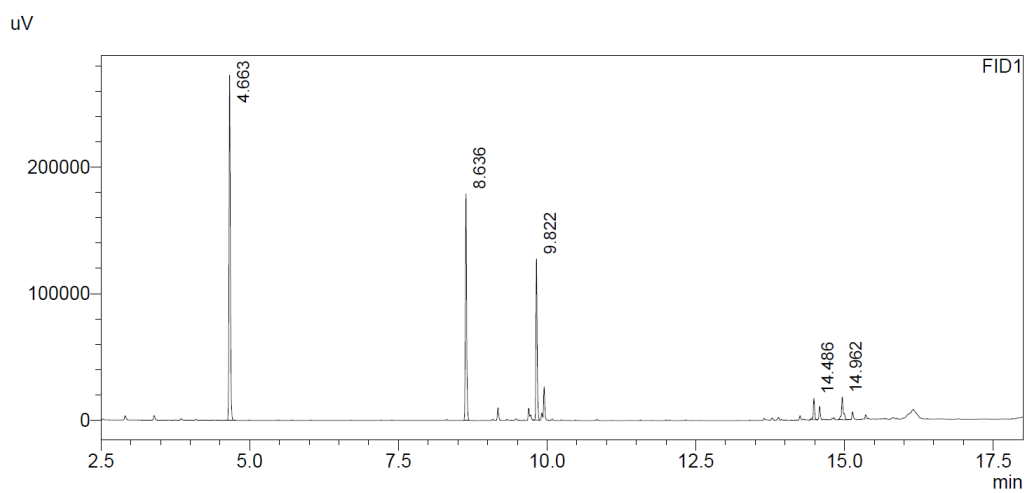


Figure 90 GC: conversion after 5 d, 40 % HCl, 60 °C for aldehyde (A) and 1-methylcyclohexene (B) 1:4 (entry 5, similar signal pattern for entry 3, Table 18)

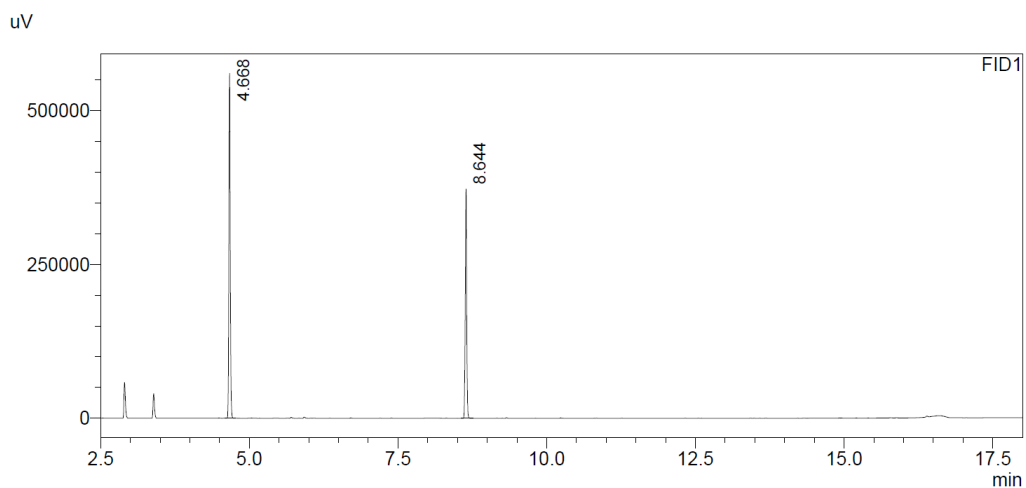


Figure 91 GC: start point 0 d, 30 % HCl, 30 °C for aldehyde (A) and 1-methylcyclohexene (B) 1:4 (entry 2, similar signal pattern for entry 4, Table 18)

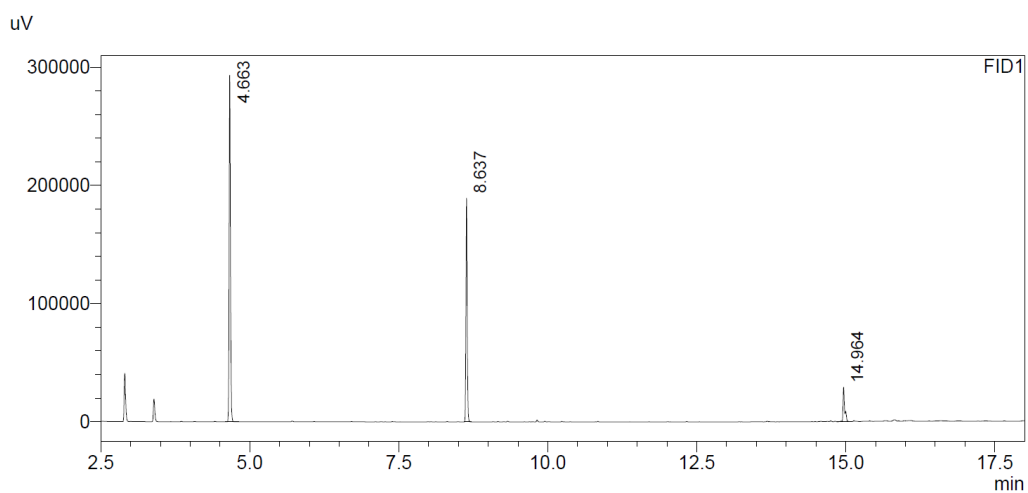
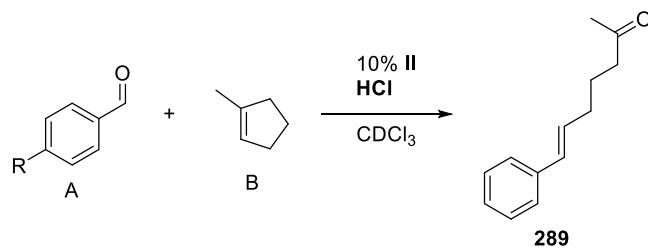


Figure 92 GC: conversion after 5 d, 30 % HCl, 30 °C for aldehyde (A) and 1-methylcyclohexene (B) 1:4 (entry 2, similar signal pattern for entry 4, Table 18)



Table 19: Screening for reaction conditions for 1-methylcyclopentene with benzaldehyde and 4-nitrobenzaldehyde



entry	R	ratio A:B	HCl	time	T	Consumption A
1	H	2:1	30%	5 d	30 °C	35%
2	H	2:1	30%	5 d	50 °C	51%
3	H	1:4	30%	3 d	50 °C	17%
4	NO <sub>2</sub>	1:4	30%	5 d	30 °C	80%
5	NO <sub>2</sub>	1:4	30%	5 d	60 °C	86%
6	NO <sub>2</sub>	1:4	40%	5 d	30 °C	65%
7	NO <sub>2</sub>	1:4	40%	5 d	60 °C	84%
8	NO <sub>2</sub>	1:100	30%	5 d	60 °C	100%
9	NO <sub>2</sub>	2:1	30%	5 d	30 °C	40%
10	NO <sub>2</sub>	2:1	30%	5 d	30 °C	40%
236	NO <sub>2</sub>	2:1	30%	5 d	50 °C	52%

GC-data with a similar signal pattern will be summarized by one representative chromatogram

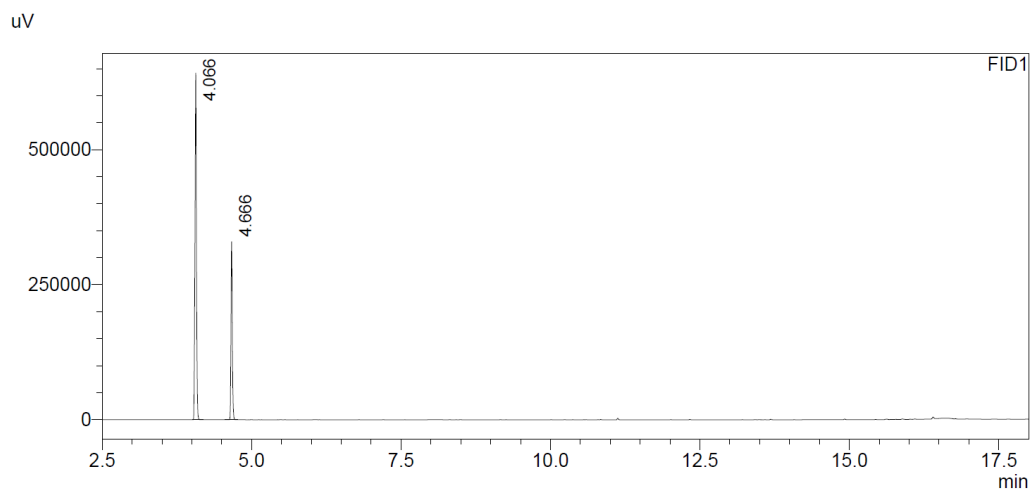


Figure 93 GC: start point 0 d, 30 % HCl, 30 °C for aldehyde (A) and 1-methylcyclohexene (B) 2:1 (entry 1, Table 19)

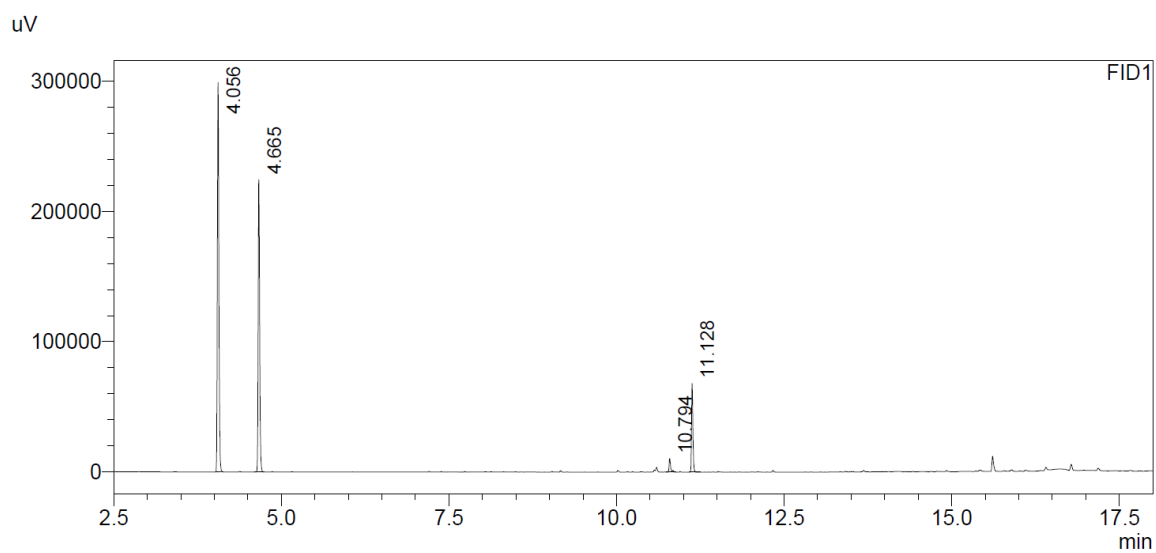


Figure 94 GC: conversion after 5 d, 30 % HCl, 30 °C for aldehyde (A) and 1-methylcyclohexene (B) 2:1 (entry 1, Table 19)

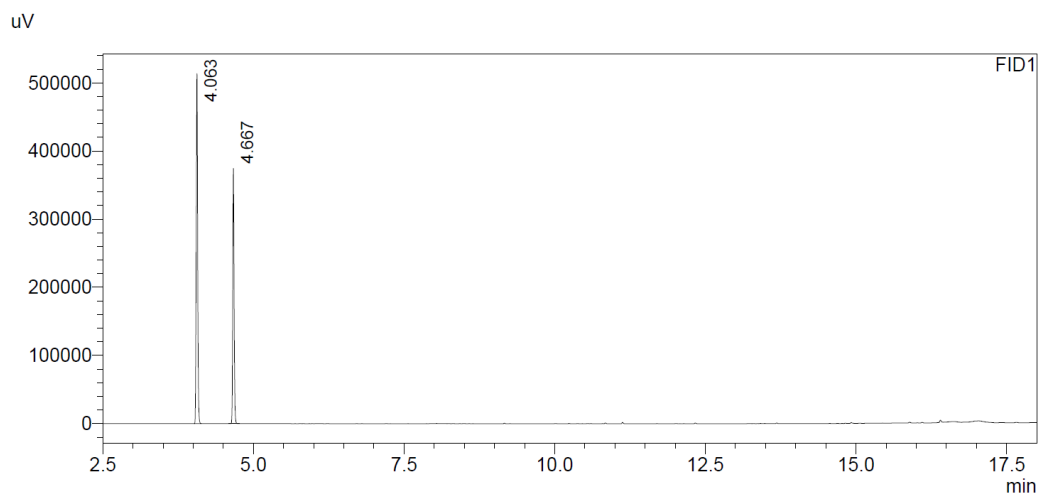


Figure 95 GC: start point 0 d, 30 % HCl, 50 °C for aldehyde (A) and 1-methylcyclohexene (B) 2:1 (entry 2, similar signal pattern for entry 3 Table 19)

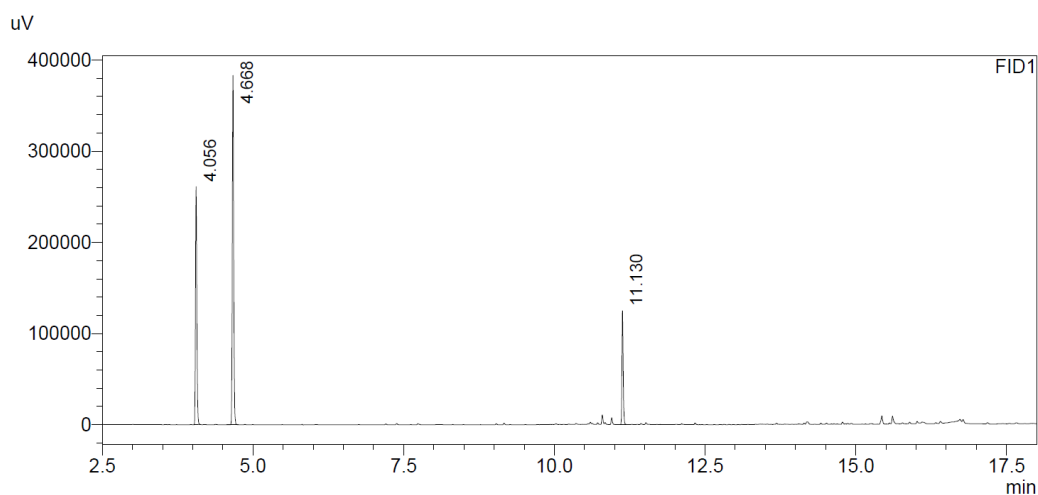


Figure 96 GC: conversion after 5 d, 30 % HCl, 50 °C for aldehyde (A) and 1-methylcyclohexene (B) 2:1 (entry 2, similar signal pattern for entry 3 Table 19)

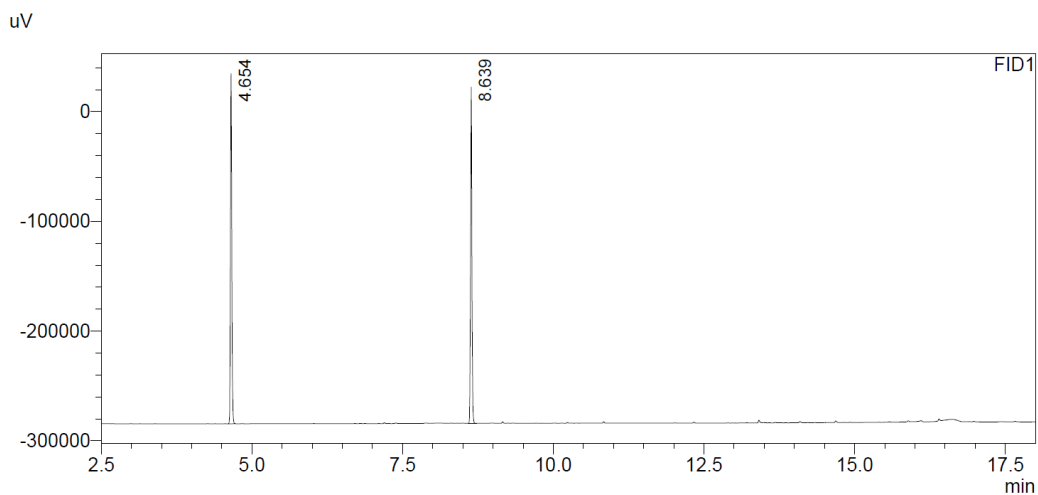


Figure 97 GC: start point 0 d, 30 % HCl, 60 °C for aldehyde (A) and 1-methylcyclohexene (B) 1:4 (entry 5, similar signal pattern for entry 7, 8 Table 19)

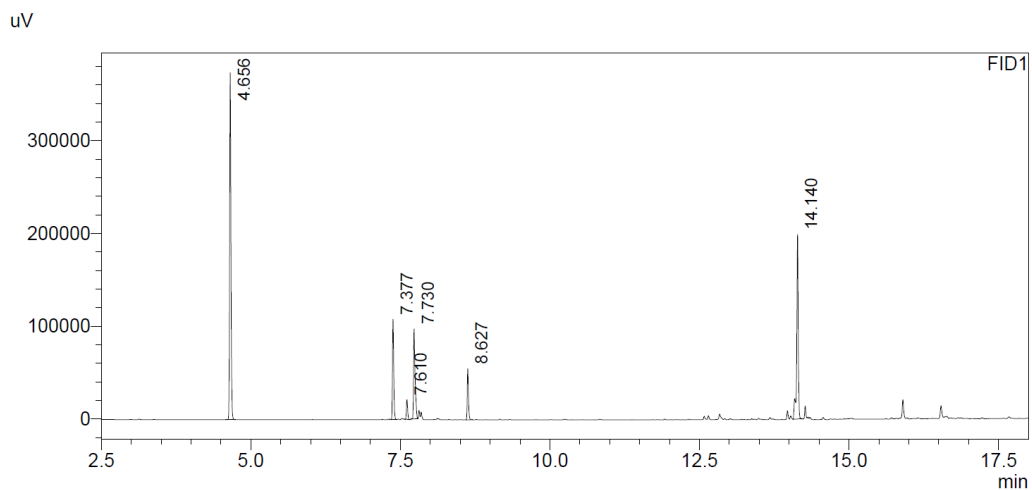


Figure 98 GC: conversion 5 d, 30 % HCl, 60 °C for aldehyde (A) and 1-methylcyclohexene (B) 1:4 (entry 5, similar signal pattern for entry 7, 8 Table 19)

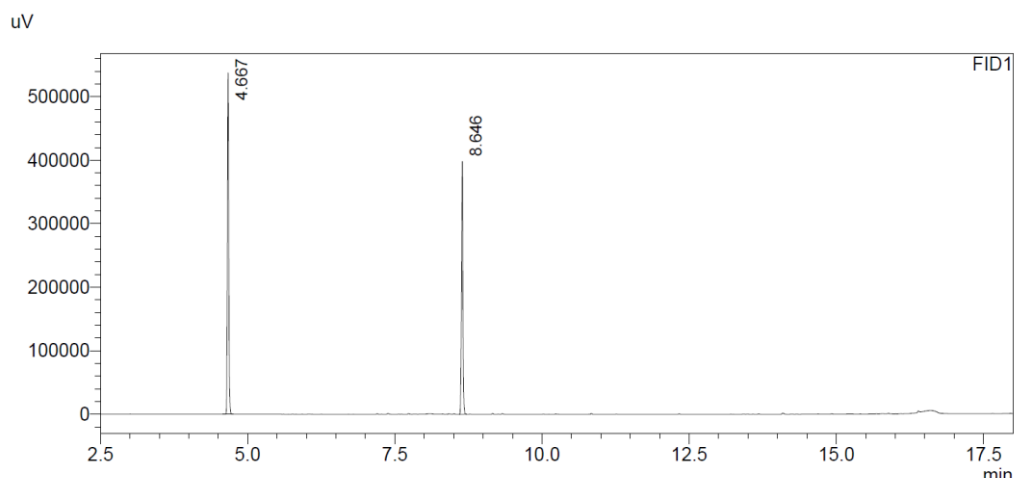


Figure 99 GC: start point 0 d, 30 % HCl, 30 °C for aldehyde (A) and 1-methylcyclohexene (B) 1:4 (entry 4, similar signal pattern for entry 6, 9, 10 Table 19)

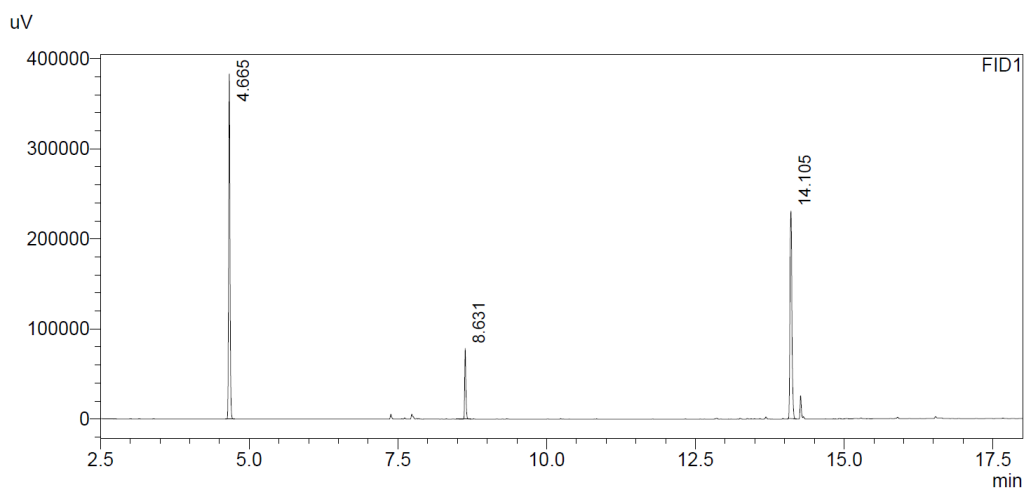


Figure 100 GC: conversion after 5 d, 30 % HCl, 30 °C for aldehyde (A) and 1-methylcyclohexene (B) 1:4 (entry 4, similar signal pattern for entry 6, 9, 10 Table 19)



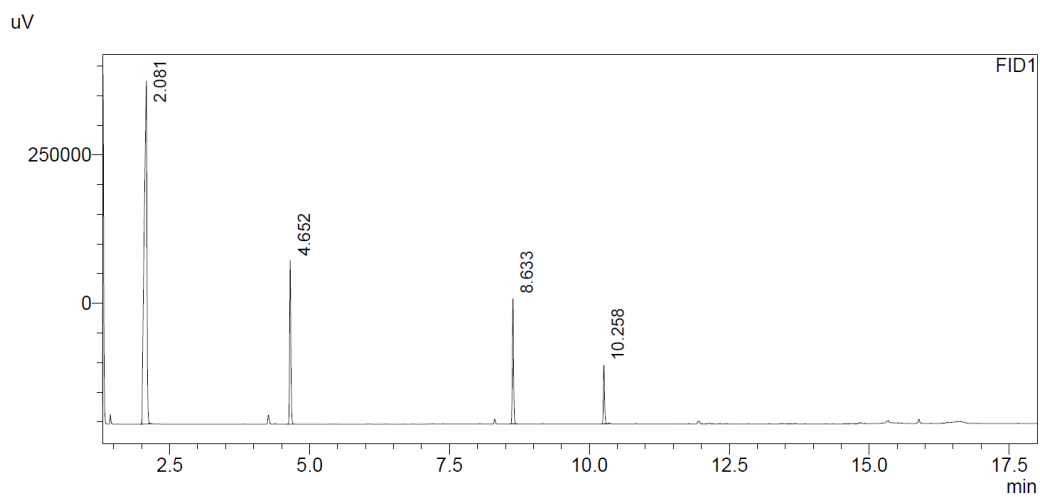


Figure 102 GC: conversion after 7 d, 30 % HCl, 60 °C for aldehyde (A) and 1-methylcyclohexene (B) 1:4 (entry 4, similar signal pattern for entry 5 Table 20)

## 7.3 Glycosylation

### 7.3.1 Reaction Order

#### 7.3.1.1 Rate dependence of the glycosylation on MeOH

To gain insight into the mechanism of the  $\beta$ -selective glycosylation, we tested the rate dependence of the reaction regarding the methanol concentration. The rate was determined by conducting the reactions of the  $\alpha$ -glycosyl donor to different concentrations of methanol. Every reaction was performed three times, in 2 mL GC vials in an aluminum heating block. Before every reaction, stock solutions of the resorcinarene capsule (**II**) and the substrate (**331**) were prepared. Two sets of experiments were performed. Each set contained two different concentrations. Stock solutions were prepared before every set.

**Resorcinarene stock solution:** Resorcinarene (266 mg, 0.240 mmol) was suspended in  $\text{CDCl}_3$  (filtered through basic aluminum oxide) (3.60 mL) leading to 0.011 M solution referred to the assembled capsule. Upon gentle heating, the solution became clear. Tetraethylsilane (9.48  $\mu\text{L}$ , 50.0  $\mu\text{mol}$ ) was added to the solution as an internal standard.

**Substrate stock solution: 331** (83.4mg, 0.35 mmol) was dissolved in  $\text{CDCl}_3$  (filtered through basic aluminum oxide) (350  $\mu\text{L}$ )

Resorcinarene (450  $\mu\text{L}$ , 0.005 mmol) and **331** (50.0  $\mu\text{L}$ , 0.05 mmol) were added to a 2 mL GC vial together with dry alumina (neutral, 50.0 mg). MeOH was added and the closed vial was placed inside an aluminum heating block, set to 50 °C. For methanol volumes < 10  $\mu\text{L}$ , methanol was added as a stock solution (50.0  $\mu\text{L}$ ). To compensate for the additional volume of the stock solution, the resorcinarene solution was prepared in a higher concentration (0.0125 M referred to the assembled capsule) and added to 400  $\mu\text{L}$ . Aliquots of 25.0  $\mu\text{L}$  were taken every 30 min and diluted with 500  $\mu\text{L}$  of acetone- $d_6$ , over a period of 3 h. The samples were analyzed by  $^1\text{H}$  NMR (d1= 3 s and 64 scans).



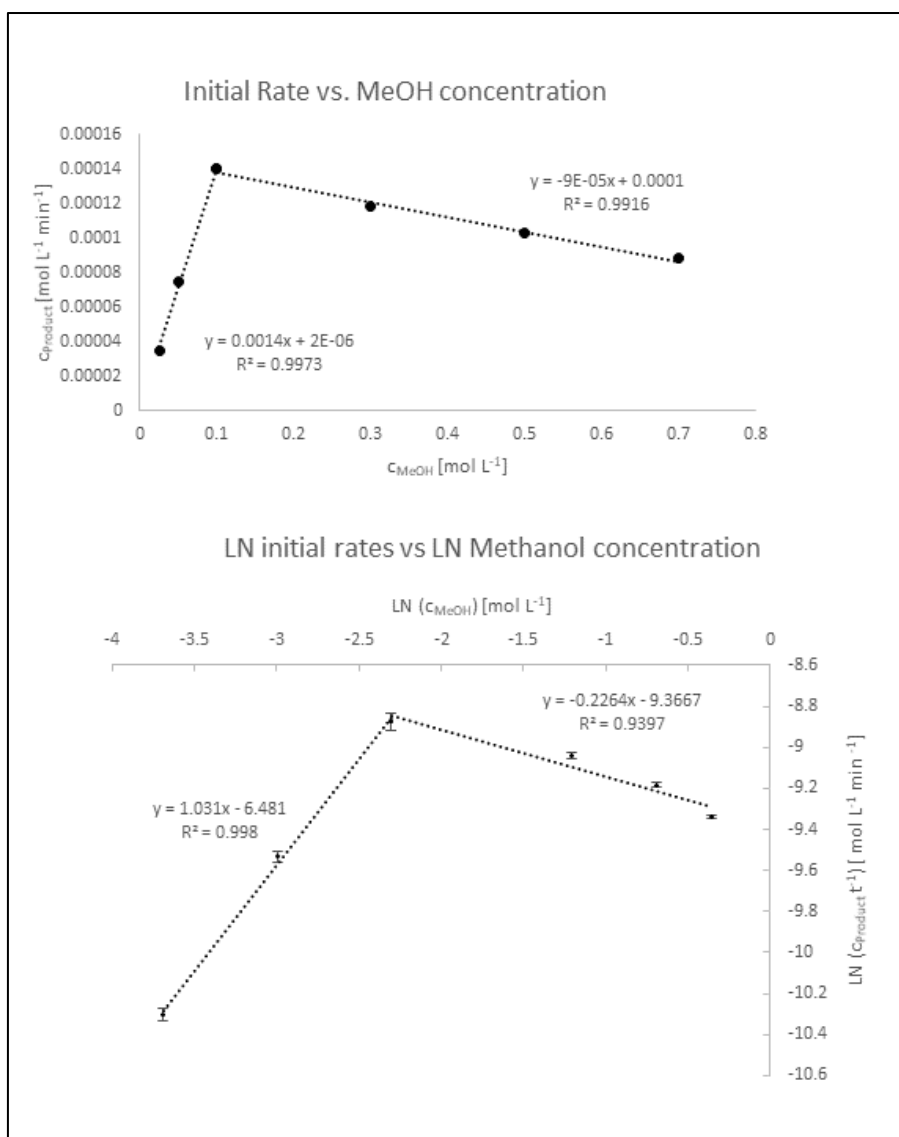
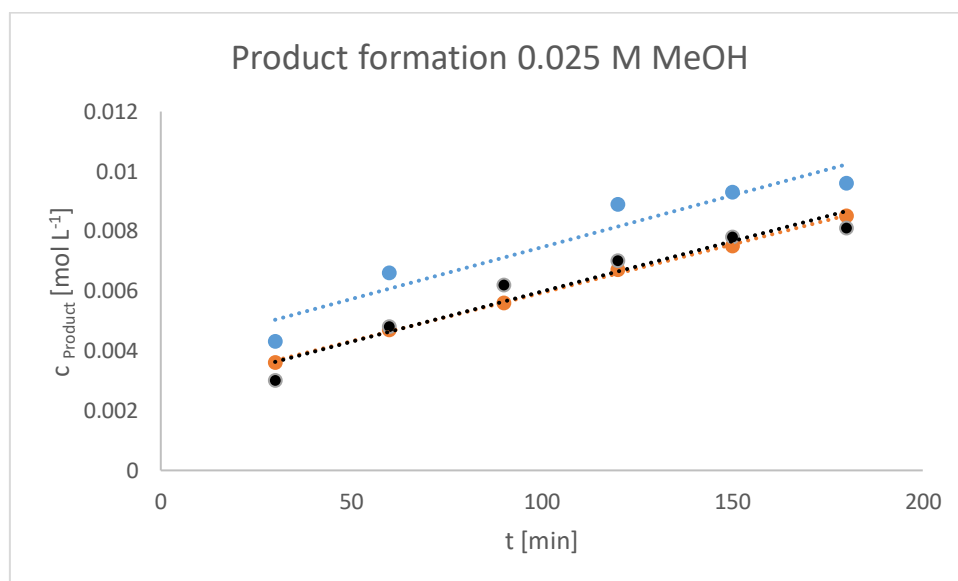
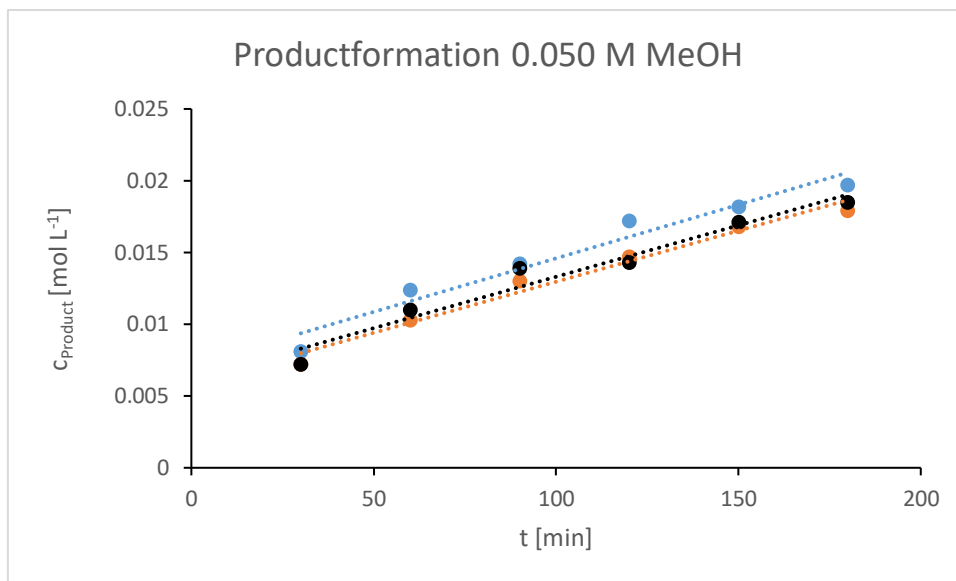


Figure 103 (**top**) Linear dependence of the initial rates on the methanol concentration until a concentration of 0.1 M. For concentrations  $> 0.1$  M, the initial rates decrease linearly with the methanol concentration, which indicates a saturation with methanol and deactivation of the catalyst. (**below**) Logarithmic plot of the initial rates vs methanol concentration gives the reaction order as the slope of the trendline. For concentrations  $< 0.1$  M, a reaction with 1<sup>st</sup> order kinetic on methanol can be observed. For concentrations  $> 0.1$  M a reaction with approx. 0<sup>th</sup> order on methanol can be observed.

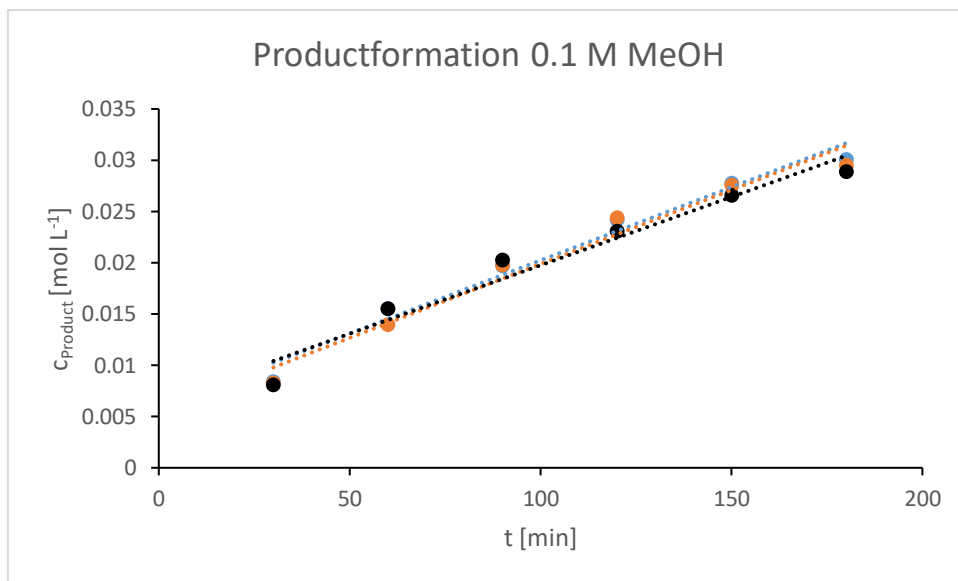
7.3.1.1.1 Initial rates with  $c_{\text{MeOH}}$  (0.025 M – 0.700 M)



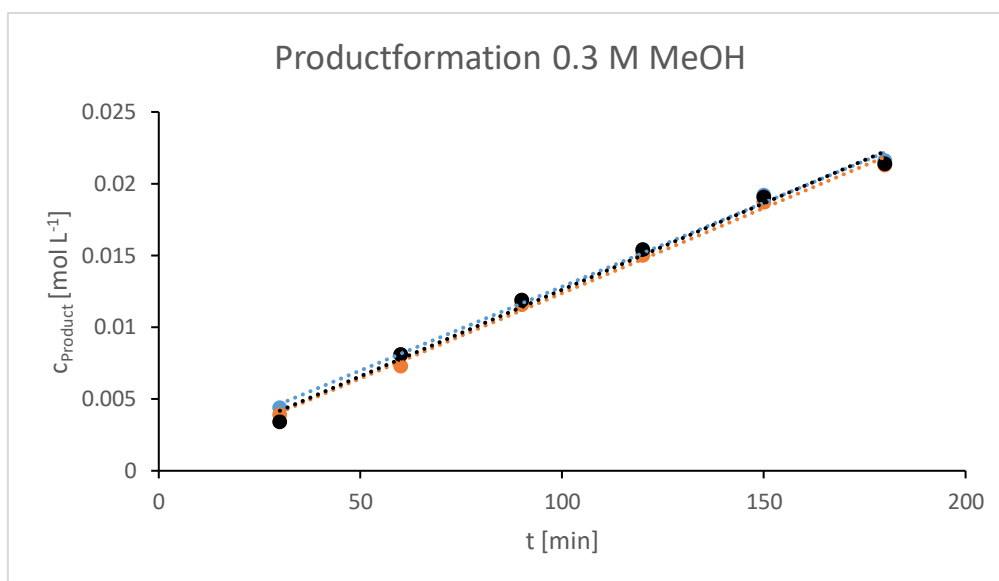
Time [min]	C [mol L <sup>-1</sup> ]			Stdev.	0.0339
	A	B	C		
30	4.30E-03	3.60E-03	3.00E-03		
60	6.60E-03	4.70E-03	4.80E-03		
90	-	5.60E-03	6.20E-03		
120	8.90E-03	6.70E-03	7.00E-03		
150	9.30E-03	7.50E-03	7.80E-03		
180	9.60E-03	8.50E-03	8.10E-03		
slope	3.47E-05	3.24E-05	3.36E-05		
ln slope	-10.270	-10.338	-10.300		
R <sup>2</sup>	0.912	0.998	0.937		



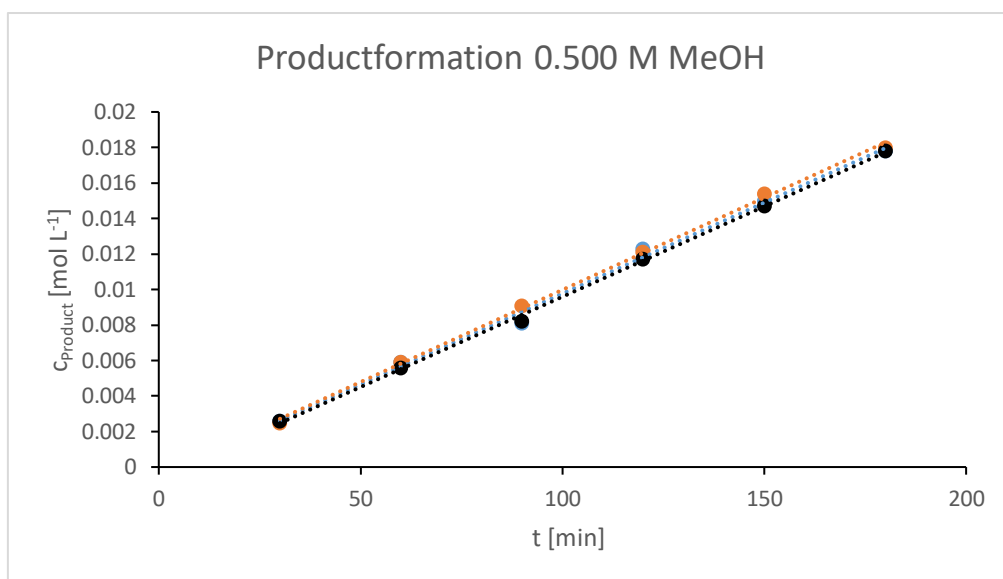
Time [min]	C [mol L <sup>-1</sup> ]			Stdev.	0.026
	A	B	C		
30	8.10E-03	7.20E-03	7.20E-03		
60	1.24E-02	1.03E-02	1.10E-02		
90	1.42E-02	1.30E-02	1.39E-02		
120	1.72E-02	1.47E-02	1.43E-02		
150	1.82E-02	1.68E-02	1.71E-02		
180	1.97E-02	1.79E-02	1.85E-02		
slope	7.47E-05	7.11E-05	7.16E-05		
ln slope	-9.502	-9.551	-9.544		
R <sup>2</sup>	0.952	0.976	0.956		



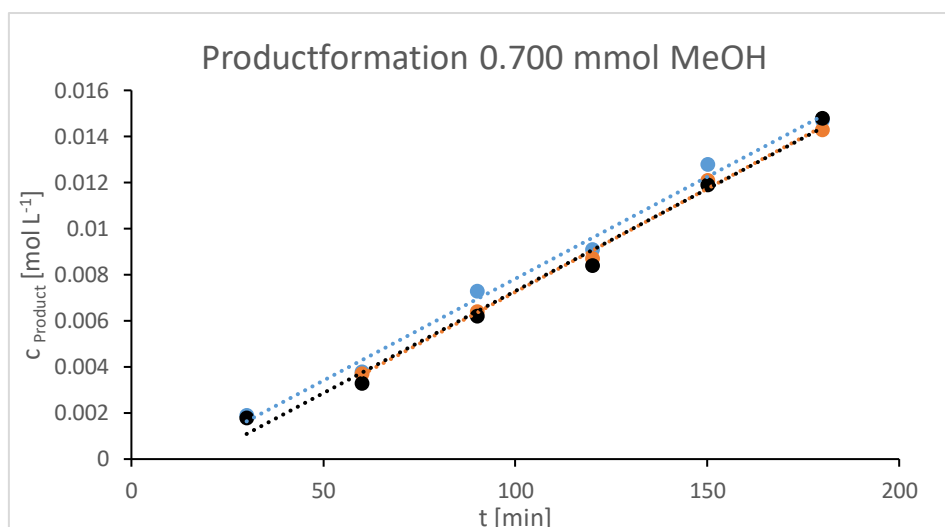
Time [min]	C [mol L <sup>-1</sup> ]			Stdev.	0.0422
	A	B	C		
30	8.40E-03	8.30E-03	8.10E-03		
60	1.55E-02	1.40E-02	1.55E-02		
90	1.97E-02	1.98E-02	2.03E-02		
120	2.42E-02	2.44E-02	2.31E-02		
150	2.78E-02	2.76E-02	2.66E-02		
180	3.01E-02	2.95E-02	2.89E-02		
slope	1.43E-04	1.44E-04	1.33E-04		
ln slope	-8.854	-8.844	-8.922		
R <sup>2</sup>	0.973	0.968	0.9560		



Time [min]	C [mmol L <sup>-1</sup> ]			Stdev.	0.015
	A	B	C		
30	3.00E-04	3.00E-04	3.00E-04		
60	4.40E-03	3.90E-03	3.40E-03		
90	8.10E-03	7.30E-03	8.10E-03		
120	1.19E-02	1.16E-02	1.19E-02		
150	1.53E-02	1.50E-02	1.54E-02		
180	1.92E-02	1.87E-02	1.91E-02		
slope	1.17E-04	1.19E-04	1.20E-04		
ln slope	-9.054	-9.039	-9.024		
R <sup>2</sup>	0.996	0.996	0.991		



Time [min]	C [mol L <sup>-1</sup> ]			Stdev.	0.010
	A	B	C		
30	2.60E-03	2.50E-03	2.60E-03		
60	5.90E-03	5.90E-03	5.60E-03		
90	8.10E-03	9.10E-03	8.20E-03		
120	1.23E-02	1.21E-02	1.17E-02		
150	1.50E-02	1.54E-02	1.47E-02		
180	1.78E-02	1.80E-02	1.78E-02		
slope	1.02E-04	1.04E-04	1.02E-04		
ln slope	-9.187	-9.173	-9.193		
R <sup>2</sup>	0.996	0.996	0.991		



Time [min]	C [mol L <sup>-1</sup> ]			Stdev.	0.009
	A	B	C		
30	1.90E-03	1.50E-03	1.80E-03		
60	3.80E-03	3.70E-03	3.30E-03		
90	7.30E-03	6.40E-03	6.20E-03		
120	9.10E-03	8.70E-03	8.40E-03		
150	1.28E-02	1.21E-02	1.19E-02		
180	1.47E-02	1.43E-02	1.48E-02		
slope	8.8381E-05	8.71E-05	8.86E-05		
ln slope	-9.334	-9.348	-9.332		
R <sup>2</sup>	0.992	0.997	0.989		

### 7.3.1.2 Rate dependence of the glycosylation on **331**

The rate dependence of glycosylation was determined by the initial rates at different concentrations of the  $\alpha$ -glycosyl donor. The reactions were performed in 2 mL GC vials, in an aluminum heating block. Before every reaction, stock solutions of the resorcinarene capsule and the substrate (**331**) were prepared.

**Resorcinarene stock solution:** Resorcinarene (266 mg, 0.24 mmol) was suspended in CDCl<sub>3</sub> (filtered through basic aluminum oxide) (3.20 mL) leading to 0.0125 M solution referred to the

assembled capsule. Upon gentle heating, the solution became clear. Tetraethylsilane (9.48  $\mu\text{L}$ , 50.0  $\mu\text{mol}$ ) was added to the solution as an internal standard.

**Substrate stock solution: 331** (59.6 mg, 0.25 mmol) was dissolved in filtered  $\text{CDCl}_3$  (250  $\mu\text{L}$ ) Resorcinarene (400  $\mu\text{L}$ , 0.005 mmol) and **331** were added to a 2 mL GC vial together with dry alumina (neutral, 50.0 mg). Depending on the amount of added **331** stock solution,  $\text{CDCl}_3$  was added to reach a total volume of 500  $\mu\text{L}$ . MeOH (20.2  $\mu\text{L}$ , 0.5 mmol) was added and the vial was placed inside an aluminum heating block, set to 50  $^\circ\text{C}$ . Aliquots of 25.0  $\mu\text{L}$  were taken every 30 min and diluted with 500  $\mu\text{L}$  of acetone- $\text{d}_6$  over a period of 6 h. The samples were analyzed by  $^1\text{H}$  NMR (d1= 3 s and 64 scans).



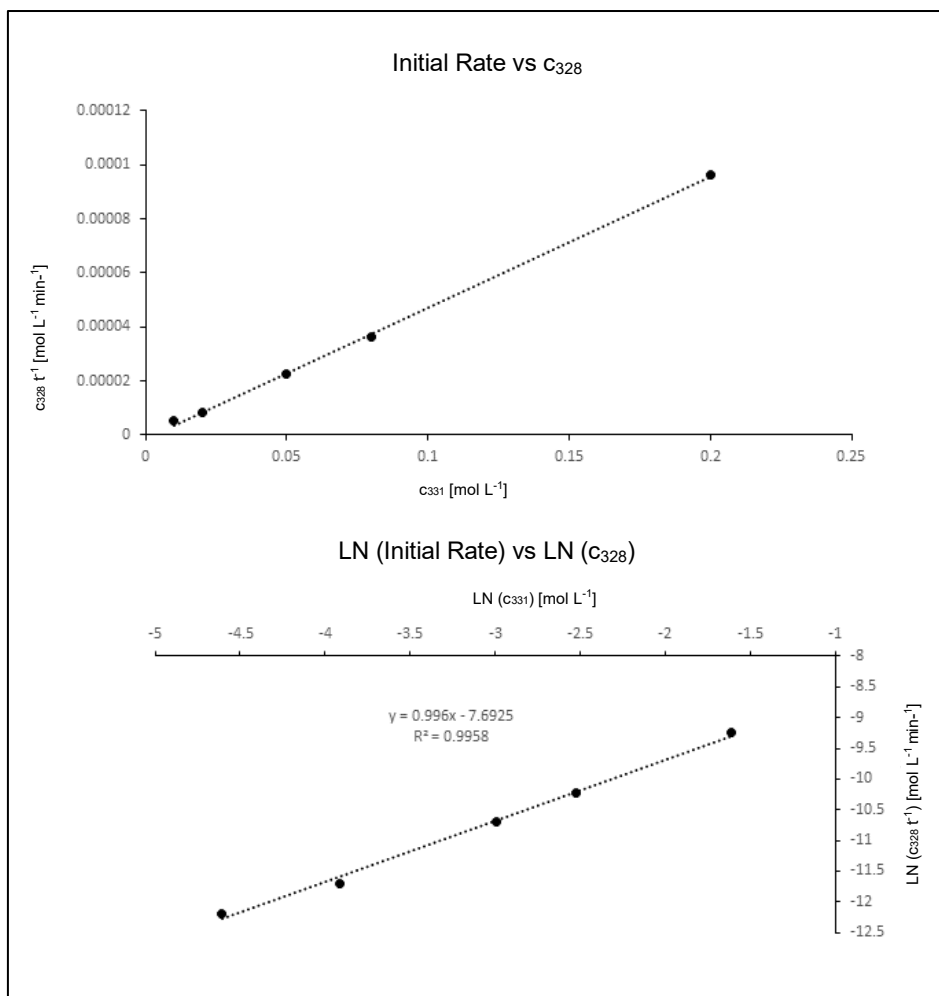
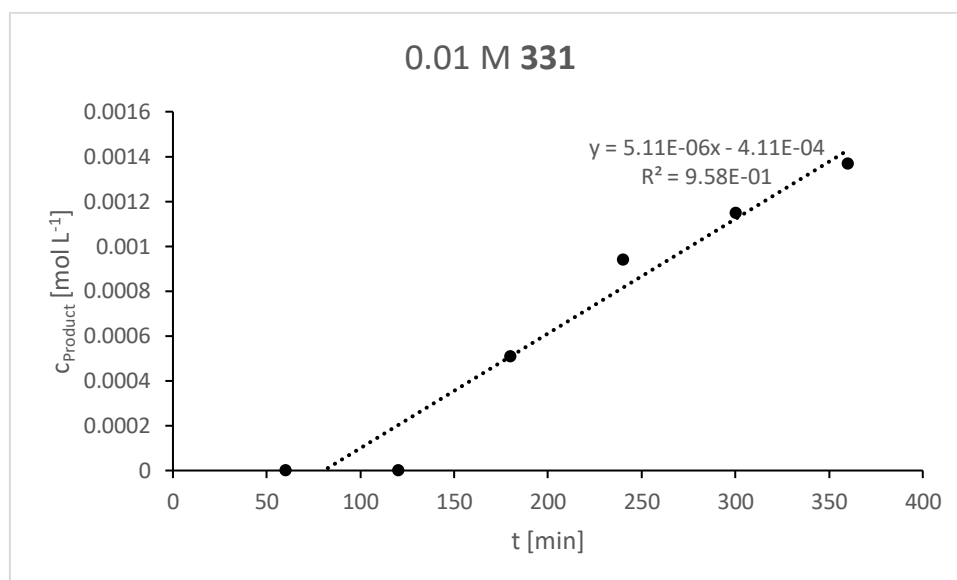
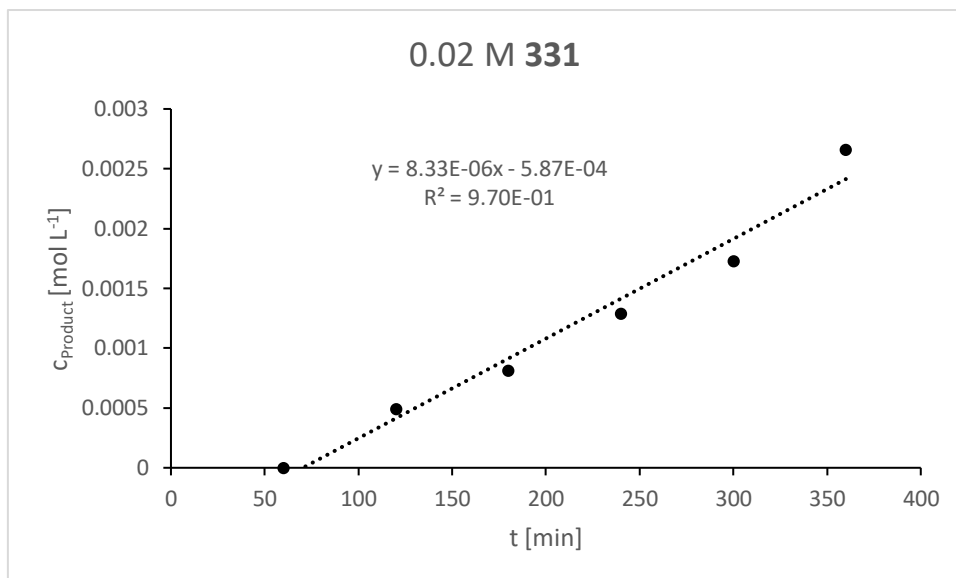


Figure 104 **(top)** Linear dependence of the initial rates on **331** concentration **(below)** Logarithmic plot of the initial rates vs **331** concentration gives the reaction order as the slope of the trendline.

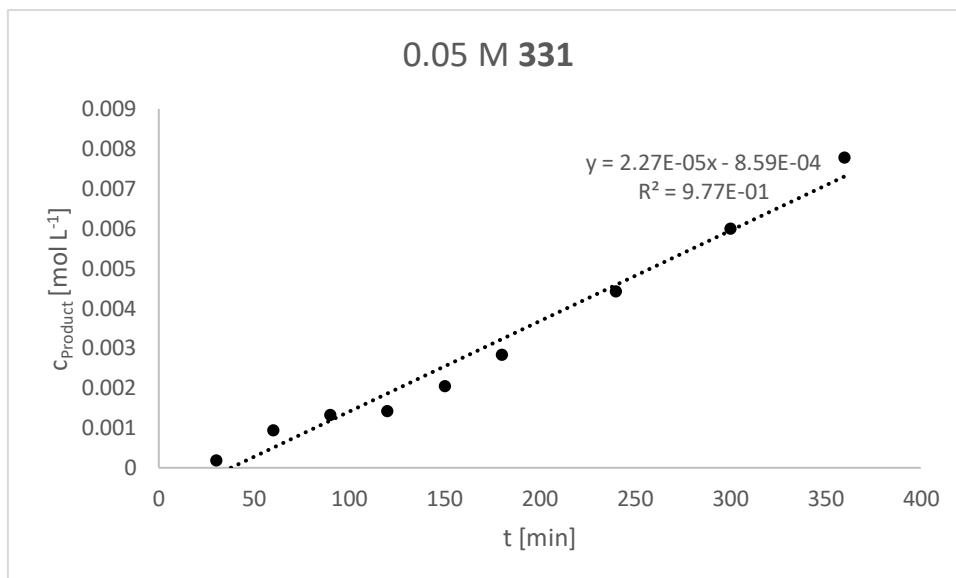
7.3.1.2.1 Initial rates with  $c_{331}$  (0.01M – 0.20 M)



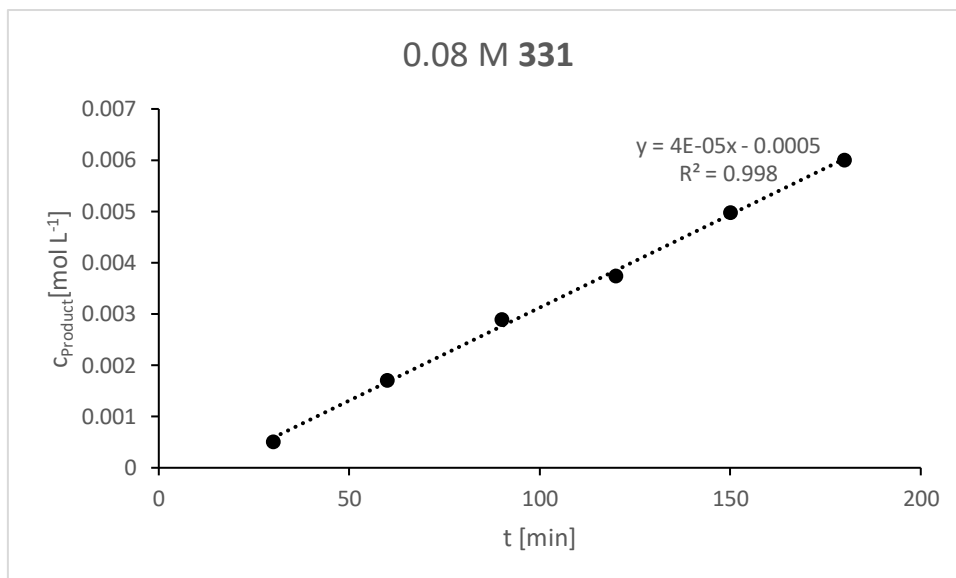
Time [min]	C [mol L <sup>-1</sup> ]
60	0.00E+00
120	0.00E+00
180	5.10E-04
240	9.40E-04
300	1.15E-03
360	1.37E-03
slope	5.11E-06
ln slope	-12.184
R <sup>2</sup>	0.958



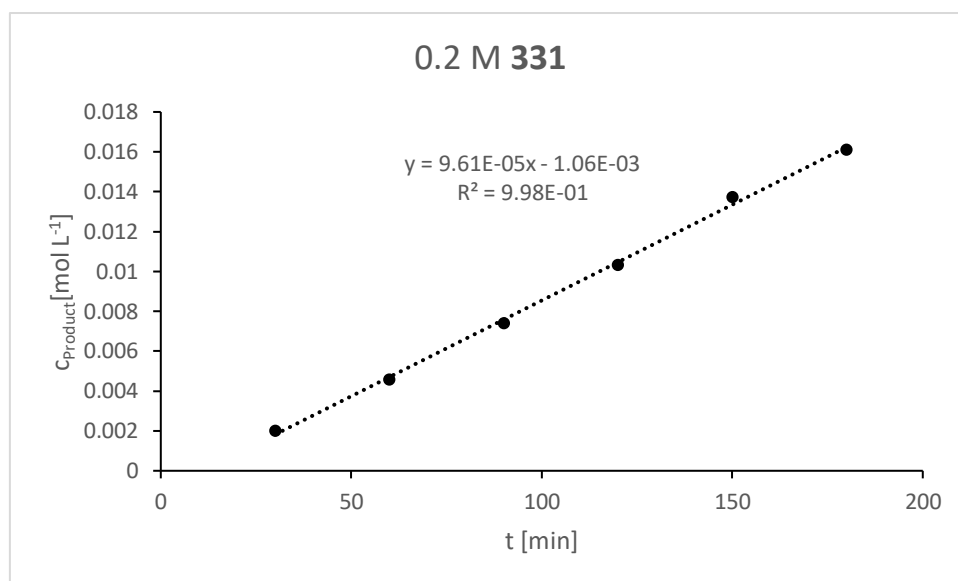
Time [min]	C [mol L <sup>-1</sup> ]
60	0.00E+00
120	4.90E-04
180	8.10E-04
240	1.29E-03
300	1.73E-03
360	2.66E-03
slope	8.33E-06
ln slope	-11.695
R <sup>2</sup>	0.970



Time [min]	C [mol L <sup>-1</sup> ]
30	1.90E-04
60	9.50E-04
90	1.33E-03
120	1.43E-03
150	2.05E-03
180	2.83E-03
240	4.42E-03
300	6.00E-03
360	7.78E-03
slope	2.27E-05
ln slope	-10.694
R <sup>2</sup>	0.956



Time [min]	C [mol L <sup>-1</sup> ]
30	0.00E+00
60	4.90E-04
90	8.10E-04
120	1.29E-03
150	1.73E-03
180	2.66E-03
slope	3.63E-05
ln slope	-10.224
R <sup>2</sup>	0.998



Time [min]	C [mol L <sup>-1</sup> ]
30	2.00E-03
60	4.57E-03
90	7.42E-03
120	1.03E-02
150	1.37E-02
180	1.61E-02
slope	9.61E-05
ln slope	-9.250
R <sup>2</sup>	0.998

### 7.3.2 Secondary Kinetic Isotopic Effect

#### 7.3.2.1 Secondary Kinetic Isotope Effect:

**Resorcinarene stock solution:** Resorcinarene (1.07 g, 0.968 mmol) was suspended in CDCl<sub>3</sub> (filtered through basic aluminum oxide) (12.8 mL) leading to 0.012 M solution referred to the assembled capsule. Upon gentle heating, the solution became clear.

**Substrate stock solution unlabelled: 331** (180 mg, 0.755 mmol) was dissolved in CDCl<sub>3</sub> (filtered through basic aluminum oxide) (1.80 mL)

**Substrate stock solution labelled: 331D** (174 mg, 0.726 mmol) was dissolved in  $\text{CDCl}_3$  (filtered through basic aluminum oxide) (1.73 mL)

**331** (525  $\mu\text{L}$ , 0.201 mmol) and **331D** (525  $\mu\text{L}$ , 0.201 mmol) were mixed in a 10 mL flask. An aliquot of 25.0  $\mu\text{L}$  was taken and diluted in acetone- $\text{d}_6$  (500  $\mu\text{L}$ ). Dry aluminum oxide (412 mg, neutral) tetraethylsilane (9.53  $\mu\text{L}$ , 50.0  $\mu\text{mol}$ ), and resorcinarene (3.20 mL, 40.0  $\mu\text{mol}$ ) were added and the flask was placed in a 50 °C oil bath to equilibrate for 5 min. Methanol (81.4  $\mu\text{L}$ , 2.01 mmol) was added and the flask was sealed with a rubber septum. After 6 h, an aliquot of 25.0  $\mu\text{L}$  was taken and diluted in acetone- $\text{d}_6$ . The reaction was quenched by the addition of triethylamine (400  $\mu\text{L}$ ) and the mixture was directly loaded onto a silica column (DCM :  $\text{Et}_2\text{O}$  = 9:1 with  $\text{NEt}_3$  1 %). To obtain the pure product, the purification had to be performed twice. The isolated product was analyzed by  $^1\text{H}$  NMR (acetone- $\text{d}_6$ ).

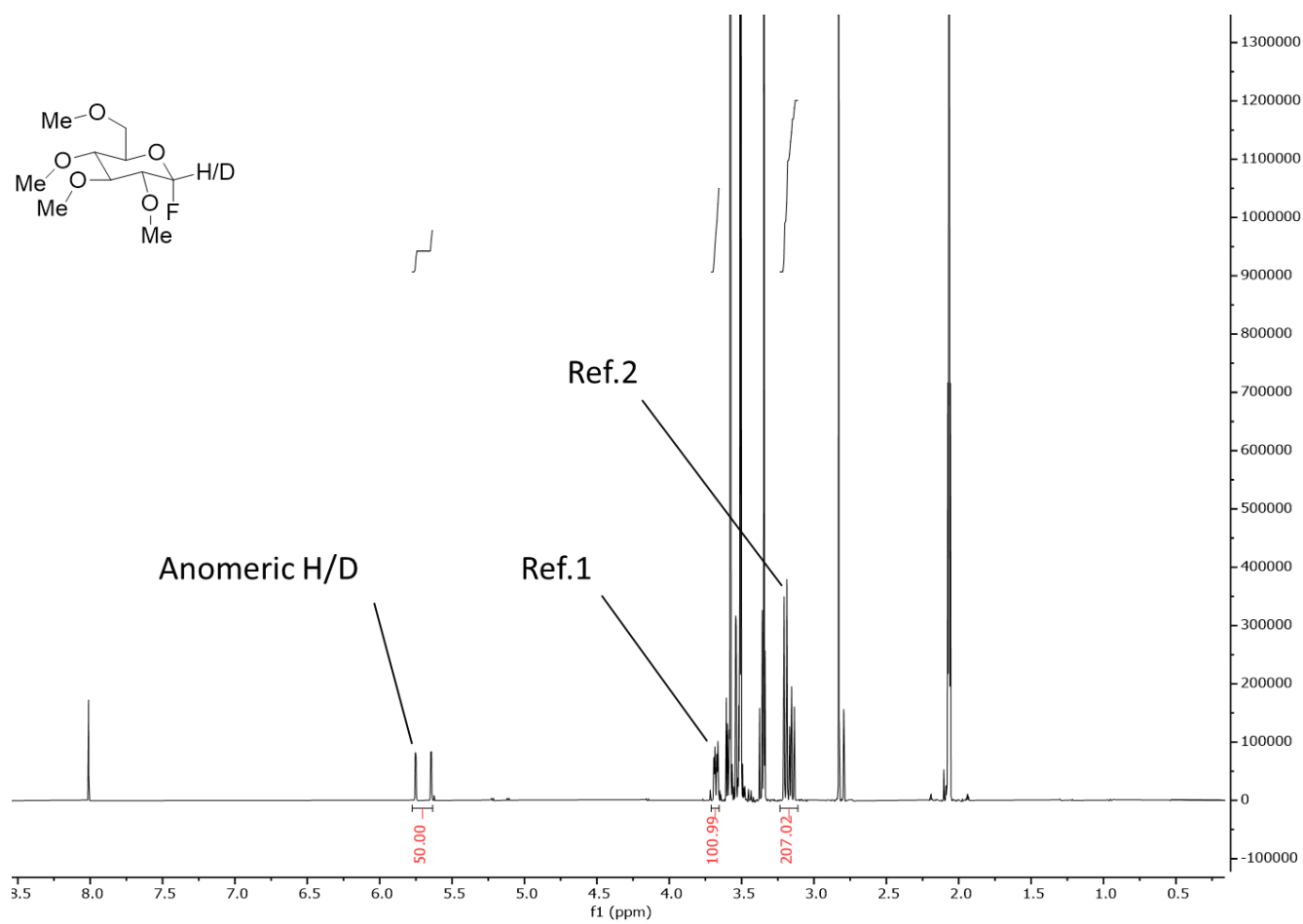


Figure 105  $^1\text{H}$  NMR spectra of partially deuterated compounds (starting material **331/ 331D**).



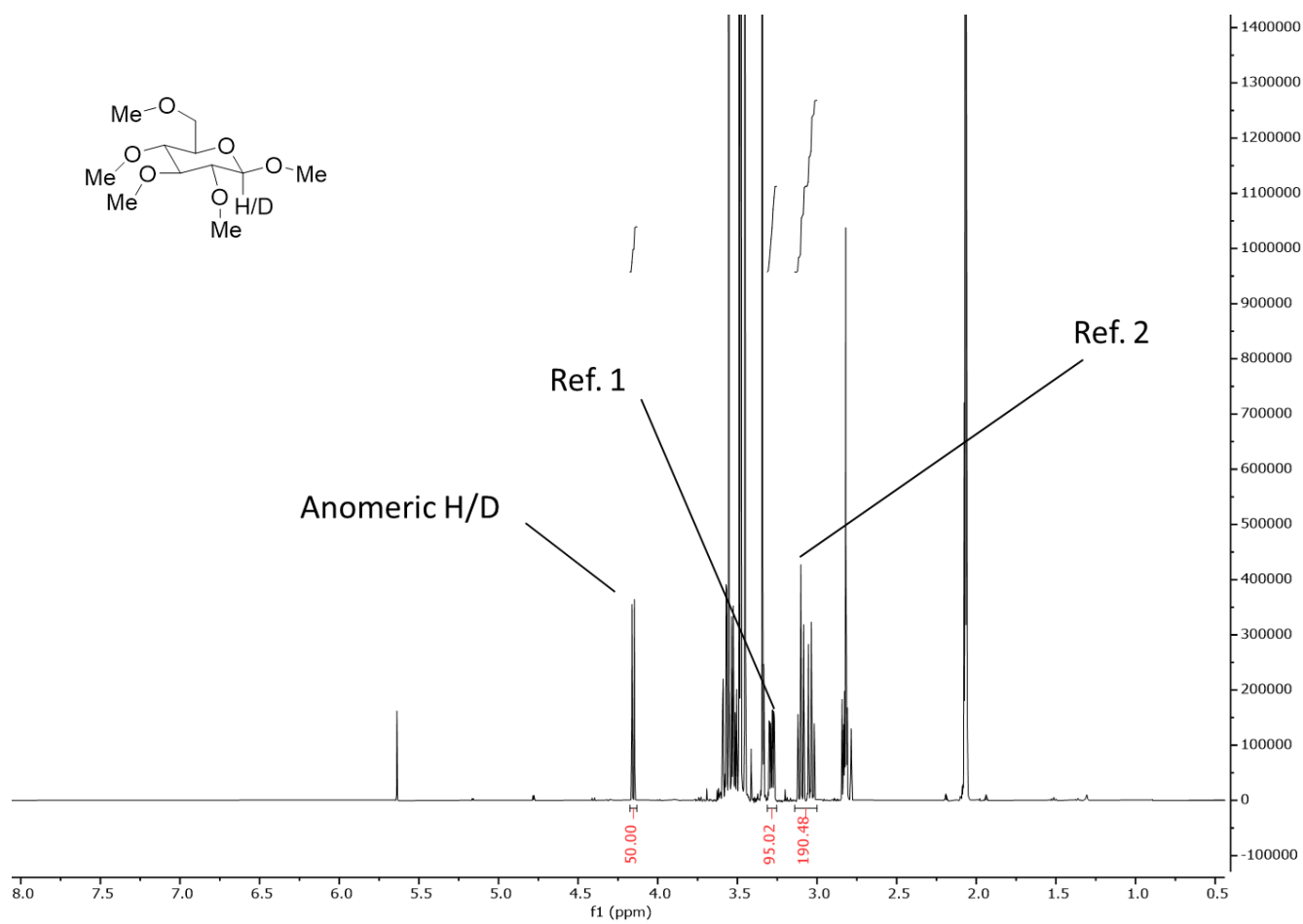


Figure 106 <sup>1</sup>H NMR spectra of partially deuterated compounds (product **328/ 328D**).

KIE values were calculated for every experiment by

Equation 4, where R is the isotopic ratio between the partially labeled anomeric center and a protonated reference signal and F is the partial conversion. R was calculated by subtracting the integral of the partially labeled anomeric center from the protonated signals of the C5 (Ref 1) and C6 (Ref 2) positions (Figure 106). The average between Ref 1 and Ref 2 was taken to determine R<sub>0</sub> respectively R<sub>P</sub>. F was determined by <sup>1</sup>H NMR quantification of the integral from the anomeric signal of the product **328/ 328D** with the signal of tetraethylsilane (0.54 ppm, acetone-d<sub>6</sub>).

Equation 3: Calculation Heavy/Light Isotope

$$R = \frac{[integral\ Reference]^* - [integral\ anomeric\ centre]}{[integral\ anomeric\ centre]}$$

\* in case of Ref 2, the integral has to be divided by two

Equation 4 Calculation KIE

$$KIE = \frac{\ln(1 - F)}{\ln(1 - (F * \frac{R_p}{R_0}))} = 1.19$$

Run	Integral Anomeric	Ref 1	Ref 2	R <sub>01</sub>	R <sub>02</sub>	Ø
1	50	100.74	206.93	1.015	1.069	1.042
2	50	102.26	208.15	1.045	1.081	1.063
3	50	101.36	207.1	1.027	1.071	1.049

Run	Integral Anomeric	Ref 1	Ref 2	R <sub>p1</sub>	R <sub>p2</sub>	Ø
1	50	95.02	190.67	0.900	0.907	0.903
2	50	92.81	192.74	0.856	0.927	0.892
3	50	95.71	188.46	0.914	0.885	0.899

Run	F
1	0.23
2	0.21
3	0.25

Run	R <sub>0</sub>	R <sub>p</sub>	F	SKIE
1	1.04205	0.90355	0.23	1.175
2	1.06335	0.8918	0.21	1.217
3	1.0491	0.8994	0.25	1.192
Ø				1.195
Stdev.				0.0214

### 7.3.3 Proton inventory study

Proton inventory studies are used to evaluate the number of protic sites involved in the transition state. For that, the exchangeable protons are substituted successively with deuterons. The quotient of the reaction rate at 0 % deuteration and of the reaction rate at X % deuteration is plotted against the ratio of protium to deuterium (D/H). The shape of the resulting curve provides information about the participating protic sites<sup>129, 130</sup>

In a classical proton inventory experiment, the amount of deuterium is regulated via the ratio of H<sub>2</sub>O to D<sub>2</sub>O. In the case of **II**, the reaction is performed in CDCl<sub>3</sub> which has no exchangeable protons/deuterons under the reaction conditions. The following molecules in the reaction can exchange protons/deuterons.

1. H<sub>2</sub>O/ D<sub>2</sub>O [in CDCl<sub>3</sub>]
2. Phenol groups and residual water of resorcinarene (RS)
3. Hydroxy group [methanol]

**H<sub>2</sub>O/ D<sub>2</sub>O [in CDCl<sub>3</sub>]:** The reactions were carried out in H<sub>2</sub>O or D<sub>2</sub>O saturated CDCl<sub>3</sub>. To determine the amount of water solvated in CDCl<sub>3</sub>, three samples of 500 μL were analyzed by NMR with tetraethyl silane (1.89 μL, 9.95 μmol) as an internal standard:

	A	B	C	Average	Stdev.
H <sub>2</sub> O [mmol]	3.26E-02	3.13E-02	3.27E-02	3.22E-02	7.77E-04
Protons [mmol]	6.53E-02	6.27E-02	6.55E-02	6.45E-02	1.55E-03

**Phenol groups and residual water of resorcinarene (II):** Resorcinarene was dried for 1 week under reduced pressure until the water content was stable. The residual water was determined by suspending resorcinarene (11.0 mg, 9.95 μmol) in H<sub>2</sub>O saturated CDCl<sub>3</sub> (500 μL). Under gentle heating, the suspension turned clear and was allowed to cool to room temperature. (Note: Using dry CDCl<sub>3</sub> for the water determination would lead to solubility problems.) Tetraethyl silane (1.89 μL, 9.95 μmol) was added as an internal standard, and the solution was analyzed by NMR. Subtraction of the amount of protons added by the solvent from the capsule solution results in the amount of exchangeable protons from the capsule. As mentioned above, the capsule not only features protons from the phenol groups but also residual crystal water.

	A	B	C	Average	Stdev.
Phenol protons [mmol]	7.45E-02	7.90E-02	7.83E-02	7.73E-02	2.41E-03
H <sub>2</sub> O protons [mmol]	6.95E-02	7.13E-02	7.28E-02	7.12E-02	1.70E-03
Sum				1.48E-01	
Protons from CDCl <sub>3</sub> [mmol]				6.45E-02	
Protons from II [mmol]				8.40E-02	
Exchang. Proton per resorcinarene [mmol /mmol]				8.44E+00	

The overall exchangeable protons for the reaction conditions with RS (30.0  $\mu\text{mol}$ , 6 eq. RS = 1 eq. capsule), methanol (250  $\mu\text{mol}$ , 5 eq.) and H<sub>2</sub>O/D<sub>2</sub>O saturated CDCl<sub>3</sub> (500  $\mu\text{L}$ , 6.23 mmol) are summed up:

Proton Source	Protons [mmol]	Proportion
CDCl <sub>3</sub>	6.45E-02	11.3 %
RS	2.54E-01	44.7 %
MeOH	2.50E-01	44.0 %
Sum	5.67E-01	100 %

**Deuteration of II:** To achieve a high deuteration, the phenolic protons and the capsule water was exchanged with deuterons: **II** was dissolved in a mixture of dry THF and 20 % (v/v) D<sub>2</sub>O and stirred for 24 h at 50 °C. The solvent mixture was removed under reduced pressure and the remaining solid was stored under high vacuum for one week.

To determine the degree of deuteration, **II<sub>d</sub>** (11 mg, 9.95  $\mu\text{mol}$ ) was suspended in H<sub>2</sub>O-sat CDCl<sub>3</sub> (500  $\mu\text{L}$ ). Under gentle heating, the suspension turned clear and was allowed to cool to room temperature. Tetraethyl silane (1.89  $\mu\text{L}$ , 9.95  $\mu\text{mol}$ ) was added and the solution was analyzed by NMR.

Under the assumption, that the water content of the  $\text{II}/\text{II}_d$  samples is approximately the same, the total amount of protons from the phenols and water was determined for  $\text{II}_d$ .

	A	B	C	Average	Stdev.
Phenol <sub>d</sub> protons [mmol]	4.33E-02	3.84E-02	3.63E-02	3.93E-02	3.57E-03
H <sub>2</sub> O protons [mmol]	3.79E-02	3.07E-02	2.67E-02	3.18E-02	5.69E-03
Sum				7.11E-02	
Protons from regular II [mmol]				1.48E-01	
1 – (II <sub>d</sub> /II)				52.1 %	

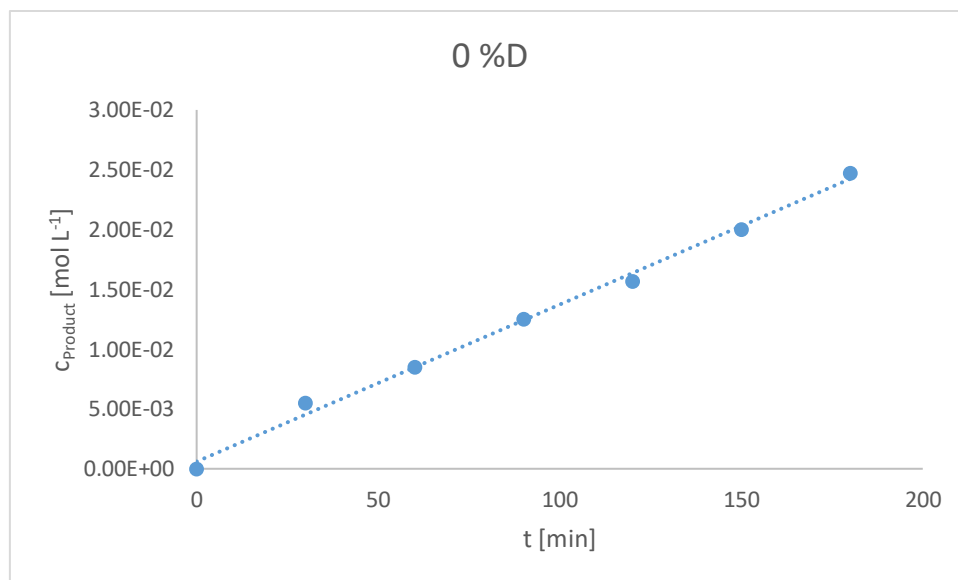
By mixing different proportions of the protonated/deuterated species, different D/H ratios can be achieved in the reaction:

Proportion of the deuterated species	Hydrons [mmol]	% D
100 % D <sub>2</sub> O	6.45E-02	11.3 %
25 % MeOD + 100 % D <sub>2</sub> O	1.26E-01	22.3 %
50 % MeOD + 100 % D <sub>2</sub> O	1.88E-01	33.3 %
75 % MeOD + 100 % D <sub>2</sub> O	2.51E-01	44.3 %
100 % MeOD + 100 % D <sub>2</sub> O	3.13E-01	55.3 %
100 % MeOD + 100 % D <sub>2</sub> O + 50 % II <sub>d</sub>	3.79E-01	67.0 %
100 % MeOD + 100 % D <sub>2</sub> O + 100 % II <sub>d</sub>	4.45E-01	78.6 %

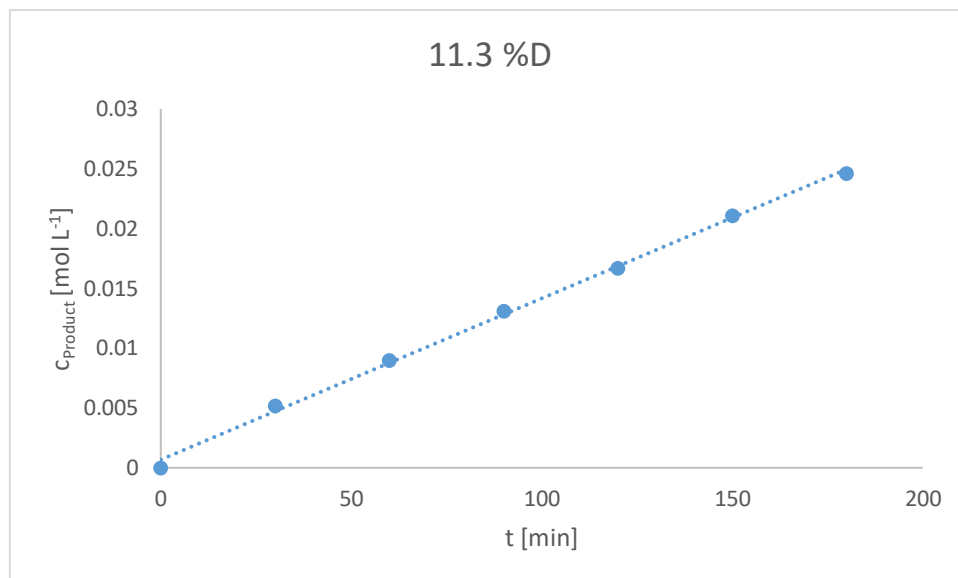
The reaction rates were determined for the different D/H ratios, including 0 % D.

Resorcinarene (30.0  $\mu\text{mol}$ , 0.6 eq. = 5.00  $\mu\text{mol}$  capsule, 0.1 eq.) was suspended in  $\text{CDCl}_3$  (500  $\mu\text{L}$ , H<sub>2</sub>O or D<sub>2</sub>O sat.). Under gentle heating, the suspension turned clear and was allowed to cool to room temperature. The solution was transferred to a 2 mL GC vial with **331** (11.9 mg,

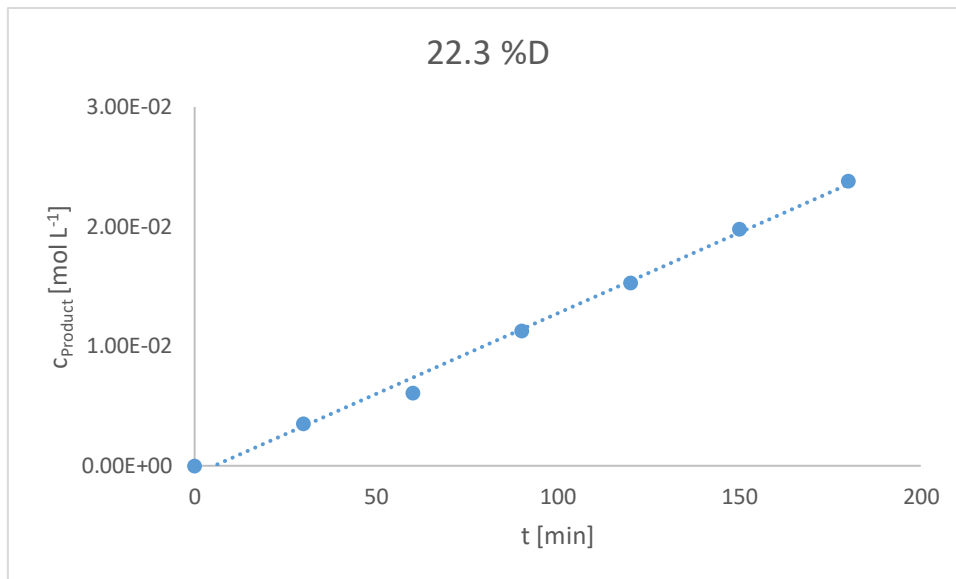
50.0  $\mu\text{mol}$ , 1 eq.). After mixing, the solution was transferred to a new 2 mL GC vial containing dry alumina (neutral, 50.0 mg). Methanol (250.0  $\mu\text{mol}$ , 5 eq.) was added and the closed vial was placed inside an aluminum heating block, set to 50 °C. Aliquots of 25.0  $\mu\text{L}$  were taken every 30 min over a period of 3 h. The samples were diluted with 500  $\mu\text{L}$  of acetone- $\text{d}_6$  and analyzed by NMR (d1=3 s and 64 scans).



Time [min]	C [mol L <sup>-1</sup> ]
0	0.00E+00
30	5.50E-03
60	8.50E-03
90	1.25E-02
120	1.57E-02
150	2.00E-02
180	2.47E-02
slope	1.31E-04
R <sup>2</sup>	9.95E-01

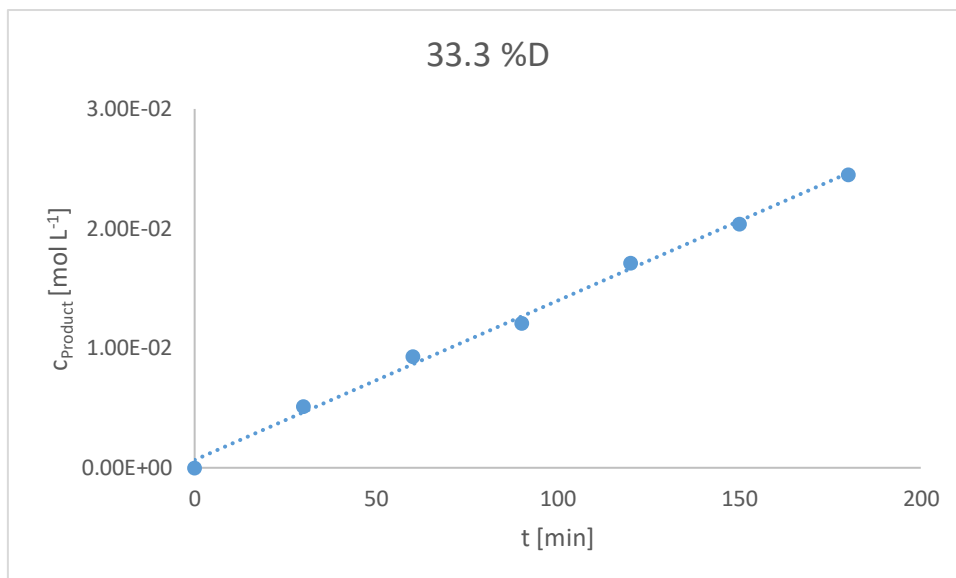


Time [min]	C [mol L <sup>-1</sup> ]
0	0
30	5.20E-03
60	9.00E-03
90	1.31E-02
120	1.67E-02
150	2.11E-02
180	2.46E-02
slope	1.35E-04
R <sup>2</sup>	9.98E-01

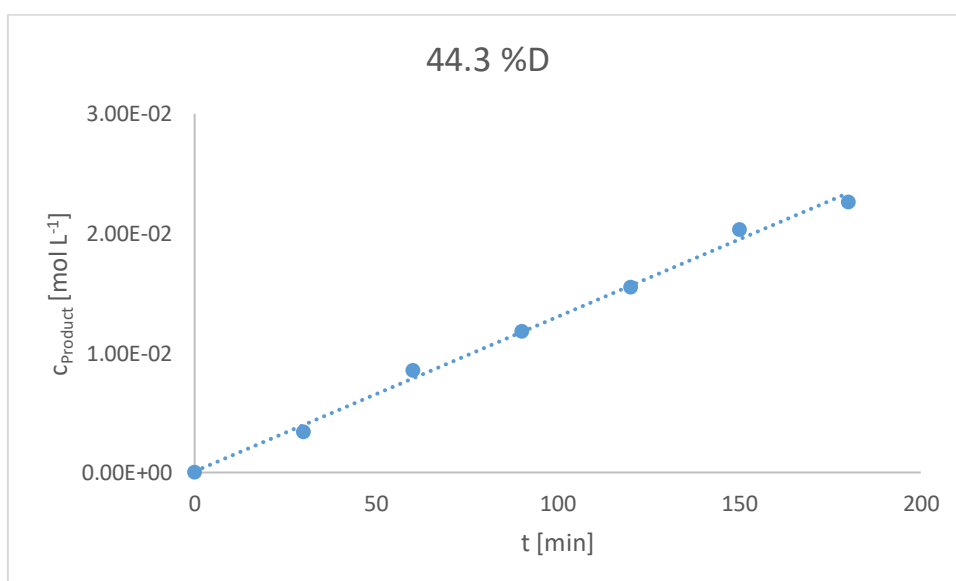


Time [min]	C [mol L <sup>-1</sup> ]
0	0.00E+00
30	3.50E-03
60	6.10E-03
90	1.13E-02
120	1.53E-02
150	1.98E-02
180	2.38E-02
slope	1.35E-04
R <sup>2</sup>	9.95E-01

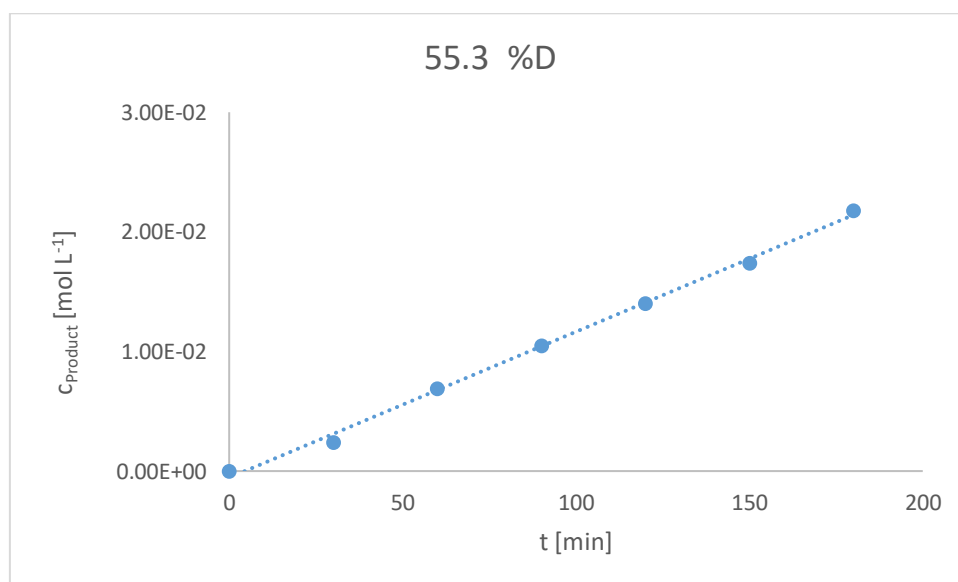




Time [min]	C [mol L <sup>-1</sup> ]
0	0.00E+00
30	5.10E-03
60	9.30E-03
90	1.21E-02
120	1.71E-02
150	2.04E-02
180	2.45E-02
slope	1.33E-04
R <sup>2</sup>	9.96E-01



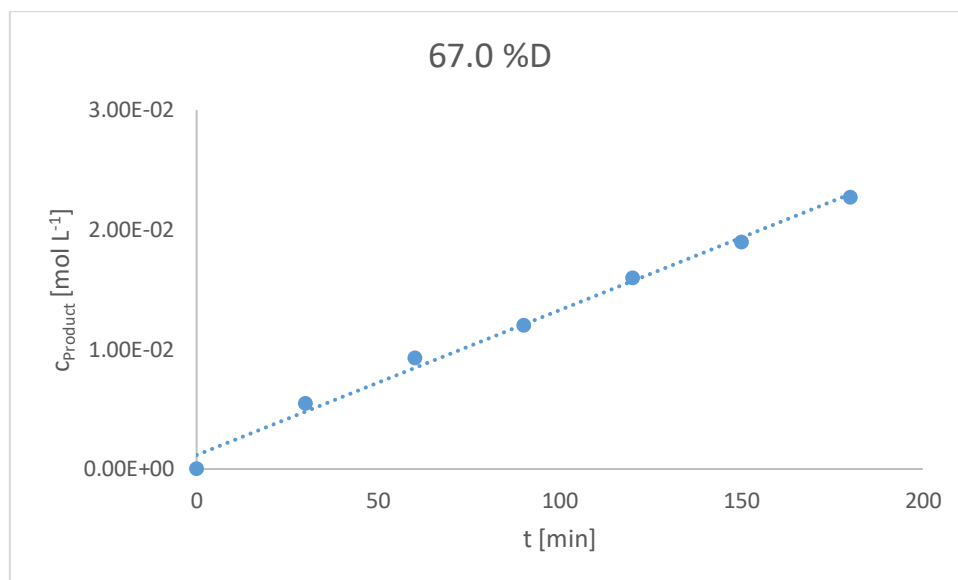
Time [min]	C [mol L <sup>-1</sup> ]
0	0.00E+00
30	3.40E-03
60	8.50E-03
90	1.18E-02
120	1.55E-02
150	2.03E-02
180	2.26E-02
slope	1.29E-04
R <sup>2</sup>	9.95E-01



Time [min]	C [mol L <sup>-1</sup> ]
0	0.00E+00
30	2.40E-03
60	6.90E-03
90	1.05E-02
120	1.40E-02
150	1.74E-02
180	2.18E-02

---

slope	1.22E-04
R <sup>2</sup>	9.97E-01

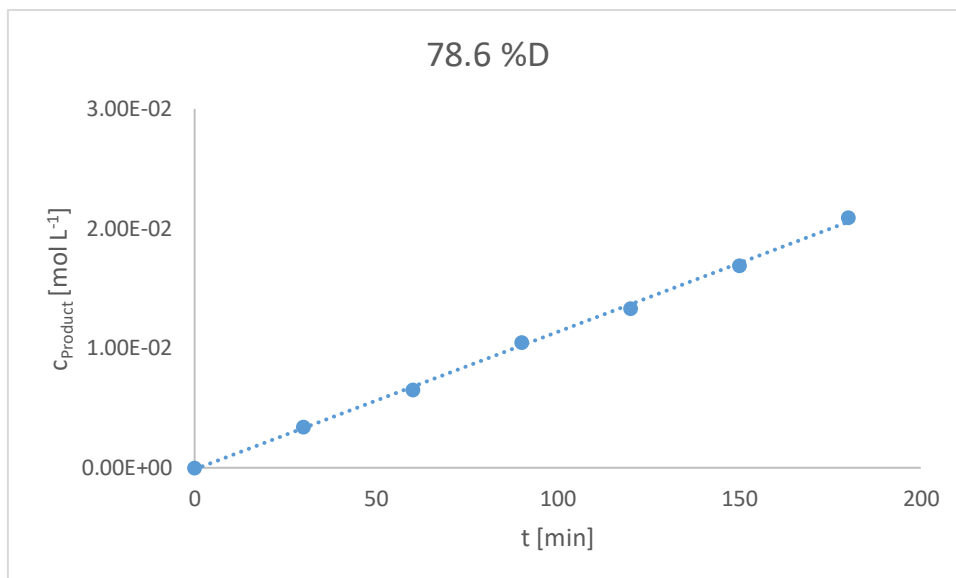



---

Time [min]	C [mol L <sup>-1</sup> ]
0	0.00E+00
30	5.50E-03
60	9.30E-03
90	1.20E-02
120	1.60E-02
150	1.90E-02
180	2.27E-02

---

slope	1.21E-04
R <sup>2</sup>	9.92E-01



Time [min]	C [mol L <sup>-1</sup> ]
0	0.00E+00
30	3.40E-03
60	6.50E-03
90	1.05E-02
120	1.33E-02
150	1.69E-02
180	2.09E-02
slope	1.15E-04
R <sup>2</sup>	9.99E-01

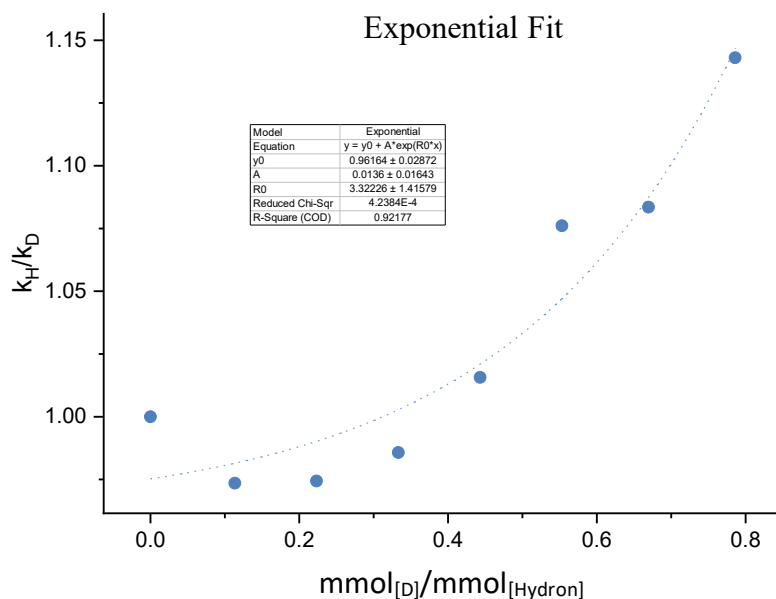


Figure 107 Kinetic isotope effect ( $k_H/k_D$ ) vs. the D/H (%D) ratio with an exponential fit

D/H	$k_H/k_D$
0.0	1.000E+00
0.113	9.735E-01
0.223	9.744E-01
0.333	9.857E-01
0.443	1.016E+00
0.553	1.076E+00
0.670	1.083E+00
0.786	1.143E+00

If one protic site is involved in the rate-limiting transition state, a linear plot is expected. For two protic sites, the plot of the square root of the KIE versus the D/H ratio should provide a linear relation. The linear regression of the data (Figure 108) does not provide a satisfactory fit ( $R^2 = 79\%$ ). This indicates that more than two protic sites are involved in the rate-limiting transition state.<sup>129, 135</sup> To determine the total amount of protic sites, a different model equation for the expected number of protic sites has to be fitted to the data. This is the subject of current investigations and will be treated in future publications.

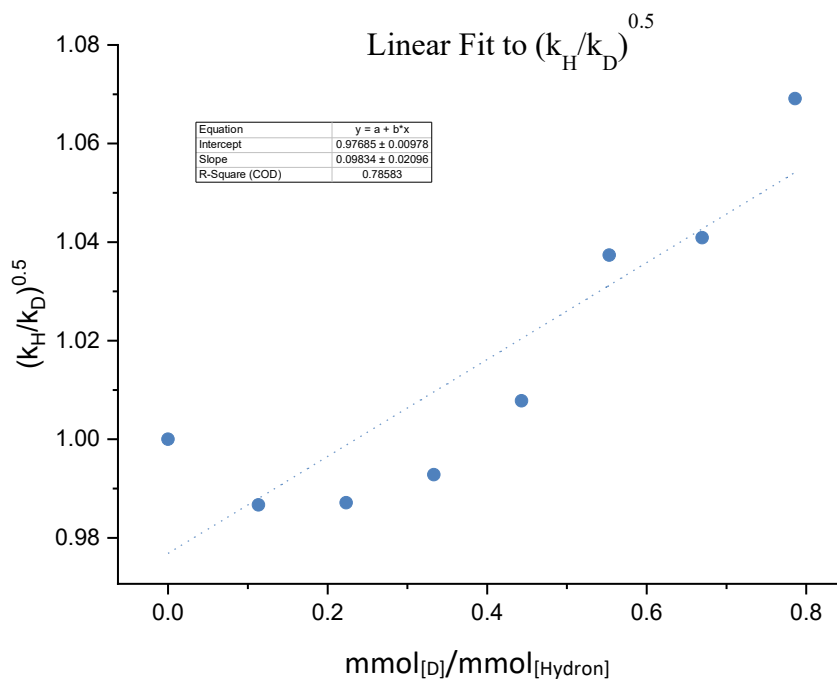


Figure 108 Square root of the kinetic isotope effect ( $k_H/k_D$ ) vs. the D/H ratio with a linear fit

D/H	$(k_H/k_D)^{0.5}$
0.0	1.000E+00
0.113	9.867E-01
0.223	9.871E-01
0.333	9.928E-01
0.443	1.008E+00
0.553	1.037E+00
0.670	1.041E+00
0.786	1.069E+00
<b>R<sup>2</sup></b>	<b>7.858E-01</b>

## 8. References

- (1) Heckmann, C. M.; Paradisi, F. Looking Back: A Short History of the Discovery of Enzymes and How They Became Powerful Chemical Tools. *ChemCatChem* **2020**, *12* (24), 6082-6102,
- (2) Lindström, B.; Pettersson, L. J. A Brief History of Catalysis. *CATTECH* **2003**, *7* (4), 130-138,
- (3) Ertl, G. Reactivity of Surfaces. In *Chemistry and Physics of Solid Surfaces VIII*, Vanselow, R., Howe, R. Eds.; Springer Berlin Heidelberg, 1990; pp 1-22.
- (4) Erisman, J. W.; Sutton, M. A.; Galloway, J.; Klimont, Z.; Winiwarter, W. How a century of ammonia synthesis changed the world. *Nat. Geosci.* **2008**, *1* (10), 636-639,
- (5) Chapter 1 History of catalysis. In *Studies in Surface Science and Catalysis*, Moulijn, J. A., van Leeuwen, P. W. N. M., van Santen, R. A. Eds.; Vol. 79; Elsevier, 1993; pp 3-21.
- (6) Anastas, P.; Eghbali, N. Green Chemistry: Principles and Practice. *Chem. Soc. Rev.* **2010**, *39* (1), 301-312,
- (7) Anastas, P. T.; Kirchhoff, M. M.; Williamson, T. C. Catalysis as a foundational pillar of green chemistry. *Appl Catal A Gen* **2001**, *221* (1), 3-13,
- (8) Sheldon, R. A. Engineering a more sustainable world through catalysis and green chemistry. *J. R. Soc. Interface* **2016**, *13* (116), 20160087,
- (9) Hoveyda, A. H.; Zhugralin, A. R. The remarkable metal-catalysed olefin metathesis reaction. *Nature* **2007**, *450*, 243,
- (10) Grubbs, R. H. Olefin metathesis. *Tetrahedron* **2004**, *60* (34), 7117-7140,
- (11) Fürstner, A. Metathesis in total synthesis. *Chem. Commun.* **2011**, *47* (23), 6505-6511,
- (12) Tomasek, J.; Schatz, J. Olefin metathesis in aqueous media. *Green Chem.* **2013**, *15* (9), 2317-2338,
- (13) Hong, S. H.; Grubbs, R. H. Highly Active Water-Soluble Olefin Metathesis Catalyst. *J. Am. Chem. Soc.* **2006**, *128* (11), 3508-3509,
- (14) Abbas, M.; Neubauer, M.; Slugovc, C. Converting natural rubber waste into ring-opening metathesis polymers with oligo-1,4-cis-isoprene sidechains. *Polym. Chem.* **2018**, *9* (14), 1763-1766,
- (15) Mouawia, A.; Nourry, A.; Gaumont, A.-C.; Pilard, J.-F.; Dez, I. Controlled Metathetic Depolymerization of Natural Rubber in Ionic Liquids: From Waste Tires to Telechelic Polyisoprene Oligomers. *ACS Sustain. Chem. Eng.* **2017**, *5* (1), 696-700,
- (16) Nagyházi, M.; Turczel, G.; Balla, Á.; Szálás, G.; Tóth, I.; Gál, G. T.; Petra, B.; Anastas, P. T.; Tuba, R. Towards Sustainable Catalysis – Highly Efficient Olefin Metathesis in Protic Media Using Phase Labelled Cyclic Alkyl Amino Carbene (CAAC) Ruthenium Catalysts. *ChemCatChem* **2020**, *12* (7), 1953-1957,
- (17) Burdett, K. A.; Harris, L. D.; Margl, P.; Maughon, B. R.; Mokhtar-Zadeh, T.; Saucier, P. C.; Wasserman, E. P. Renewable Monomer Feedstocks via Olefin Metathesis: Fundamental Mechanistic Studies of Methyl Oleate Ethenolysis with the First-Generation Grubbs Catalyst. *Organometallics* **2004**, *23* (9), 2027-2047,
- (18) Mol, J. C. Application of olefin metathesis in oleochemistry: an example of green chemistry. *Green Chem.* **2002**, *4* (1), 5-13,
- (19) Mol, J. C. Industrial applications of olefin metathesis. *J. Mol. Catal. A: Chem.* **2004**, *213* (1), 39-45,
- (20) Wittig, G.; Geissler, G. Zur Reaktionsweise des Pentaphenyl-phosphors und einiger Derivate. *Liebigs Ann. Chem.* **1953**, *580* (1), 44-57,
- (21) Wittig, G.; Schöllkopf, U. Über Triphenyl-phosphin-methylene als olefinbildende Reagenzien (I. Mitteil. *Chem. Ber.* **1954**, *87* (9), 1318-1330,
- (22) Wittig, G.; Wetterling, M.-H. Darstellung und Eigenschaften des Trimethyl-ammonium-methylids. *Liebigs Ann. Chem.* **1947**, *557* (1), 193-201,
- (23) Pommer, H. The Wittig Reaction in Industrial Practice. *Angew. Chem. Int. Ed.* **1977**, *16* (7), 423-429,
- (24) Edmonds, M.; Abell, A. The Wittig Reaction. In *Modern Carbonyl Olefination*, Takeda, T. Ed.; Wiley-VCH, 2003; pp 1-17.
- (25) van Kalker, H. A.; Blom, A. L.; Rutjes, F. P. J. T.; Huijbregts, M. A. J. On the usefulness of life cycle assessment in early chemical methodology development: the case of organophosphorus-catalyzed Appel and Wittig reactions. *Green Chem.* **2013**, *15* (5), 1255-1263,

- (26) Vedejs, E.; Marth, C. F. Mechanism of Wittig reaction: evidence against betaine intermediates. *J. Am. Chem. Soc.* **1990**, *112* (10), 3905-3909,
- (27) Byrne, P. A.; Gilheany, D. G. The modern interpretation of the Wittig reaction mechanism. *Chem. Soc. Rev.* **2013**, *42* (16), 6670-6696,
- (28) Farfán, P.; Gómez, S.; Restrepo, A. Dissection of the Mechanism of the Wittig Reaction. *J. Org. Chem.* **2019**, *84* (22), 14644-14658,
- (29) Robiette, R.; Richardson, J.; Aggarwal, V. K.; Harvey, J. N. Reactivity and Selectivity in the Wittig Reaction: A Computational Study. *J. Am. Chem. Soc.* **2006**, *128* (7), 2394-2409,
- (30) Maryanoff, B. E.; Reitz, A. B. The Wittig olefination reaction and modifications involving phosphoryl-stabilized carbanions. Stereochemistry, mechanism, and selected synthetic aspects. *Chem. Rev.* **1989**, *89* (4), 863-927,
- (31) M–L Multiple Bonds. In *The Organometallic Chemistry of the Transition Metals*, 2014; pp 290-316.
- (32) Hartley, R. C.; McKiernan, G. J. Titanium reagents for the alkylidenation of carboxylic acid and carbonic acid derivatives. *J. Chem. Soc., Perkin Trans. 1* **2002**, (24), 2763-2793,
- (33) Tebbe, F. N.; Parshall, G. W.; Ovenall, D. W. Titanium-catalyzed olefin metathesis. *J. Am. Chem. Soc.* **1979**, *101* (17), 5074-5075,
- (34) Stille, J. R.; Grubbs, R. H. Synthesis of (+)- $\Delta^9,12$ -capnellene using titanium reagents. *J. Am. Chem. Soc.* **1986**, *108* (4), 855-856,
- (35) Nicolaou, K. C.; Postema, M. H. D.; Yue, E. W.; Nadin, A. An Olefin Metathesis Based Strategy for the Construction of the JKL, OPQ, and UVW Ring Systems of Maitotoxin. *J. Am. Chem. Soc.* **1996**, *118* (42), 10335-10336,
- (36) Scharf, D.; Korte, F. Photosensibilisierte Cyclodimerisierung von Norbornen. In *Tetrahedron Letters*, Martin, R. H., Wasserman, H. H., Nesmeyanov, A. N., Weygand, F. Eds.; Pergamon, 1963; pp 821-823.
- (37) Fréneau, M.; Hoffmann, N. The Paternò-Büchi reaction—Mechanisms and application to organic synthesis. *J. Photochem. Photobiol. C: Photochem. Rev* **2017**, *33*, 83-108,
- (38) Turro, N. J.; Dalton, J. C.; Dawes, K.; Farrington, G.; Hautala, R.; Morton, D.; Niemczyk, M.; Schore, N. Molecular photochemistry. L. Molecular photochemistry of alkanones in solution.  $\alpha$ -Cleavage, hydrogen abstraction, cycloaddition, and sensitization reactions. *Acc. Chem. Res.* **1972**, *5* (3), 92-101,
- (39) Griesbeck, A. G.; Stadtmueller, S. Photocycloaddition of benzaldehyde to cyclic olefins: electronic control of endo stereoselectivity. *J. Am. Chem. Soc.* **1990**, *112* (3), 1281-1283,
- (40) Kutateladze, A. G. Conformational Analysis of Singlet-Triplet State Mixing in Paternò-Büchi Diradicals. *J. Am. Chem. Soc.* **2001**, *123* (38), 9279-9282,
- (41) Iriando-Alberdi, J.; Perea-Buceta, J. E.; Greaney, M. F. A Paternò-Büchi Approach to the Synthesis of Merrilactone A. *Org. Lett.* **2005**, *7* (18), 3969-3971,
- (42) Jones, G.; Acquadro, M. A.; Carmody, M. A. Long-chain enals via carbonyl-olefin metathesis. An application in pheromone synthesis. *J. Chem. Soc., Chem. Commun.* **1975**, (6), 206-207,
- (43) Jones, G.; Schwartz, S. B.; Marton, M. T. Regiospecific thermal cleavage of some oxetan photoadducts: carbonyl-olefin metathesis in sequential photochemical and thermal steps. *J. Chem. Soc., Chem. Commun.* **1973**, (11), 374-375,
- (44) Valiulin, R. A.; Kutateladze, A. G. Harvesting the Strain Installed by a Paternò-Büchi Step in a Synthetically Useful Way: High-Yielding Photoprotolytic Oxametathesis in Polycyclic Systems. *Org. Lett.* **2009**, *11* (17), 3886-3889,
- (45) Valiulin, R. A.; Arisco, T. M.; Kutateladze, A. G. Photoinduced Intramolecular Cyclopentation vs Photoprotolytic Oxametathesis in Polycyclic Alkenes Outfitted with Conformationally Constrained Aroylmethyl Chromophores. *J. Org. Chem.* **2013**, *78* (5), 2012-2025,
- (46) Valiulin, R. A.; Arisco, T. M.; Kutateladze, A. G. Double-Tandem  $[4\pi+2\pi]$ - $[2\pi+2\pi]$ - $[4\pi+2\pi]$ - $[2\pi+2\pi]$  Synthetic Sequence with Photoprotolytic Oxametathesis and Photoepoxidation in the Chromone Series. *J. Org. Chem.* **2011**, *76* (5), 1319-1332,
- (47) Albright, H.; Davis, A. J.; Gomez-Lopez, J. L.; Vonesh, H. L.; Quach, P. K.; Lambert, T. H.; Schindler, C. S. Carbonyl-Olefin Metathesis. *Chem. Rev.* **2021**, *121* (15), 9359-9406,



- (48) Wang, R.; Chen, Y.; Shu, M.; Zhao, W.; Tao, M.; Du, C.; Fu, X.; Li, A.; Lin, Z. AuCl<sub>3</sub>-Catalyzed Ring-Closing Carbonyl–Olefin Metathesis. *Eur. J. Chem.* **2020**, *26* (9), 1941-1946,
- (49) Naidu, V. R.; Bah, J.; Franzén, J. Direct Organocatalytic Oxo-Metathesis, a trans-Selective Carbocation-Catalyzed Olefination of Aldehydes. *Eur. J. Org. Chem.* **2015**, *2015* (8), 1834-1839,
- (50) Tran, U. P. N.; Oss, G.; Pace, D. P.; Ho, J.; Nguyen, T. V. Tropylium-promoted carbonyl–olefin metathesis reactions. *Chem. Sci.* **2018**, *9* (23), 5145-5151,
- (51) Albright, H.; Vonesh, H. L.; Schindler, C. S. Superelectrophilic Fe(III)–Ion Pairs as Stronger Lewis Acid Catalysts for (E)-Selective Intermolecular Carbonyl–Olefin Metathesis. *Org. Lett.* **2020**, *22* (8), 3155-3160,
- (52) Tran, U. P. N.; Oss, G.; Breugst, M.; Detmar, E.; Pace, D. P.; Liyanto, K.; Nguyen, T. V. Carbonyl–Olefin Metathesis Catalyzed by Molecular Iodine. *ACS Catal.* **2018**, 912-919,
- (53) Albright, H.; Vonesh, H. L.; Becker, M. R.; Alexander, B. W.; Ludwig, J. R.; Wiscons, R. A.; Schindler, C. S. GaCl<sub>3</sub>-Catalyzed Ring-Opening Carbonyl–Olefin Metathesis. *Org. Lett.* **2018**, *20* (16), 4954-4958,
- (54) Griffith, A. K.; Vanos, C. M.; Lambert, T. H. Organocatalytic Carbonyl–Olefin Metathesis. *J. Am. Chem. Soc.* **2012**, *134* (45), 18581-18584,
- (55) Jermaks, J.; Quach, P. K.; Seibel, Z. M.; Pomarole, J.; Lambert, T. H. Ring-opening carbonyl–olefin metathesis of norbornenes. *Chem. Sci.* **2020**, *11* (30), 7884-7895,
- (56) Becker, M. R.; Watson, R. B.; Schindler, C. S. Beyond olefins: new metathesis directions for synthesis. *Chem. Soc. Rev.* **2018**, *47* (21), 7867-7881,
- (57) Lambert, T. H. Development of a Hydrazine-Catalyzed Carbonyl–Olefin Metathesis Reaction. *Synlett* **2019**, *30* (17), 1954-1965,
- (58) Demole, E.; Enggist, P.; Borer, M. C. Applications synthétiques de la cyclisation d'alcools tertiaires  $\gamma$ -éthyléniques en  $\alpha$ -bromotétrahydrofurannes sous l'action du N-bromosuccinimide. II. Cyclisation du ( $\pm$ )-nérolidol en diméthyl-2,5-(méthyl-4-pentène-3-yl)-2-cycloheptène-4-one, tétraméthyl-3, 3, 7, 10-oxa-2-tricyclo[5.5.0.0.1,4]-dodécène-9,  $\beta$ -acoratriène, cédradiène-2,8, épi-2- $\alpha$ -cédrene et  $\alpha$ -cédrene. *Helv. Chim. Acta* **1971**, *54* (7), 1845-1864,
- (59) van Schaik, H.-P.; Vijn, R.-J.; Bickelhaupt, F. Acid-Catalyzed Olefination of Benzaldehyde. *Angew. Chem. Int. Ed.* **1994**, *33* (15-16), 1611-1612,
- (60) Slavov, N.; Cvengroš, J.; Neudörfl, J.-M.; Schmalz, H.-G. Total Synthesis of the Marine Antibiotic Pestalone and its Surprisingly Facile Conversion into Pestalalactone and Pestalachloride A. *Angew. Chem. Int. Ed.* **2010**, *49* (41), 7588-7591,
- (61) Soicke, A.; Slavov, N.; Neudörfl, J.-M.; Schmalz, H.-G. Metal-Free Intramolecular Carbonyl–Olefin Metathesis of ortho-Prenylaryl Ketones. *Synlett* **2011**, *2011* (17), 2487-2490,
- (62) Khripach, V. A.; Zhabinskii, V. N.; Kuchto, A. I.; Zhiburtovich, Y. Y.; Gromak, V. V.; Groen, M. B.; van der Louw, J.; de Groot, A. Intramolecular cycloaddition/cycloreversion of (E)-3 $\beta$ ,17 $\beta$ -diacetoxy-5,10-secoandrost-1(10)-en-5-one. *Tetrahedron Lett.* **2006**, *47* (38), 6715-6718,
- (63) Ludwig, J. R.; Zimmerman, P. M.; Gianino, J. B.; Schindler, C. S. Iron(III)-catalysed carbonyl–olefin metathesis. *Nature* **2016**, *533* (7603), 374-379,
- (64) Ludwig, J. R.; Phan, S.; McAtee, C. C.; Zimmerman, P. M.; Devery, J. J.; Schindler, C. S. Mechanistic Investigations of the Iron(III)-Catalyzed Carbonyl–Olefin Metathesis Reaction. *J. Am. Chem. Soc.* **2017**, *139* (31), 10832-10842,
- (65) Ma, L.; Li, W.; Xi, H.; Bai, X.; Ma, E.; Yan, X.; Li, Z. FeCl<sub>3</sub>-Catalyzed Ring-Closing Carbonyl–Olefin Metathesis. *Angew. Chem. Int. Ed.* **2016**, *55* (35), 10410-10413,
- (66) Groso, E. J.; Golonka, A. N.; Harding, R. A.; Alexander, B. W.; Sodano, T. M.; Schindler, C. S. 3-Aryl-2,5-Dihydropyrroles via Catalytic Carbonyl–Olefin Metathesis. *ACS Catal.* **2018**, 2006-2011,
- (67) Rykaczewski, K. A.; Groso, E. J.; Vonesh, H. L.; Gavia, M. A.; Richardson, A. D.; Zehnder, T. E.; Schindler, C. S. Tetrahydropyridines via FeCl<sub>3</sub>-Catalyzed Carbonyl–Olefin Metathesis. *Org. Lett.* **2020**, *22* (7), 2844-2848,
- (68) Becker, M. R.; Rykaczewski, K. A.; Ludwig, J. R.; Schindler, C. S. Carbonyl–olefin metathesis for the synthesis of cyclic olefins. *Org. Synth.* **2018**, *95*, 472-485, 477 plates,

- (69) Albright, H.; Riehl, P. S.; McAtee, C. C.; Reid, J. P.; Ludwig, J. R.; Karp, L. A.; Zimmerman, P. M.; Sigman, M. S.; Schindler, C. S. Catalytic Carbonyl-Olefin Metathesis of Aliphatic Ketones: Iron(III) Homo-Dimers as Lewis Acidic Superelectrophiles. *J. Am. Chem. Soc.* **2019**, *141* (4), 1690-1700,
- (70) Olah, G. A. Superelectrophiles. *Angew. Chem. Int. Ed.* **1993**, *32* (6), 767-788,
- (71) Hong, X.; Liang, Y.; Griffith, A. K.; Lambert, T. H.; Houk, K. N. Distortion-accelerated cycloadditions and strain-release-promoted cycloreversions in the organocatalytic carbonyl-olefin metathesis. *Chem. Sci.* **2014**, *5* (2), 471-475,
- (72) Zhang, Y.; Jermaks, J.; MacMillan, S. N.; Lambert, T. H. Synthesis of 2H-Chromenes via Hydrazine-Catalyzed Ring-Closing Carbonyl-Olefin Metathesis. *ACS Catal.* **2019**, *9* (10), 9259-9264,
- (73) Zhang, Y.; Sim, J. H.; MacMillan, S. N.; Lambert, T. H. Synthesis of 1,2-Dihydroquinolines via Hydrazine-Catalyzed Ring-Closing Carbonyl-Olefin Metathesis. *Org. Lett.* **2020**,
- (74) Ni, S.; Franzén, J. Carbocation catalysed ring closing aldehyde-olefin metathesis. *Chem. Commun.* **2018**, *54* (92), 12982-12985,
- (75) Minegishi, S.; Mayr, H. How Constant Are Ritchie's "Constant Selectivity Relationships"? A General Reactivity Scale for  $n$ -,  $\pi$ -, and  $\sigma$ -Nucleophiles. *J. Am. Chem. Soc.* **2003**, *125* (1), 286-295,
- (76) Mayr, H.; Kempf, B.; Ofial, A. R.  $\pi$ -Nucleophilicity in Carbon-Carbon Bond-Forming Reactions. *Acc. Chem. Res.* **2003**, *36* (1), 66-77,
- (77) Horn, M.; Mayr, H. Electrophilicity versus Electrofugality of Tritylium Ions in Aqueous Acetonitrile. *Eur. J. Chem.* **2010**, *16* (25), 7478-7487,
- (78) Horn, M.; Mayr, H. Electrophilicities of Acceptor-Substituted Tritylium Ions. *Eur. J. Org. Chem.* **2011**, *2011* (32), 6470-6475,
- (79) Horn, M.; Mayr, H. A comprehensive view on stabilities and reactivities of triarylmethyl cations (tritylium ions). *J. Phys. Org. Chem.* **2012**, *25* (11), 979-988,
- (80) Horn, M.; Schappele, L. H.; Lang-Wittkowski, G.; Mayr, H.; Ofial, A. R. Towards a Comprehensive Hydride Donor Ability Scale. *Eur. J. Chem.* **2013**, *19* (1), 249-263,
- (81) Jereb, M.; Vražič, D.; Zupan, M. Iodine-catalyzed transformation of molecules containing oxygen functional groups. *Tetrahedron* **2011**, *67* (7), 1355-1387,
- (82) Oss, G.; Nguyen, T. V. Iodonium-Catalyzed Carbonyl-Olefin Metathesis Reactions. *Synlett* **2019**, *30* (17), 1966-1970,
- (83) MacGillivray, L. R.; Atwood, J. L. A chiral spherical molecular assembly held together by 60 hydrogen bonds. *Nature* **1997**, *389* (6650), 469-472,
- (84) Atwood, J. L.; Barbour, L. J.; Jerga, A. Hydrogen-bonded molecular capsules are stable in polar media. *Chem. Commun.* **2001**, (22), 2376-2377,
- (85) Avram, L.; Cohen, Y. Spontaneous Formation of Hexameric Resorcinarene Capsule in Chloroform Solution as Detected by Diffusion NMR. *J. Am. Chem. Soc.* **2002**, *124* (51), 15148-15149,
- (86) Avram, L.; Cohen, Y. The Role of Water Molecules in a Resorcinarene Capsule As Probed by NMR Diffusion Measurements. *Org. Lett.* **2002**, *4* (24), 4365-4368,
- (87) Avram, L.; Cohen, Y. Hexameric Capsules of Lipophilic Pyrogallolarene and Resorcinarene in Solutions as Probed by Diffusion NMR: One Hydroxyl Makes the Difference. *Org. Lett.* **2003**, *5* (18), 3329-3332,
- (88) Avram, L.; Cohen, Y.; Rebek Jr, J. Recent advances in hydrogen-bonded hexameric encapsulation complexes. *Chem. Commun.* **2011**, *47* (19), 5368-5375,
- (89) Cavarzan, A.; Scarso, A.; Sgarbossa, P.; Strukul, G.; Reek, J. N. H. Supramolecular Control on Chemo- and Regioselectivity via Encapsulation of (NHC)-Au Catalyst within a Hexameric Self-Assembled Host. *J. Am. Chem. Soc.* **2011**, *133* (9), 2848-2851,
- (90) Zhang, Q.; Tiefenbacher, K. Hexameric Resorcinarene Capsule is a Brønsted Acid: Investigation and Application to Synthesis and Catalysis. *J. Am. Chem. Soc.* **2013**, *135* (43), 16213-16219,
- (91) Catti, L.; Tiefenbacher, K. Intramolecular hydroalkoxylation catalyzed inside a self-assembled cavity of an enzyme-like host structure. *Chem. Commun.* **2015**, *51* (5), 892-894,
- (92) Lorenzo, C.; Alexander, P.; Konrad, T. Host-Catalyzed Cyclodehydration-Rearrangement Cascade Reaction of Unsaturated Tertiary Alcohols. *Adv. Synth. Catal.* **2017**, *359* (8), 1331-1338,

- (93) Zhang, Q.; Tiefenbacher, K. Terpene cyclization catalysed inside a self-assembled cavity. *Nat. Chem.* **2015**, *7*, 197,
- (94) Croteau, R. Biosynthesis and catabolism of monoterpenoids. *Chem. Rev.* **1987**, *87* (5), 929-954,
- (95) Zhang, Q.; Tiefenbacher, K. Sesquiterpene Cyclizations inside the Hexameric Resorcinarene Capsule: Total Synthesis of  $\delta$ -Selinene and Mechanistic Studies. *Angew. Chem. Int. Ed.* **2019**, *58* (36), 12688-12695,
- (96) Syntrivanis, L.-D.; Némethová, I.; Schmid, D.; Levi, S.; Prescimone, A.; Bissegger, F.; Major, D. T.; Tiefenbacher, K. Four-Step Access to the Sesquiterpene Natural Product Presilphiperfolan-1 $\beta$ -ol and Unnatural Derivatives via Supramolecular Catalysis. *J. Am. Chem. Soc.* **2020**, *142* (12), 5894-5900,
- (97) Merget, S.; Catti, L.; Piccini, G.; Tiefenbacher, K. Requirements for Terpene Cyclizations inside the Supramolecular Resorcinarene Capsule: Bound Water and Its Protonation Determine the Catalytic Activity. *J. Am. Chem. Soc.* **2020**, *142* (9), 4400-4410,
- (98) Catti, L.; Tiefenbacher, K. Brønsted Acid-Catalyzed Carbonyl-Olefin Metathesis inside a Self-Assembled Supramolecular Host. *Angew. Chem. Int. Ed.* **2018**, *57* (44), 14589-14592,
- (99) La Manna, P.; De Rosa, M.; Talotta, C.; Gaeta, C.; Soriente, A.; Floresta, G.; Rescifina, A.; Neri, P. The hexameric resorcinarene capsule as an artificial enzyme: ruling the regio and stereochemistry of a 1,3-dipolar cycloaddition between nitrones and unsaturated aldehydes. *Org. Chem. Front.* **2018**, *5* (5), 827-837,
- (100) La Manna, P.; Talotta, C.; Floresta, G.; De Rosa, M.; Soriente, A.; Rescifina, A.; Gaeta, C.; Neri, P. Mild Friedel-Crafts Reactions inside a Hexameric Resorcinarene Capsule: C-Cl Bond Activation through Hydrogen Bonding to Bridging Water Molecules. *Angew. Chem. Int. Ed.* **2018**, *57* (19), 5423-5428,
- (101) Gaeta, C.; Talotta, C.; De Rosa, M.; La Manna, P.; Soriente, A.; Neri, P. The Hexameric Resorcinarene Capsule at Work: Supramolecular Catalysis in Confined Spaces. *Eur. J. Chem.* **2019**, *25* (19), 4899-4913,
- (102) Gambaro, S.; De Rosa, M.; Soriente, A.; Talotta, C.; Floresta, G.; Rescifina, A.; Gaeta, C.; Neri, P. A hexameric resorcinarene capsule as a hydrogen bonding catalyst in the conjugate addition of pyrroles and indoles to nitroalkenes. *Org. Chem. Front.* **2019**, *6* (14), 2339-2347,
- (103) La Manna, P.; De Rosa, M.; Talotta, C.; Rescifina, A.; Floresta, G.; Soriente, A.; Gaeta, C.; Neri, P. Synergic Interplay Between Halogen Bonding and Hydrogen Bonding in the Activation of a Neutral Substrate in a Nanoconfined Space. *Angew. Chem. Int. Ed.* **2020**, *59* (2), 811-818,
- (104) Li, T.-R.; Huck, F.; Piccini, G.; Tiefenbacher, K. Hydrogen Bond Synchronized Dual Activation Enables the Unified  $\beta$ -Selective O-Glycosylation Inside a Molecular Capsule. *ChemRxiv. Preprint.* **2021**, <https://doi.org/10.26434/chemrxiv.14199443.v14199441>,
- (105) Huck, F.; Catti, L.; Reber, G. L.; Tiefenbacher, K. Expanding the Protecting Group Scope for the Carbonyl Olefin Metathesis Approach to 2,5-Dihydropyrroles. *J. Org. Chem.* **2022**, *87* (1), 419-428,
- (106) Naito, H.; Hata, T.; Urabe, H. Selective Deprotection of Methanesulfonamides to Amines. *Org. Lett.* **2010**, *12* (6), 1228-1230,
- (107) Griffin, R. H.; Jewett, J. G. Remote secondary deuterium isotope effects. II. Allylic systems. *J. Am. Chem. Soc.* **1970**, *92* (4), 1104-1105,
- (108) Thibblin, A. Borderline between E1 and E2 mechanisms. Bimolecular base-promoted elimination via ion pairs competing with concerted E2 elimination. *J. Am. Chem. Soc.* **1989**, *111* (14), 5412-5416,
- (109) Choi, S.-r.; Breugst, M.; Houk, K. N.; Poulter, C. D.  $\delta$ -Deuterium Isotope Effects as Probes for Transition-State Structures of Isoprenoid Substrates. *J. Org. Chem.* **2014**, *79* (8), 3572-3580,
- (110) Nagorski, R. W.; Slebocka-Tilk, H.; Brown, R. S. Observation of an unusually large inverse secondary deuterium kinetic isotope effect for the reaction of a sterically congested olefin with bromine. *J. Am. Chem. Soc.* **1994**, *116* (1), 419-420,
- (111) Vassilikogiannakis, G.; Stratakis, M.; Orfanopoulos, M. Isotope Effects and syn Selectivity in the Ene Reaction of Triazolinedione with Conjugated Enones: Aziridinium Imide or an Open Intermediate Mechanism? *Org. Lett.* **2000**, *2* (15), 2245-2248,
- (112) Jencks, W. P. Ingold Lecture. How does a reaction choose its mechanism? *Chem. Soc. Rev.* **1981**, *10* (3), 345-375,

- (113) Young, P. R.; Jencks, W. P. Separation of polar and resonance substituent effects in the reactions of acetophenones with bisulfite and of benzyl halides with nucleophiles. *J. Am. Chem. Soc.* **1979**, *101* (12), 3288-3294,
- (114) Stein, A. R.; Tencer, M.; Moffatt, E. A.; Dawe, R.; Sweet, J. Nonlinearity of Hammett  $\rho$  correlations for benzylic systems: activation parameters and their mechanistic implications. *J. Org. Chem.* **1980**, *45* (17), 3539-3540,
- (115) Michael, A. On the synthesis of Helicin and Phenolglucoside. *Am. Chem. J.* **1879**, *1*, 305. **1879**,
- (116) Fischer, E. Ueber die Glucoside der Alkohole. *Chem. Ber.* **1893**, *26* (3), 2400-2412,
- (117) Toshima, K.; Tatsuta, K. Recent progress in O-glycosylation methods and its application to natural products synthesis. *Chem. Rev.* **1993**, *93* (4), 1503-1531,
- (118) W.Koenigs, E. K. Some derivatives of grape sugars and galactose. *Ber.* 1901, *34*, 957-981. *Ber.* **1901**, (Koenigs, W., Knorr, E. Some derivatives of grape sugars and galactose. *Ber.* 1901, *34*, 957-981.), 957-981,
- (119) Kotke, M.; Schreiner, P. R. Acid-free, organocatalytic acetalization. *Tetrahedron* **2006**, *62* (2), 434-439,
- (120) Kotke, M.; Schreiner, P. R. Generally Applicable Organocatalytic Tetrahydropyranylation of Hydroxy Functionalities with Very Low Catalyst Loading. *Synthesis* **2007**, *2007* (05), 779-790,
- (121) Balmond, E. I.; Coe, D. M.; Galan, M. C.; McGarrigle, E. M.  $\alpha$ -Selective Organocatalytic Synthesis of 2-Deoxygalactosides. *Angew. Chem. Int. Ed.* **2012**, *51* (36), 9152-9155,
- (122) Sun, L.; Wu, X.; Xiong, D.-C.; Ye, X.-S. Stereoselective Koenigs–Knorr Glycosylation Catalyzed by Urea. *Angew. Chem. Int. Ed.* **2016**, *55* (28), 8041-8044,
- (123) Park, Y.; Harper, K. C.; Kuhl, N.; Kwan, E. E.; Liu, R. Y.; Jacobsen, E. N. Macrocyclic bis-thioureas catalyze stereospecific glycosylation reactions. *Science* **2017**, *355* (6321), 162-166,
- (124) Nakamura, A.; Ishida, T.; Kusaka, K.; Yamada, T.; Fushinobu, S.; Tanaka, I.; Kaneko, S.; Ohta, K.; Tanaka, H.; Inaka, K.; et al. "Newton's cradle" proton relay with amide–imidic acid tautomerization in inverting cellulase visualized by neutron crystallography. *Sci. Adv.* **2015**, *1* (7), e1500263,
- (125) Adero, P. O.; Amarasekara, H.; Wen, P.; Bohé, L.; Crich, D. The Experimental Evidence in Support of Glycosylation Mechanisms at the SN1–SN2 Interface. *Chem. Rev.* **2018**, *118* (17), 8242-8284,
- (126) Singleton, D. A.; Thomas, A. A. High-Precision Simultaneous Determination of Multiple Small Kinetic Isotope Effects at Natural Abundance. *J. Am. Chem. Soc.* **1995**, *117* (36), 9357-9358,
- (127) Matsui, H.; Blanchard, J. S.; Brewer, C. F.; Hehre, E. J. Alpha-secondary tritium kinetic isotope effects for the hydrolysis of alpha-D-glucopyranosyl fluoride by exo-alpha-glucanases. *J. Biol. Chem.* **1989**, *264* (15), 8714-8716,
- (128) Chan, J.; Sannikova, N.; Tang, A.; Bennet, A. J. Transition-State Structure for the Quintessential SN2 Reaction of a Carbohydrate: Reaction of  $\alpha$ -Glucopyranosyl Fluoride with Azide Ion in Water. *J. Am. Chem. Soc.* **2014**, *136* (35), 12225-12228,
- (129) Schowen, R. L. The use of solvent isotope effects in the pursuit of enzyme mechanisms. *J. Labelled Compd. Radiopharm.* **2007**, *50* (11-12), 1052-1062,
- (130) Venkatasubban, K. S.; Schowen, R. L. The Proton Inventory Techniqu. *Crit. Rev. Biochem. Mol. Biol.* **1984**, *17* (1), 1-44,
- (131) Catti, L.; Pöthig, A.; Tiefenbacher, K. Host-Catalyzed Cyclodehydration–Rearrangement Cascade Reaction of Unsaturated Tertiary Alcohols. *Adv. Synth. Catal.* **2017**, *359* (8), 1331-1338,
- (132) Fujiwara, T.; Okabayashi, T.; Takahama, Y.; Matsuo, N.; Tanabe, Y. Ring-Closing Strategy Utilizing Nitrile  $\alpha$ -Anions: Chiral Synthesis of (+)-Norchrysanthemide Acid and Expedient Asymmetric Total Synthesis of (+)-Grandisol. *Eur. J. Org. Chem.* **2018**, *2018* (43), 6018-6027,
- (133) Zhang, J.; Xue, W.; Wang, P.; Wang, T.; Liang, Y.; Zhang, Z. One-pot synthesis of 3-(furan-2-yl)-4-hydroxy-2H-chromen-2-ones using K10 montmorillonite clay as heterogeneous catalyst. *Tetrahedron* **2018**, *74* (36), 4712-4720,
- (134) Ganiu, M. O.; Cleveland, A. H.; Paul, J. L.; Kartika, R. Triphosgene and DMAP as Mild Reagents for Chemoselective Dehydration of Tertiary Alcohols. *Org. Lett.* **2019**, *21* (14), 5611-5615,

(135) Castro, C.; Smidansky, E.; Maksimchuk, K. R.; Arnold, J. J.; Korneeva, V. S.; Götte, M.; Konigsberg, W.; Cameron, C. E. Two proton transfers in the transition state for nucleotidyl transfer catalyzed by RNA- and DNA-dependent RNA and DNA polymerases. *PNAS* **2007**, *104* (11), 4267-4272,

